frontiers | Research Topics

Novel diagnostic and therapeutic strategies in pediatric vitreoretinal disease

Edited by
Xiaoyan Ding, Peiquan Zhao and Chi-Chao Chan

Published in
Frontiers in Medicine

ISSN 1664-8714
ISBN 978-2-8325-2912-6
DOI 10.3389/978-2-8325-2912-6

About Frontiers

Frontiers is more than just an open access publisher of scholarly articles: it is a pioneering approach to the world of academia, radically improving the way scholarly research is managed. The grand vision of Frontiers is a world where all people have an equal opportunity to seek, share and generate knowledge. Frontiers provides immediate and permanent online open access to all its publications, but this alone is not enough to realize our grand goals.

Frontiers journal series

The Frontiers journal series is a multi-tier and interdisciplinary set of open-access, online journals, promising a paradigm shift from the current review, selection and dissemination processes in academic publishing. All Frontiers journals are driven by researchers for researchers; therefore, they constitute a service to the scholarly community. At the same time, the *Frontiers journal series* operates on a revolutionary invention, the tiered publishing system, initially addressing specific communities of scholars, and gradually climbing up to broader public understanding, thus serving the interests of the lay society, too.

Dedication to quality

Each Frontiers article is a landmark of the highest quality, thanks to genuinely collaborative interactions between authors and review editors, who include some of the world's best academicians. Research must be certified by peers before entering a stream of knowledge that may eventually reach the public - and shape society; therefore, Frontiers only applies the most rigorous and unbiased reviews. Frontiers revolutionizes research publishing by freely delivering the most outstanding research, evaluated with no bias from both the academic and social point of view. By applying the most advanced information technologies, Frontiers is catapulting scholarly publishing into a new generation.

What are Frontiers Research Topics?

Frontiers Research Topics are very popular trademarks of the *Frontiers journals series*: they are collections of at least ten articles, all centered on a particular subject. With their unique mix of varied contributions from Original Research to Review Articles, Frontiers Research Topics unify the most influential researchers, the latest key findings and historical advances in a hot research area.

Find out more on how to host your own Frontiers Research Topic or contribute to one as an author by contacting the Frontiers editorial office: frontiersin.org/about/contact

Novel diagnostic and therapeutic strategies in pediatric vitreoretinal disease

Topic editors

Xiaoyan Ding — Sun Yat-sen University, China

Peiquan Zhao — Shanghai Jiao Tong University, China

Chi-Chao Chan — National Eye Institute (NIH), United States

Citation

Ding, X., Zhao, P., Chan, C.-C., eds. (2023). *Novel diagnostic and therapeutic strategies in pediatric vitreoretinal disease*. Lausanne: Frontiers Media SA.

doi: 10.3389/978-2-8325-2912-6

Table of contents

frontiers in Medicine

REVIEW
published: 02 February 2022
doi: 10.3389/fmed.2022.840030

Novel Potential Biomarkers for Retinopathy of Prematurity

Wei Tan[1,2], *Bingyan Li*[1,2], *Zicong Wang*[1,2], *Jingling Zou*[1,2], *Yang Jia*[3], *Shigeo Yoshida*[4] *and Yedi Zhou*[1,2]*

[1] Department of Ophthalmology, The Second Xiangya Hospital of Central South University, Changsha, China, [2] Hunan Clinical Research Center of Ophthalmic Disease, Changsha, China, [3] Department of Pediatrics, The Second Xiangya Hospital of Central South University, Changsha, China, [4] Department of Ophthalmology, Kurume University School of Medicine, Kurume, Japan

Retinopathy of prematurity (ROP) is the main risk factor for vision-threatening disease in premature infants with low birth weight. An accumulating number of independent studies have focused on ROP pathogenesis and have demonstrated that laser photocoagulation therapy and/or anti-VEGF treatment are effective. However, early diagnosis of ROP is still critical. At present, the main method of ROP screening is based on binocular indirect ophthalmoscopy. However, the judgment of whether ROP occurs and whether treatment is necessary depends largely on ophthalmologists with a great deal of experience. Therefore, it is essential to develop a simple, accurate and effective diagnostic method. This review describes recent findings on novel biomarkers for the prediction, diagnosis and prognosis of ROP patients. The novel biomarkers were separated into the following categories: metabolites, cytokines and growth factors, non-coding RNAs, iconography, gut microbiota, oxidative stress biomarkers, and others. Biomarkers with high sensitivity and specificity are urgently needed for the clinical applications of ROP. In addition, using non-invasive or minimally invasive methods to obtain samples is also important. Our review provides an overview of potential biomarkers of ROP.

Keywords: biomarker, retinopathy of prematurity, metabolites, cytokines and growth factors, non-coding RNAs, gut microbiota, oxidative stress biomarkers, iconography

OPEN ACCESS

Edited by:
Xiaoyan Ding,
Sun Yat-sen University, China

Reviewed by:
Ye Liu,
Zhejiang University, China
Wencui Wan,
The First Affiliated Hospital of Zhengzhou University, China

***Correspondence:**
Yedi Zhou
zhouyedi@csu.edu.cn

Specialty section:
This article was submitted to Ophthalmology, a section of the journal Frontiers in Medicine

Received: *20 December 2021*
Accepted: *12 January 2022*
Published: *02 February 2022*

Citation:
Tan W, Li B, Wang Z, Zou J, Jia Y, Yoshida S and Zhou Y (2022) Novel Potential Biomarkers for Retinopathy of Prematurity. Front. Med. 9:840030. doi: 10.3389/fmed.2022.840030

INTRODUCTION

Retinopathy of prematurity (ROP) is a major cause of vision loss and blindness in children worldwide (1–3). As perinatal oxygen metabolism disorder causes hypoxia-ischemia, the compensatory secretion of pathological angiogenic factors and then the formation of retinal neovascularization contributes to abnormal retinal blood vessel development and even tractional retinal detachment (4–6). Preterm infants have immature retinal tissue, shorter axial lengths and thicker corneas and are more likely to suffer from ROP (7, 8). Epidemiological studies have shown that the incidence of premature newborns is approximately 10%, and infants with lower birth weight and gestational age have a higher incidence and severity of ROP. A total of 65.8% of preterm infants with a birth weight of < 1,251 g suffer from ROP to a certain degree; 81.6% of infants with a birth weight of < 1,000 g suffer from ROP (9, 10). However, ROP is a largely preventable disease. Reducing the incidence of blindness is related to high-quality newborn care, a comprehensive ROP screening program, and experienced ROP ophthalmologists (11). Laser photocoagulation combined with intravitreal injection of anti-vascular endothelial growth factor (VEGF) drugs after early detection is effective (12–14).

At present, ROP screening is based on birth weight and gestational age. Binocular indirect ophthalmoscopy (BIO) bedside examination, as well as wide-field fundus imaging system, are widely applied for ROP screening (15, 16). Recently, telemedicine and artificial intelligence-based ROP screening are considered to be more suitable in remote areas that are lack trained ophthalmologists (16–18). However, these screening methods have not been widely implemented, and the judgment of whether the therapeutic treatment is required for ROP infants mainly depends on the clinical experiences of the ophthalmologists (19–21). Furthermore, the molecular diagnostic methods and diagnostic criteria of ROP have not yet been clarified. A balance between the accurate identification of newborns with ROP that need therapy and a reduction in workload is required to save resources and avoid the unnecessary inspection of prematurity (22).

Biomarkers are indicators that are defined as objective measurements and evaluations that are used to evaluate normal biological processes, pathogenic processes, and responses to intervention or exposure (23). Biomarkers are mainly divided into seven categories, including diagnosis, monitoring, drug efficacy/response, prediction, prognosis, safety and susceptibility/risk biomarkers (23, 24). Blood is easy to obtain, and blood draw is a relatively non-invasive method (25). Some diseases have been distinguished using blood-based biomarkers, such as human epidermal growth factor receptor 2 (HER2) for breast cancer (26, 27) and epidermal growth factor receptor (EGFR) for lung cancer (28, 29). In addition to blood biomarkers, biomarkers from urine, feces and cerebrospinal fluid can be used to identify diseases. One such biomarker in the spinal fluid is myelin oligodendrocyte glycoprotein (MOG-IgG) and aquaporin-4 (AQP4), which are used to identify neuromyelitis optica spectrum disorders (30). In the field of ophthalmology, imaging findings and artificial intelligence analysis have been used as biomarkers for prediction and therapy response of choroidal diseases (31–33), and intraretinal cysts can be used for the prognosis of neovascular age-related macular (AMD) disease (34). Our review provides an overview of biomarkers in ROP and summarized in **Figure 1**.

CANDIDATES OF NOVEL POTENTIAL BIOMARKERS

Metabolites

ROP is related to hypoxia and nutrient deprivation in the maturation of retinal blood vessels, and regulation of retinal metabolism can prevent pathological angiogenesis. Recent research on the metabolic changes of ROP shows that metabolites can serve as biomarkers (35). Metabolomics affects cell physiology by regulating the genome, epigenome, transcriptome, and proteome (36). A study on targeted blood metabolomics in premature neonates showed that elevated levels of malonyl carnitine (C3DC) and glycine in the blood are promising biomarkers for prediction but cannot judge severity (37). Another plasma metabolomics study on treatment-requiring ROP indicated that altered metabolites may be used as diagnostic and prognostic biomarkers, including the majority of altered amino acids and their derivatives (38). Further targeted metabolomics research found that plasma citrulline, arginine and aminoadipate were increased in patients with ROP, but creatine was reduced. They are all potential biomarkers (39). The oxygen-induced retinopathy (OIR) model is an animal model that has been widely used in the study of retinal neovascular diseases and is similar to the pathological process of ROP (40, 41). By analyzing the plasma from an OIR rat model, Lu et al. found that proline and "arginine and proline metabolism" pathways are potential biomarkers for the diagnosis of ROP (42). A prospective study by Nilsson et al. analyzed the changes in serum sphingolipidome in very preterm infants and concluded that a low concentration of sphingosine-1-phosphate signaling lipid is strongly related to severe ROP (43). Lower levels of the ω-6 long-chain polyunsaturated fatty acid arachidonic acid (AA) are closely related to the development of ROP and is beneficial for the prediction of ROP (44). **Table 1** summarizes these metabolism biomarkers.

Cytokines and Growth Factors

The immune-inflammatory environment before and after delivery of preterm infants may be a crucial factor leading to the progression of ROP (45). Various inflammatory cytokines and chemokines have been extensively investigated, and changes in their levels may be potential candidates for novel biomarkers of ROP. A study indicated that the increase in inflammatory factors (interleukin (IL)-6 and IL-8) and angiogenic mediators (endoglin, endostatin and insulin-like growth factor-binding protein (IGFBP)-2) in amniotic fluid is related to the occurrence and development of ROP. The use of these biomarkers in combination with prenatal factors can establish a prenatal prediction pattern of ROP (46). Another similar study suggested that an increase in IL-6 in umbilical cord plasma can predict ROP severity, and the elevated concentration of C5a can be used to assess whether laser treatment is required. Furthermore, the combined application is more accurate in the prediction of ROP development (45). In umbilical cord serum, elevated levels of IL-7, monocyte chemotactic protein-1 (MCP-1), macrophage inflammatory protein 1α (MIP-1α) and MIP-1β contribute to predicting the risk of ROP, while MIP-1β is related to ROP severity (47). High levels of VEGF-Receptor 1, IL-8, matrix metalloproteinase 9 (MMP-9), erythropoietin (EPO), tumor necrosis factor (TNF)-α and basic fibroblast growth factor (bFGF) are related to a risk factor for prethreshold ROP in the first three postnatal weeks (48). A similar study showed that IL-6 is significantly increased and IL-17 is decreased on Days 0–3 after birth. On Days 7–21, transforming growth factor-β (TGF-β), brain-derived neurotrophic factor (BDNF), and regulated upon activation, normal T cell expressed and secreted (RANTES) were significantly reduced. IL-18, CRP and NT-4 concentrations were changed in both time periods (49). On Day 28, elevated concentrations of IL-6, TNF-α, TNF-R1/-R2, and IL-8 were related to the risk of ROP (48), and decreased serum levels of EPO was determined to be an independent factor for ROP prediction (50). In the tears of severe ROP, MMP-9 is elevated. Moreover, in the ROP vitreous, MMP9, complement factor H (CFH), C3,

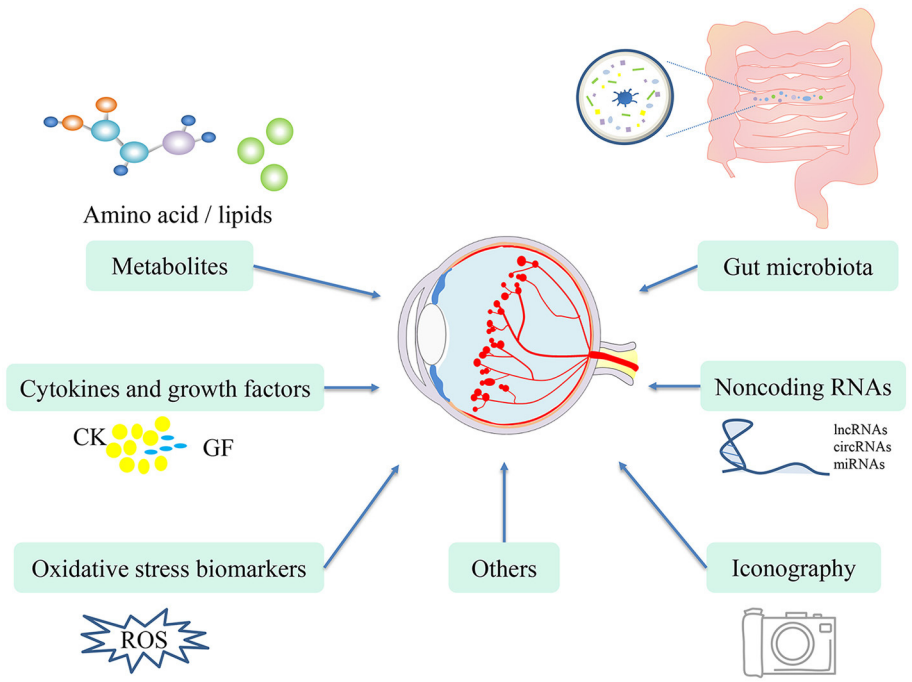

FIGURE 1 | Novel potential biomarkers for ROP, including metabolites, cytokines and growth factors, ncRNAs, iconography, gut microbiota, oxidative stress biomarkers and others.

TABLE 1 | Metabolites as potential biomarkers for ROP patients.

Sample source	Method	Potential biomarker	Correlation
Infant-blood	Targeted metabolomic	C3DC and glycine	Elevated levels of C3DC and glycine in premature infants are promising biomarkers for ROP prediction, not for severity (37).
Infant-plasma	Untargeted metabolomics analysis	altered metabolites	Altered metabolites may be used as diagnostic and prognostic biomarkers, especially altered amino acids and their derivatives (38).
Infant-plasma	Targeted metabolomics analysis	citrulline, arginine,aminoadipate and creatine	Citrulline, arginine and aminoadipate in patients with ROP were increased, while creatine was reduced (39).
OIR rat-plasma	Untargeted metabolomics analysis	proline and "arginine and proline metabolism" pathways	Proline and "arginine and proline metabolism" pathways are potential biomarkers for the diagnosis of ROP (42).
Infant-serum	Lipid analysis	sphingosine-1-phosphate	Low levels of the sphingosine-1-phosphate signaling lipid is strongly related to severe ROP (43).
Infant-serum	Lipid analysis	AA	Low levels of AA are closely related to the development of ROP and benefit prediction (44).

C4, IL-1ra, VEGF and granulocyte colony-stimulating factor (G-CSF) are also increased (51). VEGF is elevated, and insulin-like growth factor 1 (IGF-1) is reduced in the cord blood of ROP patients. Serum IL-33 and endocan could be predictive biomarkers for severe ROP. These serum concentrations were higher and then significantly reduced after laser treatment (52). VEGF, interferon-γ (IFN-γ), IL-10 and IL-12 are elevated in the aqueous humor of ROP patients, and higher levels of VEGF and MIP-1β are independently associated with ROP retreatment (53). At birth, infants with proliferative ROP have a low level of serum IL-5. Ten to 14 days after birth, babies without ROP have higher levels of serum BDNF and RANTES than infants with proliferative ROP (54). At 24 h after birth, the levels of proinflammatory cytokines (IL-6 and TNF-α) were increased in children who received ROP therapeutic treatment. However, the concentration of IL-6 was negatively correlated with IGF-1 in ROP infants of 5–8 weeks after birth (55).

IGF-1 is the primary factor involved in the growth of fetal tissues. Under normal circumstances, sufficient levels of serum IGF-1 are required for VEGF-stimulated retinal angiogenesis, but premature delivery causes a sudden decrease in serum IGF-1 levels (56, 57). Clinical studies in the United States (56) and

Europe (58) have shown that a low concentration of IGF-1 is related to the subsequent progression of severe ROP, so it is a risk predictor. The early return of IGF-1 to normal levels in premature infants can prevent ROP (59). The critical time for the detection of serum IGF-1 is in the third week after delivery (57). Visfatin is an adipocytokine that has a similar to insulin function and IGF-1 level, and it could be considered to be a predictor of ROP (60). Serum VEGF levels at birth are reduced in premature newborns who develop ROP later and may be an ROP predictor (61). VEGF and stromal cell-derived factor 1α (SDF-1α) are elevated in the vitreous of stage 4 ROP (62). Among the proangiogenic factors in infant tears, angiogenin/VEGF can be used as a potential non-invasive screening biomarker for ROP (63). However, Woo et al. found that inflammatory cytokines (IL-1β, IL-4, IL-6, IL-8, IL-10, IL12, IFN-γ, and TNF-α) and growth factors (IGF-1 and VEGF) in cord blood samples may not predict ROP (64). Lymphocyte count is negatively correlated with ROP and may have an independent predictive value. However, the neutrophil-to-lymphocyte ratio (NLR) is not an independent predictor of ROP (65). **Table 2** summarizes the cytokine and growth factor biomarkers.

Non-coding RNA

Non-coding RNAs (ncRNAs) are a type of RNA that does not encode proteins (66). However, they can still affect normal gene expression and participate in physiological and pathological processes through various mechanisms (67–69). Types of ncRNAs include long non-coding RNAs (lncRNAs), circular RNAs (circRNAs), and microRNAs (miRNAs), etc. (70). CircRNA is a single-stranded closed circular ncRNA. Compared to other RNAs, it has a longer half-life, better stability and increased resistance to RNase R, making it a potential biomarker and therapeutic target (71–73). In fact, the expression and function of various circRNAs have been indicated in different cancers (74) and ocular diseases (75). Based on an OIR mouse model, Liu et al. found that the expression of cZNF609 in the retina was largely reduced during the vascular occlusion phase and significantly increased during the neovascularization phase. It combines with miR-615-5p as a miRNA sponge to regulate the gene expression of human umbilical vein endothelial cells (76). MiRNAs are small ncRNAs that can influence gene expression by influencing transcription, translation and epigenetics (77). At present, most studies on miRNAs and ROP are derived from research in animal models (78, 79). Metin et al. (80) performed the first clinical study. Through the analysis of 13 cases of ROP and 15 cases of premature infants without ROP, they found that miR-23a and miR-200b-3p were significantly elevated in premature infants with ROP, while miR-27b-3p and miR-214-3p were reduced. These altered miRNAs could be considered as possible biomarkers of ROP (80). Furthermore, there are some related transcriptomics and bioinformatics analyses that can also provide novel for ncRNA as ROP biomarkers (81–83).

Oxidative Stress Biomarkers

ROP is a neonatal disease that is associated with oxidative stress. When a premature baby is born, it suddenly changes from a very low oxygen intrauterine environment to an artificial hyperoxia treatment environment. Due to an insufficient antioxidant protection capacity, it is in a state of oxidative stress, and the retina is particularly sensitive to oxidative stress (84, 85). The glutathione status of red blood cells is an indicator of oxidative stress in preterm infants, and it aids in the early identification of children at risk of ROP (86). The acrolein-lysine adduct was elevated in the premature infant group with active retinopathy compared with the preterm group without retinopathy (87).

The levels of 8-hydroxy 2-deoxyguanosine (8-OHdG) and malondialdehyde (MDA) are significantly higher in the blood and urine of ROP patients than in non-ROP patients. Based on this correlation, they could be used as screening indicators for ROP (88). In umbilical cord plasma, elevated levels of the oxidative stress biomarker MDA and reduced levels of the micronutrient vitamin A in infants are independent predictors of ROP (89). Other studies also recognized that total oxidative status (TOS) and MDA are satisfactory markers of oxidative stress, which is increased in the ROP group (90). Peroxidant antioxidant balance (PAB) contributes to the incidence of ROP, and the severity of ROP increases with PAB (91).

Gut Microbiome

Although the human intestine is far from the eye, ophthalmological diseases are related to the regulation of systemic immunity. Emerging investigations into changes in the gut microbiota have been reported with a focus on uveitis (92, 93) and AMD (94, 95), and the concept of the gut-retina axis has emerged (94, 96). The maternal gut microbiota plays a key role in the health of infants (97). We can screen out differentially expressed gut microbes and explore the potential biomarkers of ROP. Such biomarkers could have important clinical significance and application value for the preliminary screening of certain concealed and difficult-to-diagnose ROPs. Westaway et al. suggested that preterm birth-related diseases are associated with the gut microbiome and that α-diversity in ROP infants was significantly reduced (98). Other studies proposed that Enterobacteriaceae species are enriched a few weeks before the diagnosis of ROP, while amino acid synthesis is more abundant in the non-ROP group (99, 100). Changes in the intestinal flora are promising targets for prevention and therapy in ROP patients. Such changes are closely related to metabolites. Therefore, it might be effective to utilize beneficial bacteria or produce antibodies against pathogenic bacteria to prevent or treat ROP in infants.

Iconography

In some remote regions, telemedicine technology with a digital fundus camera has been used for the screening and diagnosis of ROP (101). The swept-source optical coherence tomography imaging is used to determine the choroidal vascularity index (CVI), which is more sensitive than subfoveal choroidal thickness in assessing related choroidal structural changes in premature infants with a history of ROP. A decrease in CVI indicates impaired choroidal vascular function (102).

TABLE 2 | Cytokines and growth factors as potential biomarkers for ROP patients.

Sample source	Method	Potential biomarker	Correlation
Infant-amniotic fluid	ELISA	IL-6, IL-8, endoglin, endostatin and IGFBP-2	Inflammatory factors (IL-6 and IL-8) and angiogenic mediators (endoglin, endostatin and IGFBP-2) in amniotic fluid are related to the occurrence and development of ROP (46).
Infant-plasma	ELISA	IL-6 and C5a	High IL-6 levels predict ROP severity, while elevated concentrations of C5a assess whether laser treatment is required. The combined application is more accurate in predicting ROP development (45).
Infant-serum	multiplex protein arrays	IL-7, MCP-1, MIP-1α and MIP-1β	Elevated levels of IL-7, MCP-1, MIP-1α and MIP-1β contribute to prediction of the risk of ROP, and MIP-1β is related to ROP severity (47).
Infant-blood	meso scale discovery multiplex platform and microplate detection platform	VEGF-R1, IL-8, MMP-9, EPO, TNF-α and bFGF	High levels of VEGF-R1, IL-8, MMP-9, EPO, TNF-α and bFGF are related to a risk factor for prethreshold ROP in the first three postnatal weeks. On Day 28, elevated concentrations of IL-6, TNF-α, TNF-R1/-R2, IL-8 are still related to the risk (48).
Infant-blood	Multiplex Luminex assay	IL-6, IL-17, TGF-β, BDNF, RANTES, IL-18, CRP and NT-4	IL-6 is significantly increased and IL-17 is decreased on Days 0–3 after birth. On Days 7–21, TGF-β, BDNF, and RANTES are significantly reduced. IL-18, CRP and NT-4 were changed in both time periods (49).
Infant-serum	ELISA	EPO	On Day 28, decreased serum levels of EPO were determined to be independent factors for ROP prediction (50).
Infant-vitreous and tear	multiplex bead arrays	MMP9, CFH, C3, C4, IL-1ra, VEGF and G-CSF	In tears of severe ROP, MMP-9 is elevated. In the ROP vitreous, MMP9, CFH, C3, C4, IL-1ra, VEGF and G-CSF are also increased (51).
Infant-blood	ELISA	VEGF, IGF-1, IL-33 and endocan	VEGF is elevated and IGF-1 is reduced in cord blood of ROP patients. Serum IL-33 and endocan could be predictive biomarkers for severe ROP (52).
Infant-aqueous humor	multiplex bead assay	VEGF, IFN-γ, IL-10, IL-12 and MIP-1β	VEGF, IFN-γ, IL-10 and IL-12 in ROP patients are elevated, and higher levels of VEGF and MIP-1β are independently associated with ROP retreatment (53).
Infant-serum	multiplex immunoassay	IL-5, BDNF and RANTES	Infants at birth with proliferative ROP have a low level of serum IL-5. Ten to 14 days after birth, babies without ROP have higher levels of serum BDNF and RANTES than infants with proliferative ROP (54).
Infant-blood	human Luminex xMAP assay	IL-6, TNF-α and IGF-1	At 24 h after birth, the levels of IL-6 and TNF-α are both increased in children who received ROP treatment, while the concentration of IL-6 is negatively correlated with IGF-1 between 5–8 weeks after birth (55).
Infant-serum	ELISA and IGF binding protein-blocked radioimmunoassay	IGF-1	A low concentration of IGF-1 is related to the subsequent progression of severe ROP, so it is a risk predictor (56, 58). In addition, the early return of IGF-1 to normal levels in premature infants can prevent ROP (59). The critical time for the detection of serum IGF-1 is in the third week after delivery (57).
Infant-blood	Enzyme immunoassay	IGF-1 and Visfatin	Visfatin is an adipocytokine that has a similar to insulin function and IGF-1 level, and could be considered a predictor of ROP (60).
Infant-blood	ELISA	VEGF	Serum VEGF levels are reduced in premature newborns who develop ROP, and may be a predictor of ROP (61).
Infant-vitreous	ELISA	VEGF and SDF-1α	VEGF and SDF-1α are elevated in the vitreous of stage 4 ROP (62).
Infant-tear fluid	multiplex ELISA	Angiogenin and VEGF	Among the pro-angiogenic factors in the tears of infants, angiogenin/VEGF may be a potential non-invasive screening biomarker for ROP (63).
Infant-blood	ABX Pentra DF120/USA biochemical analyzer	Lymphocyte count	Lymphocyte count is negatively correlated with ROP and may be an independent predictor (65).

Other Biomarkers

There is significant thrombocytopenia in the blood samples of infants with treatment-requiring ROP, and this could be a predictor of disease progression (103). Platelet mass index is a reliable monitoring indicator for the prognosis of ROP in very premature newborns (104). The percentage of fetal hemoglobin after birth is negatively correlated with the severity of ROP (105). The complete blood count, including low concentrations of hemoglobin, can be a simple screening indicator for ROP; this is especially true for the mean corpuscular hemoglobin (106). Mutations in a Wnt signaling receptor protein (FZD4) gene may be an indicator of ROP (107). High levels of neonatal hemoglobin A1C are a feasible biomarker for proliferative ROP, and low levels of A1C are a feasible biomarker for non-proliferative ROP (108). Elevated plasma E-selection levels and recombinant human erythropoietin (rhEPO) are independent risk predictors for the progression of ROP (109–111). The serine protease HTRA-1 is the basis of protection against preeclampsia-mediated ROP and prevents the occurrence of diseases (112). An increase in the concentration of lactate and a low value for the perfusion index may be early parameters that can be used to predict ROP (113). The lack of human chorionic gonadotropin (hCG) at 4

weeks after birth may be related to non-proliferative ROP (114). The increase in urinary N-terminal B-type natriuretic peptide (NT-proBNP) in the early stage of preterm infants (<30 weeks of gestational age) and the NT-proBNP/creatinine ratio can identify the risk of severe ROP (115, 116). However, the changes in NT-proBNP disappear in more mature infants (117). Cluster analysis showed that an early increase in the levels of Parkinson disease protein 7 (PARK7), vimentin, myeloperoxidase (MPO), CD69, and NF-κB essential modulator (NEMO) in plasma is related to a decrease in ROP risk. However, lower levels of tumor necrosis factor receptor superfamily member 4 (TNFRSF4) and higher levels of HER2 and galanin could predict the progression of ROP (118). In addition, a meta-analysis suggested that polymorphisms in the angiotensin-converting enzyme (ACE) I/D may be a genetic biomarker of an increased risk of ROP (119). The mean blur rate (MBR) was higher in OIR rats than in the control group, and it was significantly correlated with avascular area/total retinal area (%AVA) and retinal VEGF, therefore, MBR could be used to assess the severity of OIR (120).

COMPARISON OF DIFFERENT DETECTION METHODS

Although various biomarkers are associated with ROP, whether their different detection methods are easy and fast is an important part of determining the feasibility of their final application in premature infants. Premature infants are fragile, and thus, it is highly important to avoid invasive operations, such as obtaining aqueous humor. Less invasive examinations, such as blood tests, are reliable sources of biomarkers, and most of the potential biomarkers we summarized above are also obtained from blood. In addition to collecting plasma or serum, peripheral blood mononuclear cells (PBMCs) could be obtained during the blood examination. PBMCs are an essential part of the immune system. They are related to inflammatory cells and can release a large number of paracrine factors (121–124). They are potentially an important source of biomarkers that are related to cytokines and growth factors. In addition, saliva has been used to determine the level of melatonin in premature infants. No significant difference in the level of melatonin between serum and saliva has been demonstrated, and a high degree of correlation was observed (125). Perhaps these findings can provide new ideas for exploring biomarkers. It is convenient to collect urine. Urine is rich in metabolites and can reflect the total imbalance of all biochemical pathways in the body (126). It is worth further exploring the value of such non-invasive, pain-free and easy-to-obtain samples as potential monitoring, diagnostic and prognostic biomarkers in ROP.

CONCLUSION

All over the world, the incidence of ROP is increasing in countries that have the technology to save premature infants (127, 128). If patients can be diagnosed in a timely manner, an effective treatment could restore vision. However, regrettably, the diagnosis of ROP depends on pediatric ophthalmologists with a great deal of clinical experience, and this diagnosis has a high degree of subjectivity and variability (129). It is easy to ignore abnormal conditions of the eyes because infants are unable to speak, but it could eventually lead to irreversible vision loss in some cases. Therefore, it is believed that the discovery of effective ROP biomarkers is very important. Reliable and easily available biomarkers will provide considerable information on diseases and aid in the development of new effective therapies (130). With the development of emerging laboratory medical technologies, microfluidic chips (131), proteomics (132) and single-cell technologies (133), also contribute to the exploration of biomarkers, which also deserve to be further revealed in ROP studies. In this review, we summarized several strong potential biomarkers including metabolites, cytokines and growth factors, ncRNAs, gut microbiota, iconography, oxidative stress biomarkers, etc. Since newborns are fragile, these markers should preferably be found in non-invasive and easily accessible samples, such as blood, urine and feces. Those studies and methods might contribute to the identification of effective biomarkers that shed light to the prediction and treatment of ROP.

AUTHOR CONTRIBUTIONS

YZ contributed to the conceptualization, design, and outline of this review. WT prepared the draft of the manuscript with tables and figures. BL, ZW, and JZ contributed to the literature search. YJ and SY contributed to the revision and editing. All authors have read and approved the final manuscript.

FUNDING

This work was supported by Changsha Science and Technology Project (kq1907075) and the Fundamental Research Funds for the Central Universities of Central South University (No. 2021zzts1056).

ACKNOWLEDGMENTS

The authors would like to thank Prof. Yun Li for important advice regarding the manuscript.

REFERENCES

1. Kim SJ, Port AD, Swan R, Campbell JP, Chan RVP, Chiang MF. Retinopathy of prematurity: a review of risk factors and their clinical significance. *Surv Ophthalmol.* (2018) 63:618–37. doi: 10.1016/j.survophthal.2018.04.002
2. Solebo AL, Teoh L, Rahi J. Epidemiology of blindness in children. *Arch Dis Child.* (2017) 102:853–7. doi: 10.1136/archdischild-2016-310532
3. Good WV. Retinopathy of prematurity incidence in children. *Ophthalmology.* (2020) 127:S82–3. doi: 10.1016/j.ophtha.2019.11.026
4. GBD 2019 Blindness and Vision Impairment Collaborators, Vision Loss Expert Group of the Global Burden of Disease Study. Causes of blindness and vision impairment in 2020 and trends over 30 years, and prevalence of avoidable blindness in relation to VISION 2020: the Right to Sight: an analysis for the Global Burden of Disease Study.

Lancet Glob Health. (2021) 9:e144–60. doi: 10.1016/S2214-109X(20)30489-7
5. Hellström A, Smith LE, Dammann O. Retinopathy of prematurity. *Lancet*. (2013) 382:1445–57. doi: 10.1016/S0140-6736(13)60178-6
6. Patel CK, Carreras E, Henderson RH, Wong SC, Berg S. Evolving outcomes of surgery for retinal detachment in retinopathy of prematurity: the need for a national service in the United Kingdom: an audit of surgery for acute tractional retinal detachment complicating ROP in the UK. *Eye*. (2021). doi: 10.1038/s41433-021-01679-8. [Epub ahead of print].
7. Fierson WM. Screening examination of premature infants for retinopathy of prematurity. *Pediatrics*. (2018) 142:e20183061. doi: 10.1542/peds.2018-3061
8. Kardaras D, Papageorgiou E, Gaitana K, Grivea I, Dimitriou VA, Androudi S, et al. The association between retinopathy of prematurity and ocular growth. *Invest Ophthalmol Vis Sci.* (2019) 60:98–106. doi: 10.1167/iovs.18-24776
9. Palmer EA, Flynn JT, Hardy RJ, Phelps DL, Phillips CL, Schaffer DB, et al. Incidence and early course of retinopathy of prematurity. *Ophthalmology*. (2020) 127:S84–96. doi: 10.1016/j.ophtha.2020.01.034
10. Goldenberg RL, Culhane JF, Iams JD, Romero R. Epidemiology and causes of preterm birth. *Lancet*. (2008) 371:75–84. doi: 10.1016/S0140-6736(08)60074-4
11. Adams GGW. ROP in Asia. *Eye*. (2020) 34:607–8. doi: 10.1038/s41433-019-0620-y
12. Daruich A, Bremond-Gignac D, Behar-Cohen F, Kermorvant E. [Retinopathy of prematurity: from prevention to treatment]. *Med Sci*. (2020) 36:900–7. doi: 10.1051/medsci/2020163
13. Laveti V, Balakrishnan D, Rani PK, Mohamed A, Jalali S. Prospective clinical study of two different treatment regimens of combined laser photocoagulation and intravitreal bevacizumab for retinopathy of prematurity: the Indian Twin Cities ROP study (ITCROPS) database report number 9. *Int Ophthalmol*. (2020) 40:3539–45. doi: 10.1007/s10792-020-01543-w
14. Sen P, Wu WC, Chandra P, Vinekar A, Manchegowda PT, Bhende P. Retinopathy of prematurity treatment: Asian perspectives. *Eye*. (2020) 34:632–42. doi: 10.1038/s41433-019-0643-4
15. Wu C, Petersen RA, VanderVeen DK. RetCam imaging for retinopathy of prematurity screening. *J AAPOS*. (2006) 10:107–11. doi: 10.1016/j.jaapos.2005.11.019
16. Yonekawa Y, Thomas BJ, Thanos A, Todorich B, Drenser KA, Trese MT, et al. The cutting edge of retinopathy of prematurity care: expanding the boundaries of diagnosis and treatment. *Retina*. (2017) 37:2208–25. doi: 10.1097/IAE.0000000000001719
17. Scruggs BA, Chan RVP, Kalpathy-Cramer J, Chiang MF, Campbell JP. Artificial intelligence in retinopathy of prematurity diagnosis. *Transl Vis Sci Technol*. (2020) 9:5. doi: 10.1167/tvst.9.2.5
18. Patel TP, Aaberg MT, Paulus YM, Lieu P, Dedania VS, Qian CX, et al. Smartphone-based fundus photography for screening of plus-disease retinopathy of prematurity. *Graefes Arch Clin Exp Ophthalmol*. (2019) 257:2579–85. doi: 10.1007/s00417-019-04470-4
19. Chawla D, Deorari A. Retinopathy of prematurity prevention, screening and treatment programmes: progress in India. *Semin Perinatol*. (2019) 43:344–7. doi: 10.1053/j.semperi.2019.05.006
20. Yu TY, Donovan T, Armfield N, Gole GA. Retinopathy of prematurity: the high cost of screening regional and remote infants. *Clin Exp Ophthalmol*. (2018) 46:645–51. doi: 10.1111/ceo.13160
21. Quinn GE, Vinekar A. The role of retinal photography and telemedicine in ROP screening. *Semin Perinatol*. (2019) 43:367–74. doi: 10.1053/j.semperi.2019.05.010
22. Mgharbil E, Raffa LH, Alessa S, Alamri A. Screening premature infants for retinopathy of prematurity in a tertiary hospital in Saudi Arabia. *Ann Saudi Med*. (2020) 40:87–93. doi: 10.5144/0256-4947.2020.87
23. Califf RM. Biomarker definitions and their applications. *Exp Biol Med*. (2018) 243:213–21. doi: 10.1177/1535370217750088
24. Pitkänen A, Ekolle Ndode-Ekane X, Lapinlampi N, Puhakka N. Epilepsy biomarkers - toward etiology and pathology specificity. *Neurobiol Dis*. (2019) 123:42–58. doi: 10.1016/j.nbd.2018.05.007
25. Best MG, Wesseling P, Wurdinger T. Tumor-educated platelets as a noninvasive biomarker source for cancer detection and progression monitoring. *Cancer Res*. (2018) 78:3407–12. doi: 10.1158/0008-5472.CAN-18-0887
26. Dieci MV, Miglietta F, Griguolo G, Guarneri V. Biomarkers for HER2-positive metastatic breast cancer: beyond hormone receptors. *Cancer Treat Rev*. (2020) 88:102064. doi: 10.1016/j.ctrv.2020.102064
27. Loibl S, Gianni L. HER2-positive breast cancer. *Lancet*. (2017) 389:2415–29. doi: 10.1016/S0140-6736(16)32417-5
28. Sigismund S, Avanzato D, Lanzetti L. Emerging functions of the EGFR in cancer. *Mol Oncol*. (2018) 12:3–20. doi: 10.1002/1878-0261.12155
29. Hastings K, Yu HA, Wei W, Sanchez-Vega F, DeVeaux M, Choi J, et al. EGFR mutation subtypes and response to immune checkpoint blockade treatment in non-small-cell lung cancer. *Ann Oncol*. (2019) 30:1311–20. doi: 10.1093/annonc/mdz141
30. Thoman ME, McKarns SC. Metabolomic profiling in neuromyelitis optica spectrum disorder biomarker discovery. *Metabolites*. (2020) 10:374. doi: 10.3390/metabo10090374
31. Schmidt-Erfurth U, Waldstein SM, Klimscha S, Sadeghipour A, Hu X, Gerendas BS, et al. Prediction of individual disease conversion in early amd using artificial intelligence. *Invest Ophthalmol Vis Sci*. (2018) 59:3199–208. doi: 10.1167/iovs.18-24106
32. Waldstein SM, Vogl WD, Bogunovic H, Sadeghipour A, Riedl S, Schmidt-Erfurth U. Characterization of drusen and hyperreflective foci as biomarkers for disease progression in age-related macular degeneration using artificial intelligence in optical coherence tomography. *JAMA Ophthalmol*. (2020) 138:740–7. doi: 10.1001/jamaophthalmol.2020.1376
33. Pichi F, Aggarwal K, Neri P, Salvetti P, Lembo A, Nucci P, et al. Choroidal biomarkers. *Indian J Ophthalmol*. (2018) 66:1716–26. doi: 10.4103/ijo.IJO_893_18
34. Ritter M, Simader C, Bolz M, Deák GG, Mayr-Sponer U, Sayegh R, et al. Intraretinal cysts are the most relevant prognostic biomarker in neovascular age-related macular degeneration independent of the therapeutic strategy. *Br J Ophthalmol*. (2014) 98:1629–35. doi: 10.1136/bjophthalmol-2014-305186
35. Tomita Y, Usui-Ouchi A, Nilsson AK, Yang J, Ko M, Hellström A, et al. Metabolism in retinopathy of prematurity. *Life*. (2021) 11:1119. doi: 10.3390/life11111119
36. Rinschen MM, Ivanisevic J, Giera M, Siuzdak G. Identification of bioactive metabolites using activity metabolomics. *Nat Rev Mol Cell Biol*. (2019) 20:353–67. doi: 10.1038/s41580-019-0108-4
37. Yang Y, Wu Z, Li S, Yang M, Xiao X, Lian C, et al. targeted blood metabolomic study on retinopathy of prematurity. *Invest Ophthalmol Vis Sci*. (2020) 61:12. doi: 10.1167/iovs.61.2.12
38. Zhou Y, Xu Y, Zhang X, Zhao P, Gong X, He M, et al. Plasma metabolites in treatment-requiring retinopathy of prematurity: potential biomarkers identified by metabolomics. *Exp Eye Res*. (2020) 199:108198. doi: 10.1016/j.exer.2020.108198
39. Zhou Y, Xu Y, Zhang X, Huang Q, Tan W, Yang Y, et al. Plasma levels of amino acids and derivatives in retinopathy of prematurity. *Int J Med Sci*. (2021) 18:3581–7. doi: 10.7150/ijms.63603
40. Connor KM, Krah NM, Dennison RJ, Aderman CM, Chen J, Guerin KI, et al. Quantification of oxygen-induced retinopathy in the mouse: a model of vessel loss, vessel regrowth and pathological angiogenesis. *Nat Protoc*. (2009) 4:1565–73. doi: 10.1038/nprot.2009.187
41. Vähätupa M, Järvinen TAH, Uusitalo-Järvinen H. Exploration of oxygen-induced retinopathy model to discover new therapeutic drug targets in retinopathies. *Front Pharmacol*. (2020) 11:873. doi: 10.3389/fphar.2020.00873
42. Lu F, Liu Y, Guo Y, Gao Y, Piao Y, Tan S, et al. Metabolomic changes of blood plasma associated with two phases of rat OIR. *Exp Eye Res*. (2020) 190:107855. doi: 10.1016/j.exer.2019.107855
43. Nilsson AK, Andersson MX, Sjöbom U, Hellgren G, Lundgren P, Pivodic A, et al. Sphingolipidomics of serum in extremely preterm infants: association between low sphingosine-1-phosphate levels and severe retinopathy of prematurity. *Biochim Biophys Acta Mol Cell Biol Lipids*. (2021) 1866:158939. doi: 10.1016/j.bbalip.2021.158939
44. Löfqvist CA, Najm S, Hellgren G, Engström E, Sävman K, Nilsson AK, et al. Association of retinopathy of prematurity with low levels of arachidonic acid: a secondary analysis of a randomized clinical trial. *JAMA Ophthalmol*. (2018) 136:271–7. doi: 10.1001/jamaophthalmol.2017.6658

45. Park YJ, Woo SJ, Kim YM, Hong S, Lee YE, Park KH. Immune and inflammatory proteins in cord blood as predictive biomarkers of retinopathy of prematurity in preterm infants. *Invest Ophthalmol Vis Sci.* (2019) 60:3813–20. doi: 10.1167/iovs.19-27258
46. Woo SJ, Park JY, Hong S, Kim YM, Park YH, Lee YE, et al. Inflammatory and angiogenic mediators in amniotic fluid are associated with the development of retinopathy of prematurity in preterm infants. *Invest Ophthalmol Vis Sci.* (2020) 61:42. doi: 10.1167/iovs.61.5.42
47. Yu H, Yuan L, Zou Y, Peng L, Wang Y, Li T, et al. Serum concentrations of cytokines in infants with retinopathy of prematurity. *Apmis.* (2014) 122:818–23. doi: 10.1111/apm.12223
48. Holm M, Morken TS, Fichorova RN, VanderVeen DK, Allred EN, Dammann O, et al. Systemic inflammation-associated proteins and retinopathy of prematurity in infants born before the 28th week of gestation. *Invest Ophthalmol Vis Sci.* (2017) 58:6419–28. doi: 10.1167/iovs.17-21931
49. Sood BG, Madan A, Saha S, Schendel D, Thorsen P, Skogstrand K, et al. Perinatal systemic inflammatory response syndrome and retinopathy of prematurity. *Pediatr Res.* (2010) 67:394–400. doi: 10.1203/PDR.0b013e3181d01a36
50. Yang X, Ze B, Dai Y, Zhu L, Chen C. The alteration and significance of erythropoietin serum levels in preterm infants with retinopathy of prematurity. *Am J Perinatol.* (2017) 34:1020–5. doi: 10.1055/s-0037-1601486
51. Rathi S, Jalali S, Patnaik S, Shahulhameed S, Musada GR, Balakrishnan D, et al. Abnormal complement activation and inflammation in the pathogenesis of retinopathy of prematurity. *Front Immunol.* (2017) 8:1868. doi: 10.3389/fimmu.2017.01868
52. Cakir U, Tayman C, Yucel C, Ozdemir O. Can IL-33 and endocan be new markers for retinopathy of prematurity? *Comb Chem High Throughput Screen.* (2019) 22:41–8. doi: 10.2174/1386207322666190325120244
53. Lyu J, Zhang Q, Jin H, Xu Y, Chen C, Ji X, et al. Aqueous cytokine levels associated with severity of type 1 retinopathy of prematurity and treatment response to ranibizumab. *Graefes Arch Clin Exp Ophthalmol.* (2018) 256:1469–77. doi: 10.1007/s00417-018-4034-5
54. Hellgren G, Willett K, Engstrom E, Thorsen P, Hougaard DM, Jacobsson B, et al. Proliferative retinopathy is associated with impaired increase in BDNF and RANTES expression levels after preterm birth. *Neonatology.* (2010) 98:409–18. doi: 10.1159/000317779
55. Hellgren G, Löfqvist C, Hansen-Pupp I, Gram M, Smith LE, Ley D, et al. Increased postnatal concentrations of pro-inflammatory cytokines are associated with reduced IGF-I levels and retinopathy of prematurity. *Growth Horm IGF Res.* (2018) 39:19–24. doi: 10.1016/j.ghir.2017.11.006
56. Jensen AK, Ying GS, Huang J, Quinn GE, Binenbaum G. Postnatal serum insulin-like growth factor I and retinopathy of. prematurity. *Retina.* (2017) 37:867–72. doi: 10.1097/IAE.0000000000001247
57. Pérez-Muñuzuri A, Fernández-Lorenzo JR, Couce-Pico ML, Blanco-Teijeiro MJ, Fraga-Bermúdez JM. Serum levels of IGF1 are a useful predictor of retinopathy of prematurity. *Acta Paediatr.* (2010) 99:519–25. doi: 10.1111/j.1651-2227.2009.01677.x
58. Hellström A, Engström E, Hård AL, Albertsson-Wikland K, Carlsson B, Niklasson A, et al. Postnatal serum insulin-like growth factor I deficiency is associated with retinopathy of prematurity and other complications of premature birth. *Pediatrics.* (2003) 112:1016–20. doi: 10.1542/peds.112.5.1016
59. Hellstrom A, Perruzzi C, Ju M, Engstrom E, Hard AL, Liu JL, et al. Low IGF-I suppresses VEGF-survival signaling in retinal endothelial cells: direct correlation with clinical retinopathy of prematurity. *Proc Natl Acad Sci U S A.* (2001) 98:5804–8. doi: 10.1073/pnas.101113998
60. Cekmez F, Canpolat FE, Çetinkaya M, Pirgon O, Aydinoz S, Ceylan OM, et al. IGF-I and visfatin levels in retinopathy of prematurity. *J Pediatr Ophthalmol Strabismus.* (2012) 49:120–4. doi: 10.3928/01913913-20110531-01
61. Yenice O, Cerman E, Ashour A, Firat R, Haklar G, Sirikci O, et al. Serum erythropoietin, insulin-like growth factor 1, and vascular endothelial growth factor in etiopathogenesis of retinopathy of prematurity. *Ophthalmic Surg Lasers Imaging Retina.* (2013) 44:549–54. doi: 10.3928/23258160-20131105-05
62. Sonmez K, Drenser KA, Capone A, Trese MT. Vitreous levels of stromal cell-derived factor 1 and vascular endothelial growth factor in patients with retinopathy of prematurity. *Ophthalmology.* (2008) 115:1065–70. doi: 10.1016/j.ophtha.2007.08.050
63. Vinekar A, Nair AP, Sinha S, Vaidya T, Chakrabarty K, Shetty R, et al. Tear fluid angiogenic factors: potential noninvasive biomarkers for retinopathy of prematurity screening in preterm infants. *Invest Ophthalmol Vis Sci.* (2021) 62:2. doi: 10.1167/iovs.62.3.2
64. Woo SJ, Park KH, Lee SY, Ahn SJ, Ahn J, Park KH, et al. The relationship between cord blood cytokine levels and perinatal factors and retinopathy of prematurity: a gestational age-matched case-control study. *Invest Ophthalmol Vis Sci.* (2013) 54:3434–9. doi: 10.1167/iovs.13-11837
65. Kurtul BE, Kabatas EU, Zenciroglu A, Ozer PA, Ertugrul GT, Beken S, et al. Serum neutrophil-to-lymphocyte ratio in retinopathy of prematurity. *J AAPOS.* (2015) 19:327–31. doi: 10.1016/j.jaapos.2015.04.008
66. Liu Y, Liu X, Lin C, Jia X, Zhu H, Song J, et al. Non-coding RNAs regulate alternative splicing in cancer. *J Exp Clin Cancer Res.* (2021) 40:11. doi: 10.1186/s13046-020-01798-2
67. Mattick JS, Makunin IV. Non-coding RNA. *Hum Mol Genet.* (2006) 15:R17–29. doi: 10.1093/hmg/ddl046
68. Matsui M, Corey DR. Non-coding RNAs as drug targets. *Nat Rev Drug Discov.* (2017) 16:167–79. doi: 10.1038/nrd.2016.117
69. Panni S, Lovering RC, Porras P, Orchard S. Non-coding RNA regulatory networks. *Biochim Biophys Acta Gene Regul Mech.* (2020) 1863:194417. doi: 10.1016/j.bbagrm.2019.194417
70. Filardi T, Catanzaro G, Mardente S, Zicari A, Santangelo C, Lenzi A, et al. Non-coding RNA: role in gestational diabetes pathophysiology and complications. *Int J Mol Sci.* (2020) 21:4020. doi: 10.3390/ijms21114020
71. Jeck WR, Sharpless NE. Detecting and characterizing circular RNAs. *Nat Biotechnol.* (2014) 32:453–61. doi: 10.1038/nbt.2890
72. Memczak S, Jens M, Elefsinioti A, Torti F, Krueger J, Rybak A, et al. Circular RNAs are a large class of animal RNAs with regulatory potency. *Nature.* (2013) 495:333–8. doi: 10.1038/nature11928
73. Zhou WY, Cai ZR, Liu J, Wang DS, Ju HQ, Xu RH. Circular RNA: metabolism, functions and interactions with proteins. *Mol Cancer.* (2020) 19:172. doi: 10.1186/s12943-020-01286-3
74. Lei B, Tian Z, Fan W, Ni B. Circular RNA: a novel biomarker and therapeutic target for human cancers. *Int J Med Sci.* (2019) 16:292–301. doi: 10.7150/ijms.28047
75. Zhang C, Hu J, Yu Y. CircRNA is a rising star in researches of ocular diseases. *Front Cell Dev Biol.* (2020) 8:850. doi: 10.3389/fcell.2020.00850
76. Liu C, Yao MD, Li CP, Shan K, Yang H, Wang JJ, et al. Silencing of circular RNA-ZNF609 ameliorates vascular endothelial dysfunction. *Theranostics.* (2017) 7:2863–77. doi: 10.7150/thno.19353
77. Chen L, Heikkinen L, Wang C, Yang Y, Sun H, Wong G. Trends in the development of miRNA bioinformatics tools. *Brief Bioinform.* (2019) 20:1836–52. doi: 10.1093/bib/bby054
78. Chen XK, Ouyang LJ, Yin ZQ, Xia YY, Chen XR, Shi H, et al. Effects of microRNA-29a on retinopathy of prematurity by targeting AGT in a mouse model. *Am J Transl Res.* (2017) 9:791–801.
79. Fan YY, Liu CH, Wu AL, Chen HC, Hsueh YJ, Chen KJ, et al. MicroRNA-126 inhibits pathological retinal neovascularization via suppressing vascular endothelial growth factor expression in a rat model of retinopathy of prematurity. *Eur J Pharmacol.* (2021) 900:174035. doi: 10.1016/j.ejphar.2021.174035
80. Metin T, Dinç E, Görür A, Erdogan S, Ertekin S, Sari AA, et al. Evaluation of the plasma microRNA levels in stage 3 premature retinopathy with plus disease: preliminary study. *Eye.* (2018) 32:415–20. doi: 10.1038/eye.2017.193
81. Zhao R, Qian L, Jiang L. Identification of retinopathy of prematurity related miRNAs in hyperoxia-induced neonatal rats by deep sequencing. *Int J Mol Sci.* (2014) 16:840–56. doi: 10.3390/ijms16010840
82. Cao M, Zhang L, Wang JH, Zeng H, Peng Y, Zou J, et al. Identifying circRNA-associated-ceRNA networks in retinal neovascularization in mice. *Int J Med Sci.* (2019) 16:1356–65. doi: 10.7150/ijms.35149
83. Peng Y, Zou J, Wang JH, Zeng H, Tan W, Yoshida S, et al. Small RNA sequencing reveals transfer RNA-derived small RNA expression profiles in retinal neovascularization. *Int J Med Sci.* (2020) 17:1713–22. doi: 10.7150/ijms.46209

84. Graziosi A, Perrotta M, Russo D, Gasparroni G, D'Egidio C, Marinelli B, et al. Oxidative stress markers and the retinopathy of prematurity. *J Clin Med.* (2020) 9:2711. doi: 10.3390/jcm9092711
85. Stone WL, Shah D, Hollinger SM. Retinopathy of prematurity: an oxidative stress neonatal disease. *Front Biosci.* (2016) 21:165–77. doi: 10.2741/4382
86. Oziebło-Kupczyk M, Bakunowicz-Lazarczyk A, Dzienis K, Skrzydlewska E, Szczepański M, Waszkiewiczz E. [The estimation of selected parameters in antioxidant system in red blood cells in ROP screening of premature infants]. *Klin Oczna.* (2006) 108:413–5.
87. Tsukahara H, Jiang MZ, Ohta N, Sato S, Tamura S, Hiraoka M, et al. Oxidative stress in neonates: evaluation using specific biomarkers. *Life Sci.* (2004) 75:933–8. doi: 10.1016/j.lfs.2004.01.025
88. Ates O, Alp HH, Caner I, Yildirim A, Tastekin A, Kocer I, et al. Oxidative DNA damage in retinopathy of prematurity. *Eur J Ophthalmol.* (2009) 19:80–5. doi: 10.1177/112067210901900112
89. Agrawal G, Dutta S, Prasad R, Dogra MR. Fetal oxidative stress, micronutrient deficiency and risk of retinopathy of prematurity: a nested case-control study. *Eur J Pediatr.* (2021) 180:1487–96. doi: 10.1007/s00431-020-03896-x
90. Banjac L, Banjac G, Kotur-Stevuljević J, Spasojević-Kalimanovska V, Gojković T, Bogavac-Stanojević N, et al. Pro-oxidants and antioxidants in retinopathy of prematurity. *Acta Clin Croat.* (2018) 57:458–63. doi: 10.20471/acc.2018.57.03.08
91. Boskabadi H, Marefat M, Maamouri G, Abrishami M, Abrishami M, Shoeibi N, et al. Evaluation of pro-oxidant antioxidant balance in retinopathy of prematurity. *Eye.* (2021) 36:148-52. doi: 10.1038/s41433-021-01465-6
92. Jayasudha R, Kalyana Chakravarthy S, Sai Prashanthi G, Sharma S, Tyagi M, Shivaji S. Implicating dysbiosis of the gut fungal microbiome in uveitis, an inflammatory disease of the eye. *Invest Ophthalmol Vis Sci.* (2019) 60:1384–93. doi: 10.1167/iovs.18-26426
93. Horai R, Caspi RR. Microbiome and autoimmune uveitis. *Front Immunol.* (2019) 10:232. doi: 10.3389/fimmu.2019.00232
94. Rowan S, Jiang S, Korem T, Szymanski J, Chang ML, Szelog J, et al. Involvement of a gut-retina axis in protection against dietary glycemia-induced age-related macular degeneration. *Proc Natl Acad Sci U S A.* (2017) 114:E4472–e81. doi: 10.1073/pnas.1702302114
95. Rowan S, Taylor A. Gut microbiota modify risk for dietary glycemia-induced age-related macular degeneration. *Gut Microbes.* (2018) 9:452–7. doi: 10.1080/19490976.2018.1435247
96. Rinninella E, Mele MC, Merendino N, Cintoni M, Anselmi G, Caporossi A, et al. The role of diet, micronutrients and the gut microbiota in age-related macular degeneration: new perspectives from the gut?retina axis. *Nutrients.* (2018) 10:1677. doi: 10.3390/nu10111677
97. Nyangahu DD, Jaspan HB. Influence of maternal microbiota during pregnancy on infant immunity. *Clin Exp Immunol.* (2019) 198:47–56. doi: 10.1111/cei.13331
98. Westaway JAF, Huerlimann R, Kandasamy Y, Miller CM, Norton R, Staunton KM, et al. The bacterial gut microbiome of probiotic-treated very-preterm infants: changes from admission to discharge. *Pediatr Res.* (2021). doi: 10.1038/s41390-021-01888-7. [Epub ahead of print].
99. Mammas IN, Spandidos DA. Retinopathy of prematurity and neonatal gut microbiome: an interview with professor dimitra skondra, associate professor of ophthalmology and vitreoretinal surgeon at the university of chicago (USA). *Exp Ther Med.* (2020) 20:294. doi: 10.3892/etm.2020.9424
100. Skondra D, Rodriguez SH, Sharma A, Gilbert J, Andrews B, Claud EC. The early gut microbiome could protect against severe retinopathy of prematurity. *J aapos.* (2020) 24:236–8. doi: 10.1016/j.jaapos.2020.03.010
101. Chan-Ling T, Gole GA, Quinn GE, Adamson SJ, Darlow BA. Pathophysiology, screening and treatment of ROP: a multi-disciplinary perspective. *Prog Retin Eye Res.* (2018) 62:77–119. doi: 10.1016/j.preteyeres.2017.09.002
102. Lavric A, Tekavcic Pompe M, Markelj S, Ding J, Mahajan S, Khandelwal N, et al. Choroidal structural changes in preterm children with and without retinopathy of prematurity. *Acta Ophthalmol.* (2019). doi: 10.1111/aos.14324
103. Parrozzani R, Nacci EB, Bini S, Marchione G, Salvadori S, Nardo D, et al. Severe retinopathy of prematurity is associated with early post-natal low platelet count. *Sci Rep.* (2021) 11:891. doi: 10.1038/s41598-020-79535-0
104. Korkmaz L, Baştug O, Özdemir A, Korkut S, Karaca Ç, Akin MA, et al. Platelet mass index can be a reliable marker in predicting the prognosis of retinopathy of prematurity in very preterm infants. *Pediatr Neonatol.* (2018) 59:455–63. doi: 10.1016/j.pedneo.2017.11.001
105. Stutchfield CJ, Jain A, Odd D, Williams C, Markham R. Foetal haemoglobin, blood transfusion, and retinopathy of prematurity in very preterm infants: a pilot prospective cohort study. *Eye.* (2017) 31:1451–5. doi: 10.1038/eye.2017.76
106. Akyüz Ünsal A, Key Ö, Güler D, Kurt Omurlu I, Anik A, Demirci B, et al. Can complete blood count parameters predict retinopathy of prematurity? *Turk J Ophthalmol.* (2020) 50:87–93. doi: 10.4274/tjo.galenos.2019.45313
107. Dailey WA, Gryc W, Garg PG, Drenser KA. Frizzled-4 variations associated with retinopathy and intrauterine growth retardation: a potential marker for prematurity and retinopathy. *Ophthalmology.* (2015) 122:1917–23. doi: 10.1016/j.ophtha.2015.05.036
108. Movsas TZ, Muthusamy A. Feasibility of neonatal haemoglobin A1C as a biomarker for retinopathy of prematurity. *Biomarkers.* (2020) 25:468–73. doi: 10.1080/1354750X.2020.1783573
109. Pieh C, Krüger M, Lagrèze WA, Gimpel C, Buschbeck C, Zirrgiebel U, et al. Plasma sE-selectin in premature infants: a possible surrogate marker of retinopathy of prematurity. *Invest Ophthalmol Vis Sci.* (2010) 51:3709–13. doi: 10.1167/iovs.09-4723
110. Suk KK, Dunbar JA, Liu A, Daher NS, Leng CK, Leng JK, et al. Human recombinant erythropoietin and the incidence of retinopathy of prematurity: a multiple regression model. *J AAPOS.* (2008) 12:233–8. doi: 10.1016/j.jaapos.2007.08.009
111. Manzoni P, Memo L, Mostert M, Gallo E, Guardione R, Maestri A, et al. Use of erythropoietin is associated with threshold retinopathy of prematurity (ROP) in preterm ELBW neonates: a retrospective, cohort study from two large tertiary NICUs in Italy. *Early Hum Dev.* (2014) 90:S29–33. doi: 10.1016/S0378-3782(14)50009-6
112. Owen LA, Shirer K, Collazo SA, Szczotka K, Baker S, Wood B, et al. The serine protease HTRA-1 is a biomarker for ROP and mediates retinal neovascularization. *Front Mol Neurosci.* (2020) 13:605918. doi: 10.3389/fnmol.2020.605918
113. Tuten A, Dincer E, Topcuoglu S, Sancak S, Akar S, Hakyemez Toptan H, et al. Serum lactate levels and perfusion index: are these prognostic factors on mortality and morbidity in very low-birth weight infants? *J Matern Fetal Neonatal Med.* (2017) 30:1092–5. doi: 10.1080/14767058.2016.1205019
114. Movsas TZ, Paneth N, Gewolb IH, Lu Q, Cavey G, Muthusamy A. The postnatal presence of human chorionic gonadotropin in preterm infants and its potential inverse association with retinopathy of prematurity. *Pediatr Res.* (2020) 87:558–63. doi: 10.1038/s41390-019-0580-8
115. Czernik C, Metze B, Müller C, Müller B, Bührer C. Urinary N-terminal B-type natriuretic peptide predicts severe retinopathy of prematurity. *Pediatrics.* (2011) 128:e545–9. doi: 10.1542/peds.2011-0603
116. Bührer C, Erdeve Ö, van Kaam A, Berger A, Lechner E, Bar-Oz B, et al. N-terminal B-type natriuretic peptide urinary concentrations and retinopathy of prematurity. *Pediatr Res.* (2017) 82:958–63. doi: 10.1038/pr.2017.179
117. Berrington JE, Clarke P, Embleton ND, Ewer AK, Geethanath R, Gupta S, et al. Retinopathy of prematurity screening at ≥30 weeks: urinary NTpro-BNP performance. *Acta Paediatr.* (2018) 107:1722–5. doi: 10.1111/apa.14354
118. Markasz L, Olsson KW, Holmström G, Sindelar R. Cluster analysis of early postnatal biochemical markers may predict development of retinopathy of prematurity. *Transl Vis Sci Technol.* (2020) 9:14. doi: 10.1167/tvst.9.13.14
119. Gohari M, Dastgheib SA, Noorishadkam M, Lookzadeh MH, Mirjalili SR, Akbarian-Bafghi MJ, et al. Association of eNOS and ACE polymorphisms with retinopathy of prematurity: a systematic review and meta-analysis. *Fetal Pediatr Pathol.* (2020) 39:334–45. doi: 10.1080/15513815.2019.1652378
120. Matsumoto T, Saito Y, Itokawa T, Shiba T, Oba MS, Takahashi H, et al. Retinal VEGF levels correlate with ocular circulation measured by a laser speckle-micro system in an oxygen-induced retinopathy rat model. *Graefes Arch Clin Exp Ophthalmol.* (2017) 255:1981–90. doi: 10.1007/s00417-017-3756-0
121. Becker PS, Suck G, Nowakowska P, Ullrich E, Seifried E, Bader P, et al. Selection and expansion of natural killer cells for NK cell-based immunotherapy. *Cancer Immunol Immunother.* (2016) 65:477–84. doi: 10.1007/s00262-016-1792-y

122. Chanput W, Mes JJ, Wichers HJ. THP-1 cell line: an in vitro cell model for immune modulation approach. *Int Immunopharmacol.* (2014) 23:37–45. doi: 10.1016/j.intimp.2014.08.002
123. Beer L, Mildner M, Gyöngyösi M, Ankersmit HJ. Peripheral blood mononuclear cell secretome for tissue repair. *Apoptosis.* (2016) 21:1336–53. doi: 10.1007/s10495-016-1292-8
124. Xiao D, Ling KHJ, Custodio J, Majeed SR, Tarnowski T. Quantitation of intracellular triphosphate metabolites of antiretroviral agents in peripheral blood mononuclear cells (PBMCs) and corresponding cell count determinations: review of current methods and challenges. *Expert Opin Drug Metab Toxicol.* (2018) 14:781–802. doi: 10.1080/17425255.2018.1500552
125. Bagci S, Mueller A, Reinsberg J, Heep A, Bartmann P, Franz AR. Saliva as a valid alternative in monitoring melatonin concentrations in newborn infants. *Early Hum Dev.* (2009) 85:595–8. doi: 10.1016/j.earlhumdev.2009.06.003
126. Khamis MM, Adamko DJ, El-Aneed A. Mass spectrometric based approaches in urine metabolomics and biomarker discovery. *Mass Spectrom Rev.* (2017) 36:115–34. doi: 10.1002/mas.21455
127. Hartnett ME, Penn JS. Mechanisms and management of retinopathy of prematurity. *N Engl J Med.* (2012) 367:2515–26. doi: 10.1056/NEJMra1208129
128. Reich ES. Pre-term births on the rise. *Nature.* (2012) 485:20. doi: 10.1038/485020a
129. Brown JM, Campbell JP, Beers A, Chang K, Ostmo S, Chan RVP, et al. Automated diagnosis of plus disease in retinopathy of prematurity using deep convolutional neural networks. *JAMA Ophthalmol.* (2018) 136:803–10. doi: 10.1001/jamaophthalmol.2018.1934
130. Kaštelan S, Orešković I, Bišćan F, Kaštelan H, Gverović Antunica A. Inflammatory and angiogenic biomarkers in diabetic retinopathy. *Biochem Med (Zagreb).* (2020) 30:030502. doi: 10.11613/BM.2020.030502
131. Hosokawa K. Biomarker analysis on a power-free microfluidic chip driven by degassed poly(dimethylsiloxane). *Anal Sci.* (2021) 37:399–406. doi: 10.2116/analsci.20SCR04
132. Sobsey CA, Ibrahim S, Richard VR, Gaspar V, Mitsa G, Lacasse V, et al. Targeted and untargeted proteomics approaches in biomarker development. *Proteomics.* (2020) 20:e1900029. doi: 10.1002/pmic.201900029
133. Gohil SH, Iorgulescu JB, Braun DA, Keskin DB, Livak KJ. Applying high-dimensional single-cell technologies to the analysis of cancer immunotherapy. *Nat Rev Clin Oncol.* (2021) 18:244–56. doi: 10.1038/s41571-020-00449-x

Conflict of Interest: The authors declare that the research was conducted in the absence of any commercial or financial relationships that could be construed as a potential conflict of interest.

Publisher's Note: All claims expressed in this article are solely those of the authors and do not necessarily represent those of their affiliated organizations, or those of the publisher, the editors and the reviewers. Any product that may be evaluated in this article, or claim that may be made by its manufacturer, is not guaranteed or endorsed by the publisher.

frontiers in Medicine

ORIGINAL RESEARCH
published: 28 March 2022
doi: 10.3389/fmed.2022.838800

The Value of the Antibody Detection in the Diagnosis of Ocular Toxocariasis and the Aqueous Cytokine Profile Associated With the Condition

Xiang Zhang†, Yuan Yang†, Yan Zheng, Yiqian Hu, Yuqing Rao, Jiakai Li, Peiquan Zhao and Jing Li**

Department of Ophthalmology, Xinhua Hospital Affiliated to Shanghai Jiao Tong University School of Medicine, Shanghai, China

OPEN ACCESS

Edited by:
Alan G. Palestine, University of Colorado Anschutz Medical Campus, United States

Reviewed by:
Bahador Sarkari (Shahriari), Shiraz University of Medical Sciences, Iran
Funda Dikkaya, Istanbul Medipol University, Turkey
Chan Zhao, Peking Union Medical College Hospital (CAMS), China

***Correspondence:**
Jing Li
lijing@xinhuamed.com.cn
Peiquan Zhao
zhaopeiquan@xinhuamed.com.cn

†These authors have contributed equally to this work and share first authorship

Specialty section:
This article was submitted to Ophthalmology, a section of the journal Frontiers in Medicine

Received: *18 December 2021*
Accepted: *28 February 2022*
Published: *28 March 2022*

Citation:
Zhang X, Yang Y, Zheng Y, Hu Y, Rao Y, Li J, Zhao P and Li J (2022) The Value of the Antibody Detection in the Diagnosis of Ocular Toxocariasis and the Aqueous Cytokine Profile Associated With the Condition. Front. Med. 9:838800. doi: 10.3389/fmed.2022.838800

Introduction: To evaluate and compare the specificity of Toxocara *canis*-specific antibody detection in the serum and aqueous samples for the diagnosis of ocular toxocariasis (OT) and explore the cytokine profiles associated with the condition in children.

Materials and Methods: This is a prospective cohort study. The inclusion criteria were the clinical presentations of OT, which included unilateral vision reduction, typical peripheral or posterior pole granuloma with variable degrees of vitritis, and exclusion of other diagnoses. The titer of antibody against the excretory-secretory antigen of Toxocara *canis* [T-immunoglobulin G (IgG)] was measured in serum and aqueous samples that were taken from the affected eyes. The diagnosis of OT was made upon positive detection of T-IgG either in the serum or aqueous. The rest with typical clinical presentations as described above but a positive serum or aqueous T-IgG could not be confirmed were diagnosed as suspected OT. Cytokines were measured using multiplexed cytometric bead array system.

Results: Two hundred and eleven eyes of 211 patients had participated in the study. One hundred and twenty-eight eyes were diagnosed as OT. The median age of the cohort was 7.7 years with a male to female ratio of 2.5:1. Major initial symptoms were decreased vision (74%) and strabismus (22%). The percentages of eyes with peripheral granuloma, posterior granuloma, and endophthalmitis were 40, 18, and 41%, respectively. Vitritis (100%), vitreous strands (64%), retinal fibrotic bands (57%), and retinal detachment (42%) were the most common signs. T-IgG was positive in 66.7% of the aqueous and 57.2% of the serum samples. Forty-four patients were diagnosed T-IgG negative in both serum and aqueous of the affected eyes. Interleukin (IL)-6, monocyte chemoattractant protein (MCP)-1, IL-8, eosinophil chemotactic protein (Eotaxin), MCP-1β, and vascular endothelial growth factor (VEGF) were higher in T-IgG negative eyes when compared to controls and further increased in T-IgG positive eyes.

However, only T-IgG positive eyes showed increased IL-5, IL-13, and IL-10. IL-1β, tumor necrosis factor-alpha (TNF-α), IL-12, IL-2, interferon-gamma (IFN-γ), and IL-4 were undetectable in all eyes.

Conclusions: Pediatric OT is often present with severe retinal complications. Polarized intraocular Th2 response was only found in aqueous T-IgG positive eyes. Our results supported an aqueous sample-based antibody test for the more specific diagnosis of OT.

Keywords: ocular toxocariasis, diagnosis, aqueous humor, antibody detection, Th2 response, cytokines

INTRODUCTION

Ocular toxocariasis (OT) is a condition caused by the infection of roundworms, mainly *Toxocara canis*, less frequently by *Toxocara cati* and other helminth species in the eyes (1, 2). Humans become infected through unintentional ingestion of the infective eggs. The eggs hatch in the digestive tract, penetrate the intestine, and spread *via* circulation. The larva is not able to mature within the human body and instead encysts in tissues. Migrating, dying, or dead larva could stimulate eosinophilic responses in host tissues. Increased number of eosinophils, increased concentrations of total immunoglobulin E (IgE), and increased levels of interleukin (IL)-4, IL-6, IL-5, IL-10, IL-13, and interferon-gamma (IFN-γ) were reported in peripheral blood of patients with systemic signs of Toxocara infection (3, 4). However, there was a paucity of data on intraocular immunological responses associated with OT.

The human eye is one of the organs that the larva prefers to stay. However, the diagnosis of OT could be challenging due to the lack of pathognomonic signs. The main symptoms of OT include decreased vision, strabismus, and leukocoria. OT can manifest in three major types (5): 1. Peripheral granulomatous type, which is featured by a focal, increased, white nodule granuloma located at the peripheral retina. 2. Posterior granulomatous type, which is featured by granuloma at the posterior pole. 3. Chronic endophthalmitis type, which is featured by diffuse intraocular inflammation, often more severe in the vitreous cavity than in the anterior chamber. The granulomatous types appeared to be the dominant types of OT manifestation, often accounting for more than 70% of the affected eyes (6, 7). However, endophthalmitis type may be more frequently seen in children, as reported by an early study from Poland (8). Other clinical signs include vitreous bands, epiretinal membrane, fibrotic retinal bands, retinal folds, partial, or total retinal detachment. Posterior synechiae and signs of inflammation in the anterior chamber are less frequently seen (7). The antibodies against excretory-secretory proteins of *T. canis* [T-immunoglobulin G (T-IgG)] in serum or intraocular fluid are often measured to aid the diagnosis of OT (6). However, many studies have reported negative T-IgG in serum or aqueous samples taken from clinically diagnosed OT patients (7, 9–14). These patients were clinically undistinguishable from the T-IgG positive patients. Whether there were differences in the underlying immunological responses between T-IgG positive and negative eyes were unknown.

Due to the nature of the infection, Toxocara infection is more often seen in children than in adults. Toxocara seroprevalence ranged from 4 to 46% in adults and can be as high as 77.6% in school children (9, 15, 16). The reported seroprevalence among children in China varied from 5.14 to 19.3% (17–19). Data on the prevalence of OT were scarce, the reported prevalence varied from 1 case per 1,000 persons in the general population to 7 ophthalmologist-diagnosed OT cases in 100,000 school children (20, 21). OT is one of the main causes of uveitis and blindness in children. Since children are less likely to notice and report changes in vision acuity, the symptoms and clinical signs of pediatric OT could be more complicated than the adult version. In this prospective study, we characterized the clinical and immunological features of 211 consecutive pediatric cases seen in a tertiary ophthalmology clinic from June 2014 to June 2018. Their T-IgG was measured in both aqueous and serum samples and the association between intraocular cytokine responses and T-IgG status was explored.

MATERIALS AND METHODS

Patients and Ethical Statement

This is a prospective study carried out at the Department of Ophthalmology, Xinhua Hospital affiliated to Shanghai Jiao Tong University School of Medicine between June 2014 and June 2018. In total, 128 consecutive pediatric patients (1–18 years old) who were diagnosed with OT, and 83 pediatric patients who were presented with unilateral retinal granuloma or vitritis without explainable causes but a positive serum or aqueous T-IgG could not be confirmed were enrolled upon consent by their parent(s) or legal guardian(s). Twenty-five children with congenital cataracts but otherwise quiescent eyes who underwent cataract surgery at the same time period were recruited and their aqueous samples were used as controls for cytokine analysis as described below. The study protocol was approved by the Institutional Review Board of Xinhua Hospital and adhered to the tenets of the Declaration of Helsinki. All examinations and procedures were performed in accordance with the approved protocol. Informed written consent was obtained from the parents/guardians of the patients.

Patient Evaluation and the Diagnostic Criteria for OT

For all enrolled patients, the medical history and information about the patient's living environment and previous contact with animals, especially dogs, were obtained. The ophthalmic

examinations included vision acuity test, intraocular pressure measurement, slit-lamp examination, B-scan ultrasonography, and funduscopic examinations. Depending on the conditions of the eyes, ultrasound biomicroscopy (UBM) (SW-3200, Suoer, Tianjin, China), scanning laser ophthalmoscopy (Optomap 200Tx; Optos, Inc., Marlborough, MA, USA), optical coherence tomography (RTVue XR AVANTI with AngioVue; Optovue Inc., Fremont, CA, USA), and fundus fluorescein angiography (HRA2; Heidelberg Engineering GmbH, Heidelberg, Germany) were also performed. For children < 3-year old, RetCam imaging (RetCam-120 digital retinal camera; Clarity Medical Systems, Pleasanton, CA, USA) was performed.

Ocular toxocariasis was diagnosed by the same senior retina specialist based on the following criteria: 1. Unilateral vision reduction, strabismus, leukocoria, red or painful eye, or photophobia. 2. The existence of peripheral or posterior pole granuloma with variable degrees of vitritis or moderate to severe vitritis with vitreous strands, or layered vitreous veil or retinal fibrosis. 3. Positive serum or aqueous T-IgG (see next section for details). The severity of vitritis was graded as mild, moderate, and severe based on vitreous haze according to the grading system proposed by the National Eye Institute and agreed by two doctors (22). The suspected cases were those with typical clinical presentations, such as OT, as described above but a positive serum or aqueous T-IgG could not be confirmed.

For all patients, the following conditions were excluded: retinoblastoma, toxoplasmic retinochoroiditis, retinopathy of prematurity (ROP), familial exudative vitreoretinopathy (FEVR), persistent fetal vasculature, Coats' disease, ocular tuberculosis, syphilis, retinitis, and organized vitreous hemorrhage.

T-IgG and Total IgG Measurement and the Calculation of Goldmann-Witmer Co-efficient

Aqueous samples were taken under sterile conditions using a 30-gauge needle on a tuberculin syringe *via* an anterior chamber paracentesis as previously described (23). T-IgG was measured using a qualitative ELISA kit (*Toxocara canis* IgG ELISA, IBL International, Hamburg, Germany). The specificity and sensitivity were both above 95%. Serum and aqueous samples were 100 times diluted and analyzed in duplicates. The titer of the antibody was calculated as follows: (absorbance of sample × 10)/absorbance of cutoff control. According to the manufacturer's instructions, a serum sample with a titer of < 9 units was determined as negative, higher than 11 was positive, between 9 and 11 was uncertain. Since the manufacturer did not provide a cutoff value for aqueous samples, we measured T-IgG in 25 aqueous samples that were taken from patients with no clinical signs of OT or uveitis in general. The mean titer was 0.880, with a range between 0.000 and 2.953 and a standard deviation (SD) of 0.677. Based on these values, we set a cutoff value of 2.234 (mean + 2 SD) for aqueous samples.

To calculate GWC, total IgG levels in serum and aqueous samples were quantitated using an ELISA kit (Abnova, KA3976). Serum and aqueous samples were 5,000 and 50 times diluted, respectively, and analyzed in duplicates. GWC was calculated as follows: (T-IgG/total IgG) aqueous/(T-IgG/total IgG) serum.

Cytokine Analysis

Bio-Plex Pro^{TM} magnetic color-bead-based multiplex assay (Bio-Rad Laboratories, Inc., Hercules, CA, USA) was used to measure the concentrations of the following human cytokines: IL-1β, IL-2, IL-4, IL-5, IL-6, IL-8, IL-10, IL-12(p70), IL-13, IL-17, IFN-γ, tumor necrosis factor-alpha (TNF-α), monocyte chemoattractant protein (MCP-1, CCL2), macrophage inflammatory protein-1α (MIP-1α, CCL3), macrophage inflammatory protein-1β (MIP-1β, CCL4), regulated on activation normal T cell expressed and secreted (RANTES, CCL5), eosinophil chemotactic protein (Eotaxin, CCL11), granulocyte-colony stimulating factor (GCSF), and vascular endothelial growth factor (VEGF). The assay was performed according to the manufacturer's instructions and analyzed using Bio-Plex^{TM} 200 System (software version 6.0). Fifty microliters (50 μl) of aqueous humor sample were used in each reaction. All concentrations that were determined as <out of range (OOR) by the software were arbitrarily determined as 0 for data analysis.

Statistical Analysis

Statistical analysis was conducted using Statistical Package for the Social Sciences (SPSS) Version 19 (IBM Corporation, Armonk, NY, USA). We used the unpaired *t*-test or the Mann-Whitney U test to compare the differences in cytokines between 2 groups, depending on the distribution of data. A significance value of or < 0.05 was accepted as statistically significant.

RESULTS

Demographic Information of Patients Involved in the Study

Two hundred and eleven consecutive pediatric patients with typical clinical presentation of OT were enrolled. One hundred and twenty-eight were diagnosed with OT since their serum or aqueous was T-IgG positive. The rest were diagnosed as suspected OT. Among those, 44 were confirmed both serum and aqueous T-IgG negative.

The demographic information of all 211 patients is summarized in **Table 1**. The male to female ratio was 2.5:1. The median age of patients at the time of diagnosis was 7.68 years. There was no significant difference in age between male and female patients. About 46.4% of the patients had lived in the rural areas (villages), 20.4% lived in a town or city, 33.2% had lived in both village and town areas before the onset of the symptoms. Most of the patients had gone to other ophthalmology clinics before coming to us. About 74.4% of the patients had initial signs of reduced vision, 22.3% had strabismus, 7.1% had leukocoria. The median time from the notice of the symptoms to the diagnosis of OT was 2 months, with a range of 3 days to 6 years.

Ophthalmic Findings

The entire cohort was separated into three conventional groups based on clinical presentations, and the major ophthalmic

TABLE 1 | Demographic information and initial symptoms.

No. of patients	211
Gender (No. of patients, % in the cohort)	
Male	151 (70.9%)
Female	60 (28.2%)
Age (Median and range, in years)	7.7 (1–18)
Time till diagnosis (Median and IQR, in days)	60 (3->3 yrs)
Living environment (No. of patients, % in the cohort)	
Town or city	43 (20.4%)
Rural area	98 (46.4%)
Mixed	70 (33.2%)
History of dog contact (No. of patients, % in the cohort)	
Yes	158 (74.9%)
No	46 (21.8%)
Initial symptoms (No. of patients, % in the cohort)	
Decreased vision	157 (74.4%)
Strabismus	47 (22.3%)
Leukocoria	15 (7.1%)
Red eye	8 (3.8%)
Pain	3 (1.4%)
Photophobia	2 (1.0%)

findings are summarized in **Table 2**. Four eyes from 4 patients had both peripheral and posterior granulomas. They were not included because we were not sure which group they belong to. Therefore, 207 eyes from the original 211 patients were further analyzed. In total, 86 eyes (41.5%) were of the endophthalmitis type, 38 eyes (18.4%) and 83 eyes (40.1%) were of the posterior and peripheral granuloma types, respectively. Typical clinical presentations of the affected eyes are shown in **Figure 1**.

There were significant differences in the severity of vitritis among three types (Kruskal-Wallis analysis, $p < 0.001$). Severe vitritis was most frequently found in the endophthalmitis type (57%). There were 12 endophthalmitis-type eyes with mild vitritis; however, they all had either vitreous bands or retinal fibrosis without other explainable causes. The endophthalmitis type also had a higher percentage of posterior synechiae (18.6%) than other types. The occurrence of anterior keratic precipitates (KP) and band keratopathy was similar among the three groups.

Fibrotic changes of the vitreous and retina were common. Vitreous strands were found in 71.1, 47.4, and 62.8% of the peripheral granuloma, posterior granuloma, and endophthalmitis types, respectively. Retinal fibrotic changes were found in 67.5, 84.2, and 33.7% of the peripheral granuloma, posterior granuloma, and endophthalmitis types, respectively. The posterior granuloma type had the highest percentage of eyes with optic disc involvement (47.4%) and the epiretinal membrane (26.3%).

Within the entire cohort, about 42% of eyes had varying degrees of retinal detachment. In the granulomatous types, the partial detachment was more frequently seen than complete detachment. However, in the endophthalmitis type, 48.8% of eyes had retinal detachment and 83.3% of those had complete detachment.

Other less frequently seen clinical signs included cataracts, which occurred in < 10% of eyes. Since most patients were too young to cooperate with UBM examinations, cyclitic membrane was found in about 2% of eyes during vitrectomy.

Aqueous and Serum T-IgG

One hundred and eighty aqueous and 207 serum samples, including 172 aqueous and serum pairs were tested for T-IgG. The results are shown in **Table 3**. The grouping of all participated patients according to their clinical features and aqueous and serum T-IgG status are shown in **Figure 2**. Six blood samples were not measured because of hemolysis. The results of the 5 samples were not conclusive since the T-IgG values fell into the gray area as defined by the kit. GWC was calculated in all aqueous T-IgG positive samples. The lowest GWC was 6, suggesting the intraocular origin of the antibody.

Overall, 66.7% of the aqueous in this cohort was T-IgG positive. When separated by groups, 78.6, 48.6, and 66.2% of the peripheral granulomatous, posterior granuloma, and endophthalmitis OT eyes were positive, respectively. About 70, 28.8, and 52.4% of the patients were serum T-IgG positive.

In 42 patients (24.4% of all measured pairs), the T-IgG status of the serum and the aqueous of the affected eye were not consistent. There were 28 patients who were aqueous T-IgG positive but serum T-IgG negative and 14 patients who were aqueous T-IgG negative but serum T-IgG positive. To explore the agreement between the aqueous and serum T-IgG, when separated by groups, the kappa values of peripheral granulomatous, posterior granuloma, and endophthalmitis OT eyes were 0.454, 0.311, and 0.533, respectively.

There were 44 patients who were T-IgG negative in both serum and the aqueous samples, suggesting the absence of OT. Their collective clinical features are summarized in **Table 4**. The posterior granuloma group had the highest percentage of double-negative eyes, followed by the endophthalmitis group and peripheral granuloma group. Overall, the clinical presentations of the double-negative eyes were very similar to those of the entire group. In eyes with peripheral granuloma, the double-negatives had a higher percentage of mild vitritis and a lower percentage of vitreous strands and vitreous veil. In eyes with endophthalmitis, the double-negative had a higher percentage of vitreous strands and vitreous veil.

Aqueous Cytokine Profiles

The concentrations of 19 cytokines were measured in 75 aqueous samples taken from patients who had discontinued both topical and systemic treatments for at least 5 days prior to the sampling. During the initial analysis, we separated samples into 4 groups: Group 1, T-IgG negative in both aqueous and serum; Group 2, aqueous negative but serum positive; Group 3, aqueous positive but serum negative; and Group 4, aqueous and serum both positive. We found no significant differences in cytokines between Groups 1 and 2 or between Groups 3 and 4, indicating that T-IgG seropositivity had little effect on aqueous cytokine responses. Therefore, we grouped samples by aqueous T-IgG only: the aqueous T-IgG negative (Aq^-, 35 samples) and positive (Aq^+, 40 samples) groups (**Table 5**). We used 25 aqueous samples

TABLE 2 | Clinical features.

Variables	No. of eyes (% in the group)			
	Peripheral granuloma	Posterior granuloma	Endophthal-mitis	Overall
No. of eyes	83 (40.1%)	38 (18.4%)	86 (41.5%)	207 (100%)
Vitritis				
Severe	26 (31.3%)	6 (15.8%)	49 (57.0%)	82 (38.9%)
Moderate	26 (31.3%)	11 (28.9%)	25 (29.1%)	63 (30.0%)
Mild	31 (37.3%)	21 (55.3%)	12 (14.0%)	66 (31.3%)
Vitreous strands	59 (71.1%)	18 (47.4%)	54 (62.8%)	134 (63.5%)
Vitreous veil	7 (8.4%)	0	9 (10.5%)	17 (8.1%)
Retinal fibrotic band	56 (67.5%)	32 (84.2%)	29 (33.7%)	120 (56.9%)
Dragged disc	29 (34.9%)	18 (47.4%)	10 (11.6%)	58 (27.5%)
Epiretinal membrane	8 (9.6%)	10 (26.3%)	9 (10.5%)	29 (13.7%)
Retinal detachment				
Partial	24 (28.9%)	7 (18.4%)	7 (8.1%)	39 (18.5%)
Total	13 (15.7%)	3 (7.9%)	35 (40.7%)	50 (23.7%)
Cyclitic membrane	2 (2.4%)	0	2 (2.3%)	4 (1.9%)
Posterior synechiae	7 (8.4%)	2 (5.3%)	16 (18.6%)	25 (11.8%)
Cataract	8 (9.6%)	0	8 (9.3%)	16 (7.6%)
Anterior KP	10 (12.0%)	4 (10.5%)	10 (11.6%)	25 (11.8%)
Band keratopathy	8 (9.6%)	1 (2.6%)	8 (9.3%)	17 (8.1%)

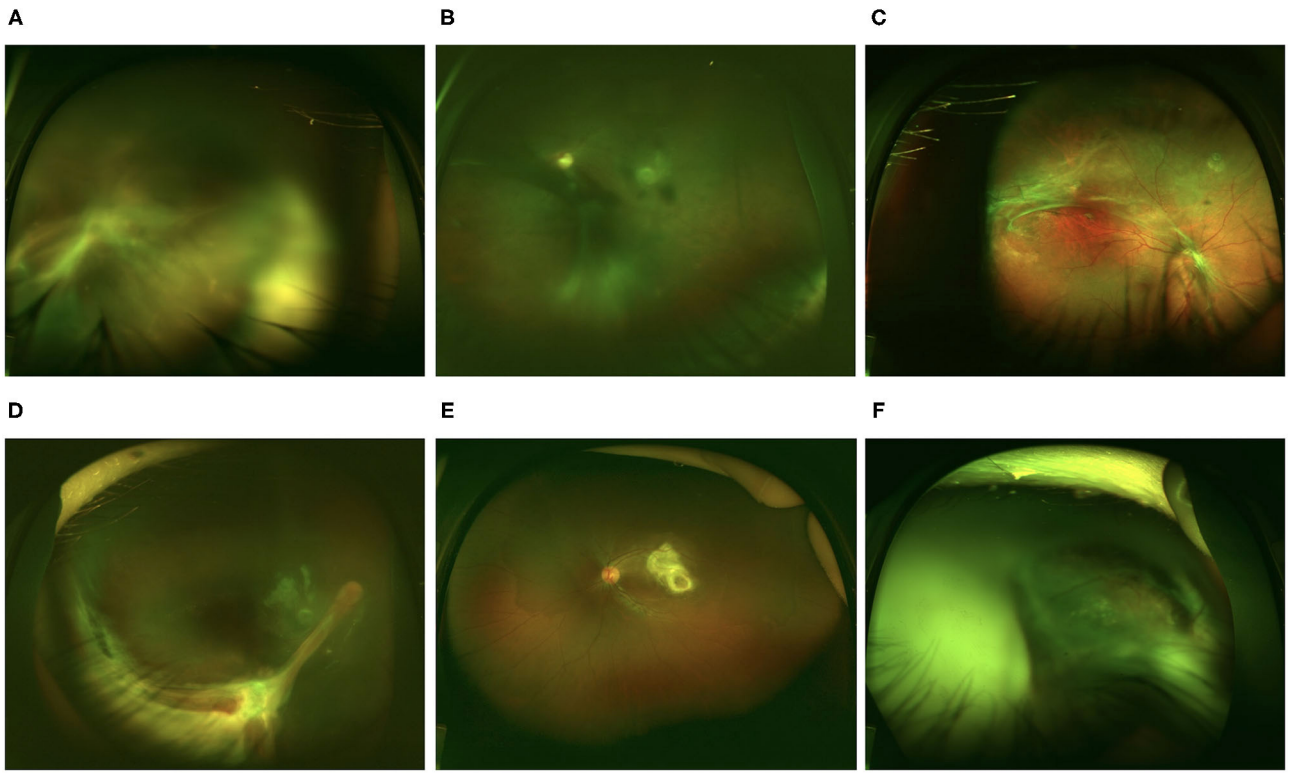

FIGURE 1 | Representative retinal images of eyes with ocular toxocariasis (OT). **(A–C)** Endophthalmitis type OT. **(A)** Diffusive vitritis with vitreous strands extending to the retina. **(B)** Diffusive vitritis with vitreous membrane. **(C)** Fibrotic membrane at the retina surface with relatively clear vitreous. **(D)** Peripheral granuloma with retinal fold extending to the optic disc. **(E)** Posterior pole granuloma. **(F)** Total retinal detachment with vitritis.

TABLE 3 | Aqueous and serum T-IgG status.

Category	Number of eyes/patients (% in all measured samples in each group)		
	Peripheral granuloma	Posterior granuloma	Endophthalmitis
Aqueous			
Positive	55 (78.6%)	18 (48.6%)	47 (66.2%)
Negative	15 (21.4%)	19 (51.4%)	26 (33.8%)
Not Measured	13	1	13
Serum			
Positive	56 (70.0%)	15 (28.8%)	44 (52.4%)
Negative	23 (28.8%)	21 (56.8%)	37 (44.0%)
Uncertain	1	1	3
Not Measured	3	1	2
T-IgG consistency			
Both positive	43 (64.2%)	10 (28.6%)	33 (47.1%)
Both negative	10 (14.9%)	13 (37.1%)	21 (30.0%)
Aq+/Serum-	10 (14.9%)	7 (20.0%)	11 (15.7%)
Aq-/Serum+	4 (6.0%)	5 (14.3%)	5 (7.1%)
Kappa value	0.454	0.311	0.533

T-IgG status referred to positive, negative, or uncertain of the anti-T. canis antibody in samples. The definition for positive, negative, and uncertain T-IgG status was described in the Methods. T-IgG consistency referred to the number of patients whose aqueous and serum samples showed the same T-IgG status. + referred to T-IgG positive, – referred to T-IgG negative. Aq, aqueous.

taken from eyes with congenital cataract but otherwise quiescent eyes as control. The average age of the children in the control group was 4.5 years, which was significantly younger than the OT patients (unpaired *t*-test, $p = 0.003$).

Both T-IgG negative and positive groups showed very low concentrations of IL-12 (p70), IFN-γ, IL-2, IL-17, TNF-α, IL-1β, and MIP-1α. The T-IgG positive group (Aq^+) showed significantly higher IL-6, MCP-1, IL-5, IL-13, Eotaxin, RANTES, IL-8, MIP-1β, and IL-10 than the T-IgG negative group (Aq^-) and controls. A small yet significant increase of IL-6, MCP-1, IL-8, IL-5, and Eotaxin was observed in the Aq^- group compared to controls.

We also compared cytokine concentrations by three clinical types. No statistically significant differences were found among groups (data not shown).

DISCUSSION

This is probably the largest pediatric OT series reported. Demographically, this cohort of patients recapitulated features reported by previous studies, i.e., boy and rural living environment predominant (6, 10, 11, 14, 21, 24–26). A previous study in China also reported a similar male predominance in OT patients (14). The average age of this cohort was 7.7 years old, which was within the age range with a high seroprevalence of anti-*T. canis* antibody (16, 27). Overall, these demographic features represented factors leading to increased exposure to infectious sources.

We found two clinical features that were not often reported by previous studies. Firstly, the endophthalmitis type constituted 41.5% of the entire cohort. After we excluded patients who were T-IgG antibody-negative in both serum and aqueous, the percentage remained 39.9%. Many studies reported a 25% or less endophthalmitis type in OT (6, 11, 28). However, this number was calculated in cohorts mixed with pediatric and adult patients. There was one study from Poland that reported 48% endophthalmitis type in 94 OT eyes from patients of 3–18 years old, and their diagnosis was based on both clinical presentations and positive serum antibody (8). The ratio of the peripheral granuloma type to the posterior granuloma type in this cohort (2:1) was similar to published data (6, 28).

Another interesting feature of the cohort was the high incidence of retinal detachment (42.2% eyes). In the granuloma types, partial detachment was more frequently seen than total detachment. In the endophthalmitis group, about 83.3% (35 out of 42 eyes) was total detachment. Studies based on patients of all ages in the United States reported < 30% retinal detachment in OT eyes (11, 29). In adult OT patients, the retinal detachment was even less frequently seen (10, 24, 30). However, in another study of 35 Chinese OT patients (mostly granulomatous type), a 45.7% retinal detachment was reported (14). We believe that this was largely due to the fact that children were less likely to notice and report vision changes than adults, especially when it occurred only in one eye.

Although aqueous T-IgG positive and negative eyes presented with similar clinical features, they showed different aqueous cytokine profiles. Only aqueous T-IgG positive eyes had increased IL-5, IL-13, IL-10, GCSF, MIP-1β, and RANTES, suggesting a polarized Th2 response. The concentrations of IL-6, MCP-1, IL-8, and Eotaxin were increased in both T-IgG positive and negative eyes, but were higher in the former group. IL-2, IL-4, IFN-γ, TNF-α, IL-12p70, IL-17, and MIP-1α were undetectable in both groups, suggesting the absence of Th1 or Th17 responses.

Interleukin-4 subverts the host tissue immune responses and cell metabolism in favor of parasite survival and growth (31). During the establishment of *T. canis* infection in mice, a synchronized increase of IL-4, IL-5, and IL-13 was found. However, IL-4 was not always increased in serum of patients with systemic *T. canis* infection (3, 4, 32–34). Although IL-4 and IL-13 (or IL-5, which largely tracks with IL-13) are both cytokines central to type-2 inflammation, there do exist some occasions where IL-13 production outweighs IL-4 production in type-2 inflammation. Th2 cells produce IL-13 in peripheral tissues, such as the lung and eye, while IL-4 protein production is centralized to germinal center reactions within B follicles in lymphoid tissues. Since IL-13 drives peripheral hallmarks of type-2 inflammation, IL-13 expression may predominate over IL-4 in non-lymphoid tissues and at mucosal barriers. This phenomenon has been detected in many settings of allergic type-2 lung inflammation (35). As we know, the eye is one of the immunoprivileged organs mainly due to the lack of lymphatic drainage of the retina. Therefore, IL-13 and IL-5 expressions predominate over IL-4 in these none-lymphoid tissues, which may explain why IL-4 was undetectable in our OT groups. Moreover, previous infection and anthelmintic treatment could

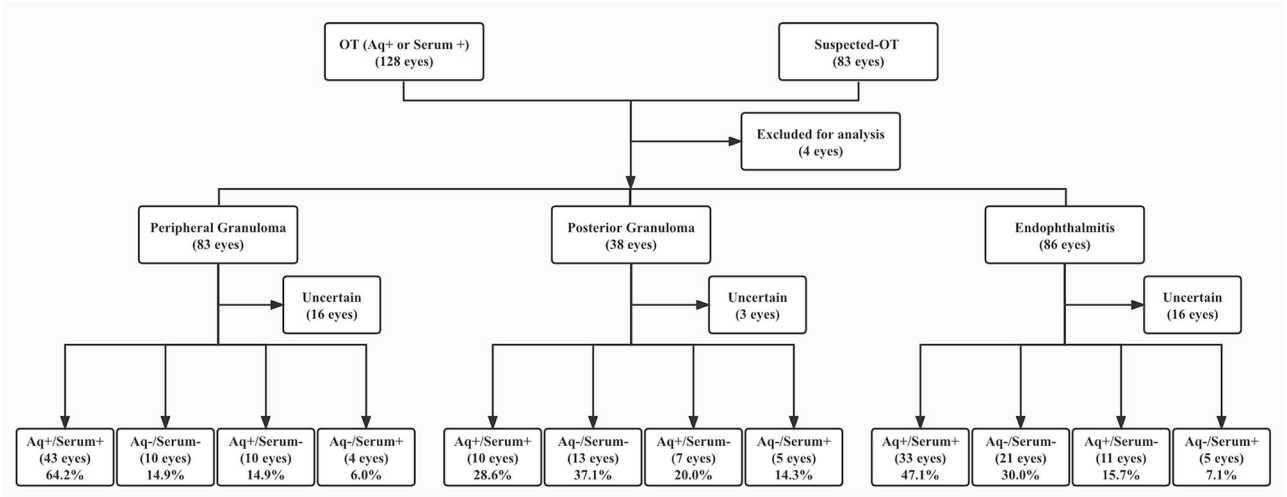

FIGURE 2 | Patient groups according to clinical features and aqueous and serum T-IgG status. T-IgG status referred to positive, negative, or uncertain of the anti-*T. canis* antibody in samples. + referred to T-IgG positive, – referred to T-IgG negative. OT, ocular toxocariasis; Aq, aqueous. Patients whose samples were not measured or with uncertain values (for serum samples) were put in the Uncertain group.

TABLE 4 | Major clinical features of the serum and aqueous T-IgG negative eyes.

Variables	No. of eyes (% in the group)			
	Peripheral granuloma	Posterior granuloma	Endophthal-mitis	Overall
No. of eyes	11	13	20	44
% in the initial group	13.3%	34.2%	23.3%	21.3%
Vitritis				
Severe	4 (36.4%)	3 (23.1%)	10 (50.0%)	17 (38.6%)
Moderate	2 (18.2%)	3 (23.1%)	8 (40.0%)	13 (29.5%)
Mild	5 (45.5%)	7 (53.8%)	2 (10.0%)	14 (31.8%)
Vitreous strands	6 (54.5%)	5 (38.5%)	14 (70.0%)	25 (56.8%)
Vitreous veil	0 (0.0%)	0 (0.0%)	4 (20.0%)	4 (9.1%)
Retinal fibrotic band	6 (54.5%)	12 (92.3%)	7 (35.0%)	25 (56.8%)
Dragged disc	6 (54.5%)	8 (61.5%)	2 (10.0%)	16 (36.4%)
Epiretinal membrane	2 (18.2%)	6 (46.2%)	2 (10.0%)	10 (22.7%)
Retinal detachment				
Partial	3 (27.3%)	3 (23.1%)	3 (15.0%)	9 (20.5%)
Total	2 (18.2%)	0 (0.0%)	6 (30.0%)	8 (18.2%)

affect the production of IL-4 or IL-5 (36). Ocular immune responses could be activated by live larva entering the eye or larva dying in the cyst. There were few reports on aqueous cytokine changes associated with OT. Additional analysis, such as the measurement of IgE, could provide more useful information. Unfortunately, there were not enough samples left after T-IgG and cytokine analysis in this study.

Many labs measure T-IgG in serum or intraocular samples to confirm the diagnosis of OT (9–11, 13, 14). Serum samples were much easier to obtain than intraocular fluids. However, the present study showed that aqueous cytokine changes were not associated with serum T-IgG status. Furthermore, the consistency of T-IgG between serum and aqueous samples was about 75%. Therefore, our results suggested that T-IgG should be analyzed in the aqueous instead of serum to provide accurate data on *T. canis* infection.

Negative T-IgG in intraocular fluid samples or serum was often reported in clinically diagnosed OT patients, the percentage of which varied between 15 and 75% in the intraocular fluid and 30 and 87% in the serum (9–11, 13, 14). However, OT cannot be excluded on the basis of negative T-IgG. Factors, such as the low number of larva in the eye, history of the previous infection, insufficient time for the development of immune reactions and antibodies, and the efficiency of the host immune systems could all lead to negative T-IgG (37). Furthermore, the cutoff values for antibody titer of serum and intraocular fluid remain to be further

TABLE 5 | Aqueous cytokine concentrations.

Cytokines	Concentrations (average ± std in pg/mL)			*p*-values		
	Cataract ($n = 25$)	Aq- ($n = 35$)	Aq+ ($n = 40$)	Aq+/Aq-	Aq-/Cat	LOD
IL-6	3.3 ± 2.6	23.3 ± 30.6	250.1 ± 383.1	<0.01	<0.01	2.6
MCP-1	158.2 ± 53.6	239.3 ± 164.2	354.8 ± 237.2	<0.01	<0.01	1.1
IL-4	<LOD	<LOD	<LOD			0.7
IL-5	<LOD	0.7 ± 1.1	4.1 ± 5.7	<0.01	0.04	0.6
IL-13	3.2 ± 2.2	0.7±1.2	10.1 ± 12.2	<0.01	<0.01	0.7
IL-10	2.5 ± 1.6	0.7 ± 1	11.2 ± 20.4	<0.01	<0.01	0.3
Eotaxin	<LOD	3.6 ± 1.7	10.5 ± 11.8	<0.01	<0.01	2.5
RANTES	<LOD	<LOD	4.3 ± 9.6	<0.01	0.08	1.8
IL-8	6.3 ± 7.4	13.2 ± 20.1	28.2 ± 30	0.02	<0.01	1.0
TNF-α	<LOD	<LOD	<LOD			6.0
IL-1β	<LOD	<LOD	<LOD			0.6
IL-12p70	8.9 ± 8.7	<LOD	<LOD	<0.01	<0.01	3.5
IFN-γ	10.1 ± 1.6	<LOD	<LOD			6.4
IL-2	<LOD	<LOD	<LOD			1.6
IL-17	<LOD	<LOD	<LOD			3.3
MIP-1α	<LOD	<LOD	<LOD			0.2
MIP-1β	6.0 ± 2.9	4.3 ± 1.5	19.3 ± 18.9	<0.01	0.78	0.8
GCSF	2.8 ± 1.7	4.1 ± 2	8.2 ± 11.9	<0.01	<0.01	1.7
VEGF	52.7 ± 32.6	29.7 ± 26.9	70.4 ± 53.5	<0.01	<0.01	3.1

Cataract, children with congenital cataract; Aq, aqueous. – and + stood for T-IgG negative or positive in the aqueous, respectively; LOD, limit of the detection as provided by manufacturer.

defined. In a most recent study on OT with 290 participants, new diagnostic cutoff values for serum (8.2 U) and intraocular fluid (1.8 U) T-IgG were proposed with increased sensitivity and specificity (38). These cutoff values were lower than what we used in the current study. Using the proposed cutoff values, 3 patients were re-diagnosed as serum T-IgG positive and 1 was re-diagnosed as aqueous T-IgG positive (data not shown). However, the discordant T-IgG titer between aqueous and serum samples of the same patient remained. In the present cohort, there were 11 patients with very low T-IgG in the aqueous (< 1 U) and high T-IgG in the serum (> 20 U) and 12 patients with low T-IgG in the serum (< 5 U) and high T-IgG in the aqueous (> 10 U).

In this study, most patients were treated with systemic plus topical anti-inflammation medication, depending on the severity of the condition. Anthelmintic medicine was often prescribed. Surgical intervention was given to eyes with vitreous haze and partial retinal detachment. Our treatment strategy was similar to most of the studies published (28, 39). Frequent follow-up was necessary to monitor and adjust treatment strategies.

CONCLUSIONS

In summary, this study provided evidence to suggest the measurement of anti-*T. canis* antibody in aqueous for more specific diagnosis of clinically suspected OT. The analysis of aqueous cytokines could unveil molecular targets for the development of more specific and effective treatment options. However, future studies with fine control of patient history are needed to confirm and further understand the immunological features associated with OT.

DATA AVAILABILITY STATEMENT

The raw data supporting the conclusions of this article will be made available by the authors, without undue reservation.

ETHICS STATEMENT

The studies involving human participants were reviewed and approved by Institutional Review Board of Xinhua Hospital. Written informed consent to participate in this study was provided by the participants' legal guardian/next of kin. Written informed consent was obtained from the individual(s), and minor(s)' legal guardian/next of kin, for the publication of any potentially identifiable images or data included in this article.

AUTHOR CONTRIBUTIONS

Conceptualized, design, and provided fundings for the study: JinL and PZ. Clinical examination and evaluation of the patients: PZ, YH, and XZ. Patient data curation: XZ, YZ, YY, YR, and JiaL. Laboratory investigation: XZ, YR, and JinL. Manuscript writing and editing: JinL, YY, and XZ. All authors contributed to the article and approved the submitted version.

FUNDING

This research was supported by grants from the National Natural Science Foundation of China (NFSC) 81873679 to JinL and 82171069 to PZ.

ACKNOWLEDGMENTS

The authors would like to thank the patients who participated in this study and thereby made this work possible.

REFERENCES

1. Macpherson CN. The epidemiology and public health importance of toxocariasis: a zoonosis of global importance. *Int J Parasitol.* (2013) 43:999–1008. doi: 10.1016/j.ijpara.2013.07.004
2. Hotez PJ, Wilkins PP. Toxocariasis: America's most common neglected infection of poverty and a helminthiasis of global importance? *PLoS Negl Trop Dis.* (2009) 3:e400. doi: 10.1371/journal.pntd.0000400
3. Nagy D, Bede O, Danka J, Szenasi Z, Sipka S. Analysis of serum cytokine levels in children with chronic cough associated with toxocara *canis* infection. *Parasite Immunol.* (2012) 34:581–8. doi: 10.1111/pim.12010
4. Mazur-Melewska K, Jonczyk K, Modlinska-Cwalinska A, Figlerowicz M, Sluzewski W. Visceral larva migrans syndrome: analysis of serum cytokine levels in children with hepatic lesions confirmed in radiological findings. *Parasite Immunol.* (2014) 36:668–73. doi: 10.1111/pim.12143
5. Wilkinson CP, Welch RB. Intraocular toxocara. *Am J Ophthalmol.* (1971) 71:921–930. doi: 10.1016/0002-9394(71)90267-4
6. Arevalo JF, Espinoza JV, Arevalo FA. Ocular toxocariasis. *J Pediatr Ophthalmol Strabismus.* (2013) 50:76–86. doi: 10.3928/01913913-20120821-01
7. Martinez-Pulgarin DF, Munoz–Urbano M, Gomez–Suta LD, Delgado OM, Rodriguez-Morales AJ. Ocular toxocariasis: new diagnostic and therapeutic perspectives. *Recent Pat Antiinfect Drug Discov.* (2015) 10:35–41. doi: 10.2174/1574891X10666150410125057
8. Zygulska-Mach H, Krukar-Baster K, Ziobrowski S. Ocular toxocariasis in children and youth. *Doc Ophthalmol.* (1993) 84:145–54. doi: 10.1007/BF01206249
9. de Visser L, Rothova A, de Boer JH, van Loon AM, Kerkhoff FT. Canninga-van Dijk MR, et al. Diagnosis of ocular toxocariasis by establishing intraocular antibody production. *Am J Ophthalmol.* (2008) 145:369–74. doi: 10.1016/j.ajo.2007.09.020
10. Yokoi K, Goto H, Sakai J, Usui M. Clinical features of ocular toxocariasis in Japan. *Ocul Immunol Inflamm.* (2003) 11:269–75. doi: 10.1076/ocii.11.4.269.18266
11. Stewart JM, Cubillan LD, Cunningham ET Jr. Prevalence, clinical features, and causes of vision loss among patients with ocular toxocariasis. *Retina.* (2005) 25:1005–13. doi: 10.1097/00006982-200512000-00009
12. Lee RM, Moore LB, Bottazzi ME, Hotez PJ. Toxocariasis in North America: a systematic review. *PLoS Negl Trop Dis.* (2014) 8:e3116. doi: 10.1371/journal.pntd.0003116
13. Wang ZJ, Zhou M, Cao WJ, et al. Evaluation of the Goldmann-Witmer coefficient in the immunological diagnosis of ocular toxocariasis. *Acta Trop.* (2016) 158:20–3. doi: 10.1016/j.actatropica.2016.02.013
14. Zhou M, Chang Q, Gonzales JA, et al. Clinical characteristics of ocular toxocariasis in eastern China. *Graefes Arch Clin Exp Ophthalmol.* (2012) 250:1373–8. doi: 10.1007/s00417-012-1971-2
15. Phasuk N, Punsawad C. Seroprevalence of Toxocara *canis* infection and associated risk factors among primary school children in rural southern Thailand. *Trop Med Health.* (2020) 48:23. doi: 10.1186/s41182-020-00211-0
16. Won KY. Kruszon–Moran D, Schantz PM, Jones JL. National seroprevalence and risk factors for zoonotic toxocara spp infection. *Am J Trop Med Hyg.* (2008) 79:552–7. doi: 10.4269/ajtmh.2008.79.552
17. Cong W, Meng QF, You HL, Zhou N, Dong XY, Dong W, et al. Seroprevalence and risk factors of toxocara infection among children in Shandong and Jilin provinces, China. *Acta Trop.* (2015) 152:215–9. doi: 10.1016/j.actatropica.2015.09.008
18. Wang S, Li H, Yao Z, Li P, Wang D, Zhang H, et al. Toxocara infection: seroprevalence and associated risk factors among primary school children in central China. *Parasite.* (2020) 27:30. doi: 10.1051/parasite/2020028
19. Yang GL, Zhang XX, Shi CW, Yang WT, Jiang YL, Wei ZT, et al. Seroprevalence and associated risk factors of toxocara infection in Korean, Manchu, Mongol, and Han ethnic groups in northern China. *Epidemiol Infect.* (2016) 144:3101–7. doi: 10.1017/S0950268816001631
20. Maetz HM, Kleinstein RN, Federico D, Wayne J. Estimated prevalence of ocular toxoplasmosis and toxocariasis in Alabama. *J Infect Dis.* (1987) 156:414. doi: 10.1093/infdis/156.2.414
21. Good B, Holland CV, Taylor MR, Larragy J, Moriarty P, O'Regan M. Ocular toxocariasis in schoolchildren. *Clin Infect Dis.* (2004) 39:173–8. doi: 10.1086/421492
22. Nussenblatt RB, Palestine AG, Chan CC, Roberge F. Standardization of vitreal inflammatory activity in intermediate and posterior uveitis. *Ophthalmology.* (1985) 92:467–71. doi: 10.1016/S0161-6420(85)34001-0
23. Li J, Ang M, Cheung CM, Vania M, Chan AS, Waduthantri S, et al. Aqueous cytokine changes associated with Posner-Schlossman syndrome with and without human cytomegalovirus. *PLoS ONE.* (2012) 7:e44453. doi: 10.1371/journal.pone.0044453
24. Ahn SJ, Woo SJ, Jin Y, Chang YS, Kim TW, Ahn J, et al. Clinical features and course of ocular toxocariasis in adults. *PLoS Negl Trop Dis.* (2014) 8:e2938. doi: 10.1371/journal.pntd.0002938
25. Jee D, Kim KS, Lee WK, Kim W, Jeon S. Clinical features of ocular toxocariasis in adult Korean patients. *Ocul Immunol Inflamm.* (2016) 24:207–16. doi: 10.3109/09273948.2014.994783
26. Yoshida M, Shirao Y, Asai H, Nagase H, Nakamura H, Okazawa T, et al. A retrospective study of ocular toxocariasis in Japan: correlation with antibody prevalence and ophthalmological findings of patients with uveitis. *J Helminthol.* (1999) 73:357–61. doi: 10.1017/S0022149X99000608
27. Jarosz W. Mizgajska-Wiktor H, Kirwan P, Konarski J, Rychlicki W, Wawrzyniak G. developmental age, physical fitness and toxocara seroprevalence amongst lower-secondary students living in rural areas contaminated with toxocara eggs. *Parasitology.* (2010) 137:53–63. doi: 10.1017/S0031182009990874
28. Despreaux R, Fardeau C, Touhami S, Brasnu E, Champion E, Paris L, et al. Ocular toxocariasis: clinical features and long-term visual outcomes in adult patients. *Am J Ophthalmol.* (2016) 166:162–8. doi: 10.1016/j.ajo.2016.03.050
29. Centers for Disease C, Prevention. ocular toxocariasis-United States, 2009–2010. *MMWR Morb Mortal Wkly Rep.* (2011) 60:734–6.
30. Kwon SI, Lee JP, Park SP, Lee EK, Huh S, Park IW. Ocular toxocariasis in Korea. *Jpn J Ophthalmol.* (2011) 55:143–7. doi: 10.1007/s10384-010-0909-7
31. Huang L, Beiting DP, Gebreselassie NG, Gagliardo LF, Ruyechan MC, Lee NA, et al. Eosinophils and IL-4 support nematode growth coincident with an innate response to tissue injury. *PLoS Pathog.* (2015) 11:e1005347. doi: 10.1371/journal.ppat.1005347
32. Resende NM, Gazzinelli-Guimarães PH, Barbosa FS, Oliveira LM, Nogueira DS, Gazzinelli-Guimarães AC, et al. New insights into the immunopathology of early toxocara *canis* infection in mice. *Parasit Vectors.* (2015) 8:354. doi: 10.1186/s13071-015-0962-7
33. Huang L, Appleton JA. Eosinophils in helminth infection: defenders and dupes. *Trends Parasitol.* (2016) 32:798–807. doi: 10.1016/j.pt.2016.05.004
34. Waindok P, Strube C. Neuroinvasion of toxocara *canis* and T. cati-larvae mediates dynamic changes in brain cytokine and chemokine profile. *J Neuroinflammation.* (2019) 16:147. doi: 10.1186/s12974-019-1537-x

35. Bao K, Reinhardt RL. The differential expression of IL-4 and IL-13 and its impact on type-2 immunity. *Cytokine.* (2015) 75:25–37. doi: 10.1016/j.cyto.2015.05.008
36. Scott JT, Turner Cm, Mutapi F, Woolhouse ME, Chandiwana SK, Mduluza T, et al. Dissociation of interleukin-4 and interleukin-5 production following treatment for schistosoma haematobium infection in humans. *Parasite Immunol.* (2000) 22:341–8. doi: 10.1046/j.1365-3024.2000.00311.x
37. Brindley PJ, Prociv P, Creevey CA, East IJ. Regulation of toxocariasis in mice selectively reared for high and low immune responses to Nematospiroides dubius. *J Helminthol.* (1985) 59:157–66. doi: 10.1017/S0022149X0002575X
38. Huang L, Sun L, Liu C, Li S, Zhang T, Luo X, et al. Diagnosis of ocular toxocariasis by serum and aqueous humor IgG ELISA. *Transl Vis Sci Technol.* (2021) 8:33. doi: 10.1167/tvst.10.8.33
39. Moreira GM, Telmo Pde L, Mendonça M, Moreira AN, McBride AJ, Scaini CJ, et al. Human toxocariasis: current advances in diagnostics, treatment, and interventions. *Trends Parasitol.* (2014) 30:456–64. doi: 10.1016/j.pt.2014.07.003

Conflict of Interest: The authors declare that the research was conducted in the absence of any commercial or financial relationships that could be construed as a potential conflict of interest.

frontiers | Frontiers in Medicine

ORIGINAL RESEARCH
published: 07 April 2022
doi: 10.3389/fmed.2022.855661

Intra-Arterial Chemotherapy as Primary Treatment for Advanced Unilateral Retinoblastoma in China

Tingyi Liang[1†], *Xin Zhang*[2†], *Jiakai Li*[1], *Xuming Hua*[2], *Peiquan Zhao*[1*] *and Xunda Ji*[1*]

[1] Department of Ophthalmology, Xinhua Hospital Affiliated to Shanghai Jiao Tong University School of Medicine, Shanghai, China, [2] Department of Neurosurgery, Xinhua Hospital Affiliated to Shanghai Jiao Tong University School of Medicine, Shanghai, China

Purpose: This study aimed to evaluate the efficacy and complications of intra-arterial chemotherapy (IAC) as a primary treatment for advanced unilateral retinoblastoma in Chinese patients.

Methods: This study was a retrospective review of patients with advanced unilateral retinoblastoma treated with IAC as the primary treatment. The IAC procedures were performed using a balloon-assisted technique. The clinical status and treatment complications were recorded at each visit. Kaplan–Meier analysis was performed to estimate recurrence-free survival and ocular survival.

Results: In total, 116 eyes of 116 patients with advanced unilateral retinoblastoma were enrolled, including 66 eyes (57%) in group D and 50 eyes (43%) in group E. All treated eyes received a mean of 3 cycles of IAC (range, 3–5), and 66% of the eyes were combined with local consolidation therapy. The median follow-up time was 39 months (range, 22–57 months). The 3-year recurrence-free survival and ocular survival rates were 68.8% (95% CI, 59.2–76.6%) and 88.5% (95% CI, 80.9–93.2%), respectively. Moreover, the 3-year ocular survival rate in group D was significantly higher than that in group E (96.9%, 76.3%; $P < 0.01$). The common ocular complication was vitreous hemorrhage (19.8%). No deaths or severe systemic complications occurred.

Conclusion: Primary intra-arterial chemotherapy is effective for the treatment of advanced unilateral retinoblastoma, especially in group D, with acceptable toxicity.

Keywords: retinoblastoma, advanced stage, unilateral disease, intra-arterial chemotherapy, ophthalmic artery chemosurgery

OPEN ACCESS

Edited by:
Alexander C. Rokohl, University of Cologne, Germany

Reviewed by:
Wanlin Fan, University Hospital of Cologne, Germany
Senmao Li, University of Cologne, Germany

***Correspondence:**
Peiquan Zhao
zhaopeiquan@xinhuamed.com.cn
Xunda Ji
jixunda@xinhuamed.com.cn

[†]These authors have contributed equally to this work and share first authorship

Specialty section:
This article was submitted to Ophthalmology, a section of the journal Frontiers in Medicine

Received: *15 January 2022*
Accepted: *11 March 2022*
Published: *07 April 2022*

Citation:
Liang T, Zhang X, Li J, Hua X, Zhao P and Ji X (2022) Intra-Arterial Chemotherapy as Primary Treatment for Advanced Unilateral Retinoblastoma in China. Front. Med. 9:855661. doi: 10.3389/fmed.2022.855661

INTRODUCTION

Retinoblastoma is the most common primary intraocular malignant tumor in children (1). Over the past three decades, multiple treatment modalities have been applied for the management of retinoblastoma without the need for external beam radiation or enucleation. Since the mid-1990s, intravenous chemotherapy (IVC) has become the most commonly used treatment for retinoblastoma and achieved treatment success rates ranging from 90 to 100% for early-stage retinoblastoma (groups A–C) (2). However, IVC alone is rarely curative for eyes with advanced retinoblastoma (groups D and E), and the treatment success rates are less than 50% (2–4). Additionally, the systemic adverse effects associated with IVC, such as secondary acute myelogenous leukemia, are worrisome (5).

Intra-arterial chemotherapy (IAC), also known as ophthalmic artery chemosurgery (OAC), has been introduced in the management of retinoblastoma for several years (6–9). Compared with IVC, IAC directly delivers chemotherapy drugs into the eye, showing substantial advantages in increasing intraocular tumor exposure to the drugs and reducing systemic adverse effects. IAC allows many eyes with advanced retinoblastoma to be saved; previously, these eyes would have required enucleation (10). Due to the remarkable treatment effect, many centers worldwide prefer to use IAC for the treatment of retinoblastoma, especially advanced retinoblastoma (11).

Currently, there are no clear clinical guidelines regarding whether IAC can be used as a primary treatment for advanced retinoblastoma; clinicians mainly make treatment choices based on their experience. In the present study, we evaluated the efficacy and complications of IAC as the primary treatment for advanced unilateral retinoblastoma in a Chinese population. We hope that this study will serve as a powerful reference for developing clinical guidelines in the management of advanced unilateral retinoblastoma.

TABLE 1 | International intraocular retinoblastoma classification (IIRC).

Group A	Small (< 3 mm) discrete tumor at least 3 mm from foveola and 1.5 mm from optic nerve. No vitreous or subretinal seeding.
Group B	Eyes with no vitreous or subretinal seeding and discrete retinal tumor of any size and location. Subretinal fluid < 5 mm from the base of the tumor.
Group C	Eyes with only focal vitreous or subretinal seeding and discrete retinal tumor of any size and location. Subretinal fluid < 1 quadrant.
Group D	Eyes with diffuse vitreous or subretinal seeding and/or massive non-discrete endophytic or exophytic disease. Eyes with more extensive seeding than Group C. Massive and/or diffuse intraocular disseminated disease may consist of fine or greasy vitreous seeding or avascular masses. Subretinal seeding may be plaque like. Included exophytic disease and more than one quadrant of retinal detachment.
Group E	Eyes anatomically or functionally destroyed, including irreversible neovascular glaucoma, massive intraocular hemorrhage, aseptic orbital cellulitis, tumor anterior to anterior vitreous face, tumor touching the lens, diffuse infiltrating retinoblastoma, phthisis bulbi or pre-phthisis.

MATERIALS AND METHODS

Patients

This was a single-center, single-arm retrospective study. The study was approved by the Ethics Committee of Xinhua Hospital Affiliated to Shanghai Jiao Tong University School of Medicine and adhered to the tenets of the Declaration of Helsinki. Written informed consent was obtained from the guardian of each patient. The medical records of all patients diagnosed with advanced unilateral retinoblastoma and treated at Xinhua Hospital Affiliated to Shanghai Jiao Tong University School of Medicine between January 2016 and December 2018 were reviewed. The inclusion criteria were patients with advanced unilateral retinoblastoma who received IAC as the primary treatment. Advanced retinoblastoma was defined as International Intraocular Retinoblastoma Classification (IIRC) (12) groups D and E (**Table 1**). Patients were excluded if they (1) received previous treatment before referral to our hospital; (2) had high-risk retinoblastoma with tumor invasion into the anterior chamber, choroid or retrolaminar optic nerve; or (3) had extraocular tumor extension or metastatic disease.

Treatment

The IAC procedure was based on the Japanese balloon-assisted IAC infusion method (13). IAC was performed under general anesthesia and systemic intravenous heparinization. After femoral artery puncture using the Seldinger technique, a 5-French (5-F) catheter was introduced into the ipsilateral internal carotid artery under fluoroscopic guidance. Then, a microballoon catheter was passed through the introducer catheter and moved beyond the orifice of the ophthalmic artery (OA). Temporary occlusion was achieved by inflating the balloon. After fluoroscopic confirmation of balloon occlusion at the portion immediately distal to the orifice of the OA, chemotherapy drugs were injected from the introducer catheter and infused into the OA. The chemotherapy agents included carboplatin (30–60 mg), topotecan (1 mg) and melphalan (3–7 mg). The specific drug dosage was determined based on the patient's age and severity of the disease. The dosage of melphalan should be less than 0.5 mg/kg. IAC was performed at monthly intervals. As needed, local consolidation therapy, including thermotherapy, laser photocoagulation, cryotherapy and intravitreal chemotherapy, was used for tumor consolidation in conjunction with or after the completion of IAC. Thermotherapy was performed for small retinal tumors (<3 mm), and laser photocoagulation was performed for slightly larger retinal tumors by surrounding the tumor and closing off feeding vessels. Cryotherapy was mainly used for peripheral tumors. Intravitreal chemotherapy was performed for vitreous seeds control.

Follow-Up

The patients underwent monthly comprehensive ocular examinations, including anterior segment evaluation, fundus examination with indirect ophthalmoscopy, fundus photography, B-scan ultrasonography, and, as needed, fluorescein fundus angiography (FFA). The clinical status and complications were recorded at each visit. If treatment success was achieved, the follow-up time was extended to 3 and 4 months, and then every 6 months thereafter. Treatment success was defined as the complete regression of the intraocular tumor without recurrence. Recurrent disease was defined as regrowth of inactive tumor or seeds that required further treatment. Meanwhile, the patients were followed up with orbit/brain MRI every 6 months for systemic monitoring.

Statistical Analysis

The statistical analysis was performed with Prism (GraphPad Software, La Jolla California USA). Kaplan–Meier analysis was performed to estimate recurrence-free survival and

TABLE 2 | Patient characteristics.

Features	No. (%)
Treated patients	116
Treated eyes	116
Mean age (median, range), mos	22 (12, 6–120)
Sex	
Male	61 (53%)
Female	55 (47%)
Eye	
Right	56 (48%)
Left	60 (52%)
IIRC	
Group D	66 (57%)
Group E	50 (43%)
IAC cycles, mean (median, range)	3 (3, 3–5)
Local therapy	
With	76 (66%)
Without	40 (34%)
Mean follow-up (median, range), mos	38 (39, 22–57)

IIRC, International Intraocular Retinoblastoma Classification; IAC, intra-arterial chemotherapy.

ocular survival, and the Mantel–Cox test was used to compare the survival curves. A $P < 0.05$ was considered statistically significant.

RESULTS

In total, 116 eyes of 116 consecutive patients with advanced unilateral retinoblastoma were included (**Table 2**). The average age at diagnosis was 22 months (range, 6–120 months), and 61 patients (53%) were male. According to the IIRC, 116 treated eyes were classified as group D ($n = 66$, 57%) and group E ($n = 50$, 43%). The mean follow-up time was 38 months (median, 39 months; range, 22–57 months).

The treated eyes received no prior treatment and initially received an average of 3 cycles of IAC (range, 3–5). The IAC procedures were technically successful in all eyes. In addition, 76 eyes (66%) received local therapy combined with IAC: thermotherapy and/or laser photocoagulation ($n = 27$), cryotherapy ($n = 20$) and intravitreal chemotherapy ($n = 43$). Treatment success was achieved in 81 eyes (69.8%); tumor recurrence occurred in 35 eyes (30.2%) within an average of 11 months (range, 4–36 months) after completing primary treatment. Further treatment for recurrent disease was performed as follows: additional IAC ($n = 19$), local therapy ($n = 22$), and enucleation ($n = 7$). The 36-month overall recurrence-free survival rate was 68.8% (95% CI, 59.2–76.6%) and 73.7% (95% CI, 61.2–82.8%) in group D and 62.2% (95% CI, 46.3–74.6%) in group E ($P = 0.266$; **Figure 1A**). At the final follow-up, globe salvage was achieved in 106 eyes (87%). **Figures 2**, **3** show representative cases in the present study. The 36-month overall ocular survival rate was 88.5% (95% CI, 80.9–93.2%) and 96.9% (95% CI, 88.4–99.2%) in group D and 77.3% (95% CI, 62.7–86.8%) in group E ($P = 0.0006$; **Figure 1B**). The causes for enucleation included persistent dense vitreous hemorrhage and/or neovascular glaucoma (NVG) ($n = 8$) and tumor recurrence ($n = 7$). Pathological reports showed that the resection margins and optic nerve were tumor-free. One patient developed bone metastasis 6 months after enucleation and was subsequently treated with aggressive intravenous chemotherapy, achieving disease control. No deaths occurred (100% patient survival rate).

The details of the treatment complications are shown in **Table 3**. The most common ocular complication was vitreous hemorrhage ($n = 23$; 19.8%). Mild vitreous hemorrhage was observed in 15 eyes and was self-absorbed; however, the other 8 eyes, which showed persistent dense vitreous hemorrhage and NVG, lost the control of the fundus and received enucleation. Other ocular complications included lens opacity ($n = 11$; 9.5%), chorioretinal atrophy ($n = 4$; 3.4%), vitreoretinal fibrosis ($n = 2$; 1.7%), rhegmatogenous retinal detachment (RRD) ($n = 1$; 0.9%) and phthisis bulbi ($n = 1$; 0.9%). No severe systemic complications occurred. The main systemic complications included transient leukopenia ($n = 41$; 35.3%) and vomiting ($n = 21$; 18.1%).

DISCUSSION

In the present study, we reported our experience performing IAC as the primary treatment for 116 Chinese patients with advanced unilateral retinoblastoma. Our study confirms that the majority of advanced unilateral retinoblastoma could be successfully managed with primary IAC, avoiding the need for enucleation. In our study, a high rate of ocular salvage was achieved with an overall success rate of 87% ($n = 101/116$). The 36-month ocular survival rate in group D was dramatically 96.9%, which was significantly higher than that in group E (77.3%; $P < 0.01$). The results of our study are consistent with the data reported by other researchers. Shields et al. reported that primary IAC provided superior globe salvage rates for unilateral retinoblastoma of 91 and 48% in groups D and E, respectively (14). Abramson et al. showed successful IAC treatment for naïve advanced retinoblastoma with a 5-year ocular survival rate of 80.2% (10, 15). In another study focusing on group D retinoblastoma, the globe salvage rate at 110 months with primary IAC was 85% (16). According to the work by Munier and colleagues, 25 patients with unilateral group D retinoblastoma received primary IAC, and after a mean follow-up of 41.7 months, all treated eyes (100%) were saved with no need for enucleation (8). An opinion report from the above three major IAC centers agreed with the preference for IAC for the treatment of advanced unilateral retinoblastoma (17). Therefore, it seems that primary IAC shows superiority in the management of advanced unilateral retinoblastoma, achieving a globe salvage rate of approximately 90%.

Since Reese first reported the use of IAC for the treatment of retinoblastoma in 1958 (18), IAC technology has been continuously developed. Japanese investigators developed a

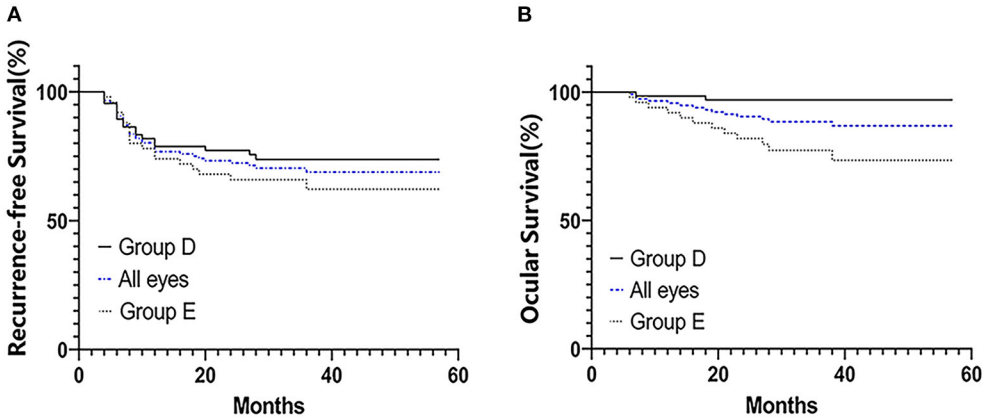

FIGURE 1 | Kaplan–Meier survival curves for 116 patients with advanced unilateral retinoblastoma who were treated with primary IAC treatment. Recurrence-free survival **(A)** and ocular survival **(B)**. Patients' eyes were divided into groups according to the IIRC.

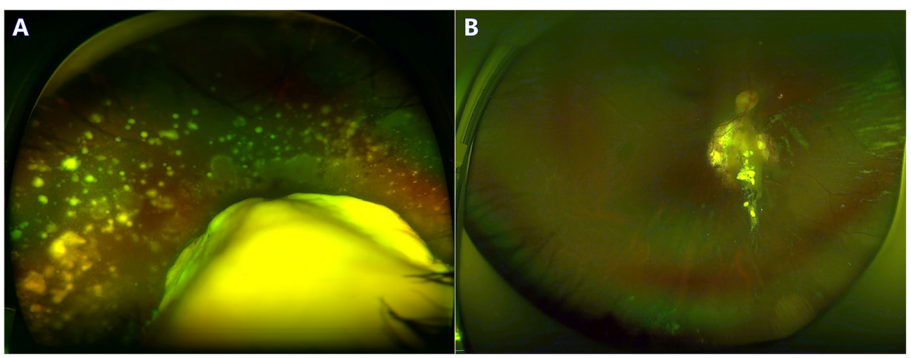

FIGURE 2 | A 3-year-old boy with group D retinoblastoma presented with a large retinal tumor and massive subretinal seeds. The regression of tumor and seeds was noted at the 24-month follow-up. Before **(A)** and after **(B)** 3 cycles of primary IAC infusion and laser consolidation treatment.

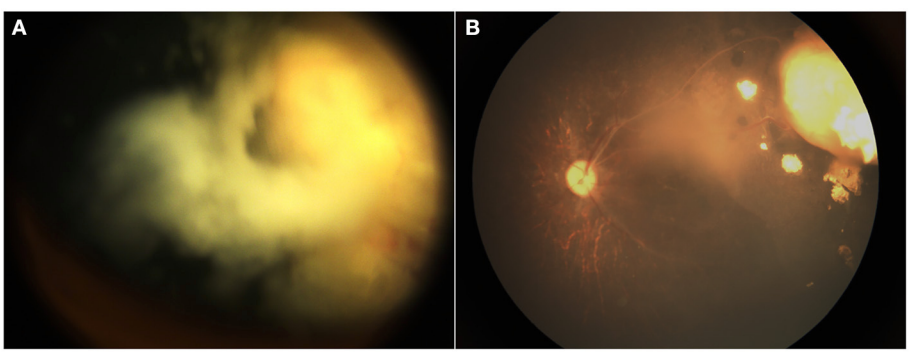

FIGURE 3 | A 12-month-old boy with group D retinoblastoma presented with a peripheral retinal tumor and diffuse vitreous seeds. The regression of tumor and seeds was noted at the 18-month follow-up. Before **(A)** and after **(B)** 3 cycles of primary IAC infusion combined with intravitreal chemotherapy.

technique referred to as "selective ophthalmic artery infusion (SOAI)" with a balloon catheter, which temporarily occludes the internal carotid artery (distal to the OA orifice) and allows chemotherapy drugs to be infused into the OA (13). More recently, Abramson et al. introduced another SOAI technique, superselective OA catheterization, involving a microcatheter directly introduced into the OA through which high doses of chemotherapy drugs could be directly administered into the

TABLE 3 | Treatment complications.

Complications	No. (%)
Ocular	
Vitreous hemorrhage	23 (19.8%)
Lens opacity	11 (9.5%)
Chorioretinal atrophy	4 (3.4%)
Vitreoretinal fibrosis	2 (1.7%)
RRD	1 (0.9%)
Phthisis bulbi	1 (0.9%)
Systemic	
Transient leukopenia	41 (35.3%)
Vomiting	21 (18.1%)
Rash	6 (5.1%)
Epistaxis	4 (3.4%)
Periocular erythema	3 (2.6%)
Fever	2 (1.7%)

RRD, rhegmatogenous retinal detachment.

eye (6, 19). However, compared with the Japanese method, the treatment failure rate of superselective OA catheterization was higher due to the technical difficulty of inserting the microcatheter into the OA, especially in an infant; moreover, there was a higher risk of damage to the vascular intima during OA catheterization, which could lead to a series of ophthalmic vascular events (20). In our study, the average age of the treated patients was young (mean, 22 months), and in our experience, East Asians generally grow slowly with relatively narrow ophthalmic arteries, which may increase the difficulty of superselective OA catheterization. We adopted the Japanese balloon-assisted IAC infusion method; as a result, technical success of IAC procedures was achieved in all treated eyes, and we did not experience serious adverse events associated with IAC.

In our study, all eyes were primarily treated with an average of 3 cycles of IAC infusion, which resulted in significant intraocular tumor shrinkage and regression. Meanwhile, the treated eyes also benefited from additional local consolidation therapies for tumor control. Combined with chemoreduction, local therapy including thermotherapy, laser photocoagulation and cryotherapy were beneficial for retinal tumor control (21); in addition, intravitreal chemotherapy was particularly effective in treating vitreous seeds, which commonly resulted in treatment failure with IAC alone in eyes with severe vitreous disease (22). Recurrent disease was observed in 35 (30.2%) treated eyes, while we did not observe a difference in the recurrence rate between group D and group E ($P = 0.266$). Seven eyes were enucleated due to recurrent disease, while the other eyes with recurrence achieved tumor control with additional IAC and/or local therapies. In addition, 8 eyes were enucleated due to persistent dense vitreous hemorrhage and NVG. Considering the continuous development of eye-preserving management of advanced retinoblastoma, secondary neovascularization may become an important cause of globe salvage failure (23, 24). The exact causes of neovascularization in a treated eye with advanced retinoblastoma may be complicated, not only related to treatment side effects but also related to the malignancy of the tumor, tumor progression/recurrence, chronic retinal detachment, and other factors (23). In our opinion, we recommended early enucleation in cases that lost the control of the fundus due to fear of neovascularization concomitant with active tumor.

With the widespread use of IAC, it was noted that the outstanding tumor response was followed by IAC-related ophthalmic vascular events, including chorioretinal ischemia, ophthalmic artery occlusion, intraocular hemorrhage, retinal artery/vein occlusion and others (25–29). The exact causes of these vascular complications remain undetermined, which may be due to vascular injury during IAC infusion or chemotherapy drug-mediated toxicity (26). Chorioretinal ischemia, also called chorioretinal occlusive vasculopathy or chorioretinal atrophy, was the most frequently reported vascular complication, developing in 7% (28, 29) to 47% (25, 30) of the eyes. In our study, chorioretinal atrophy was observed in 3.4% of the treated eyes; the low incidence may be attributed to the balloon-assisted technique, which eliminates the need for OA catheterization and thus avoids direct vascular injury. Vitreous hemorrhage was commonly observed in 19.8% of the eyes in the present study; except for 7 cases that showed persistent dense vitreous hemorrhage and NVG and required enucleation, the other cases showed mild vitreous hemorrhage, which was self-absorbed. We speculate that the occurrence of vitreous hemorrhage is not entirely due to IAC but also includes malignancy of the intraocular tumor (all advanced stage), retinal detachment, and side effects of tumor regression. In addition, we did not observe ophthalmic artery occlusion, which is considered a serious vision-threatening complication (28). During the follow-up time, severe life-threatening complications, such as cerebrovascular accident, retinal failure, or secondary cancer, were not observed. It seems that primary IAC with the balloon-assisted technique is a safe treatment modality for advanced retinoblastoma, achieving effective tumor control with acceptable toxicity.

Although primary IAC achieves a high globe salvage rate in advanced unilateral retinoblastoma, patient survival must not be compromised. In our study, no deaths occurred until the final follow-up; however, one patient developed bone metastases and received aggressive systemic chemotherapy, achieving tumor control. Theoretically, IAC had minimal systemic effects and would likely be insufficient in preventing metastatic disease. However, several studies mentioned below have reported that the use of IAC did not increase the risk of metastatic deaths. A comparative study found that there was no significant difference in the metastatic mortality rate between patients treated with primary IAC and those treated with IAC plus IVC (3 vs. 7%; $P = 0.51$) for advanced retinoblastoma; additional IVC combined with IAC did not show superiority in systemic control (31). A report from four major IAC centers worldwide showed that the use of IAC did not increase metastasis or metastasis-related deaths (17). Another worldwide report ($n = 1{,}139$) demonstrated that the risk of metastatic deaths in IAC-treated patients was < 0.01 (32). It seems that the

timely and effective control of intraocular retinoblastoma is the key to treatment and can reduce the risk of metastasis; however, high-risk retinoblastoma presenting with choroid or retrolaminar optic nerve invasion should be treated with primary enucleation and postoperative adjuvant chemotherapy to avoid metastatic disease.

This study had several limitations. First, this is a single-center retrospective study. Second, this study lacks a control group to evaluate the true benefit of primary IAC for advanced unilateral retinoblastoma. However, the rarity of retinoblastoma limited the present study to a retrospective, non-comparative cases series. A multicenter, randomized controlled trial will be valuable in the future. Last but not least, we reported 3-year survival outcomes, which may not be sufficient to represent long-term success, and it is necessary to determine 5-, 10-, and 15-year survival rates to assess long-term survival outcomes in these patients.

In summary, the findings from our relatively large cohort confirm the superiority of primary IAC for advanced unilateral retinoblastoma with acceptable ocular toxicity and minimal systemic adverse effects. For group D unilateral retinoblastoma, we strongly recommend that IAC should be the preferred treatment modality, achieving an impressive 3-year survival rate of 96.9% in the present study. We believe our study can serve as a powerful reference for clinicians' decision making in the future.

DATA AVAILABILITY STATEMENT

The original contributions presented in the study are included in the article/supplementary material, further inquiries can be directed to the corresponding authors.

ETHICS STATEMENT

The studies involving human participants were reviewed and approved by the Ethics Committee of the Xinhua Hospital Affiliated to Shanghai Jiao Tong University School of Medicine. Written informed consent to participate in this study was provided by the participants' legal guardian/next of kin.

AUTHOR CONTRIBUTIONS

XJ, PZ, and XH: conception and design. TL, XZ, and JL: collection and assembly of data. All authors contributed to the production of this manuscript and approved the final version.

FUNDING

This study was supported by the Clinical Research Plan of SHDC (Grant No: SHDC2020CR1009A) and Hospital Funded Clinical Research Plan of the Xinhua Hospital Affiliated to Shanghai Jiao Tong University School of Medicine (Grant No: 21XHDB08).

REFERENCES

1. Kivelä T. The epidemiological challenge of the most frequent eye cancer: retinoblastoma, an issue of birth and death. *Br J Ophthalmol.* (2009) 93:1129–31. doi: 10.1136/bjo.2008.150292
2. Shields CL, Mashayekhi A, Au AK, Czyz C, Leahey A, Meadows AT, et al. The international classification of retinoblastoma predicts chemoreduction success. *Ophthalmology.* (2006) 113:2276–80. doi: 10.1016/j.ophtha.2006.06.018
3. Shields CL, Ramasubramanian A, Thangappan A, Hartzell K, Leahey A, Meadows AT, et al. Chemoreduction for group E retinoblastoma: comparison of chemoreduction alone versus chemoreduction plus low-dose external radiotherapy in 76 eyes. *Ophthalmology.* (2009) 116:544–551 e1. doi: 10.1016/j.ophtha.2008.10.014
4. Cohen VML, Kingston J, Hungerford JL. The success of primary chemotherapy for group D heritable retinoblastoma. *Br J Ophthalmol.* (2009) 93:887–90. doi: 10.1136/bjo.2008.142679
5. Gombos DS, Hungerford J, Abramson DH, Kingston J, Chantada G, Dunkel IJ, et al. Secondary acute myelogenous leukemia in patients with retinoblastoma: is chemotherapy a factor? *Ophthalmology.* (2007) 114:1378–83. doi: 10.1016/j.ophtha.2007.03.074
6. Abramson DH, Dunkel IJ, Brodie SE, Kim JW, Gobin YP. A phase I/II study of direct intraarterial (ophthalmic artery) chemotherapy with melphalan for intraocular retinoblastoma initial results. *Ophthalmology.* (2008) 115:1398–1404, 1404.e1. doi: 10.1016/j.ophtha.2007.12.014
7. Shields CL, Bianciotto CG, Jabbour P, Ramasubramanian A, Lally SE, Griffin GC, et al. Intra-arterial chemotherapy for retinoblastoma: report No. 1, control of retinal tumors, subretinal seeds, and vitreous seeds. *Arch Ophthalmol.* (2011) 129:1399–406. doi: 10.1001/archophthalmol.2011.150
8. Munier FL, Mosimann P, Puccinelli F, Gaillard MC, Stathopoulos C, Houghton S, et al. First-line intra-arterial versus intravenous chemotherapy in unilateral sporadic group D retinoblastoma: evidence of better visual outcomes, ocular survival and shorter time to success with intra-arterial delivery from retrospective review of 20 years of treatment. *Br J Ophthalmol.* (2017) 101:1086–93. doi: 10.1136/bjophthalmol-2016-309298
9. Suzuki S, Yamane T, Mohri M, Kaneko A. Selective ophthalmic arterial injection therapy for intraocular retinoblastoma: the long-term prognosis. *Ophthalmology.* (2011) 118:2081–7. doi: 10.1016/j.ophtha.2011.03.013
10. Abramson DH, Fabius AW, Francis JH, Marr BP, Dunkel IJ, Brodie SE, et al. Ophthalmic artery chemosurgery for eyes with advanced retinoblastoma. *Ophthalmic Genet.* (2017) 38:16–21. doi: 10.1080/13816810.2016.1244695
11. Grigorovski N, Lucena E, Mattosinho C, Parareda A, Ferman S, Catalá J, et al. Use of intra-arterial chemotherapy for retinoblastoma: results of a survey. *Int J Ophthalmol.* (2014) 7:726–30. doi: 10.3980/j.issn.2222-3959.2014.04.26
12. Linn Murphree A. Intraocular retinoblastoma: the case for a new group classification. *Ophthalmol Clin North Am.* (2005) 18:41–53, viii. doi: 10.1016/j.ohc.2004.11.003
13. Yamane T, Kaneko A, Mohri M. The technique of ophthalmic arterial infusion therapy for patients with intraocular retinoblastoma. *Int J Clin Oncol.* (2004) 9:69–73. doi: 10.1007/s10147-004-0392-6
14. Shields CL, Jorge R, Say EA, Magrath G, Alset A, Caywood E, et al. Unilateral retinoblastoma managed with intravenous chemotherapy versus intra-arterial chemotherapy. Outcomes based on the International Classification of Retinoblastoma. *Asia Pac J Ophthalmol.* (2016) 5:97–103. doi: 10.1097/APO.0000000000000172
15. Abramson DH, Fabius AW, Issa R, Francis JH, Marr BP, Dunkel IJ, et al. Advanced unilateral retinoblastoma: the impact of ophthalmic artery chemosurgery on enucleation rate and patient survival at MSKCC. *PLoS ONE.* (2015) 10:e0145436. doi: 10.1371/journal.pone.0145436
16. Abramson DH, Daniels AB, Marr BP, Francis JH, Brodie SE, Dunkel IJ, et al. Intra-Arterial Chemotherapy (Ophthalmic Artery Chemosurgery) for Group D Retinoblastoma. *PLoS ONE.* (2016) 11:e0146582. doi: 10.1371/journal.pone.0146582
17. Abramson DH, Shields CL, Munier FL, Chantada GL. Treatment of Retinoblastoma in 2015: agreement and disagreement. *JAMA Ophthalmol.* (2015) 133:1341–7. doi: 10.1001/jamaophthalmol.2015.3108

18. Reese AB, Hyman GA, Tapley ND, Forrest AW. The treatment of retinoblastoma by x-ray and triethylene melamine. *AMA Arch Ophthalmol.* (1958) 60:897–906. doi: 10.1001/archopht.1958.00940080917010
19. Abramson DH, Dunkel IJ, Brodie SE, Marr B, Gobin YP. Superselective ophthalmic artery chemotherapy as primary treatment for retinoblastoma (chemosurgery). *Ophthalmology.* (2010) 117:1623–9. doi: 10.1016/j.ophtha.2009.12.030
20. Stathopoulos C, Bartolini B, Marie G, Beck-Popovic M, Saliou G, Munier FL. Risk factors for acute choroidal ischemia after intra-arterial melphalan for retinoblastoma: the role of the catheterization approach. *Ophthalmology.* (2021) 128:754–64. doi: 10.1016/j.ophtha.2020.09.021
21. Friedman DL, Himelstein B, Shields CL, Shields JA, Needle M, Miller D, et al. Chemoreduction and local ophthalmic therapy for intraocular retinoblastoma. *J Clin Oncol.* (2000) 18:12–7. doi: 10.1200/JCO.2000.18.1.12
22. Francis JH, Iyer S, Gobin YP, Brodie SE, Abramson DH. Retinoblastoma Vitreous Seed Clouds (Class 3): a comparison of treatment with ophthalmic artery chemosurgery with or without intravitreous and periocular chemotherapy. *Ophthalmology.* (2017) 124:1548–55. doi: 10.1016/j.ophtha.2017.04.010
23. Stathopoulos C, Gaillard MC, Moulin A, Puccinelli F, Beck-Popovic M, Munier FL. Intravitreal anti-vascular endothelial growth factor for the management of neovascularization in retinoblastoma after intravenous and/or intraarterial chemotherapy: long-term outcomes in a series of 35 eyes. *Retina.* (2018) 39:2273–82. doi: 10.1097/IAE.0000000000002339
24. Berry JL, Kogachi K, Jubran R, Kim JW. Loss of fundus view as an indication for secondary enucleation in retinoblastoma. *Pediatr Blood Cancer.* (2018) 65:10.1002/pbc.26908. doi: 10.1002/pbc.26908
25. Shields CL, Bianciotto CG, Jabbour P, Griffin GC, Ramasubramanian A, Rosenwasser R, et al. Intra-arterial chemotherapy for retinoblastoma: report No. 2, treatment complications. *Arch Ophthalmol.* (2011) 129:1407–15. doi: 10.1001/archophthalmol.2011.151
26. Munier FL, Beck-Popovic M, Balmer A, Gaillard MC, Bovey E, Binaghi S. Occurrence of sectoral choroidal occlusive vasculopathy and retinal arteriolar embolization after superselective ophthalmic artery chemotherapy for advanced intraocular retinoblastoma. *Retina.* (2011) 31:566–73. doi: 10.1097/IAE.0b013e318203c101
27. Bianciotto C, Shields CL, Iturralde JC, Sarici A, Jabbour P, Shields JA. Fluorescein angiographic findings after intra-arterial chemotherapy for retinoblastoma. *Ophthalmology.* (2012) 119:843–9. doi: 10.1016/j.ophtha.2011.09.040
28. Dalvin LA, Ancona-Lezama D, Lucio-Alvarez JA, Masoomian B, Jabbour P, Shields CL. Ophthalmic vascular events after primary unilateral intra-arterial chemotherapy for retinoblastoma in early and recent eras. *Ophthalmology.* (2018) 125:1803–11. doi: 10.1016/j.ophtha.2018.05.013
29. Ancona-Lezama D, Dalvin LA, Lucio-Alvarez JA, Jabbour P, Shields CL. Ophthalmic vascular events after intra-arterial chemotherapy for retinoblastoma: real-world comparison between primary and secondary treatments. *Retina.* (2019) 39:2264–72. doi: 10.1097/IAE.0000000000002315
30. Muen WJ, Kingston JE, Robertson F, Brew S, Sagoo MS, Reddy MA. Efficacy and complications of super-selective intra-ophthalmic artery melphalan for the treatment of refractory retinoblastoma. *Ophthalmology.* (2012) 119:611–6. doi: 10.1016/j.ophtha.2011.08.045
31. Chen Q, Zhang B, Dong Y, Mo X, Zhang L, Xia J, et al. Evaluating primary intra-arterial chemotherapy versus intravenous plus intra-arterial chemotherapy for advanced intraocular retinoblastoma. *Cancer Chemother Pharmacol.* (2020) 85:723–30. doi: 10.1007/s00280-020-04036-w
32. Abramson DH, Shields CL, Jabbour P, Teixeira LF, Fonseca JRF, Marques MCP, et al. Metastatic deaths in retinoblastoma patients treated with intraarterial chemotherapy (ophthalmic artery chemosurgery) worldwide. *Int J Retina Vitreous.* (2017) 3:40. doi: 10.1186/s40942-017-0093-8

Conflict of Interest: The authors declare that the research was conducted in the absence of any commercial or financial relationships that could be construed as a potential conflict of interest.

Publisher's Note: All claims expressed in this article are solely those of the authors and do not necessarily represent those of their affiliated organizations, or those of the publisher, the editors and the reviewers. Any product that may be evaluated in this article, or claim that may be made by its manufacturer, is not guaranteed or endorsed by the publisher.

frontiers | Frontiers in Medicine

ORIGINAL RESEARCH
published: 29 April 2022
doi: 10.3389/fmed.2022.850129

Dry-Lensectomy Assisted Lensectomy in the Management for End-Stage Familial Exudative Vitreoretinopathy Complicated With Anterior Segment Abnormalities

Jie Peng†, Ziwei Zhao†, Yihua Zou†, Xuerui Zhang†, Yuan Yang, Qiujing Huang, Mingpeng Xu, Yu Xu and Peiquan Zhao**

Department of Ophthalmology, Xin Hua Hospital Affiliated to Shanghai Jiao Tong University School of Medicine, Shanghai, China

Purpose: To report a modified technique of dry-lensectomy assisted lensectomy in the management of end-stage familial exudative vitreoretinopathy (FEVR) complicated with capsule-endothelial, iris-endothelial adhesion and secondary glaucoma.

Methods: 24 eyes of 16 patients with severe complications of advanced pediatric total retinal detachment caused by FEVR who received limbus-based dry-lensectomy were studied retrospectively. Preoperative and postoperative clinical information was collected and reviewed.

Results: Among the 24 eyes, three eyes (12.50%) underwent lensectomy combined with vitrectomy and membrane peeling simultaneously. 21 (87.50%) eyes underwent lensectomy without membrane peeling due to severe corneal opacity or retinal vascular activity, of which eight underwent another vitrectomy combined with membrane peeling. At the last visit (mean:13.86 ± 5.24 months of follow-up), all eyes had a reconstructed anterior chamber with normal depth. Among 21 eyes having preoperative corneal opacity, 15 (71.43%) had a clearer cornea with reduced opacity, 5 (23.81%) showed similar corneal opacification without deterioration. Among 11 eyes undergone retrolental fibroplasia peeling, seven (63.64%) eyes showed partial retinal reattachment in open-funnel type.

Conclusion: Dry-lensectomy offered a simple way to lower the intraocular pressure and simplified the surgery, which helped to solve the severe anterior segment complications and offer a chance for following retrolental fibroplasia peeling and potential visual gain for selected end-stage FEVR patients.

Keywords: lensectomy, vitrectomy, familial exudative vitreoretinopathy, retinal detachment, secondary glaucoma, capsule-endothelial adhesion

OPEN ACCESS

Edited by:
Haoyu Chen, The Chinese University of Hong Kong, China

Reviewed by:
Mohit Dogra, Post Graduate Institute of Medical Education and Research (PGIMER), India
Ludwig M. Heindl, University Hospital of Cologne, Germany
Simar Rajan Singh, Post Graduate Institute of Medical Education and Research (PGIMER), India

****Correspondence:***
Peiquan Zhao
zhaopeiquan@126.com;
zhaopeiquan@xinhuamed.com.cn
Yu Xu
drxuyu@126.com

†These authors have contributed equally to this work

Specialty section:
This article was submitted to Ophthalmology, a section of the journal Frontiers in Medicine

Received: *07 January 2022*
Accepted: *29 March 2022*
Published: *29 April 2022*

Citation:
Peng J, Zhao Z, Zou Y, Zhang X, Yang Y, Huang Q, Xu M, Xu Y and Zhao P (2022) Dry-Lensectomy Assisted Lensectomy in the Management for End-Stage Familial Exudative Vitreoretinopathy Complicated With Anterior Segment Abnormalities. Front. Med. 9:850129. doi: 10.3389/fmed.2022.850129

INTRODUCTION

Retinal vascular anomalies are one of the main causes of visual impairment (1). Among them, familial exudative vitreoretinopathy (FEVR) is a major cause of pediatric and juvenile RD in Asian populations (2, 3). FEVR is classified into five stages (4). Complications of advanced FEVR include corneal edema, cataract, secondary glaucoma and so on. Though treated, part of FEVR eyes would suffer from disease progression to retinal detachment (RD). Treatment of stage 5 FEVR is still a tough task with poor anatomical and functional results. Those eyes had no chance for any visual function or even a good appearance if left untreated. Lensectomy alone or combined with vitrectomy helped to save the opacity of cornea secondary to capsule-endothelial adhesion (3) and glaucoma (5). Vitrectomy with membrane peeling for Stage 5 FEVR is beneficial in preventing total blindness in some patients (3). Visual function of light perception is much better than no light perception at all, at least regarding maintaining the circadian rhythm (6).

In stage 5 FEVR eyes with capsule-endothelial or iris-endothelial adhesion, it was hard to separate the iris or/and the lens from the corneal endothelium with viscoelastics. The first difficulty to conquer was the capsule-endothelial adhesion separation and to reconstruct the anterior chamber (AC). Herein, we introduce a modified method to deal with this tough situation.

METHODS

This is a single-center, retrospective, consecutive, and interventional case series. This study was approved by the Ethics Committee of Xinhua Hospital affiliated to Shanghai Jiao Tong University School of Medicine. All procedures were performed in accordance with the Helsinki Declaration.

Twenty-four eyes from 16 FEVR infants with anterior segment compromise, shallow/flat AC, capsule-endothelial or iris-endothelial adhesion underwent dry-lensectomy-based surgery from April 2020 to September 2021 were studied. The clinical information has been listed in **Table 1**. The patients underwent comprehensive preoperative and postoperative ophthalmic examinations. The anterior and posterior segments were examined with binocular indirect ophthalmoscopy with a + 20D lens. Wide-field fundus images of the anterior and posterior segments were taken with RetCam III (Clarity Medical Systems, Pleasanton, California, USA). Ultrasound examinations were performed to confirm RDs. Ultrasound Biomicroscope (UBM) was done to assess the AC depth and AC angle, especially for the eyes with severe corneal opacity/edema. Intraocular pressure (IOP) was measured using a rebound tonometer (i-Care, Espoo Finnish). Sedation with oral intake of chloral hydrate (0.5 ml/kg) was provided when needed. In our hospital, only for eyes with total retinal detachment and severe anterior segment abnormalities, such as secondary glaucoma, shallow/flat AC or capsule-endothelial or iris-endothelial adhesion, with/ without corneal macula or keratoleukoma (< 2/3 corneal area), and without phthisis bulbi, the surgery was done (**Figures 1A,B**). The anatomic outcomes and the complications were recorded and analyzed.

Statistical Analysis

Statistical analysis was performed using Statistical Package for the Social Sciences (SPSS) Version 20 (IBM Corp, Armonk, NY, USA). Data were expressed as the mean ± standard deviation or as median and range. A paired-*t*-test was used to compare preoperative and postoperative IOP. Regression analysis was applied to analysis the associations between the factors (sex, gestational age, birth weight, age at the surgery, family history, preoperative IOP, postoperative IOP, existence of preoperative corneal oedema/ opacity) and the postoperative corneal status (0 = deterioration of corneal opacity; 1 = remained the same corneal opacity; 2 = reduced corneal opacity;3 = transparent cornea). A *P*-value was considered to be statistically significant if $P < 0.05$.

Surgical Techniques

Dry-lensectomy assisted lensectomy and closed-vitrectomy were performed via limbus approaches. A limbal incision was made by 20-Gauge MVR blade in a slightly downward manner. The route of the blade started from the limbus, went through the mid-periphery of the iris and then into the middle of dislocated lens, which can be easily observed under the microscope (**Figures 1C,D**). After this incision, 23-Gauge vitrector went through the same approach into the lens without AC irrigation and with cutter off (**Figures 1E,F**). As the vitrector is in the lens, the vitrector started to do the cutting with suction (cutting rate: 4,000 bpm, Vacuum: 500 mmHg), and this maneuver was called dry-lensectomy. After removal of some part of the crystalline lens, which helped to reduce the volume of intraocular content, the eye was soft with lower IOP. At this moment, Descemet's membrane folds or a flat or umbilicate cornea could be observed (**Figures 1G,H**). At this time, the viscoelastic can be easily injected into the AC, separating the capsule-endothelial, iris-endothelial, and capsule-iris adhesion, and reconstructing the AC (**Figures 1I,J**). At that, the AC maintainer could be inserted followed by the lensectomy in a traditional way (**Figures 1K,L**). The opaque corneal epithelium can be removed to offer better visualization. Vitrectomy and membrane peeling were performed only when the central part of cornea is clear and lack of retinal vascular activity. Otherwise, a second vitrectomy with membrane peeling was performed on a quiet eye several months later as our previous study (3). Iris speculum was used for retrolental fibroplasia (RLF) dissection as our previous study (7). Intraocular triamcinolone acetonide injection was applied to prevent postoperative inflammatory reactions.

RESULTS

Eight patients had bilateral surgeries and eight had unilateral surgery. The mean age at the surgery was 3.39 ± 1.24 months old, the mean gestational age was 38.91 ± 1.47 weeks, the mean birth weight was 3103.13 ± 748.41 grams, and the mean follow-up duration was 13.86 ± 5.24 months. Five (31.25%) patients had positive family history. All patients had genetic analysis and the FEVR diagnosis was confirmed.

Dry-lensectomy followed by AC reconstruction was successfully applied in all eyes without iatrogenic retinal

TABLE 1 | Clinical information of the patients.

No.	Sex	Age at surgery	GA (weeks)	BW (g)	Family history	Genetic test	Stages of FEVR disease		Eyes under went surgery	Preoperative IOP (mmHg)		Post operative IOP (mmHg)		Pre operative Corneal edema/ opacity		Follow-up durations (months)	Post operative Corneal edema/ opacity		Eye(s) under went vitrectomy and RLF peeling	Ocular examinations at the last visit
							OD	OS		OD	OS	OD	OS	OD	OS		OD	OS		
1	M	2.1	37	1500	(+)	NDP c.339 insG/chrX-43809107	5	5	OU lensectomy	8	6	5	6	(+)	(+)	21	remained	remained	/	OU pupillary block with reconstructed AC
2	M	2.3	38	2700	(+)	FZD4 C226 G>T/chr11-86665902	5	5	OU lensectomy	10	26	3	7	(–)	(+)	20	(–)	deteriorated	OU	OD partial retinal reattachment with closed-funnel type; OS pthisis bulbi
3	F	4.4	40	2950	(–)	LRP5 chr11-68177424/c.G2134A	1	5	OS lensectomy	4	6	5	5	/	(+)	20	/	better	OS	OS partial retinal reattachment with open-funnel type
4	M	3.6	40	3300	(–)	NDP c.134_135delTG/chrX-43817757 43817758	4	5	OS lensectomy	6	8	7	9	/	(+)	19	/	better	/	OS pupillary block with reconstructed AC
5	F	3.1	39	3350	(–)	FZD4 chr11-86663485/c.A313G	5	1	OD lensectomy	8	6	7	6	(+)	(–)	18.5	better	/	/	OD pupillary block with reconstructed AC
6	F	3.5	39.6	2500	(–)	FZD4 c.1176_1178 delGGC/chr11 -86662620 86662622	5	5	OU lensectomy	10	11	6	6	(+)	(–)	17.5	better	/	OS	OS partial retinal reattachment with open-funnel type
7	F	4.1	38	3100	(+)	FZD4 chr11 86663050 86663051/c747dupC	3	5	OS lensectomy	7	18	8	10	/	(+)	16.5	/	better	/	OS pupillary block with reconstructed AC
8	M	5.4	40	3750	(+)	ZNF408 chr11-46726357 46726357/c.1083delG	5	1	OD lensectomy	7	6	7	6	(+)	/	15	remained	/	/	OD pupillary block with reconstructed AC
9	M	2.1	37	2230	(–)	NDP chrX-43817758/c.134T>G	5	5	OU lensectomy	9	8	8	5	(+)	(+)	12.5	remained	remained	/	OU pupillary block with reconstructed AC
10	M	2	38	4030	(–)	NDP chrX-43809104/c.343C>T	5	5	OU lensectomy	4	5	5	5	(+)	(+)	11.5	better	better	OU	OD partial retinal reattachment with open-funnel type; OS partial retinal reattachment with closed-funnel type;

(Continued)

TABLE 1 | Continued

No.	Sex	Age at surgery	GA (weeks)	BW (g)	Family history	Genetic test	Stages of FEVR disease		Eyes under went surgery	Preoperative IOP (mmHg)		Post operative IOP (mmHg)		Pre operative Corneal edema/ opacity		Follow-up durations (months)	Post operative Corneal edema/ opacity		Eye(s) under went vitrectomy and RLF peeling	Ocular examinations at the last visit
							OD	OS		OD	OS	OD	OS	OD	OS		OD	OS		
11	F	2.2	39	2840	(–)	LRP5 chr11-68174159/c.1969A>G	5	5	OU lensectomy	7	5	5	8	(+)	(+)	11	better	better	OD	OD partial retinal reattachment with open-funnel type;
12	F	3.8	37	3100	(–)	LRP5 chr11-68115513/c.C290T	5	5	OU lensectomy +vitrectomy +RLF peeling	3	4	6	4	(+)	(+)	10.5	better	better	OU	OU partial retinal reattachment with open-funnel type with posterior pole nearly reattached.
13	M	5.8	38	2600	(+)	TSPAN12 chr7-120478883/c.233G>A	4	5	OS lensectomy	7	6	8	4	/	(+)	9	/	better	/	OS pupillary block with reconstructed AC
14	M	1.9	39	3250	(–)	FZD4 chr11-86662209/c.G1589A	1	5	OS lensectomy	6	7	6	5	/	(+)	8	/	better	OS	OS pupillary block with reconstructed AC
15	M	4.6	41	4600	(–)	LRP5 chr11-68115489/c.266A>G	5	4	OD lensectomy	9	9	8	10	(–)	/	7.5	/	/	/	OD pupillary block with reconstructed AC
16	M	3.3	42	3850	(–)	NDP chrX-43809162/c.285C>G	5	5	OD lensectomy. OS lensectomy + vitrectomy + RLF peeling	6	7	4	9	(+)	(+)	4.3	better	better	OS	OS partial retinal reattachment with open-funnel type with posterior pole nearly reattached.

No, number; M, male; F, female; GA, gestational age; BW, birth weight; g, gram; OD, oculus dexter; OS, oculus sinister; OU, oculus uterque; FEVR, familial exudative vitreoretinopathy; AC, anterior chamber; RLF, retrolental fibroplasia.

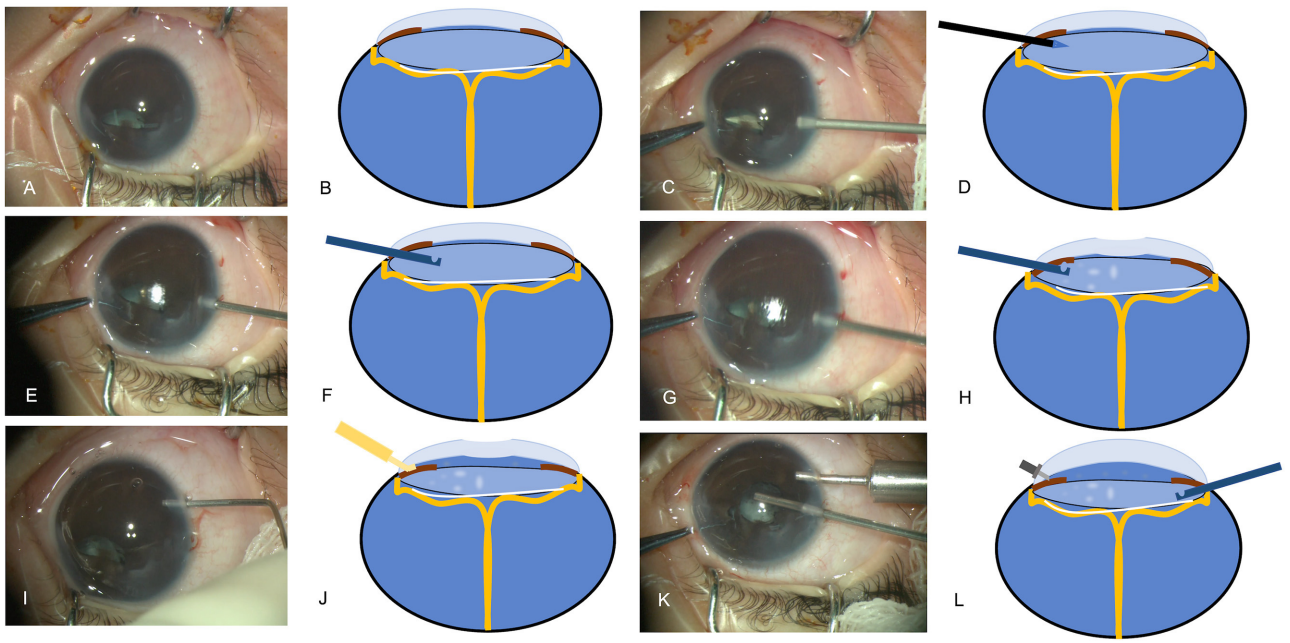

FIGURE 1 | The surgical procedures of dry-lensectomy. **(A,C,E,G,I,K)** Images acquired during the surgery, **(B,D,F,H,J,L)** schematic diagrams of the procedures. **(A,B)** A combination of anterior segment anomalies (anterior lens displacement, marked flat anterior chamber (AC), iridocapsular adhesions, capsule-endothelial adhesion with corneal opacification) was noted; **(C,D)** a limbal incision was made by 20-Gauge MVR blade in a slightly downward manner, starting from the limbus, going through the mid-periphery of the iris and then into the middle of dislocated lens; **(E,F)** the 23-Gauge vitrector went through the same approach into the lens without anterior chamber irrigation and with cutter off; **(G,H)** as the vitrector is in the lens, the vitrector started to do the cutting with suction; **(I,J)** the viscoelastic can be easily injected into the AC to reconstruct the AC; **(K,L)** the AC maintainer was inserted followed by the lensectomy in a traditional way.

holes, Descemet's membrane detachment or conversions to other surgical methods, such as external drainage of subretinal fluid to reduce the IOP.

Among the 24 eyes, three eyes (3/24, 12.50%) underwent lensectomy combined with vitrectomy and membrane peeling at the same surgery. Twenty-one (21/24, 87.50%) eyes underwent lensectomy due to the severe opacity of the cornea or vascular activity of the detached retina. All 21 eyes showed pupil block after the initial lensectomy. Among the 21 eyes, 8(38.10%) eyes had another vitrectomy and membrane peeling at the second time.

The mean preoperative IOP was 8.25 ± 4.83 mmHg. The mean postoperative IOP was 6.12 ± 1.83 mmHg, which is slightly lower than preoperative ones with statistical significance ($P = 0.03$). At the last visit (mean: 13.86 ± 5.24 months of follow-up), all eyes had a reconstructed AC. Twenty-one eyes (21/24, 87.50%) had preoperative corneal edema/opacity, among which 15 (15/21, 71.43%) eyes had a clearer cornea with reduced opacity, five (5/21, 23.81%) showed similar corneal opacification without deterioration and one (1/21, 4.76%) showed progression of corneal degeneration due to pthisis bulbi even with reconstructed AC. The surgical results were shown as **Figure 2**. UBM examinations were performed on 4 eyes of 3 patients (**Figure 3**).

In total, 11 eyes had undergone membrane peeling of the RLF, seven (7/11, 63.64%) eyes showed partial retinal reattachment with open-funnel type (three eyes showed nearly reattached posterior pole), two (2/11, 18.18%) showed partial retinal reattachment with closed-funnel type, one (1/11, 9.09%) showed pupil block and one (1/11, 9.09%) showed pthisis bulbi. Visual acuity test was not performed due to patients' incompatibility.

Regression analysis showed female ($t = 3.793$, $p = 0.001$), lower preoperative IOP ($t = -3.395$, $p = 0.003$), and larger birth weight ($t = 2.095$, $p = 0.049$) were associated with better postoperative corneal status.

DISCUSSIONS

Angle closure glaucoma (ACG) or angle closure is a rare clinical condition in children, which is always secondary condition, such in advanced stage 5 FEVR eyes at the cicatricial stage, which is hard to handle. Retinopathy of prematurity has many overlaps with FEVR, especially in the advanced stages. In 2021, the ICROP defined stage 5C as conditions that total RD with retrolental fibrovascular tissue or closed-funnel detachment and accompanied by anterior segment abnormalities (e.g., anterior lens displacement, marked AC shallowing, iridocapsular adhesions, capsule-endothelial adhesion with central corneal opacification, or a combination thereof) (8), bringing the severe anterior segment complications to our focus again.

ACG is the most frequent complication of RLF, causing pain and opacity of the cornea. The possible causes included anterior displacement of the lens-iris diaphragm due to RLF contraction, pupillary block, and ciliary block (9). Though

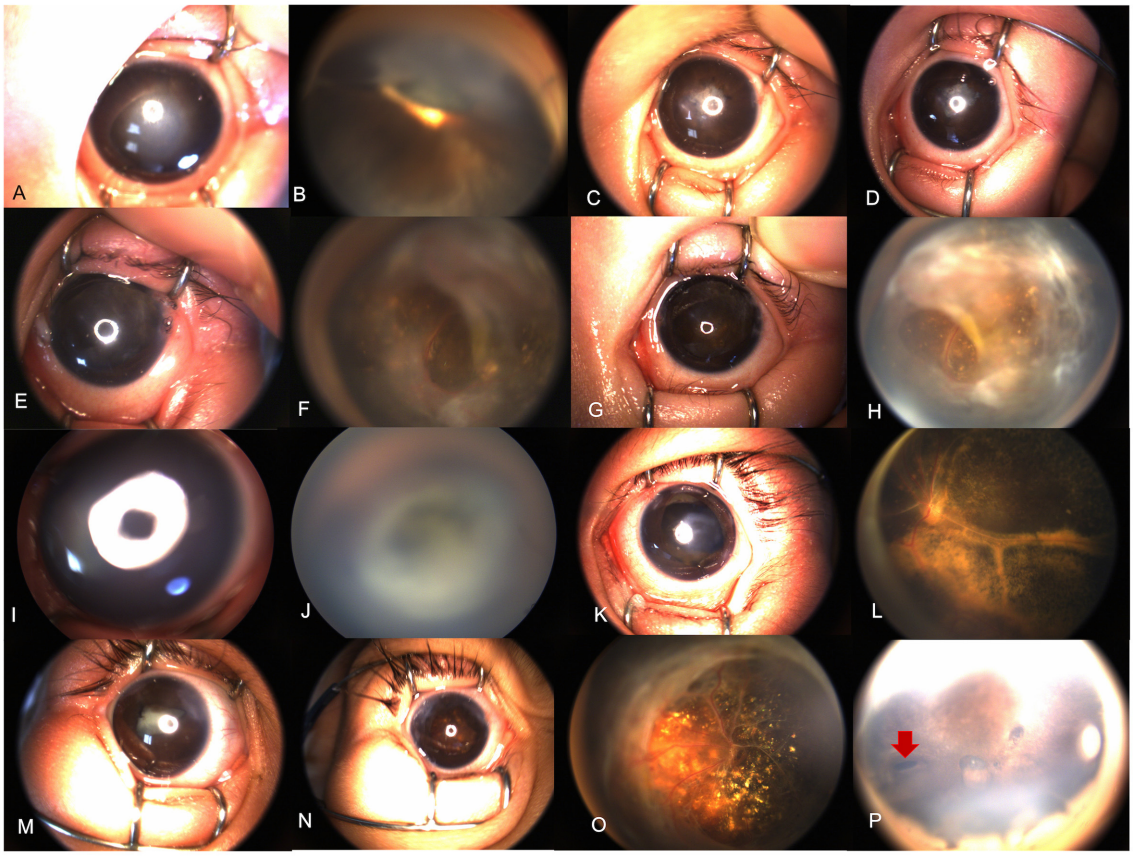

FIGURE 2 | Results of the treatment. **(A–H)** Retcam images of a 4-month-old FEVR patient (Case 3); **(A)** a combination of anterior segment anomalies (anterior lens displacement, marked AC shallowing, iridocapsular adhesions, capsule-endothelial adhesion with central corneal opacification) were noted; **(B)** 1-month after the dry-lensectomy assisted surgery, the depth of AC was normal with pupil occlusion; **(C)** 3 months after the dry-lensectomy assisted surgery, the corneal opacity was reduced; **(D)** 8 months after the dry-lensectomy assisted surgery, the corneal is nearly transparent, and a second vitrectomy and RLF peeling was performed. **(E,F)** 1 week after RLF peeling, the retina was partially reattached in an open-funnel manner; **(G,H)** 6 months after the RLF peeling, the anterior segment was in a stable and good status with clear cornea and round pupil and open-funnel retina. **(I–L)** Case 16, a 3-month-old male presented with bilateral total RD complicated with corneal opacity and flat AC. Dry-lensectomy combined with vitrectomy and RLF peeling was performed simultaneously. **(K,L)** 4 months after the surgery, the corneal opacity was limited and reduced, with nearly reattached posterior pole; **(M–O)** case 12, a 3-month-old FEVR girl received dry-lensectomy assisted surgery and RLF peeling; **(M)** before the surgery; **(N,O)** 7 months postoperatively, the corneal opacity was limited and reduced with round pupil and nearly reattached posterior pole. Subretinal exudates were noted; **(P)** case 11, 7 months after dry-lensectomy assisted lensectomy, the peripheral iridectomy could be seen (red arrow), helping to prevent secondary angle closure or glaucoma caused by pupil block.

surgical and functional outcomes of stage 5 FEVR were poor (3, 4). Lensectomy do have its merits, which was needed to cure the glaucoma and the cataract, and to set the eyes in a quiet, pain-free status (10, 11), preventing keratoleukoma and bulbi phthisis (3, 12, 13). In stage 5 FEVR with total RD, the RLF and total RD adhered to the lens, making lensectomy through par plana impossible with high risks of iatrogenic retinal breaks, a traditional limbal approach lensectomy was always performed.

In these eyes with obliterated AC, the lens-iris diagram was extremely anterior-dislocated with lens adhering to the corneal endothelium with angle closure, it was hard to separate the lens and endothelium with viscoelastics with high IOP and impossible to reconstruct the AC and insert the surgical instruments. The first step was to lower the IOP and reconstruct the AC. We tried external drainage of subretinal fluid in several cases first, but this technique had high risks of ora serrata dialysis and iatrogenic retinal breaks. As a similar concept to lower the IOP with volume depression, we came up with this idea with dry-lensectomy without irrigation initially to soften the eye to conquer the problem. After that, the irrigation tube or AC maintainer was inserted through the limbus incision, the whole traditional lensectomy with/without vitrectomy was performed. In this study, all eyes underwent dry-lensectomy as first step and successful surgery was done without intraoperative complications associated with dry-lensectomy, which is an easy and safe method. Besides, in cases receiving merely lensectomy, pupillary block was seen in all cases due to the RLF. The peripheral iridectomy during dry-lensectomy (**Figure 2P**, red arrow) helped to prevent another secondary angle closure caused by pupillary block.

Staged lensectomy and vitrectomy was recommended alternative in eyes with severe corneal opacity and vascularly

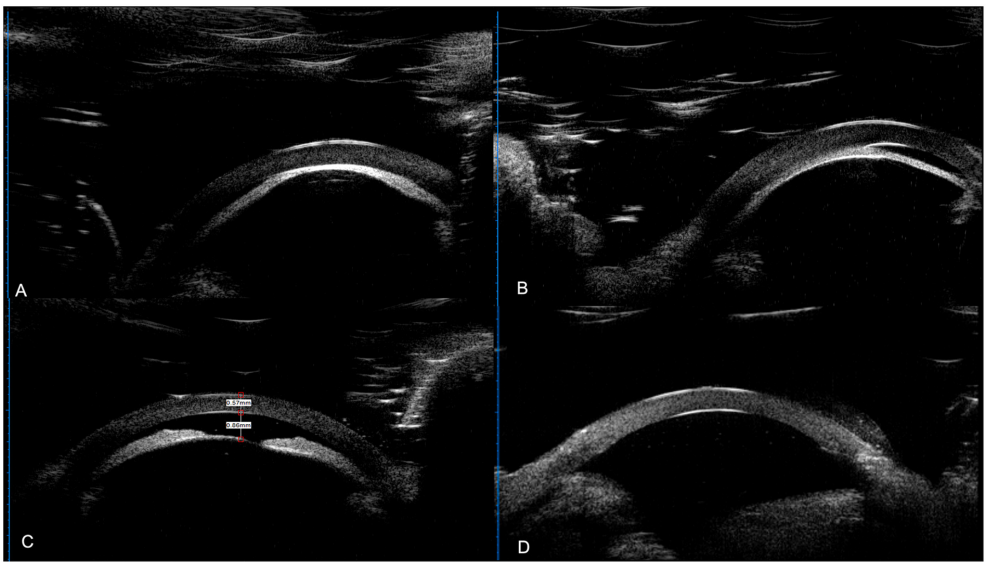

FIGURE 3 | UBM results of the patients. **(A)** UBM result of left eye of case 3 (a 3-month-old female's); **(B)** UBM result of right eye of case 8 (a 5-month-old male). A&B: anterior lens displacement, iridocapsular adhesions, capsule-endothelial adhesion, corneal thickening and edema, and obliterated anterior chamber. **(C,D)** UBM result the right eye of case 15 (a 4-month-old male). **(C)** Preoperative UBM images showed shallowing of the AC with a depth of 0.86 mm, and anterior lens displacement. **(D)** 7 months postoperatively, the AC was reconstructed with a depth of 3.2 mm with AC angle open in this aphakic eye.

activity (3). In our study, the mean age at the surgery was 3.39 ± 1.24 months, which is at the very early stage of the life. At the surgery day, most of the vitreoretinopathy (85.71%, 18/21) were vascularly active in which staged surgeries were scheduled. The AC was reconstructed in all eyes. Despite one eye (4.76%) showed phthisis bulbi after lensectomy and following membrane peeling, the anterior segment was preserved in a relatively stable status in 20(95.23%) eyes. And 71.43% eyes had a reduced corneal opacity, resulting in a better appearance.

The postoperative IOP was slightly lower than preoperative one ($p = 0.03$), though in a normal range or lower due to total RD and soft eyeball of the children. No eye had persistent elevated IOP or ocular pain in the last visit. Lensectomy, starting with dry-lensectomy, helps to reduce the corneal opacity, preserve a better outlook of the eye and offer a good basis for secondary vitrectomy in selected cases.

Besides, in this study, 63.64% of eyes that had undergone membrane peeling of the RLF showed partial retinal reattachment. And 27.27% (3/11) eyes showed nearly reattached posterior pole, which may offer visual gain in these patients. However, vitrectomy combined with RLF peeling was complicated surgery requiring enormous experience. In our opinion, lensectomy, starting with dry-lensectomy, is really recommended as the first step for stage 5 FEVR with anterior segment anomalies, offering potential chance for surgical for RLF peeling by experienced pediatric vitreoretinal surgeons and chances for potential visual gain. Besides, the surgery can be applied in similar clinical situations, such in stage 5C retinopathy of prematurity.

In this small study, female, lower preoperative IOP, and larger birth weight were associated with better postoperative anatomical outcomes. Male patients had more susceptibility for *NDP* mutation, which tended to cause severe diseases (14). Lower preoperative IOP means early surgical intervention without progression to glaucoma with elevated IOP and worse preoperative corneal compromise. However, bias do exist due to small sample size. In our opinion, these patients all presented with advanced end-stage diseases, and early presentation with early treatment should be associated with better outcomes.

In our hospital, we perform surgery with corneal keratoleukoma < 2/3 corneal area, and evaluate the AC in this transparent 1/3 corneal area. If the AC was shallow or flat, we will perform the surgery. We do believe this may differ in different hospitals without a universe consensus. This is our one-site experience. A multicenter study with large scale and long-term follow-up is needed.

Limitations include those biases intrinsic to a retrospective study. Preoperative and postoperative UBM results were not acquired for all patients. The follow-up duration was relatively short and lack of assessments of visual outcomes. Besides, the study sample was small. A further study with longer follow-up, comprehensive ophthalmic examinations and larger scale is needed.

In conclusion, lensectomy, starting with dry-lensectomy, offered a simple way to lower the IOP and made the surgery easier. Lensectomy alone helped to save the opacity of the cornea and offered a chance for following RLF peeling and potential visual gain. It is recommended in the management for eyes with end-stage FEVR or similar situations complicated with marked anterior segment complications.

DATA AVAILABILITY STATEMENT

The original contributions presented in the study are included in the article/**Supplementary Material**, further inquiries can be directed to the corresponding authors.

ETHICS STATEMENT

The studies involving human participants were reviewed and approved by Ethics Committee of Xinhua Hospital affiliated with Shanghai Jiao Tong University School of Medicine. Written informed consent to participate in this study was provided by the participants' legal guardian/next of kin.

AUTHOR CONTRIBUTIONS

JP, ZZ, YZ, XZ, YY, QH, and MX collected, analyzed, and interpreted the data. JP drafted the manuscript. ZZ, YZ, and XZ carefully revised the manuscript. YX and PZ contributed to the conception of the study. PZ came up with the surgical modification and performed all the surgeries. All authors read and approved the final manuscript.

FUNDING

This study was partially supported by Shanghai Sailing Program (Nos. 20YF1429700 and 19YF1432500), the Clinical Research Plan of SHDC (No. SHDC2020CR5014-002) and the National Natural Science Foundation of China (No. 81900908).

SUPPLEMENTARY MATERIAL

The Supplementary Material for this article can be found online at: https://www.frontiersin.org/articles/10.3389/fmed.2022.850129/full#supplementary-material

REFERENCES

1. Bek T. Regional morphology and pathophysiology of retinal vascular disease. *Prog Retin Eye Res.* (2013) 36:247–59. doi: 10.1016/j.preteyeres.2013.07.002
2. Gilmour DF. Familial exudative vitreoretinopathy and related retinopathies. *Eye Lond Engl.* (2015) 29:1–14. doi: 10.1038/eye.2014.70
3. Fei P, Yang W, Zhang Q, Jin H, Li J, Zhao P. Surgical management of advanced familial exudative vitreoretinopathy with complications. *Retina Phila Pa.* (2016) 36:1480–5. doi: 10.1097/IAE.0000000000000961
4. Pendergast SD, Trese MT. Familial exudative vitreoretinopathy. results of surgical management. *Ophthalmology.* (1998) 105:1015–23. doi: 10.1016/S0161-6420(98)96002-X
5. Nudleman E, Muftuoglu IK, Gaber R, Robinson J, Drenser K, Capone A, et al. Glaucoma after lens-sparing vitrectomy for advanced retinopathy of prematurity. *Ophthalmology.* (2018) 125:671–5. doi: 10.1016/j.ophtha.2017.11.009
6. Hartley S, Dauvilliers Y, Quera-Salva M-A. Circadian rhythm disturbances in the blind. *Curr Neurol Neurosci Rep.* (2018) 18:65. doi: 10.1007/s11910-018-0876-9
7. Lyu J, Zhang Q, Zhao P. Use of an iris speculum for retrolental membrane dissection for stage 5 prematurity of retinopathy complicated with pupillary adhesion. *Retina Phila Pa.* (2020) doi: 10.1097/IAE.0000000000002748. [Epub ahead of print].
8. Chiang MF, Quinn GE, Fielder AR, Ostmo SR, Paul Chan RV, Berrocal A, et al. International classification of retinopathy of prematurity, third edition. *Ophthalmology.* (2021) 128:e51–68. doi: 10.1016/j.ophtha.2021.05.031
9. Suzuki A, Kondo N, Terasaki H. High resolution ultrasonography in eyes with angle-closure glaucoma associated with the cicatricial stage of retinopathy of prematurity. *Jpn J Ophthalmol.* (2005) 49:312–4. doi: 10.1007/s10384-004-0206-4
10. Pollard ZF. Lensectomy for secondary angle-closure glaucoma in advanced cicatricial retrolental fibroplasia. *Ophthalmology.* (1984) 91:395–8. doi: 10.1016/S0161-6420(84)34285-3
11. Lakhanpal RR, Fortun JA, Chan-Kai B, Holz ER. Lensectomy and vitrectomy with and without intravitreal triamcinolone acetonide for vascularly active stage 5 retinal detachments in retinopathy of prematurity. *Retina Phila Pa.* (2006) 26:736–40. doi: 10.1097/01.iae.0000244257.60524.89
12. Fei P, Zhang Q, Li J, Zhao P. Clinical characteristics and treatment of 22 eyes of morning glory syndrome associated with persistent hyperplastic primary vitreous. *Br J Ophthalmol.* (2013) 97:1262–7. doi: 10.1136/bjophthalmol-2013-303565
13. Johnson DR, Swan KC. Retrolental fibroplasia-a continuing problem. *Trans Pac Coast Otoophthalmol Soc Annu Meet.* (1966) 47:129–33.
14. Li J-K, Li Y, Zhang X, Chen C-L, Rao Y-Q, Fei P, et al. Spectrum of variants in 389 chinese probands with familial exudative vitreoretinopathy. *Invest Ophthalmol Vis Sci.* (2018) 59:5368–81. doi: 10.1167/iovs.17-23541

Conflict of Interest: The authors declare that the research was conducted in the absence of any commercial or financial relationships that could be construed as a potential conflict of interest.

Publisher's Note: All claims expressed in this article are solely those of the authors and do not necessarily represent those of their affiliated organizations, or those of the publisher, the editors and the reviewers. Any product that may be evaluated in this article, or claim that may be made by its manufacturer, is not guaranteed or endorsed by the publisher.

frontiers | Frontiers in Medicine

ORIGINAL RESEARCH
published: 28 June 2022
doi: 10.3389/fmed.2022.886947

Longitudinal Photoreceptor Phenotype Observation and Therapeutic Evaluation of a Carbonic Anhydrase Inhibitor in a X-Linked Retinoschisis Mouse Model

Meng Liu[1,2], *Jingyang Liu*[1,3], *Weiping Wang*[1,3], *Guangming Liu*[1,3], *Xiuxiu Jin*[1,3] and *Bo Lei*[1,2,3*]

[1] Zhengzhou University People's Hospital, Henan Provincial People's Hospital, Zhengzhou, China, [2] Academy of Medical Sciences, Zhengzhou University, Zhengzhou, China, [3] Henan Eye Institute, Henan Eye Hospital, Henan Provincial People's Hospital, Zhengzhou, China

OPEN ACCESS

Edited by:
Peiquan Zhao,
Shanghai Jiao Tong University, China

Reviewed by:
Timothy W. Kraft,
University of Alabama at Birmingham, United States
Fabrizio Carta,
University of Florence, Italy
J. Jason McAnany,
University of Illinois at Chicago, United States
Xianjun Zhu,
Sichuan Provincial People's Hospital, China

***Correspondence:**
Bo Lei
bolei99@126.com
orcid.org/0000-0002-5497-0905

Specialty section:
This article was submitted to Ophthalmology, a section of the journal Frontiers in Medicine

Received: 01 March 2022
Accepted: 02 June 2022
Published: 28 June 2022

Citation:
Liu M, Liu J, Wang W, Liu G, Jin X and Lei B (2022) Longitudinal Photoreceptor Phenotype Observation and Therapeutic Evaluation of a Carbonic Anhydrase Inhibitor in a X-Linked Retinoschisis Mouse Model. Front. Med. 9:886947. doi: 10.3389/fmed.2022.886947

Purpose: To study the long-term photoreceptor changes and to evaluate the effects of topical application of a carbonic anhydrase inhibitor (CAI) in a mouse model of X-linked retinoschisis (XLRS).

Methods: Conventional electroretinograms (ERGs) and dark-adapted 10-Hz flicker ERGs were recorded in control and *Rs1*$^{-/Y}$ mice generated with CRISPR/Cas9. ON-pathway blocker 2-amino-4-phosphobutyric acid (APB) was injected intravitreally. Morphology was evaluated with histology and optical coherence tomography (OCT). Mice were treated with a CAI inhibitor brinzolamide eye drops (10 mg/ml) three times a day for 3 months. OCT and ERG findings at 1, 4, and 10 months were analyzed.

Results: Negative ERGs and retinal cavities were evident in *Rs1*$^{-/Y}$ mice. Both a-wave and b-wave amplitudes decreased with age when compared with age-matched controls. The APB-isolated a-wave (a′) amplitudes of *Rs1*$^{-/Y}$ mice were reduced in all age groups. In dark-adapted 10-Hz flicker ERG, the amplitude-intensity curve of *Rs1*$^{-/Y}$ mice shifted down. The thickness of ONL and IS/OS decreased in *Rs1*$^{-/Y}$ mice. CAI reduced the splitting retinal cavities but didn't affect the ERG.

Conclusions: In addition to post receptoral impairments, photoreceptor cells underwent progressive dysfunction since early age in *Rs1*$^{-/Y}$ mice. Long-term CAI treatment improved the shrinkage of the splitting retinal cavity, while no functional improvement was observed.

Keywords: retinal degeneration, X-linked juvenile retinoschisis, carbonic anhydrase inhibitor, mouse, *Rs1*, ERG

INTRODUCTION

X-Linked retinoschisis (XLRS) is the leading cause of vision loss in young men, accounting for approximately 5% of all childhood-onset inherited progressive retinal dystrophies (1). XLRS is caused by mutations in RS1 gene and affects males more than females due to its X-linked recessive inheritance (2). A hallmark of the XLRS is the splitting of the retina which frequently presents by

ophthalmoscopy as a "spoke-wheel" pattern on the macula (3, 4). These cavities are readily observed via optical coherence tomography (OCT) (5).

Another hallmark of XLRS is negative electroretinogram (ERG) response. In most cases, the b-wave amplitude is disproportionately lower than the a-wave (6), and the b/a ratio reduces to 1.0 or less. The affected males exhibit normal or nearly normal a-wave (originates from photoreceptors) amplitudes suggesting relatively preserved photoreceptor functions, but substantially reduced b-waves (originates from bipolar cells), implicating defects at or beyond synaptic transmission.

The clinical phenotype of XLRS and the severity of clinical presentation vary at different ages. Young males with XLRS usually have diminished visual acuity at school age (7). Vision usually deteriorates during the first and second decades of life and stays relatively stable until the fifth or sixth decade (8). However, progressive morphology changes are noticeable during this period. The gradual shrinkage of the split cavities in the inner retina is often seen in most cases. More importantly, some patients presenting macular atrophy and loss of macular photoreceptors (9). Nevertheless, although impaired signal transmission beyond the photoreceptors has been extensively studied, mutation associated photoreceptor degeneration in this condition has barely been documented (10, 11). Thus, the first aim of this study was focused on the longitudinal photoreceptor morphology and function changes in a mouse model of XLRS. The importance of such a study is exaggerated by the fact that the RS protein is heavily expressed in the inner segment of photoreceptor and its role in this area has been overlooked.

Recent clinical observations studies have shown that carbonic anhydrase inhibitors (CAIs) may exert multiple benefits for XLRS including reduction of the cystic cavities and modest improvement of vision (12–15). In a relevant study, CAI acted on the membrane-bound carbonic anhydrase IV (CAI-IV) receptors on the retinal pigment epithelium (RPE), and acidified the extracellular space (16). It decreased subretinal space volume by increasing the fluid transport across the RPE through changing the extracellular pH gradients. In XLRS, because the decreased visual acuity was associated with the presence of cystic cavities, it was reasonable to predict that CAI may improve the visual function by reducing the size cysts (17). However, a short-term study on $Rs1^{-/Y}$ mice denied therapeutic effect of CAI (18). To further confirm the potential beneficial roles of CAI in XLRS, we extended the study by a longitudinal observation in mice.

MATERIALS AND METHODS

Generation of $Rs1^{-/Y}$ Mouse Model

The *Rs1* knockout mouse was custom designed in our lab with CRISPR/Cas9 technique. We selected *C57BL/6J* mice as the background strain and targeted *Rs1-201* (NM_011302.3) to design a specific sgRNA to lead Cas9 endonuclease to the target region, and made specific DSBs (double-stranded Breaks) into the genome of mouse followed by non-homologous end joining (NHEJ) repair pathway and excises all coding regions, gRNAs and Cas9 mRNA were transcribed *in vitro* and injected into the pronuclei of fertilized eggs of *C57BL/6J* mouse and implanted into surrogate mothers to obtain founders. Founders were identified by PCR genotyping and confirmed by DNA sequencing analysis. They were then bred with wildtype C57BL/6J to produce generation 1 (F1), and correct transmission of the mutation was identified by PCR genotyping and confirmed by DNA sequencing analysis. Hemizygous male ($Rs1^{-/Y}$) and heterozygous female ($Rs1^{-/+}$) F1 was bred with wildtype *C57BL/6J* mice to establish mouse colonies. The $Rs1^{-/Y}$ mouse model was generated with assistance from Beijing Vital River Laboratory Animal Technologies Co. Ltd (Beijing, China). Animals were housed under 12 h light-dark cycle and given a standard chow diet. Animal care and use followed the guidelines formulated by the Association for Research in Vision and Ophthalmology (ARVO). Experimental designs and procedures were approved by the Ethics Committee of Henan Eye Hospital. Every effort was made to minimize animal discomfort and stress.

PCR Genotyping

Rs1-knockout mice were screened by PCR amplification using tail DNA as the template, with two sets of oligonucleotide primers. One set (Forward: 5′TTAGCACATTCAGAAGAGGAGCGTA3′; Reverse: 5′-CAGTTTAAGGGAAACCTCACTATCCAC-3′) was designed to amplify the wild-type *Rs1* gene, with a product size of 350 bp. The other set primer (Forward: 5′ AGTACCATGCCATTTCAATCTCAACAA3′; Reverse: 5′ CAGTTTAAGGGAAACCTCACTATCCAC3′) was used to detect the mutant *Rs1* gene with a product size of 670 bp.

Western Blot

Total retinal protein (10–50 μg) was loaded onto 10% SDS-PAGE gel. The protein was blotted onto a polyvinylidene difluoride (PVDF) membrane (Millipore, Burlington, MA, USA). Primary Rs1 antibody was used (1:1,000; Sigma-Aldrich, St. Louis, MO, USA). The bands were visualized with HRP-conjugated secondary antibody (Cell Signaling Technology, Beverly, MA, USA) and ECL detection reagents (Millipore).

Intravitreal Injection of APB

2-Amino-4-phosphobutyric acid (APB) was purchased from Sigma-Aldrich (St. Louis, MO). Injection was performed according to a protocol described previously (19, 20). Briefly, the mice were anesthetized with an intraperitoneal injection with a 4% chloralhydrate solution. The pupils were dilated with 0.5% tropicamide drops for at least 10 min prior to injection. An aperture was made through the sclera, below the *ora serrata* with a 30-gauge needle, then a blunt 33-gauge Hamilton syringe was inserted through the aperture, avoiding damage the lens and making sure that a single 1 μl APB/PBS was injected into the vitreous under a dissecting microscope (Leica, DMR, Deerfeld, IL, USA). One μl APB (8.2 mM) was injected intravitreally into the right eyes of the mice, the contralateral eyes were injected with same volume of PBS as control. One drop of Levofloxacin Eye Drops (Cravit® 0.5%) was applied topically after intravitreal injection. After injection, animals were given oxygen and were monitored in a warm recovery enclosure.

Preparation and Application of CAI

Beginning at 1 month of age, brinzolamide eye drops (Azopt® 10 mg/ml) were applied topically to the left eyes of $Rs1^{-/Y}$ mice three times a day with an 8-h interval between applications. The contralateral eyes received instillation of PBS as control. Treatment was continued for 3 months until the mice reached 4 months of age. This treatment timeline permitted us to obtain a pre-treatment baseline (1-month of age), the effects during treatment (4-months of age), and the effect after discounting treatment (10 month of age). Care was taken to avoid spilling of the solution while maintaining the fixation of the animal for at least 1 min. Efforts have been made to ensure exclusive local absorption of the drug by the ocular tissue and to prevent systemic distribution because of self-grooming of the mice after treatment (18).

ERG Assessment

ERG was recorded followed our previous protocols (21). After overnight dark adaptation, mice were anesthetized with intraperitoneal injection with a 4% chloralhydrate solution. Oxybuprocaine hydrochloride eye drops (Benoxil® 0.4%) were applied for ocular surface anesthesia. Mice were placed on a warming pad to maintain body temperature near 38°C. The pupils were dilated with tropicamide eye drops 30 mins prior to recordings. Active electrodes were gently positioned on the center of the cornea. Needle electrodes were subcutaneously inserted into the back and the tail as reference and ground leads respectively. All procedures were performed under dim red light. Full-field ERGs were recorded with a visual electrophysiology system (RetiMINER, AiErXi Medical Equipment Co., Ltd., Chongqing, China). A series of stimulus intensities ranged from −3 to 1 log cd-s/m^2 were applied for dark-adapted ERGs.

For the dark-adapted 10-Hz flicker ERG, the interval between the two consecutive flash trains was set at 200 ms (22). To increase the signal noise ratio, 10 signals were averaged.

Histologic Evaluation

The mice were sacrificed by inhalation of excessive CO_2. Eyes were enucleated and immersed in 4% paraformaldehyde/PBS (PFA/PBS) overnight (21). Fixed eyeballs were embedded in low melting temperature agarose (Sigma-Aldrich, St. Louis, MO) and sectioned. The ONL and INL thickness of inferior and superior retina were measured separately between 500 and 1,000 μm from the optic nerve head. H&E stained sagittal semithin sections including the optic nerve head were evaluated.

OCT

OCT Image Collection

Fundus photography and OCT examinations were performed using a Micron IV retinal imaging system (Phoenix Research Labs, California, USA). The pupils were dilated with 0.5% tropicamide drops for at least 10 mins. The mice were anesthetized with intraperitoneal injection of 4% chloralhydrate solution. Lubricant Eye Gel (Gen Teal® Tears) were applied on the corneal surface to keep the eyes moist. A view of the mouse retina was visible in the bright-field image. Forty OCT images were averaged to enhance the quality of the resulting image. The peripheral retina could be observed by changing the angle between the camera and the eye.

OCT Layer Thickness Measurements

The measurement area was chosen one optic head diameter away from the optic nerve. The thicknesses of the retinal layers were measured from captured images using Insight software (Phoenix Laboratories). As the OCT measurements were taken at the same distance to the optic nerve head, the data were not normalized to the total retinal thickness.

Statistics

All data were presented as mean ± standard error of the mean (SEM). Statistical analysis was undertaken using the GraphPad Prism (GraphPad Prism Software, Inc., San Diego, CA, USA). ONL, INL, and (OS+IS) thickness at three different age groups were analyzed by one-way ANOVA followed by Bonferroni correction for multiple comparisons. The rest results were analyzed by unpaired *t test*. $p < 0.05$ was considered to be statistically significant.

RESULTS

Animal Model

Mouse *Rs1* Gene (Gene ID: 20147) is located on chromosome X and contains of three transcripts, of which *Rs1-201* is the most commonly used. We targeted *Rs1-201* to design a specific sgRNA to lead Cas9 endonuclease to the target region, and made specific DSBs (double-stranded Breaks) into the genome of mouse followed by non-homologous end joining (NHEJ) repair pathway and excises all coding regions. DNA sequencing confirmed deletion of all coding regions. PCR amplification of tail DNA and horizontal gel electrophoresis were performed to verify the successful construction of $Rs1^{-/Y}$ mice. Absence of normal *Rs1h* protein was confirmed by Western blot and immunohistochemistry (IHC) (**Figures 1**, **2**).

Conventional Dark-Adapted ERG

Figure 3A showed a series of dark-adapted ERGs at 4 different ages (1, 4, 6, and 10 months). In $Rs1^{-/Y}$ mice, both the a-wave and b-wave amplitudes (**Figure 3B**) throughout the stimulus intensity range decreased with age. At 1 month, the a-wave and the b-wave amplitudes reduced by 46% and 65% respectively, compared with age-matched control WT mice at 0 log cd.s/m^2 stimulus intensity (**Table 1**).

Because of the interference of b wave, it's insufficient to evaluate photoreceptor function just by the a-wave amplitude. For better understanding of photoreceptor function of $Rs1^{-/Y}$ mice, APB was injected intravitreally to abolish the b-wave. The b-wave of the dark-adapted ERG is dominated by ON bipolar cell responses which can be excluded by APB. However, APB does not eliminate OFF bipolar cell activity, which can be eliminated by PDA. Nevertheless, the OFF-pathway contribution was proved to be minimal in mouse a-wave (22). Therefore, the residual a′ wave reflected purely the response of photoreceptor cells. About 90 mins after the injection, the dark-adapted ERG b-wave was eliminated (**Figure 4**), and the a′ wave was dominant at high

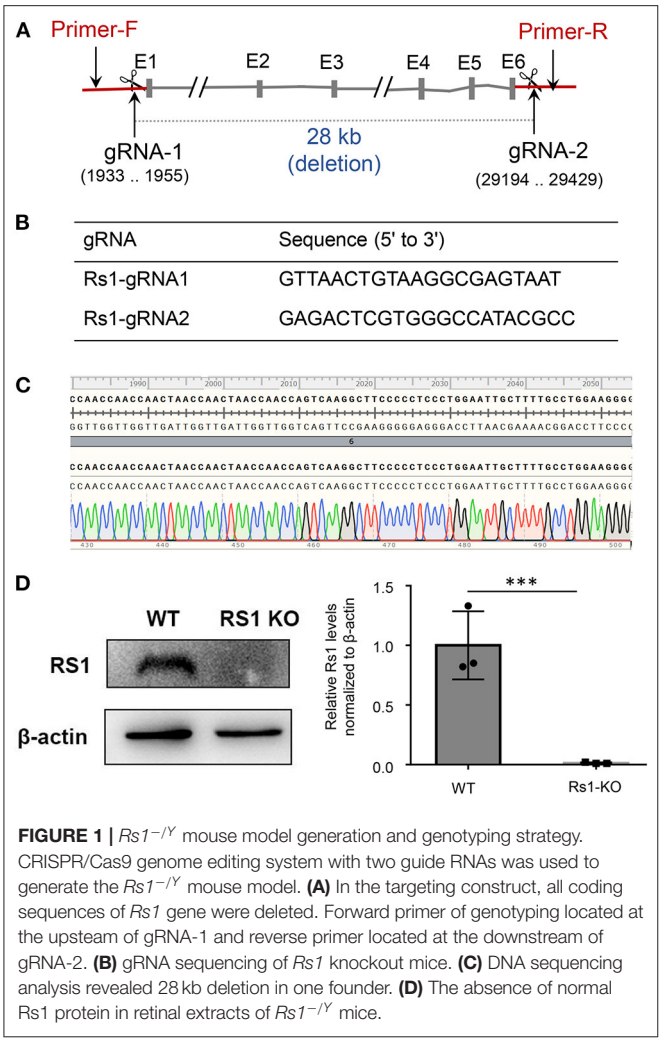

FIGURE 1 | *Rs1*$^{-/Y}$ mouse model generation and genotyping strategy. CRISPR/Cas9 genome editing system with two guide RNAs was used to generate the *Rs1*$^{-/Y}$ mouse model. **(A)** In the targeting construct, all coding sequences of *Rs1* gene were deleted. Forward primer of genotyping located at the upsteam of gRNA-1 and reverse primer located at the downstream of gRNA-2. **(B)** gRNA sequencing of *Rs1* knockout mice. **(C)** DNA sequencing analysis revealed 28 kb deletion in one founder. **(D)** The absence of normal Rs1 protein in retinal extracts of *Rs1*$^{-/Y}$ mice.

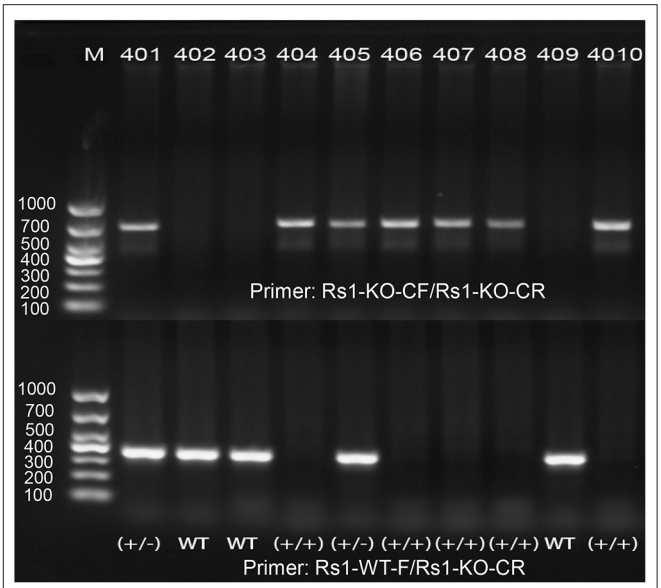

FIGURE 2 | PCR amplification demonstrates the correct targeting of *Rs1*gene. One band of 350 bp was shown in WT, one band of 670 bp was shown in *Rs1*$^{-/Y}$ mice, and both bands of 350 and 670 bp were shown in heterozygote.

intensities. The a′ wave amplitude of *Rs1*$^{-/Y}$ mice (0 log cd-s/m^2) decreased significantly compared with age-matched WT mice (**Table 2**).

And the a′ wave also declined with age. Furthermore, the a′/a ratio, which reflected the relative potential of light elicited photoreceptor response, also declined in *Rs1*$^{-/Y}$ mice when compared with WT mice. The ratio also decreased with age, further suggesting that the photoreceptor function of *Rs1*$^{-/Y}$ mice declined as the disease progresses.

The Dark-Adapted 10-Hz Flicker ERG

The dark-adapted flicker ERG is practical for evaluation of rod- and cone-driven responses simultaneously. Dark-adapted 10-Hz flicker ERGs of WT, and *Rs1*$^{-/Y}$ mice at 3 different ages were shown (**Figures 5**, **6**), and **Figure 5** showed the amplitude-intensity profiles ($n = 3$ in each age group). There were two peaks in the middle and high light intensities in the WT mice, with the first representing rod-driven and the second representing cone-driven responses.

In 1 month old *Rs1*$^{-/Y}$ mice, both the rod- and the cone-driven responses existed, while the amplitude-intensity curve shifted down significantly. The curve of the 6-month-old *Rs1*$^{-/Y}$ mice was similar to the curve at 1-month-old, except for a lower of the cone-driven response. In 10-months-old group, the rod-driven response still existed although significantly declined, but the cone-driven response was not detectable, suggesting the cone system was more vulnerable than the rod system in this model **Figure 7**.

Morphological Abnormalities

We monitored the morphological changes of *Rs1*$^{-/Y}$ mice at three different ages ($n = 4$ in each age group) by histology analysis and OCT (**Figure 8**). Large cavities within the INL were the most striking in 1-month-old Rs1$^{-/Y}$ mouse retina, and the splitting cavities gradually collapsed and shrunk at 6 and 10 months. Thickness of the retinal layers was measured on histologic sections. At 1 month, the thickness of ONL was not significantly different from WT, while the structure of the ONL was disrupted with some nuclei were displaced into the OPL and the inner segment layers. The ONL thickness declined rapidly at 6 and 10 months. The INL thickness of 1-month-old *Rs1*$^{-/Y}$ mice was larger than WT, due to the cavities within INL. With the subsequent collapse of splitting cavities, the INL became thinner gradually, but it was still thicker in *Rs1*$^{-/Y}$ mice than the age-marched WT. The thickness of OS+IS in *Rs1*$^{-/Y}$ mice decreased compared with WT at 1 month, and continued to diminish at 6 and 10 months (**Figure 8B**). OCT images of WT retina showed normal organized lamellar structure while the *Rs1*$^{-/Y}$ mouse retina showed abnormalities corresponding to those observed in

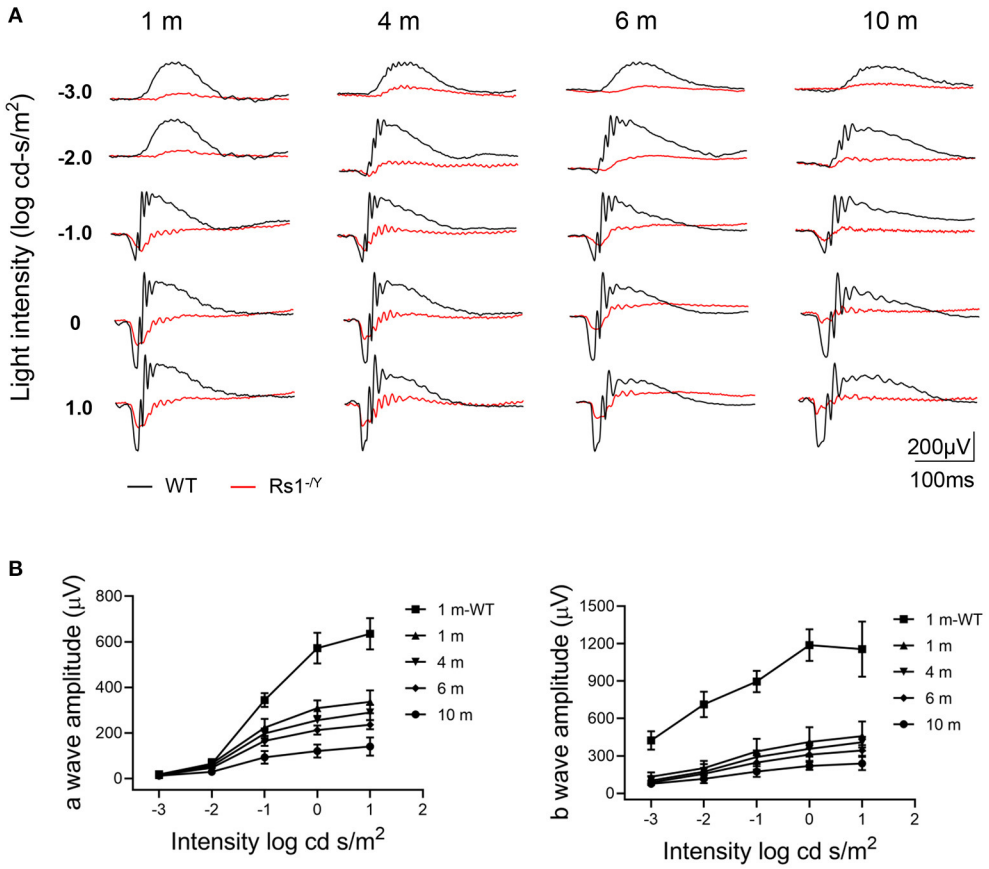

FIGURE 3 | Representative ERG amplitude changes with age in *Rs1*$^{-/Y}$ mice and age-matched WT mice. **(A)** A series of dark-adapted ERGs of *Rs1*$^{-/Y}$ and WT mice of different ages (1, 4, 6, and 10 months). **(B)** a-Wave V-log I, b-wave V-log I. $n = 9$ at each age group. WT, wild type; ERG, electroretinogram.

TABLE 1 | a-Wave and the b-wave amplitudes (0 log cd.s/m^2).

	a-wave Mean ± SE (μV)	b-wave Mean ± SE (μV)	*n*
Rs1$^{-/Y}$ (1 m)	309 ± 11	411 ± 39	9
WT (1 m)	572 ± 22	1,188 ± 42	9

histology sections, and these changes were seen across the retina from center to periphery.

CAI Treatment

We tested the potential beneficial effects of long-term CAI treatment in the *Rs1*$^{-/Y}$ mouse retina. The left eyes of 1-month-old *Rs1*$^{-/Y}$ mice were treated with brinzolamide eye drops (3 times a day for 3 consecutive months), while the right eyes were treated with PBS as control. For a detailed evaluation of retinal function and structure, ERGs and OCT were performed at three time points (1, 4, 10 months of age) ($n = 6$ in each age group). At 1 month of age, the laminar structure of *Rs1*$^{-/Y}$ mice was disrupted, and the thickness of ONL, INL showed no difference between the two eyes. After 3 months' treatment, the splitting cavities of the treated eyes were smaller, and the INL thickness decreased compared with the control eyes, while no difference in ONL thickness was observed between the two eyes. The cavities in INL continued to reduce and disappeared at the age of 10 months, but the thickness of ONL and the INL showed no difference between the two eyes. Additionally, the amplitudes of ERG a- and b-wave were similar between the treated and control eyes at all three time points (**Figure 9**).

DISCUSSION

Photoreceptors, including rods and cones, and bipolar cells are the first two order neuros in the retina. As all the three types of cells express RS1 protein, causative mutations in *RS1* gene may induce morphologic and functional damages to all these cells. However, because the most striking features of XLRS are the cystic cavities in the INL and the negative ERG waveform, both of which are convictive indicators of impairment in the inner retina, the photoreceptor impairment has relatively been overlooked. However, increasing studies reported a reduction in ERG a-wave of young XLRS patients (23, 24), indicating photoreceptor degeneration may be more prevalent in XLRS than previously thought.

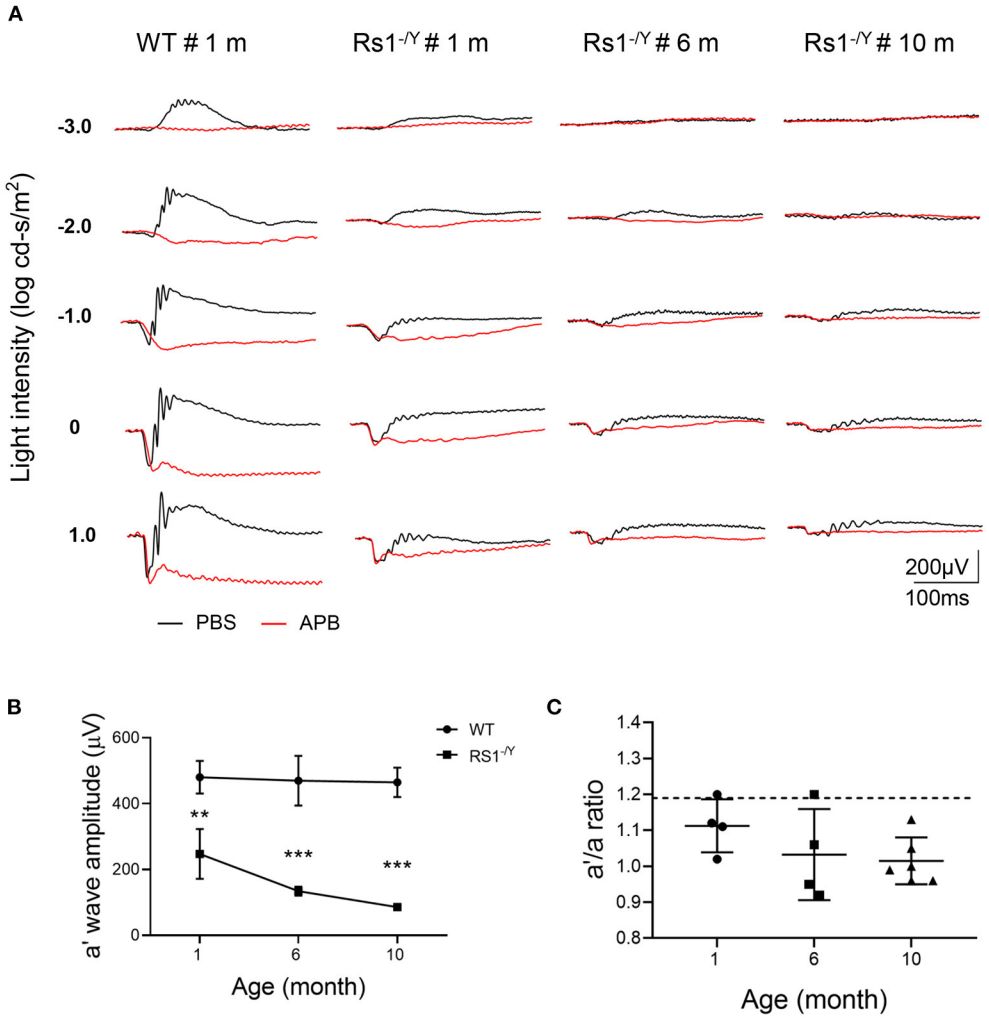

FIGURE 4 | The effect of APB on the dark-adapted ERG of *Rs1*$^{-/Y}$ mice and and age-matched WT mice. **(A)** The black traces show ERGs of the PBS-injected control eyes and the red traces show ERGs of the APB injected eyes. In the APB-injected eye, the a-wave remains but the b-waves are absent. **(B)** Left: The a′ wave amplitude changes with age in *Rs1*$^{-/Y}$ mice of 1, 6, and 10 month old. ERG stimulus, 0 log cd-s/m^2. **(C)** Right: a′/a ratio in *Rs1*$^{-/Y}$ mice of three different ages (1, 6, and 10 months). Dashed lines: the a′/a ratio mean ± SE of WT: 1.190 ± 0.127 $n = 5$. a′ wave: the negative wave in APB injected eye; APB, 2-amino-4-phosphobutyric acid. *Rs1*$^{-/Y}$ results compared to WT using Student's t-test: ***, $P < 0.001$.

TABLE 2 | a' wave of different age groups (0 log cd.s/m^2).

	1 m	6 m	10 m
Rs1$^{-/Y}$	247 ± 31 ($n = 6$)	134 ± 7 ($n = 4$)	86 ± 4 ($n = 5$)
WT	480 ± 29 ($n = 3$)	470 ± 44 ($n = 3$)	465 ± 26 ($n = 3$)

Initial evidence of abnormal cone system function came primally from photopic ERG responses recorded in patients with XLRS: Alexander et al. reported that high-frequency response attenuation of the ERG in XLRS indicated abnormalities of the photoreceptors and depolarizing bipolar cells (DBCs) (25, 26). Multifocal electroretinogram (mfERG) revealed that the cone-mediated retinal responses were more impaired in the central than peripheral retina of XLRS patients (27). A recent study that re-examined photoreceptor and post-receptor ERG responses found smaller a-wave amplitudes in some young XLRS patients (23). In addition, some XLRS animal models also showed decreased a-wave amplitude at early age. For example, Liu's group demonstrated several disease phenotypes which presented at early ages in three *Rs1* mutant mouse models. Each model developed intraretinal schisis with OCT and showed early abnormalities in outer retina neurons with immunohistochemical analysis. In consistent with the morphological changes, the decrease of ERG b-wave amplitude was more prominent than the a-wave, but the a-wave was already abnormal at P15 and remained decreased till later stage (28). These findings indicated that although the major defects were in the inner retina, outer retina photoreceptor degeneration could present concurrently. In this study, we also found that a-wave reduced significantly compared with age-matched WT mice, and

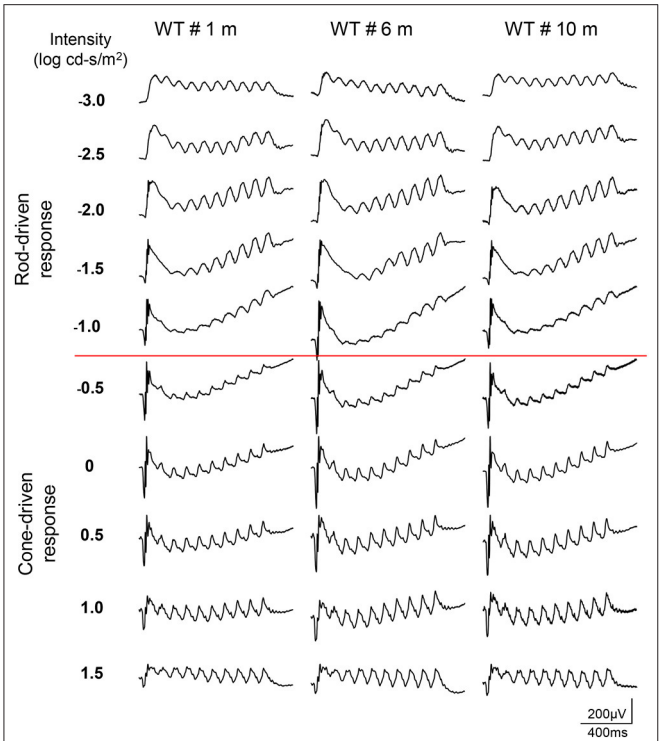

FIGURE 5 | Dark-adapted 10-Hz flicker ERGs elicited with a series of light intensity in WT mice of different ages.

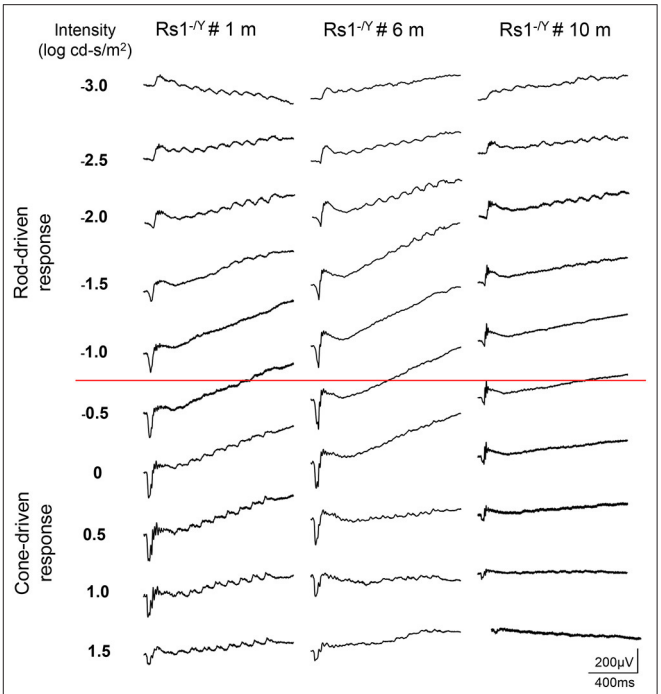

FIGURE 6 | Dark-adapted 10-Hz flicker ERGs elicited with a series of light intensity in *Rs1*$^{-/Y}$ mice of different ages.

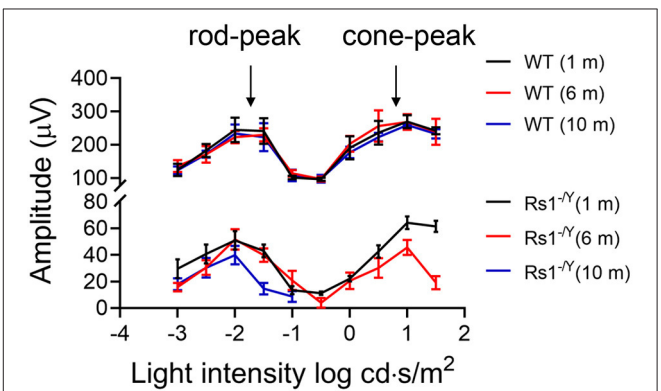

FIGURE 7 | Dark-adapted 10-Hz flicker ERG response amplitude-intensity profiles ($n = 3$ at each age group).

underwent a processive decline over time. At the same time, we found the cone system function of *Rs1*$^{-/Y}$ mice was more vulnerable than the rod system. To rule out the interference of the second order neurons, intravitreal injection of APB was applied to eliminate the b-wave. The residual a′ wave were presumably purely generated from the photoreceptors. We found that the a′ wave amplitude decreased compared with age-matched WT mice at all three age groups, and displayed a decreasing trend with age. This provided further evidence that the *Rs1*$^{-/Y}$ photoreceptor suffered from degeneration starting at early age and underwent progressive decline. However, this phenotype appeared more severe at early stage in *Rs1*$^{-/Y}$ mice than in most XLRS patients. It was reported that decreased a-wave amplitude was observed in about 1/3 of XLRS patients (29). Because photoreceptors are not regenerable, it is of great importance to evaluate their function and structure to predict the prognosis of emerging interventions. Understanding the status of photoreceptors may raise significant concerns to these crucial cells and encourage early treatment for this condition.

Except for the split cavities, abnormalities in the outer retina were also observed by OCT examinations in patients with XLRS (30, 31). All the 7 XLRS mouse models together with the *Rs1*$^{-/Y}$ rat model presented different rates of retinal degeneration (32–37). Our *Rs1*$^{-/Y}$ mice displayed similar inner retinal morphology changes and progressive loss of photoreceptors which led to a markedly reduced ONL thickness. Good corrections between the a-wave amplitude and the ONL, OS+IS thickness may partially explain the progressive reduction in overall ERG response, as has been found for other animal models with primary photoreceptor degeneration (38). It has been suggested that RS1 modulates cellular homeostasis by binding to Na/K-ATPase (39, 40). RS1 could affected the Na/K-ATPase-regulated mitogen-activated protein kinase /extracellular-signal-regulated kinase (MAPK/ERK) signaling cascade and Ca^{2+} signaling. These studies provided evidence that RS1 deficiency might be one of the initial steps that triggered XLRS pathology in retinal degeneration, rather than just the acknowledged adhesive interactions on retinal structure in inner retina.

Both XLRS patients and animal models showed natural evolution of the cystic cavities, which typically collapsed

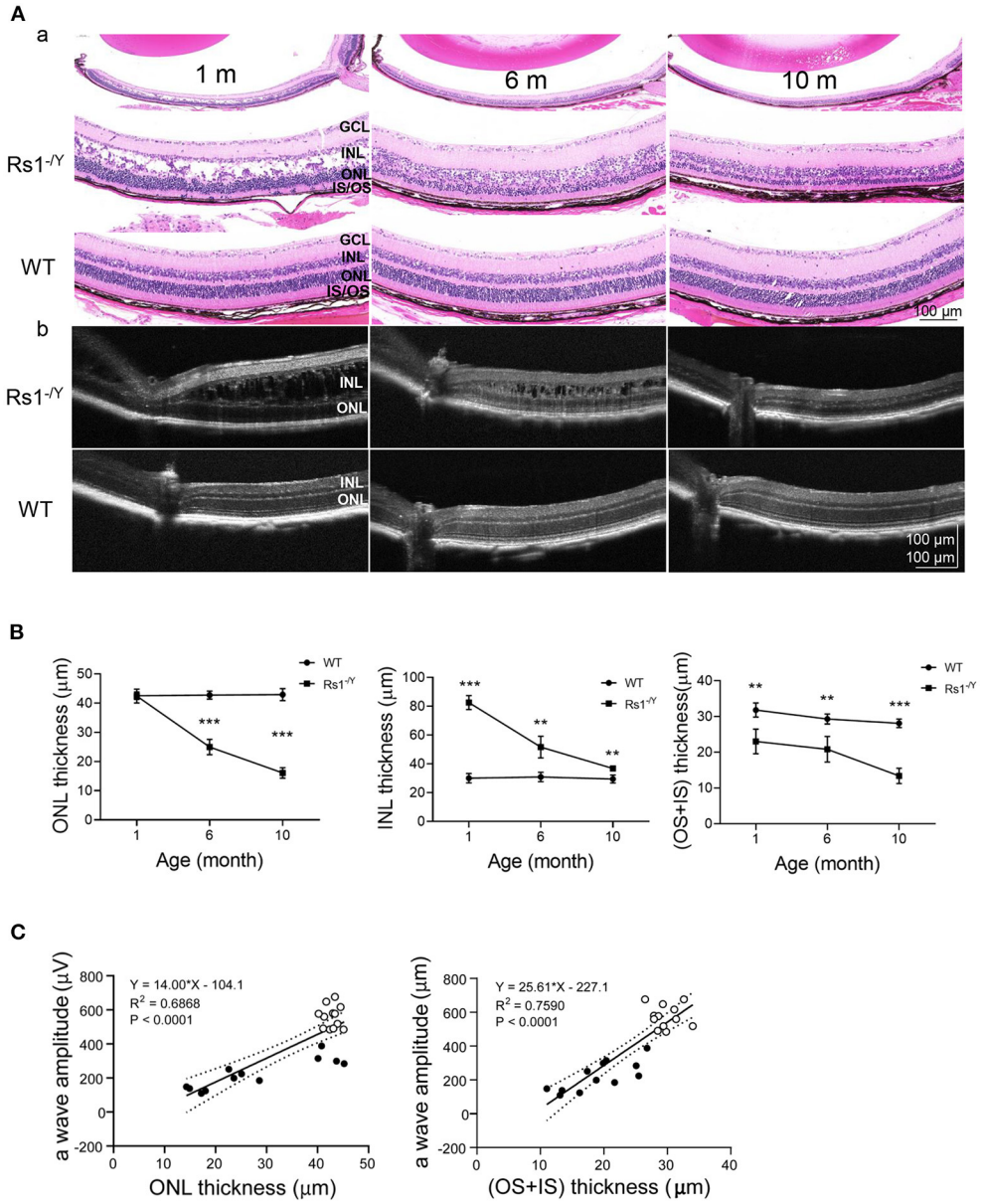

FIGURE 8 | Morphology changes in *Rs1*$^{-/Y}$ mouse and age-matched WT mice. **(A)** Representative sections from retinas of 1, 6, and 10-month-old *Rs1*$^{-/Y}$ mice and age-matched WT mice and retinal images obtained from OCT were used to evaluate the retinal morphology at three different ages. **(B)** The thickness of the ONL, INL, OS+IS 300 μm away from the optic nerve was measured ($n = 4$ at each age group). **(C)** a-Wave amplitude vs. OS+IS thickness. *Lines*: linear regression ($R^2 = 0.7590$) and 95% confidence intervals. a-Wave amplitude vs. ONL thickness. *Lines*: linear regression ($R^2 = 0.6868$) and 95% confidence intervals, $P < 0.0001$; ONL, outer nuclear layer; INL, inner nuclear layer; OS, outer segment; IS, inner segment. *Rs1*$^{-/Y}$ results compared to WT using Student's t-test: *, $P < 0.05$; **, $P < 0.01$; ***, $P < 0.001$.

overtime. Since cystic presence has been linked to decreased visual acuity (41), it was conjectured that CAI might improve the acuity and decrease the later-onset atrophy in XLRS, by reducing fluid accumulation in the cavities. We found CAI reduced cystic cavity volume in *Rs1*$^{-/Y}$ mice, while no functional improvement was detected in term of ERG responses, which were comparable to the results of clinical trials in human XLRS subjects (42–44). The reasons that the discordance between the structure and function after CAI application remained unknown. One interpretation could be the progressive structural deterioration presenting in the outer retina, including IS/OS, gap junctions, and synapses, which are indispensable for the generation of ERG. However, those damages could not be reversed by CAI treatment alone. It could also be due to the early nerve damage might occur before the treatment began. Therefore, earlier CAI intervention starting from eye opening might be more effective. Besides, the

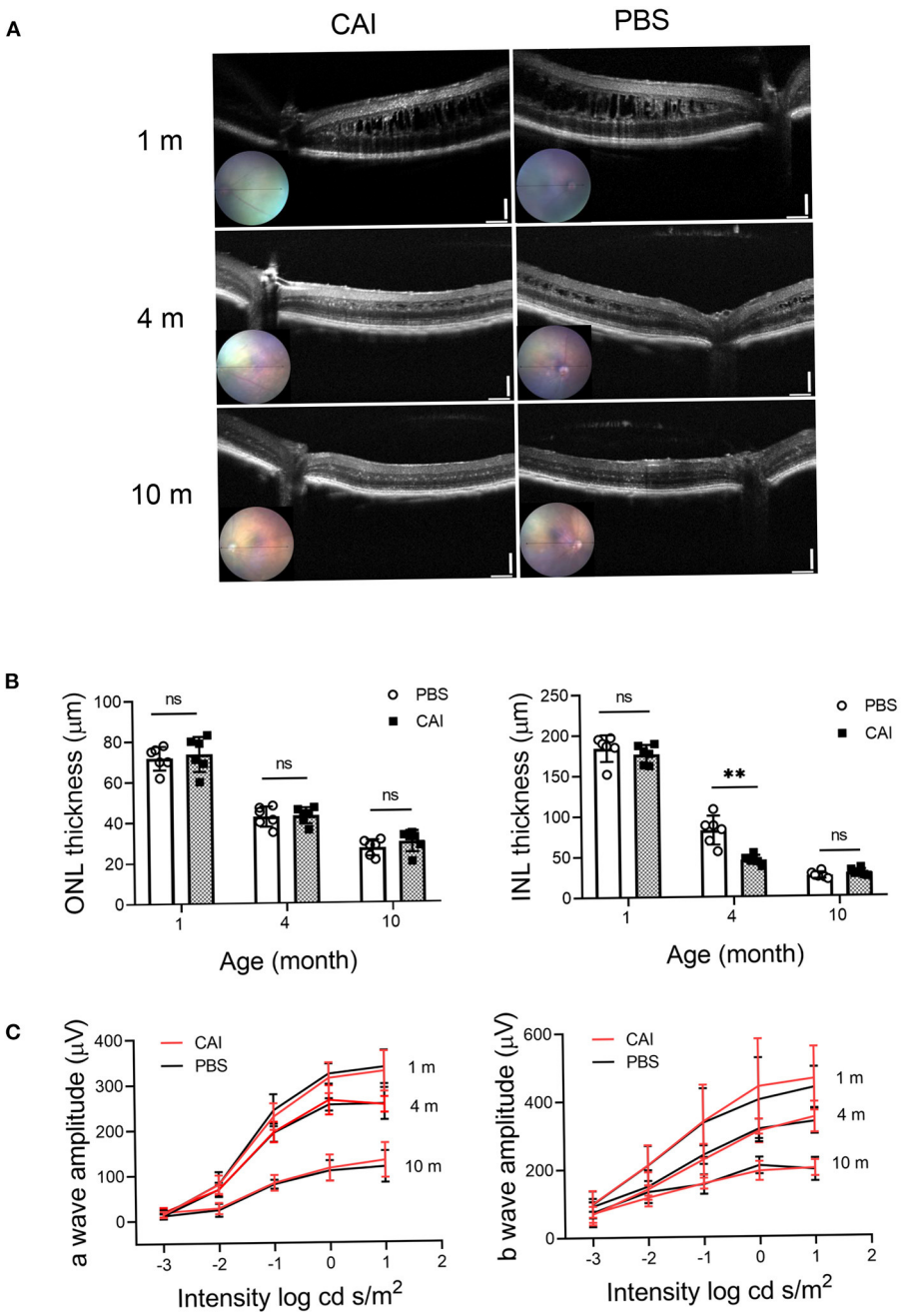

FIGURE 9 | Structural and functional changes after CAI treatment in *Rs1*$^{-/Y}$ mice retina were evaluated by OCT and ERG. **(A)** Retinal images obtained from OCT in living animals were used to evaluate the retinal morphology at 3 different ages. From 1 month, the left eyes of *Rs1*$^{-/Y}$ mice were treated with brinzolamide eye drops (10 mg/ml) for 3 continuous months, the contralateral eyes were treated with PBS as control. OCT were performed at 1, 4, 10 months of age. **(B)** ONL and INL thickness were measured from 200 to 1,200 μm inferior and superior to the optic nerve ($n = 6$ at each time point). **(C)** Functional changes by CAI treatment in *Rs1*$^{-/Y}$ mice retina were evaluated by ERG. The CAI treated eyes were compared with the control eyes using Student's *t*-test: ***, $P < 0.001$. CAI, carbonic anhydrase inhibitor; OCT, optical coherence tomography.

effect of selective inhibitors on the enzymatic isoforms expressed in the retinal/eye tissues deserves further research. Nevertheless, accelerated shrinkage of the splitting cavity by CAI could be helpful in restoring retinal anatomy, prolong the therapeutic time window for gene therapy, and thereby improve the therapeutic effect (45, 46).

In summary, we documented that photoreceptor cells underwent progressive dysfunction since early stage in an XLRS

mouse model. And the cones are more vulnerable to the genetic defect than the rods. In addition, long-term CAI treatment was beneficial in promoting the shrinkage of the splitting cavity in $Rs1^{-/Y}$ mice, while functional improvement was not observed. Nevertheless, CAI might be an adjunct medication to the emerging gene therapy for XLRS.

DATA AVAILABILITY STATEMENT

The original contributions presented in the study are included in the article/supplementary material, further inquiries can be directed to the corresponding author/s.

ETHICS STATEMENT

The animal study was reviewed and approved by Ethics Committee of Henan Eye Hospital, Henan Provincial People's Hospital.

AUTHOR CONTRIBUTIONS

BL contributed to the conceptualization, design, and outline of this review. ML conducted the experiments and prepared the draft of the manuscript. JL, WW, and GL helped in the experiment procedures. BL, XJ, and ML contributed to analyzing data, revision, and editing. All authors have read and approved the final manuscript.

FUNDING

This work was supported by grants from the National Natural Science Foundation of China (81770949 and 82071008), Key Technologies Research and Development Program of Henan Science and Technology Bureau (212102310307), and Medical Science and Technology Program of Health Commission of Henan Province (SBGJ202003014 and LHGJ20200070).

REFERENCES

1. De Silva SR, Arno G, Robson AG, Fakin A, Pontikos N, Mohamed MD, et al. The X-linked retinopathies: physiological insights, pathogenic mechanisms, phenotypic features and novel therapies. *Prog Retin Eye Res.* (2021) 82:100898. doi: 10.1016/j.preteyeres.2020.100898
2. Takada Y, Fariss RN, Muller M, Bush RA, Rushing EJ, Sieving PA. Retinoschisin expression and localization in rodent and human pineal and consequences of mouse RS1 gene knockout. *Mol Vis.* (2006) 12:1108–16. doi: 10.0000/PMID17093404
3. Fahim AT, Ali N, Blachley T, Michaelides M. Peripheral fundus findings in X-linked retinoschisis. *Br J Ophthalmol.* (2017) 101:1555–9. doi: 10.1136/bjophthalmol-2016-310110
4. Smith LM, Cernichiaro-Espinosa LA, McKeown CA, Tekin M, Lam BL, Chiang J, et al. X-linked peripheral retinoschisis without macular involvement: a case series with RS1 genetic confirmation. *Ophthalmic Genet.* (2020) 41:57–62. doi: 10.1080/13816810.2020.1723115
5. Abalem MF, Musch DC, Birch DG, Pennesi ME, Heckenlively JR, Jayasundera T. Diurnal variations of foveoschisis by optical coherence tomography in patients with RS1 X-linked juvenile retinoschisis. *Ophthalmic Genet.* (2018) 39:437–42. doi: 10.1080/13816810.2018.1466340
6. Ou J, Vijayasarathy C, Ziccardi L, Chen S, Zeng Y, Marangoni D, et al. Synaptic pathology and therapeutic repair in adult retinoschisis mouse by AAV-RS1 transfer. *J Clin Invest.* (2015) 125:2891–903. doi: 10.1172/JCI81380
7. Kjellström S, Vijayasarathy C, Ponjavic V, Sieving PA, Andréasson S. Long-term 12 year follow-up of X-linked congenital retinoschisis. *Ophthal Genet.* (2010) 31:114–25. doi: 10.3109/13816810.2010.482555
8. Wood EH, Lertjirachai I, Ghiam BK, Koulisis N, Moysidis SN, Dirani A, et al. The natural history of congenital X-linked retinoschisis and conversion between phenotypes over time. *Ophthalmol Retina.* (2019) 3:77–82. doi: 10.1016/j.oret.2018.08.006
9. Xiao Y, Liu X, Tang L, Wang X, Coursey TG, Guo X, et al. X-linked retinoschisis: phenotypic variability in a Chinese family. *Sci Rep.* (2016) 6:20118. doi: 10.1038/srep20118
10. Bradshaw K, Newman D, Allen L, Moore A. Abnormalities of the scotopic threshold response correlated with gene mutation in X-linked retinoschisis and congenital stationary night blindness. *Adv Ophthalmol.* (2003) 107:155–64. doi: 10.1023/A:1026245931580
11. Eksandh L, Andréasson S, Abrahamson M. Juvenile X-linked retinoschisis with normal scotopic b-wave in the electroretinogram at an early stage of the disease. *Ophthalmic Genet.* (2005) 26:111–7. doi: 10.1080/13816810500228688
12. Coussa RG, Kapusta MA. Treatment of cystic cavities in X-linked juvenile retinoschisis: the first sequential cross-over treatment regimen with dorzolamide. *Am J Ophthalmol Case Rep.* (2017) 8:1–3. doi: 10.1016/j.ajoc.2017.07.008
13. Genead MA, Fishman GA, Walia S. Efficacy of sustained topical dorzolamide therapy for cystic macular lesions in patients with X-linked retinoschisis. *Arch Ophthalmol* (Chicago, Ill: 1960). (2010) 128:190–7. doi: 10.1001/archophthalmol.2009.398
14. Salvatore S, Fishman GA, Genead MA. Treatment of cystic macular lesions in hereditary retinal dystrophies. *Surv Ophthalmol.* (2013) 58:560–84. doi: 10.1016/j.survophthal.2012.11.006
15. Thangavel R, Surve A, Azad S, Kumar V. Dramatic response to topical dorzolamide in X-linked retinoschisis. *Indian J Ophthalmol.* (2020) 68:1466–7. doi: 10.4103/ijo.IJO_2061_19
16. Ambrosio L, Williams JS, Gutierrez A, Swanson EA, Munro RJ, Ferguson RD, et al. Carbonic anhydrase inhibition in X-linked retinoschisis: an eye on the photoreceptors. *Exp Eye Res.* (2021) 202:108344. doi: 10.1016/j.exer.2020.108344
17. Thobani A, Fishman GA. The use of carbonic anhydrase inhibitors in the retreatment of cystic macular lesions in retinitis pigmentosa and X-linked retinoschisis. *Retina (Philadelphia, Pa).* (2011) 31:312–5. doi: 10.1097/IAE.0b013e3181e587f9
18. Zhour A, Bolz S, Grimm C, Willmann G, Schatz A, Weber BH, et al. In vivo imaging reveals novel aspects of retinal disease progression in Rs1h(-/Y) mice but no therapeutic effect of carbonic anhydrase inhibition. *Vet Ophthalmol.* (2012) 15 Suppl 2:123–33. doi: 10.1111/j.1463-5224.2012.01039.x
19. Qiu Y, Tao L, Zheng S, Lin R, Fu X, Chen Z, et al. AAV8-mediated angiotensin-converting enzyme 2 gene delivery prevents experimental autoimmune uveitis by regulating MAPK, NF-κB and STAT3 pathways. *Sci Rep.* (2016) 6:31912. doi: 10.1038/srep31912
20. Lin R, Fu X, Lei C, Yang M, Qiu Y, Lei B. Intravitreal injection of amyloid β1-42 activates the complement system and induces retinal inflammatory responses and malfunction in mouse. *Adv Exp Med Biol.* (2019) 1185:347–52. doi: 10.1007/978-3-030-27378-1_57
21. Lei C, Lin R, Wang J, Tao L, Fu X, Qiu Y, et al. Amelioration of amyloid β-induced retinal inflammatory responses by a LXR agonist TO901317 is associated with inhibition of the NF-κB signaling and NLRP3 inflammasome. *Neuroscience.* (2017) 360:48–60. doi: 10.1016/j.neuroscience.2017.07.053
22. Lei B. Rod-driven OFF pathway responses in the distal retina: dark-adapted flicker electroretinogram in mouse. *PLoS ONE.* (2012) 7:e43856. doi: 10.1371/journal.pone.0043856
23. Ambrosio L, Hansen RM, Kimia R, Fulton AB. Retinal function in x-linked juvenile retinoschisis. *Invest Ophthalmol Vis Sci.* (2019) 60:4872–81. doi: 10.1167/iovs.19-27897

24. Vincent A, Robson AG, Neveu MM, Wright GA, Moore AT, Webster AR, et al. A phenotype-genotype correlation study of X-linked retinoschisis. *Ophthalmology.* (2013) 120:1454–64. doi: 10.1016/j.ophtha.2012.12.008
25. Alexander KR, Barnes CS, Fishman GA. High-frequency attenuation of the cone ERG and ON-response deficits in X-linked retinoschisis. *Invest Ophthalmol Vis Sci.* (2001) 42:2094–101. doi: 10.1007/s004170100325
26. Alexander KR, Fishman GA, Barnes CS, Grover S. On-response deficit in the electroretinogram of the cone system in X-linked retinoschisis. *Invest Ophthalmol Vis Sci.* (2001) 42:453–9. doi: 10.1007/s004170000246
27. Piao CH, Kondo M, Nakamura M, Terasaki H, Miyake Y. Multifocal electroretinograms in X-linked retinoschisis. *Invest Ophthalmol Vis Sci.* (2003) 44:4920–30. doi: 10.1167/iovs.02-1270
28. Liu Y, Kinoshita J, Ivanova E, Sun D, Li H, Liao T, et al. Mouse models of X-linked juvenile retinoschisis have an early onset phenotype, the severity of which varies with genotype. *Hum Mol Genet.* (2019) 28:3072–90. doi: 10.1093/hmg/ddz122
29. Bowles K, Cukras C, Turriff A, Sergeev Y, Vitale S, Bush RA, et al. X-linked retinoschisis: RS1 mutation severity and age affect the ERG phenotype in a cohort of 68 affected male subjects. *Invest Ophthalmol Vis Sci.* (2011) 52:9250–6. doi: 10.1167/iovs.11-8115
30. Yang HS, Lee JB, Yoon YH, Lee JY. Correlation between spectral-domain OCT findings and visual acuity in X-linked retinoschisis. *Invest Ophthalmol Vis Sci.* (2014) 55:3029–36. doi: 10.1167/iovs.14-13955
31. Guo Q, Li Y, Li J, You Y, Liu C, Chen K, et al. Phenotype heterogeneity and the association between visual acuity and outer retinal structure in a cohort of Chinese X-Linked juvenile retinoschisis patients. *Front Genet.* (2022) 13:832814. doi: 10.3389/fgene.2022.832814
32. Ziccardi L, Vijayasarathy C, Bush RA, Sieving PA. Loss of retinoschisin (RS1) cell surface protein in maturing mouse rod photoreceptors elevates the luminance threshold for light-driven translocation of transducin but not arrestin. *J Neurosci.* (2012) 32:13010–21. doi: 10.1523/JNEUROSCI.1913-12.2012
33. Zeng Y, Takada Y, Kjellstrom S, Hiriyanna K, Tanikawa A, Wawrousek E, et al. RS-1 gene delivery to an adult Rs1h knockout mouse model restores ERG b-wave with reversal of the electronegative waveform of X-linked retinoschisis. *Invest Ophthalmol Vis Sci.* (2004) 45:3279–85. doi: 10.1167/iovs.04-0576
34. Weber BH, Schrewe H, Molday LL, Gehrig A, White KL, Seeliger MW, et al. Inactivation of the murine X-linked juvenile retinoschisis gene, Rs1h, suggests a role of retinoschisin in retinal cell layer organization and synaptic structure. *Proc Natl Acad Sci USA.* (2002) 99:6222–7. doi: 10.1073/pnas.092528599
35. Zeng Y, Qian H, Campos MM Li Y, Vijayasarathy C, Sieving PA. Rs1h(-/y) exon 3-del rat model of X-linked retinoschisis with early onset and rapid phenotype is rescued by RS1 supplementation. *Gene Ther.* (2021). doi: 10.1038/s41434-021-00290-6
36. Chen D, Xu T, Tu M, Xu J, Zhou C, Cheng L, et al. Recapitulating X-linked juvenile retinoschisis in mouse model by knock-in patient-specific novel mutation. *Front Mol Neurosci.* (2017) 10:453. doi: 10.3389/fnmol.2017.00453
37. Jablonski MM, Dalke C, Wang X, Lu L, Manly KF, Pretsch W, et al. An ENU-induced mutation in Rs1h causes disruption of retinal structure and function. *Mol Vis.* (2005) 11:569–81. doi: 10.1016/j.visres.2005.04.008
38. Kolesnikov AV, Tang PH, Kefalov VJ. Examining the role of cone-expressed RPE65 in mouse cone function. *Sci Rep.* (2018) 8:14201. doi: 10.1038/s41598-018-32667-w
39. Plössl K, Royer M, Bernklau S, Tavraz NN, Friedrich T, Wild J, et al. Retinoschisin is linked to retinal Na/K-ATPase signaling and localization. *Mol Biol Cell.* (2017) 28:2178–89. doi: 10.1091/mbc.e17-01-0064
40. Plössl K, Straub K, Schmid V, Strunz F, Wild J, Merkl R, et al. Identification of the retinoschisin-binding site on the retinal Na/K-ATPase. *PLoS ONE.* (2019) 14:e0216320. doi: 10.1371/journal.pone.0216320
41. Miller K, Fortun JA. Diabetic macular edema: current understanding, pharmacologic treatment options, and developing therapies. *Asia-Pacific J Ophthalmol (Philadelphia, Pa).* (2018) 7:28–35. doi: 10.22608/APO.2017529
42. Kousal B, Hlavata L, Vlaskova H, Dvorakova L, Brichova M, Dubska Z, et al. Clinical and genetic study of X-linked juvenile retinoschisis in the Czech Population. *Genes.* (2021) 12:1816.doi: 10.3390/genes12111816
43. Ghajarnia M, Gorin MB. Acetazolamide in the treatment of X-linked retinoschisis maculopathy. *Arch Ophthalmol.* (Chicago, Ill: 1960). (2007) 125(4):571-3.doi: 10.1001/archopht.125.4.571
44. Andreuzzi P, Fishman GA, Anderson RJ. Use of a carbonic anhydrase inhibitor in X-linked retinoschisis: effect on cystic-appearing macular lesions and visual acuity. *Retina (Philadelphia, Pa).* (2017) 37:1555–61. doi: 10.1097/IAE.0000000000001379
45. Verbakel SK, van de Ven JP, Le Blanc LM, Groenewoud JM, de Jong EK, Klevering BJ, et al. Carbonic anhydrase inhibitors for the treatment of cystic macular lesions in children with X-linked juvenile retinoschisis. *Invest Ophthalmol Vis Sci.* (2016) 57:5143–7. doi: 10.1167/iovs.16-20078
46. Vijayasarathy C, Sardar Pasha SPB, Sieving PA. Of men and mice: Human X-linked retinoschisis and fidelity in mouse modeling. *Prog Retin Eye Res.* (2022) 87:100999. doi: 10.1016/j.preteyeres.2021.100999

Conflict of Interest: The authors declare that the research was conducted in the absence of any commercial or financial relationships that could be construed as a potential conflict of interest.

The reviewer XZ declared a past co-authorship with the author BL to the handling editor.

frontiers | Frontiers in Medicine

TYPE Original Research
PUBLISHED 03 August 2022
DOI 10.3389/fmed.2022.969861

OPEN ACCESS

EDITED BY
Peiquan Zhao,
Shanghai Jiao Tong University, China

REVIEWED BY
Wei-Chi Wu,
Linkou Chang Gung Memorial Hospital, Taiwan
Gabriela Corina Zaharie,
Iuliu Haţieganu University of Medicine and Pharmacy, Romania

*CORRESPONDENCE
Yong Cheng
raccocheng@126.com
Jianhong Liang
drliangjianhong@126.com

†These authors have contributed equally to this work

SPECIALTY SECTION
This article was submitted to Ophthalmology, a section of the journal Frontiers in Medicine

RECEIVED 15 June 2022
ACCEPTED 19 July 2022
PUBLISHED 03 August 2022

CITATION
Zhong Y, Yang Y, Yin H, Zhao M, Li X, Liang J and Cheng Y (2022) Evaluation of segmental scleral buckling surgery for stage 4A retinopathy of prematurity in China.
Front. Med. 9:969861.
doi: 10.3389/fmed.2022.969861

Evaluation of segmental scleral buckling surgery for stage 4A retinopathy of prematurity in China

Yusheng Zhong[1†], Yating Yang[1†], Hong Yin[1], Mingwei Zhao[1], Xiaoxin Li[1,2], Jianhong Liang[1*] and Yong Cheng[1*]

[1]Department of Ophthalmology and Clinical Centre of Optometry, Peking University People's Hospital, Eye Diseases and Optometry Institute, Beijing Key Laboratory of Diagnosis and Therapy of Retinal and Choroid Diseases, College of Optometry, Peking University Health Science Center, Beijing, China, [2]Xiamen Eye Center, Xiamen University, Xiamen, China

Aims: To describe the long-term effect of scleral buckling (SB) surgery for stage 4A retinopathy of prematurity (ROP).

Methods: A retrospective chart review was conducted for patients with a diagnosis of stage 4A ROP who underwent SB between October 2010 and October 2021. Basic data were collected from patient charts, including gender, birth weight, gestational age at birth, disease stage, presence of plus disease, preoperative treatment [laser photocoagulation, intravitreal anti-vascular endothelial growth factor (VEGF) agent therapy, or a combination of both] and complications (vitreous hemorrhages), postmenstrual age at surgery, intraoperative combined treatment, and total length of follow-up. Retinal attachment status after surgery, postoperative complications (glaucoma, cataract), date and type of subsequent retinal surgeries (if performed), and refractive status 1 year after surgery were evaluated. The follow-up time after the first procedure was over 1 year.

Results: Six-two eyes from forty-eight patients met the inclusion criteria for this study. The initial reattachment rate was 93.5% (58/62 eyes), and the final reattachment rate was 100% after two procedures at the end of follow-up. The incidence of cataracts was 3.2% (2/62), with no eye subsequently needing lensectomy surgery. None of the patients developed glaucoma during the follow-up time. The average spherical equivalent refraction value for patients was −3.00 ± 2.51 D (−7.60 D to +2.75 D) 1 year after surgery.

Conclusion: SB, especially segmental buckling, which induces less myopia and does not require buckle removal, has the potential to provide a significant positive impact in the treatment of stage 4A ROP.

KEYWORDS

scleral buckling, retinopathy of prematurity, stage 4A, segmental, surgery

Abbreviations: SB, scleral buckling; ROP, retinopathy of prematurity; VEGF, vascular endothelial growth factor; LSV, lens-sparing vitrectomy; SE, spherical equivalent.

Introduction

Retinopathy of prematurity (ROP) is a leading cause of childhood blindness that occurs in premature infants, especially in the most immature infants throughout the world (1, 2). Although the advent of retinal ablation and intravitreal injection of anti-vascular endothelial growth factor (VEGF) drugs have improved the prognosis in threshold and prethreshold ROP, some treated eyes still experience retinal detachment (3, 4).

Surgical intervention in the early stage can yield the best chances of retinal reattachment and better functional outcomes for these eyes (5). Multiple studies have shown that scleral buckling (SB) and lens-sparing vitrectomy (LSV) are well-established techniques for the repair of ROP-related retinal detachment (6, 7). In previous literature, the success rate of LSV was higher than SB (8, 9). However, we believe that stage 4A ROP is partial retinal detachment, many of which occur in the periphery of the retina. LSV may damage the lens, resulting in cataract development and the need for cataract surgery. In addition, some studies (10, 11) have reported that LSV can result in potentially iatrogenic retinal breaks, vitreous hemorrhage and infection, which lead to a poor outcome.

It is universally acknowledged that SB can certainly neutralize the tractional forces of the extraretinal proliferation and effectively stabilize the neovascular activity of the fibrovascular tissue (12, 13). As an external surgery, SB is less invasive and carries less risk of surgical complications. However, few investigations have been published specifically focusing on the efficacy of SB for stage 4A ROP to date. Therefore, the aim of this study was to report on the long-term anatomic outcomes and complications after early SB for infants with stage 4A ROP.

Materials and methods

This was a single-center, retrospective, consecutive case series of premature infants who underwent SB surgery for stage 4A ROP from January 2010 to October 2021. This study was approved by the Ethics Committee and Institutional Review Board of Peking University People's Hospital. Written informed consent was obtained from the guardian of each participant in accordance with the Declaration of Helsinki. The stage of retinal detachment for each patient was determined during an examination under anesthesia according to the International Classification of Retinopathy of Prematurity (14). SB was selected as the most appropriate treatment for the included patient by experienced surgeons based on their best clinical judgment. We would prefer to perform SB on patients with stage 4A ROP whose tractional retinal detachment within six clock hours. All these treated cases were consecutive cases. Besides, if the patient was known any other eye disease except ROP was excluded.

The baseline characteristics of the patients, including gender, birth weight, gestational age at birth, disease stage, presence of plus disease, preoperative treatment (laser photocoagulation, intravitreal anti-VEGF agent therapy, or a combination of both) and complications (vitreous hemorrhage), postmenstrual age at surgery, intraoperative combined treatment, and total length of follow-up, were collected. Retinal attachment status after surgery, postoperative complications (glaucoma, cataract), date and type of subsequent retinal surgeries (if performed), and refractive status 1 year after surgery were evaluated.

The SB technique used in this series has been described in detail previously (15), and in this series, segmental SB was performed for all of the patients. All eyes were operated on by three surgeons (HY, JL, and YC) in the same group using the same surgical procedures and standards. The precise range and location of the tractional retinal detachment was marked on the scleral after a thorough examination under binocular indirect ophthalmoscopy. The silicone sponge was sutured to the marked area with 5-0 nylon suture. Subretinal fluid was not aspirated. Follow-up examinations were routinely performed in the first week after surgery and then at 1 month and every 3–6 months thereafter. At the follow-up sessions, all patients underwent a detailed ophthalmic examination under anesthesia, including ocular tonometry, cycloplegic refraction and a dilated fundus examination. Anatomical success was defined as total attachment of the retina. The refractive status was recorded as the spherical equivalent (SE, spherical power plus half of the cylindrical power), which was measured by a handheld autorefractometer (FR-5000; Grand Seiko Co., Ltd., Hiroshima, Japan). The average reading was obtained with at least three measurements. The follow-up time was at least 1 year after the first procedure.

The research data were uploaded to a computer environment and evaluated using SPSS V.26.0 (SPSS TM, IBM). Descriptive statistics are presented as the mean ± SD, median (minimum–maximum), frequency distribution and percentage.

Results

Our cohort consisted of 62 eyes of 48 children, of whom 24 were male and 24 were female, with an average gestational age of 29.5 ± 1.71 weeks (range 26.6–33.0 weeks) and a birth weight of 1,335.8 ± 322.93 g (range 840–2,300 g). The mean postmenstrual age at surgery was 50.7 ± 9.59 weeks (range 38.7–93.3 weeks). The mean time of the follow-up was 3.64 ± 2.53 years (range 1–10.48 years). The baseline data of the patients are presented in **Table 1**.

TABLE 1 Baseline data of the patients who underwent scleral buckling surgery for stage 4A ROP.

	Stage 4A
Eyes, *n*	62
Patients, *n*	48
Gender, male, %	24 (50%)
Mean gestational age ± SD weeks (range)	29.5 ± 1.71 (26.6–33)
Mean birth weight ± SD gram (range)	1,335.8 ± 322.93 (840–2,300)
Mean postmenstrual age at surgery ± SD weeks (range)	50.7 ± 9.59 (38.7–93.3)
Mean follow-up duration ± SD years (range)	3.64 ± 2.53 (1–10.48)

SD, standard deviation.

Traction retinal detachment spared the macula in all eyes, among which eight eyes (12.9%) had plus disease and four (6.5%) eyes had vitreous hemorrhage before surgery. Regarding previous treatments, 11 eyes (17.7%) had previously undergone laser photocoagulation therapy, 13 eyes (21.0%) only had anti-VEGF therapy, and 8 eyes (12.9%) had both anti-VEGF therapy and laser photocoagulation before surgery, as outlined in Figure 1. Thirty eyes (48.4%) had not received any treatment before surgery. For intraoperative combined treatment, nine eyes (14.5%) had combined cryotherapy, six eyes (9.7%) had combined anti-VEGF therapy, and three eyes (4.8%) had combined laser photocoagulation.

The overall anatomic success rate, evaluated as the percentage of retinal attachment on ophthalmic evaluation, was 93.5% (58/62) after the first procedure and 100% after the second procedures. Figure 2 shows examples of fundus photography before and after SB in two patients. Among the patients for whom retinal attachment failed after the first procedure, three eyes showed successful retinal attachment after SB again, and one eye showed successful attachment after vitrectomy. Regarding the complications after the surgery, two eyes developed mild cataracts during the follow-up time, but lensectomy surgery was not needed. None of the operated eyes showed signs of glaucoma or other complications. Moreover,

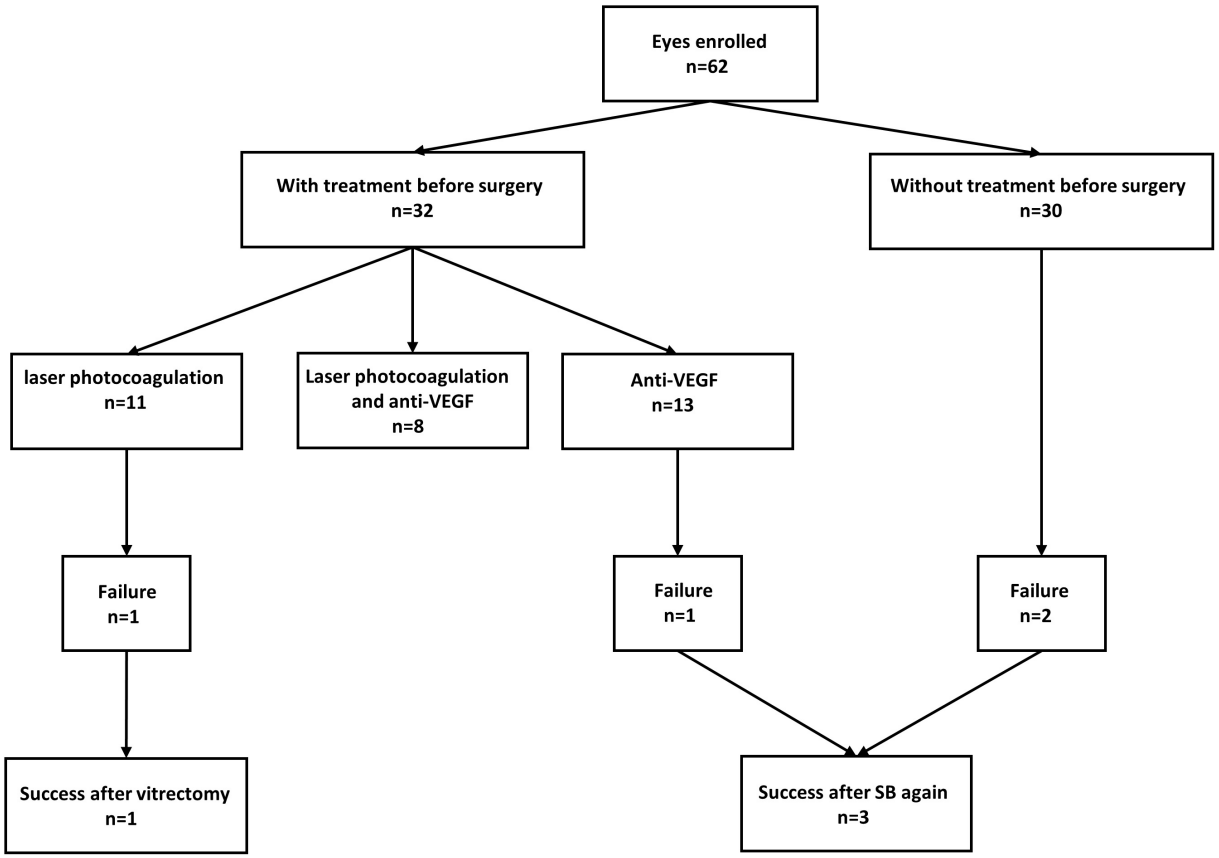

FIGURE 1
Flowchart of enrolled eyes with and without treatment before surgery and the outcome with different treatments. VEGF, vascular endothelial growth factor; SB, scleral buckling.

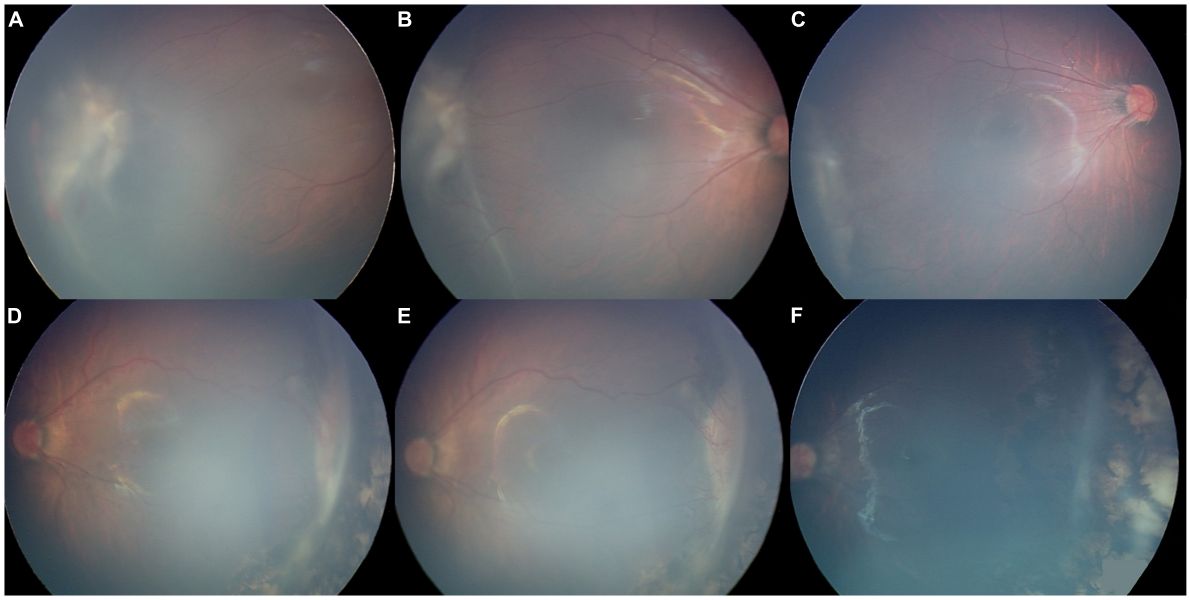

FIGURE 2
Fundus photography images from two patients in our series were obtained before and after surgery with stage 4A retinopathy of prematurity. Panels **A–C** belong to one patient. Panels **D–F** belong to another patient. **(A,D)** Fundus photograph obtained 1 week before scleral buckling showing extraretinal fibrovascular proliferation and tractional retinal detachment of the temporal retina. **(B,E)** Fundus photography obtained 1 week after scleral buckling, showing that the range of retinal detachment had no progression post-operatively. **(C,F)** Fundus photograph obtained about 6 months after scleral buckling, showing successful retinal reattachment.

the average SE refraction value for patients was -3.00 ± 2.51 D (range -7.60 D to +2.75 D) 1 year after surgery.

Discussion

Scleral buckling and LSV have been confirmed to be effective for stage 4A ROP. Although LSV has attracted much attention in the past few years, the inherent disadvantages, such as potentially iatrogenic retinal breaks, vitreous hemorrhage, and later severe proliferation after surgery, have caused wide concern. Compared with LSV, SB is less invasive and induces fewer surgical complications. However, the effectiveness of SB for stage 4A ROP has not been extensively studied.

Prior to 2003, the reattachment rates with SB were 66–75% (16–18). The initial retinal reattachment rate in our study was 93.5%. Futamura et al. (19) also reported a successful reattachment rate of 93.1% in a group of 29 eyes with stage 4A ROP after SB in 2014, which is comparable to our results. This finding suggests that the improved reattachment rates may be attributed to improvements in surgical equipment and diagnostic criteria over time. First, the considerable difference in the outcome seems to be related to the severity of the disease. Before 2003, studies followed the Cryotherapy for Retinopathy of Prematurity (CRYO-ROP) guidelines and always intervened at the threshold ROP. However, the Early Treatment for Retinopathy of Prematurity study (ETROP), published in 2003 (20), suggested that early treatment of high-risk prethreshold ROP, such as Type I ROP, can greatly improve the chance of long-term favorable structural outcomes, establishing new guidelines for the treatment of ROP. Various studies have confirmed the importance and effect of the adoption of the revised indications (21, 22). We believe that the final prognosis of disease is associated with the baseline disease condition at the time of treatment. Early treatment of prethreshold ROP can reduce the development of retinal detachment. So early treatment can reduce the severity of the disease when it comes to stage 4A ROP, such as the smaller range of retinal detachment. Therefore, this may explain the higher retinal reattachment rate in our study. Second, the average birth weight in previous studies ranged from 718 to 836 g, much less than that in our study, indicating more immature retinal nerve and vascular development and greater disease severity. Third, previous studies only combined laser photocoagulation therapy before surgery. In our study, most infants were also treated with anti-VEGF therapy, which can significantly improve the prognosis.

Several large series utilizing LSV for stage 4A ROP with adequate follow-up have reported favorable anatomical and functional success rates. In general, the successful reattachment rate of LSV for stage 4A ROP in previous studies ranged from 77 to 97% (10, 23–25). However, the complications caused by LSV surgery are a matter of great importance during the course of treatment. Bhende et al. (26) reported that the reattachment rate

was 82% (23/29) in eyes with stage 4A ROP treated with LSV as the initial surgery. While there was significant intraoperative bleeding in 8 (27.6%) eyes, only one eye had such severe bleeding that completion of the surgery was hampered. Iatrogenic retinal breaks occurred in one eye, and corneal clouding occurred in one eye. Lakhanpal et al. (27) reported that 27 of 32 (84.4%) eyes were reattached after a single LSV, in which one eye had an intraoperative retinal tear and three eyes with vitreous haze postoperatively needed a secondary procedure. Nudleman et al. (28) found in a series that the reattachment rate after a single LSV surgery was 82.1% (230/280) for stage 4A ROP. However, the rate of lens opacity was 2.1%, and the rate of lensectomy following LSV was 12.5%. One study (29) also reported that two eyes (6.25%) had cataract formation, and one eye needed lensectomy. Chandra et al. (30) reported that 5 of 90 (5.56%) eyes with stage 4A ROP were noted to have glaucoma after successful LSV, in which one eye was subsequently controlled with ocular hypotensive medication whereas four eyes required filtering surgeries. There was also one study reporting that the incidence of glaucoma after LSV in stage 4A ROP stage was 6.9% (31). The incidence of cataracts in our series was 3.2% (2/62) and no lensectomy was required for lens opacity confined to the temporal side, which was significantly lower than LSV. In addition, no eyes developed glaucoma, vitreous hemorrhage or retinal breaks in our study.

In our study, 51.6% (32/62) of patients were also treated with anti-VEGF therapy or photocoagulation before the operation. The initial reattachment rate was 90.6% (29/32) in the combined treatment group. Futamura et al. (19) compared the results of SB surgery with or without intravitreal bevacizumab and photocoagulation for stage 4A ROP. They reported that the success rate was 92% in the combined group and 93% in the non-combined group, which is comparable to our cohort. However, they also found that the retinopathy was more severe in stage 4A ROP in the combined group because the proliferative tissue in this group was larger and the VEGF concentration in the aqueous humor was higher. This indicates that the combined surgery had some positive effect on the result of treatment. Ozsaygili et al. (32) also suggested that preoperative treatment improved the functional and anatomical success rates and reduced the incidence of some complications, such as vitreous hemorrhage and retinal tears. The success rate was 89.7% in the combined group in the first year after the initial procedure, but 50% in the non-combined group. Both anti-VEGF and photocoagulation can stabilize vascular activity and plus disease, reducing the activity of retinopathy and delaying the development of lesions. Performing SB or LSV to offset the tractional forces of the extraretinal proliferation in time when the lesions are quiet after combined treatment can yield encouraging outcomes.

Although SB can clearly lead to anatomic success, the high level of myopia induced by surgery and the requirement for a second procedure to divide or remove the buckle to allow normal ocular growth are concerns for many clinicians, limiting the widespread use of SB. In one series (33), myopia (−5 D to −15 D) was found in all ten eyes that underwent SB at stage 4A ROP with a mean follow-up of 35 months; in another series (34), the mean induced myopia was −7.75 DS (−6 D to −10.25 D) with a mean follow-up of 10.5 weeks. Although the myopia caused by SB in these studies was serious, the myopia caused by LSV is not optimistic. Holz et al. (35) reported that the average SE of nine eyes with a mean follow-up of 3.6 years treated with LSV for stage 4A ROP was −6.78 D. Another study (32) showed that the average SE of 82 LSV eyes with a mean follow-up of 22.6 months was −5.91 ± 3.47 D. However, the average SE refraction value for patients in our study was −3.00 ± 2.51 D (−7.60 D to +2.75 D) 1 year after surgery. One of the most important reasons why our data were less myopic than any previous study is that all of our procedures involved segmental SB instead of scleral encircling buckling. Thus, the postoperative refractive errors and eye distortions were minimal, and no one had to undergo a second procedure to remove the buckle.

This study has inherent limitations worthy of consideration. Our series was not randomized, controlled, or prospective in nature. In addition, the high variability in the duration of follow-up has the potential to bias the reported outcomes. The short-term anatomic success rate is often higher than long-term anatomic rate, and recurrence may be occurred up to 5–6 years. In our study, the mean time of the follow-up was 3.64 ± 2.53 years and only fourteen patients were followed for more than 5 years, accounting for 29.2% (14/48) of all patients. Future studies with longer follow-up periods are needed.

To our knowledge, this is the largest study in terms of sample size for stage 4A ROP treated with segmental SB to date. Compared with LSV, SB is certainly a relatively safe, low-cost and low-technology procedure. In conclusion, SB, especially segmental SB, is effective as an initial treatment for stage 4A ROP.

Data availability statement

The raw data supporting the conclusions of this article will be made available by the authors, without undue reservation.

Ethics statement

The studies involving human participants were reviewed and approved by the Ethics Committee and Institutional Review Board of Peking University People's Hospital (2017PHB179-01). Written informed consent to participate in this study was provided by the participants' legal guardian/next of kin.

Author contributions

YC and JL conceived and designed the study. YZ, YY, HY, MZ, XL, and YC contributed important intellectual content to the study design and manuscript. YZ, YY, HY, and MZ coordinated data collection and contributed to the manuscript. YZ, YC, JL, and XL designed the analysis methods, analyzed the data, and contributed to manuscript writing. All authors contributed to the article and approved the submitted version.

Funding

This study was supported by the National Key R&D Program of China (2020YFC2008200); the Beijing Science and Technology Project (grant no. Z201100005520078); and the Beijing Bethune Charitable Foundation (grant no. 2018-Z-08).

Conflict of interest

The authors declare that the research was conducted in the absence of any commercial or financial relationships that could be construed as a potential conflict of interest.

Publisher's note

References

1. Hellström A, Smith LE, Dammann O. Retinopathy of prematurity. *Lancet.* (2013) 382:1445–57. doi: 10.1016/S0140-6736(13)60178-6

2. Cheng Y, Zhu XM, Linghu DD, Liang JH. Comparison of the effectiveness of conbercept and ranibizumab treatment for retinopathy of prematurity. *Acta Ophthalmol.* (2020) 98:e1004–8. doi: 10.1111/aos.14460

3. Barry GP, Yu Y, Ying G, Tomlinson LA, Lajoie J, Fisher M, et al. Retinal detachment after treatment of retinopathy of prematurity with laser versus intravitreal anti-vascular endothelial growth factor. *Ophthalmology.* (2021) 128:1188–96. doi: 10.1016/j.ophtha.2020.12.028

4. Cheng Y, Liu TG, Li WY, Zhao MW, Liang JH. Fluorescein angiography of retinal vascular involution after intravitreal injection of ranibizumab for retinopathy of prematurity. *Int J Ophthalmol.* (2019) 12:79–82. doi: 10.18240/ijo.2019.01.12

5. Kychenthal A, Dorta P. 25-Gauge lens-sparing vitrectomy for stage 4A retinopathy of prematurity. *Retina.* (2008) 28:S65–8. doi: 10.1097/IAE.0b013e318159ec49

6. Roohipoor R, Karkhaneh R, Riazi-Esfahani M, Ghasemi F, Nili-Ahmadabadi M. Surgical management in advanced stages of retinopathy of prematurity. *J Ophthalmic Vis Res.* (2009) 4:185–90.

7. Hubbard GB. Surgical management of retinopathy of prematurity. *Curr Opin Ophthalmol.* (2008) 19:384–90. doi: 10.1097/ICU.0b013e328309f1a5

8. Hansen ED, Hartnett ME. A review of treatment for retinopathy of prematurity. *Expert Rev Ophthalmol.* (2019) 14:73–87. doi: 10.1080/17469899.2019.1596026

9. Singh R, Reddy DM, Barkmeier AJ, Holz ER, Ram R, Carvounis PE. Long-term visual outcomes following lens-sparing vitrectomy for retinopathy of prematurity. *Br J Ophthalmol.* (2012) 96:1395–8. doi: 10.1136/bjophthalmol-2011-301353

10. Hartnett ME, Maguluri S, Thompson HW, McColm JR. Comparison of retinal outcomes after scleral buckle or lens-sparing vitrectomy for stage 4 retinopathy of prematurity. *Retina.* (2004) 24:753–7. doi: 10.1097/00006982-200410000-00011

11. Shah PK, Narendran V, Kalpana N. Safety and efficacy of simultaneous bilateral 25-gauge lens-sparing vitrectomy for vascularly active stage 4 retinopathy of prematurity. *Eye.* (2015) 29:1046–50. doi: 10.1038/eye.2015.78

12. Sears JE, Sonnie C. Anatomic success of lens-sparing vitrectomy with and without scleral buckle for stage 4 retinopathy of prematurity. *Am J Ophthalmol.* (2007) 143:810–3. doi: 10.1016/j.ajo.2007.01.017

13. Yokoi T, Yokoi T, Kobayashi Y, Hiraoka M, Nishina S, Azuma N. Evaluation of scleral buckling for stage 4A retinopathy of prematurity by fluorescein angiography. *Am J Ophthalmol.* (2009) 148:544–50. doi: 10.1016/j.ajo.2009.05.027

14. International Committee for the Classification of Retinopathy of Prematurity. The international classification of retinopathy of prematurity revisited. *Arch Ophthalmol.* (2005) 123:991–9. doi: 10.1001/archopht.123.7.991

15. Chuang YC, Yang CM. Scleral buckling for stage 4 retinopathy of prematurity. *Ophthalmic Surg Lasers.* (2000) 31:374–9. doi: 10.3928/1542-8877-20000901-04

16. Beyrau KM, Danis RM. Outcomes of primary scleral buckling for stage 4 Retinopathy of prematurity. *Can J Ophthalmol.* (2003) 38:267–71. doi: 10.1016/S0008-4182(03)80090-X

17. Trese MT. Scleral buckling for retinopathy of prematurity. *Ophthalmology.* (1994) 101:23–6. doi: 10.1016/s0161-6420(94)31362-5

18. Hinz BJ, de Juan E, Repka MX. Scleral buckling surgery for active stage 4A retinopathy of prematurity. *Ophthalmology.* (1998) 105:1827–30. doi: 10.1016/S0161-6420(98)91023-5

19. Futamura Y, Asami T, Nonobe N, Kachi S, Ito Y, Sato Y, et al. Buckling surgery and supplemental intravitreal bevacizumab or photocoagulation on stage 4 retinopathy of prematurity eyes. *Jpn J Ophthalmol.* (2015) 59:378–88. doi: 10.1007/s10384-015-0401-5

20. Early Treatment for Retinopathy of Prematurity Cooperative Group. Revised indications for the treatment of retinopathy of prematurity: results of the early treatment for retinopathy of prematurity randomized trial. *Arch Ophthalmol.* (2003) 121:1684–94. doi: 10.1001/archopht.121.12.1684

21. Alme AM, Mulhern ML, Hejkal TW, Meza JL, Qiu F, Ingvoldstad DD, et al. Outcome of retinopathy of prematurity patients following adoption of revised indications for treatment. *Bmc Ophthalmol.* (2008) 8:23. doi: 10.1186/1471-2415-8-23

22. Good WV, Early Treatment for Retinopathy Of Prematurity Cooperative Group. The early treatment for retinopathy of prematurity study: structural findings at age 2 years. *Br J Ophthalmol.* (2006) 90:1378–82. doi: 10.1136/bjo.2006.098582

23. Wu WC, Lai CC, Lin RI, Wang NK, Chao AN, Chen KJ, et al. Modified 23-gauge vitrectomy system for stage 4 retinopathy of prematurity. *Arch Ophthalmol.* (2011) 129:1326–31. doi: 10.1001/archophthalmol.2011.253

24. Prenner JL, Capone A, Trese MT. Visual outcomes after lens-sparing vitrectomy for stage 4A retinopathy of prematurity. *Ophthalmology.* (2004) 111:2271–3. doi: 10.1016/j.ophtha.2004.06.021

25. Karacorlu M, Hocaoglu M, Sayman Muslubas I, Arf S. Long-term functional results following vitrectomy for advanced retinopathy of prematurity. *Br J Ophthalmol.* (2017) 101:730–4. doi: 10.1136/bjophthalmol-2016-309198

26. Bhende P, Gopal L, Sharma T, Verma A, Biswas RK. Functional and anatomical outcomes after primary lens-sparing pars plana vitrectomy for Stage

4 retinopathy of prematurity. *Indian J Ophthalmol.* (2009) 57:267–71. doi: 10.4103/0301-4738.53050

27. Lakhanpal RR, Sun RL, Albini TA, Holz ER. Anatomic success rate after 3-port lens-sparing vitrectomy in stage 4A or 4B retinopathy of prematurity. *Ophthalmology.* (2005) 112:1569–73. doi: 10.1016/j.ophtha.2005.03.031

28. Nudleman E, Robinson J, Rao P, Drenser KA, Capone A, Trese MT. Long-term outcomes on lens clarity after lens-sparing vitrectomy for retinopathy of prematurity. *Ophthalmology.* (2015) 122:755–9. doi: 10.1016/j.ophtha.2014.11.004

29. Lakhanpal RR, Davis GH, Sun RL, Albini TA, Holz ER. Lens clarity after 3-port lens-sparing vitrectomy in stage 4A and 4B retinal detachments secondary to retinopathy of prematurity. *Arch ophthalmol.* (2006) 124:20–3. doi: 10.1001/archopht.124.1.20

30. Chandra P, Tewari R, Salunkhe N, Kumawat D, Chaurasia AK, Gupta V. Short-term incidence and management of glaucoma after successful surgery for stage 4 retinopathy of prematurity. *Indian J Ophthalmol.* (2019) 67:917–21. doi: 10.4103/ijo.IJO_33_18

31. Nudleman E, Muftuoglu IK, Gaber R, Robinson J, Drenser K, Capone A, et al. Glaucoma after lens-sparing vitrectomy for advanced retinopathy of prematurity. *Ophthalmology.* (2018) 125:671–5. doi: 10.1016/j.ophtha.2017.11.009

32. Özsaygili C, Ozdek S, Ozmen MC, Atalay HT, Yalinbas Yeter D. Parameters affecting postoperative success of surgery for stage 4A/4B ROP. *Br J Ophthalmol.* (2019) 103:1624–32. doi: 10.1136/bjophthalmol-2018-312922

33. Ricci B, Santo A, Ricci F, Minicucci G, Molle F. Scleral buckling surgery in stage 4 retinopathy of prematurity. *Graefes Arch Clin Exp Ophthalmol.* (1996) 234:S38–41. doi: 10.1007/bf02343046

34. Chow DR, Ferrone PJ, Trese MT. Refractive changes associated with scleral buckling and division in retinopathy of prematurity. *Arch Ophthalmol.* (1998) 116:1446–8. doi: 10.1001/archopht.116.11.1446

35. Holz ER. Refractive outcomes of three-port lens-sparing vitrectomy for retinopathy of prematurity. *Trans Am Ophthalmol Soc.* (2009) 107:300–10.

frontiers | Frontiers in Medicine

TYPE Original Research
PUBLISHED 04 August 2022
DOI 10.3389/fmed.2022.879110

OPEN ACCESS

EDITED BY
Xiaoyan Ding,
Sun Yat-sen University, China

REVIEWED BY
Beatrice Gallo,
Epsom and St Helier University Hospitals NHS Trust, United Kingdom
Mirella Barboni,
Semmelweis University, Hungary
Alejandra Daruich,
Hôpital Necker-Enfants Malades, France

*CORRESPONDENCE
Thibaut Chapron
tchapron@for.paris

SPECIALTY SECTION
This article was submitted to Ophthalmology, a section of the journal Frontiers in Medicine

RECEIVED 18 February 2022
ACCEPTED 04 July 2022
PUBLISHED 04 August 2022

CITATION
Piquin G, Chapron T, Abdelmassih Y, Martin G, Edelson C, Caputo G and Metge F (2022) Coats disease in female population: A comparison of clinical presentation and outcomes. *Front. Med.* 9:879110. doi: 10.3389/fmed.2022.879110

Coats disease in female population: A comparison of clinical presentation and outcomes

Gwendoline Piquin[1], Thibaut Chapron[1,2]*, Youssef Abdelmassih[1], Gilles Martin[1], Catherine Edelson[1], Georges Caputo[1] and Florence Metge[1]

[1]Pediatric Ophthalmology Department, Rothschild Foundation Hospital, Paris, France, [2]Epidemiology and Statistics Research Center/CRESS, Institut National de la Santé et de la Recherche Médicale (INSERM), Institut National de la Recherche Agronomique (INRA), Université Paris Cité, Paris, France

Purpose: To compare clinical characteristics at presentation and outcomes of Coats disease between females and males.

Methods: In this retrospective, consecutive case series we included all children diagnosed with Coats disease in a single tertiary referral center. Initial clinical presentation, treatment and outcomes were collected.

Results: A total of 158 children were included, of whom 29 (18.3%) were females and 11 (6.9%) had bilateral involvement. Age at diagnosis and disease stage were similar between females and males. Females had more bilateral involvement ($p < 0.001$) and tended to have a worse visual acuity at diagnosis ($p = 0.05$). At last follow-up, visual acuity and anatomical outcome after treatment were similar between genders.

Conclusion: Female patients with Coats disease had more bilateral involvement and tended to have worse visual acuity at presentation. Clinical presentation and outcomes seemed to be similar between genders.

KEYWORDS

pediatric retinal disease, pediatric retinal detachment, Coats disease, bilateral disease, female population

Introduction

Coats disease is a rare, idiopathic, and non-hereditary retinal vascular disorder characterized by retinal telangiectasia, intraretinal and/or subretinal exudation without vitreoretinal traction. It was first described by Georges Coats in 1908 (1). The exact prevalence of this disease is not known but may vary among populations because of ethnic genetic susceptibility and/or exposition to environmental factors. A study carried out in the United Kingdom, estimated its incidence at 0.09/100.000 inhabitants (2). Coats disease is not associated with systemic manifestations, often occurs unilaterally, and is more frequent in males. It classically starts during the first or second decade with a natural evolution toward retinal exudation which can lead to a total exudative retinal

detachment and neovascular glaucoma (3–5). The disease is staged according to Shields classification based on the presence and localization of vascular telangiectasia, exudation, exudative retinal detachment, and disease complications (3).

Although more frequent in males, Coats disease also affects females. Spitznas et al. (6) and Shields et al. (4) found a female prevalence of 28 and 24%, respectively (5). Few studies reported on Coats disease characteristics and outcomes in a female population: Shields et al. (5) reported a higher likelihood of advanced disease stages in females whereas Daruich et al. (7) reported similar disease presentation between females and males.

The purpose of our study is to compare the baseline characteristics and outcomes of Coats disease between females and males.

Methods

This retrospective consecutive case series included all children diagnosed with Coats disease at the Rothschild Foundation Hospital, a tertiary referral center, between December 1998 and October 2019. This study was approved by the institutional review and local ethics committee and adhered to the tenets of the Declaration of Helsinki.

Coats disease was defined by the presence of retinal telangiectasia with intraretinal and/or sub-retinal exudation without vitreoretinal traction. Patients with uncertain or alternative diagnosis were excluded. Patients' demographics, clinical characteristics, imaging features, treatment modalities and outcomes after management of the disease were retrospectively collected.

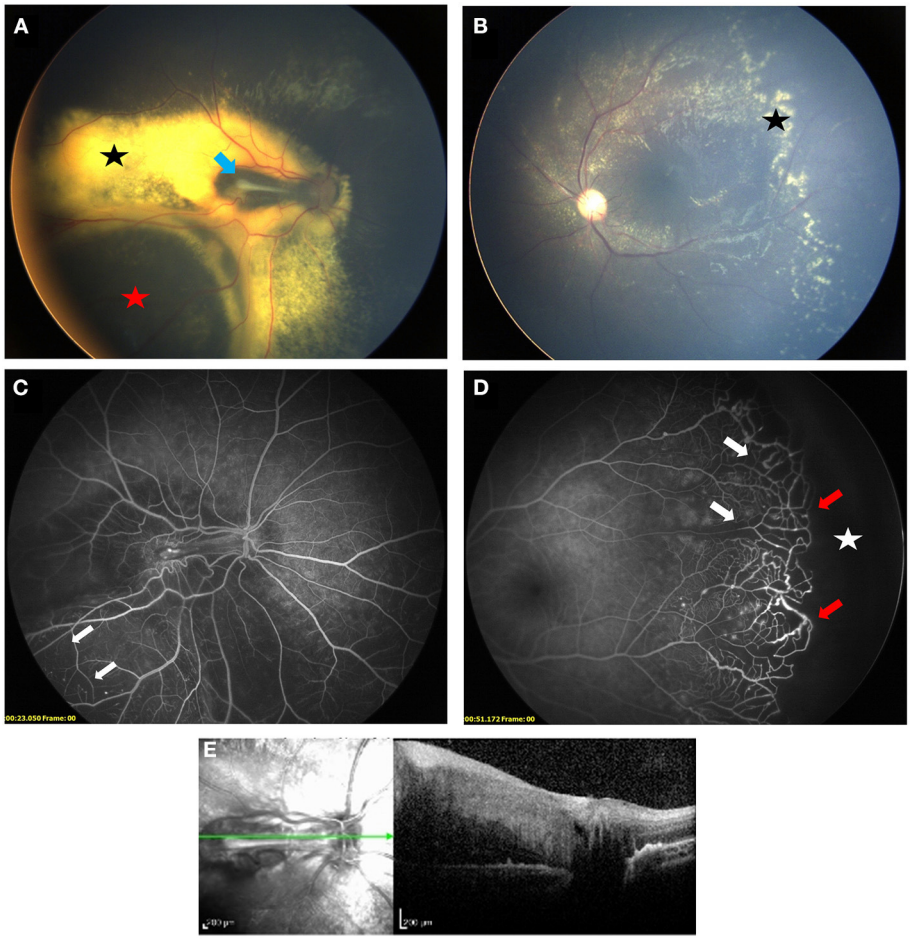

FIGURE 1
Bilateral Coats' disease in a 3-year-old girl. Right eye **(A)** is stage 3A1: fundus photograph shows an extrafoveal retinal detachment (red star) with exudates (black star) and a retinal fold at the level of the macula (blue arrow). Left eye **(B)** is stage 2A with extrafoveal exudation (black star). Fluorescein angiography shows capillary dropout (white arrows) in both eyes **(C)** right eye, **(D)** left eye) and a peripheral avascular retina (white star) lined with telangiectasia (red arrow) in the left eye. **(E)** SD-OCT section showing a thickening and hyperreflectivity of all retinal layers with preretinal fibrosis on top of the retinal fold.

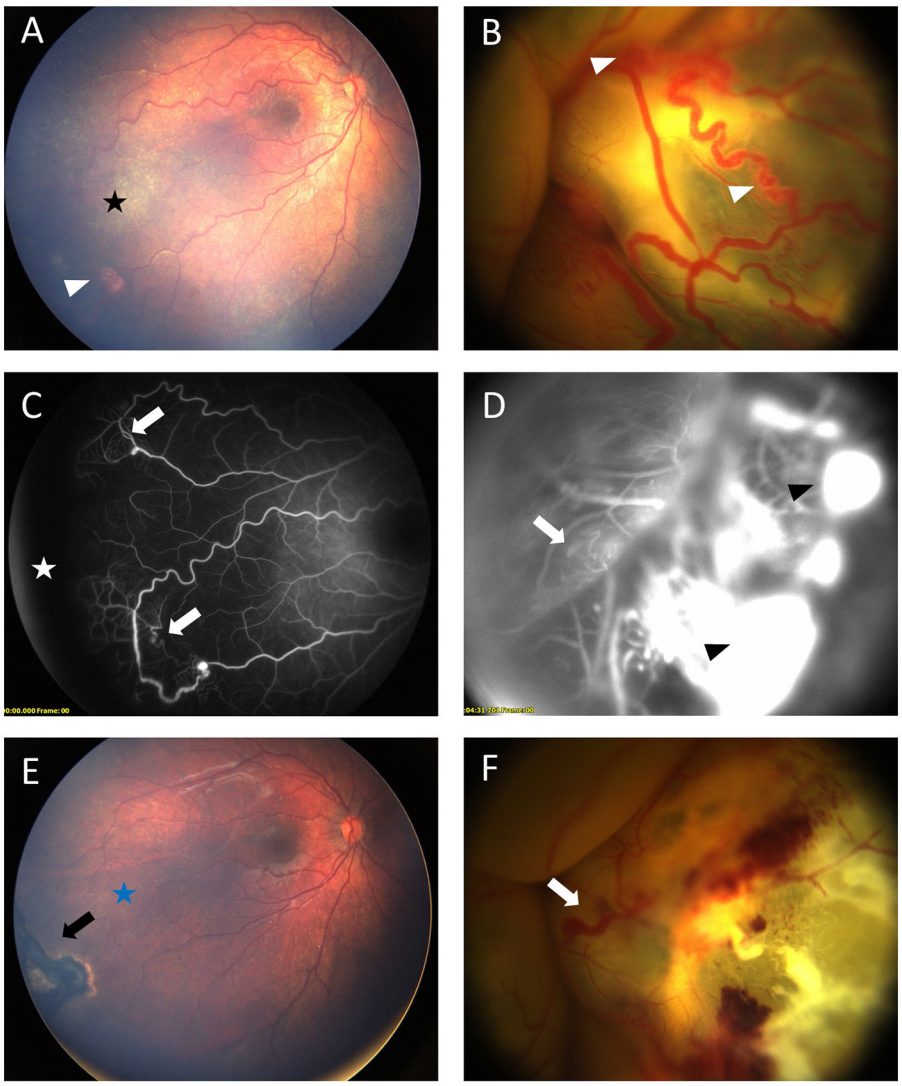

FIGURE 2
Bilateral Coats' disease in a 17-month-old girl. RetCam fundus photograph of the right eye **(A)** shows a stage 2A with moderate exudates (black star) sparing the fovea and ≪ light bulb ≫ aneurysms (white arrow head). Left eye **(B)** shows a stage 3B with a total retinal detachment covered with extensive aneurysms (white arrow head). Fluorescein angiography shows capillary dilatation and dropout (white arrows) on both eyes **(C)** right eye, **(D)** left eye and a peripheral avascular area (white star) on the right eye. Intense leakage is visible on the left eye (black arrow head). **(E,F)** shows fundus after first session of laser photocoagulation. On the right eye **(E)** black arrow shows retinal scar of photocoagulation and complete resolution of exudates (blue star). On the left eye **(F)** major exudates and dilated capillaries are still present (white arrow).

Patients' demographics and presenting characteristics included age at diagnosis, gender, laterality of the disease and presenting sign [leukocoria, strabismus, reduced visual acuity (VA), incidental finding following screening]. Clinical characteristics at diagnosis included VA (Snellen converted to logMAR), intraocular pressure (mmHg) and anterior segment findings (iris neovascularization, cataract). Visual acuity was not available for preverbal children. All patients received a thorough fundus examination using either a slit lamp or indirect ophthalmoscopy as well as fundus imaging and fluorescein angiography (FA) with either a contact wide-angle fundus camera (RetCam, Clarity Medical Systems USA) or a non-contact ultra-widefield imaging (Optos PLC, Dunfermline, Scotland, UK) depending on the child's age. We analyzed the extent and localization of telangiectasia, exudation and ischemia, and presence and extent of retinal detachment. Staging of affected eyes was based on the Shields' classification (3). In brief, stage 1 is characterized by the presence of telangiectasia only, stage 2 by the presence of both telangiectasia and exudation (A: extrafoveal exudation, B: foveal exudation), stage 3 by the presence of an exudative retinal detachment (A1 subtotal extrafoveal detachment, A2 subtotal foveal detachment,

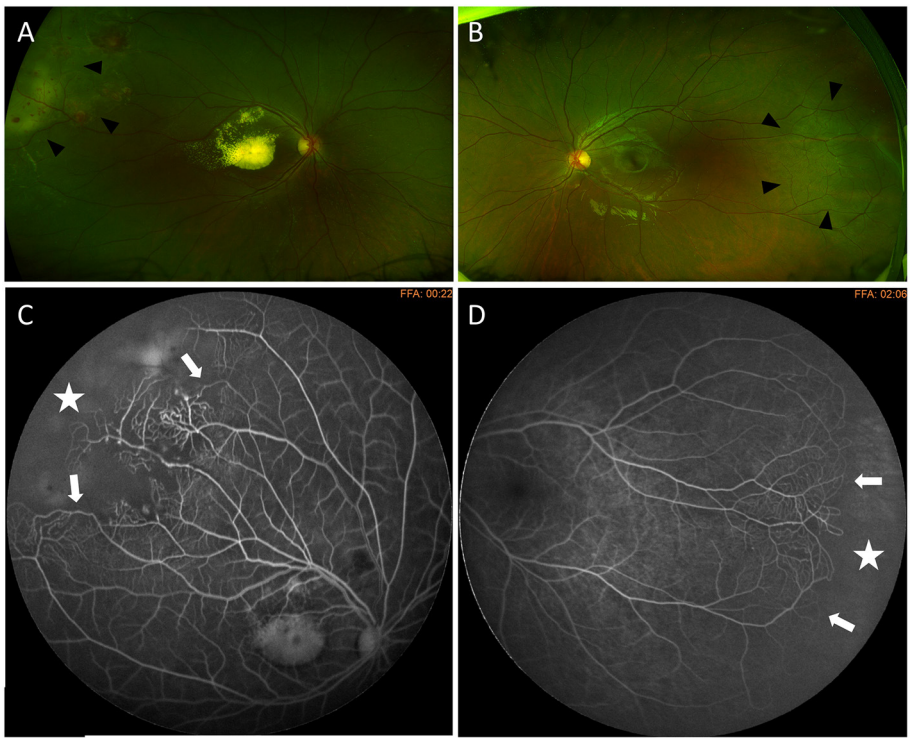

FIGURE 3
Bilateral Coats' disease in a 6-year-old girl. Optos wide-field fundus photography shows a stage 2B with macular exudation and peripheral telangiectasia (arrow heads) on the right eye **(A)** and telangiectasia located in the temporal periphery (arrow heads) on the left eye **(B)**. Fluorescein angiography shows capillary dilatation and dropout (white arrows) and a peripheral avascular area (white star) on both eyes **(C)** right eye **(D)** left eye.

B: total retinal detachment), stage 4 by the presence of a total retinal detachment with glaucoma, and stage 5 by the presence of end-stage changes: total retinal detachment, cataract, and phthisis bulbi. Contralateral eyes with anomalies such as peripheral vascular leakage, vascular tortuosity or peripheral non-perfusion were classified as "stage 0" since they didn't meet Shields' classification. Patients who were previously treated elsewhere were characterized as unknown for staging.

During examination, we paid particular attention to rule out pathologies that can mimic Coats disease such as retinoblastoma, retinopathy of prematurity (ROP), familial exudative retinopathy (FEVR), retinal capillary hemangioma, ocular toxocariasis and Coats-like syndromes combining bilateral exudative retinopathy with systemic conditions. Patients with bilateral disease underwent a brain MRI to exclude cerebro-retinal microangiopathy with calcifications and cysts (CRMCC) syndrome. When CRMCC was suspected on MRI, a genetic testing was performed.

Patients were divided into two groups according to gender. At presentation, functional and anatomical alteration was assessed. A severe functional alteration was defined by a VA less or equal to count fingers (CF) or a stage worse than 2A when the evaluation of VA was not possible. The presence of a retinal detachment defined a severe disease anatomically.

Treatment modalities included observation, laser photocoagulation, cryotherapy, intravitreal anti-vascular endothelial growth factor (anti-VEGF) injection, vitrectomy, and enucleation. At last follow-up both functional and anatomical outcomes were assessed. Some children were only referred to our institution for treatment and were therefore lost to follow-up since they went back to their referring center. Functional outcomes were evaluated based on VA at last follow-up. For anatomical outcomes, patients were classified in three categories: (1) no retinal detachment, (2) patients requiring vitrectomy, (3) anatomic failure with phthisis bulbi, total retinectomy, or enucleation.

All statistical analysis were performed using SAS 9.7 (SAS Institute Inc, Cary, NC). Descriptive statistics were reported as median and standard deviation (SD) for continuous variables, and as percentage for categorical variables. The categorical variables were tested for association with gender using Fisher exact test or Chi-square test. The continuous variables were compared between the two groups using Mann-Whitney U test. To assess the association between gender and Shields' classification, we divided the eyes into four groups as follows

stage 1 and 2A (only telangiectasia or extrafoveal exudation), stage 2B (foveal exudation), stage 3A1 and 3A2 (subtotal retinal detachment), 3B and 4 (total retinal detachment) as not all stages were present in the two groups. Concerning VA, 4 groups were also created: Hand Moving (HM) or worse, CF, VA between 20/400-20/100 and VA better than 20/100. Significance was set at $p < 0.05$.

Results

Out of the 161 patients (175 eyes) that met the clinical criteria for Coats disease, 3 (two females and one male) with a bilateral involvement were excluded because brain MRI found calcifications in favor of CRMCC syndrome, which was confirmed by the presence of a mutation on genes CTC1 or STN1. A total of 158 patients (169 eyes) were included of which 29 (18.3%) were females. Mean age at diagnosis was 7.1 +/- 6.4 years for females and 6.4 +/- 6.6 years for males ($p = 0.60$). No patient had a family history of Coats disease or other retinal vascular disease. All but 15 patients (two girls and 13 boys) received FA imaging. Children who did not received FA were not included in the bilateral involvement analysis. Bilateral disease was found in 11 (6.9%) patients and was more frequent in females (25.9 vs. 3.4%, $p < 0.001$). Bilateral involvement was clinically visible in five patients (Figures 1–3) while in the remaining six patients the involvement of the contralateral eye was only seen on FA (Figure 4). Visual acuity at diagnosis was available for 92 patients: 17.6% of girls vs. 21.3% of boys had a VA of HM or worse, 35.3% of girls vs. 10.7% of boys could count fingers, 29.4% of girls vs. 28% of boys had a VA between 20 and 400 and 20/100 and 17.6% of girls vs. 40% of boys had a VA better than 20/100. Visual acuity tended to be worse in females ($p = 0.05$). Presenting signs and symptoms were: leukocoria for 20.8% of girls vs. 19.8% of boys, strabismus for 25% of girls vs. 25.6% of boys, visual impairment for 37.5% of girls vs. 26.7% of boys, and 16.7% of girls vs. 27.9% of boys were asymptomatic. Presenting signs and symptoms were comparable between groups ($p = 0.63$). Stage of the disease at diagnosis was available for all but one girl who was initially seen and treated elsewhere. The diagnosis of Coats was never made at stage 1 for females but in 13 patients (10.1%) for males. None of the males and three females (10.7%) had a stage 4 disease. No patient had a stage 5. Baseline characteristics are shown in Table 1.

Disease classification was combined into four groups, stages 1 and 2A, stage 2B, stage 3A, and stages 3B and 4. At presentation, classification, functional and anatomical alterations were comparable between groups ($p = 0.48$, 0.21 and 0.89, respectively, see Table 2).

In the 11 patients with a bilateral form, the disease was always asymmetric. The least affected eye was classified as stage ≪0≫ in 6 patients, stage 1 in 2 patients, stage 2A in two patients, and stage 2B in one patient. The 6 eyes with stage ≪0≫ had anomalies only visible on FA: peripheral vascular leakage (two patients), vascular tortuosity (four patients) and peripheral non-perfusion associated with capillary meshwork abnormalities (dilatation and/or rarefaction) (two patients). Six of these 11 patients received laser photocoagulation on the least

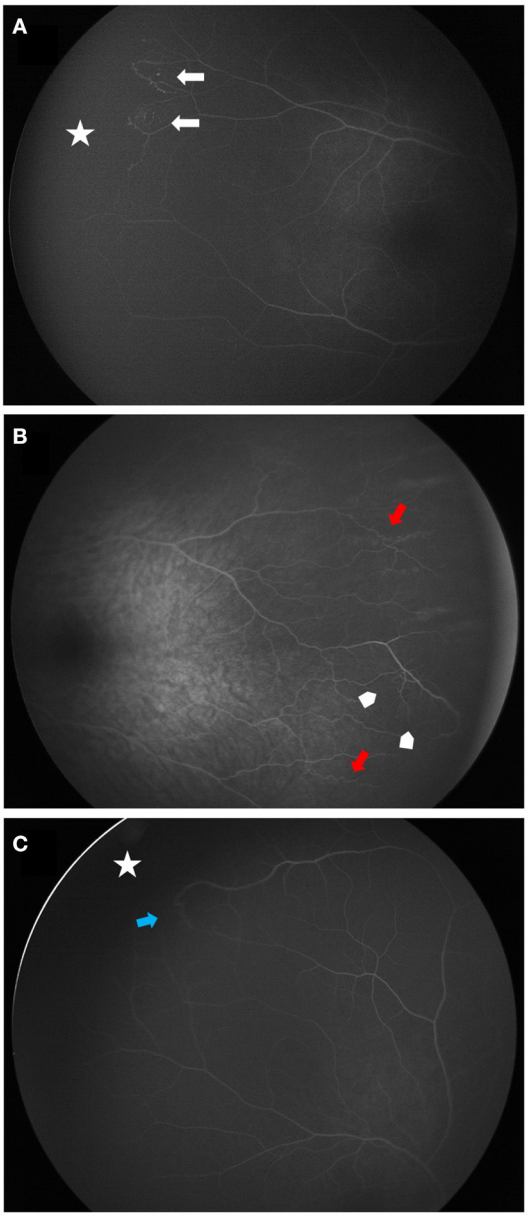

FIGURE 4
Wide angle fluorescein angiographies of contralateral vascular abnormalities in patients with Coats disease. **(A)** shows a peripheral avascular retina (white star) lined with telangiectasia (white arrows) (stage 1). **(B,C)** are classified stage 0. **(B)** demonstrates peripheral vascular tortuosity (red arrows) associated with dilatation of the capillary meshwork (arrow heads). **(C)** shows a peripheral avascular retina (white star) lined with a vascular anastomosis (blue arrow).

TABLE 1 Comparative analysis of baseline characteristics between males and females.

	Females N = 29		Males N = 129		p
Mean age at diagnosis in years ± SD ($N = 155$)		7.1 ± 6.3		6.4 ± 6.6	0.60
	n	**%**	***n***	**%**	***p***
Initial BCVA ($N = 92$)					0.05
≤HM	3	(17.6)	16	(21.3)	
CF	6	(35.3)	8	(10.7)	
20/400–20/100	5	(29.4)	21	(28.0)	
>20/100	3	(17.6)	30	(40.0)	
Presenting symptom or sign ($N = 110$)					0.63
Leukocoria	5	(20.8)	17	(19.8)	
Strabismus	6	(25.0)	22	(25.6)	
Vision impairment	9	(37.5)	23	(26.7)	
Asymptomatic (routine examination)	4	(16.7)	24	(27.9)	
Clinical staging based on Shields' classification ($N = 157$)					
1 Telangiectasia only	0	.	13	(10.1)	
2A Telangiectasia and extrafoveal exudation	3	(10.7)	14	(10.9)	
2B Telangiectasia and foveal exudation	13	(46.4)	45	(34.9)	
3A1 Extrafoveal subtotal retinal detachment	5	(17.8)	24	(18.6)	
3A2 Foveal subtotal retinal detachment	0	.	5	(3.4)	
3B Total retinal detachment	4	(14.3)	28	(21.7)	
4 Total retinal detachment and neovascular glaucoma	3	(10.7)	0	.	
Bilateral involvement ($N = 143$)					<0.001
No	20	(74.1)	112	(96.6)	
Yes	7	(25.9)	4	(3.4)	
Clinical bilateral involvement ($N = 143$)					0.004
No	23	(85.1)	115	(99.1)	
Yes	4	(14.8)	1	(0.9)	

BCVA, best-corrected visual acuity; CF, count fingers; HM: hand motion; N, number of patients and SD, standard deviation.

affected eye to treat telangiectasia in five eyes, and to treat a large peripheral avascular zone in one eye classified as stage 0. Characteristics of patients with bilateral disease are shown in Table 3.

Functional and anatomical outcomes at last follow-up were similar between both groups ($p = 0.41$ and 0.82, respectively). Twenty-one (72.4%) females and 98 (77.8%) males had an attached retina without surgery, 6 (20.7%) females and 21 (16.7%) male required vitrectomy, and 2 (6.9%) females and 7 (5.6%) males required total retinectomy, enucleation or had phthisis bulbi. Results after management are shown in Table 4.

Discussion

In this retrospective study, we reviewed all patients with Coats disease and compared the characteristics and outcomes between genders. Females represented 18.3% of patients in our study. Shields et al. and Spitznas et al. reported similar frequencies ranging from 16 to 28% (3–6, 8), while Daruich et al. found slightly lower frequencies of 14 and 11% (7, 9, 10).

Despite being usually a unilateral disease, 11 patients (6.9%) had bilateral involvement in our study. The rate of bilateral involvement showed a lot of discrepancies in literature (4–6, 8, 11–14). Some of these studies were based solely on fundus photographs (4), while others used FA imaging (6). The use of FA and more recently wide-field imaging systems helped detect more peripheral abnormalities (11–13). The improvement in detection of peripheral vascular anomalies using wide-field imaging systems may improve the detection and the classification of Coats disease, as it has already been demonstrated in other vascular pathologies such as diabetes (15). Jung et al. showed that 8.9% of patients with clinically unilateral disease had vascular abnormalities on the fellow eye revealed by FA whereas Rabiolo et al. found a higher rate

10.3389/fmed.2022.879110

TABLE 2 Comparative analysis of composite criteria at baseline between males and females.

	Females N = 29		Males N = 129		
	n	%	*n*	%	*p*
Initial presentation (*N* = 157)					0.48
Telangiectasia ± extrafoveal exudation (stage 1 + 2A)	3	(11.1)	27	(20.9)	
Foveal exudation (stage 2B)	13	(46.4)	45	(34.9)	
Subtotal exudative retinal detachment (stage 3A1 + 3A2)	5	(17.9)	29	(22.5)	
Total exudative retinal detachment (stage 3B + 4)	7	(25.0)	28	(21.7)	
Functional severity (*N* = 157)					0.21
Yes	25	(89.3)	102	(79.1)	
No	3	(10.7)	27	(20.9)	
Anatomical severity (N=157)					0.89
Yes	12	(42.9)	57	(44.2)	
No	16	(57.1)	72	(55.8)	

Functional severity was defined as best-corrected visual acuity ≤ counting fingers or a disease stage worse than 2A and anatomical severity was defined by the presence of retinal detachment. N, number of patients.

of 77.8% (12, 13). Brockmann et al. (14) reported on the presence of vascular changes on ultra wide-field FA in all the fellow eyes (100%) of middle-aged patients (mean age of 33.2 years and range between 12 and 66 years) with Coats disease and concluded that Coats disease seems to be an asymmetric bilateral disease, with abnormalities predominant in one eye. Vascular abnormalities consisted of peripheral non-perfusion, leakage, vascular tortuosity and occlusion or dilatation of capillaries (11, 12, 16–18). Among the 11 patients with bilateral involvement in our study, 6 had a normal contralateral fundus and abnormalities were only seen on FA. Since the definition of Coats disease is based on the presence of telangiectasia visible on indirect ophthalmoscopy or fundus photographs and since these angiographic abnormalities do not fit the Shields' classification, we classified these findings as "stage 0."

When the disease is bilateral, it is important to consider other etiologies that can mimic Coats disease such as ROP, FEVR, and systemic diseases that can be associated with Coats-like retinopathy such as facioscapulohumeral muscular dystrophy, aplastic anemia and CRMCC. However, in these cases the involvement is more symmetrical. It is therefore important to perform a brain MRI to look for cysts and calcifications of the brain in patients with bilateral involvement especially when anomalies are clinically visible in both eyes. A total of eight patients had a bilateral involvement that was clinically visible with no evidence of systemic manifestations on clinical examination. After brain MRI, cerebral calcifications were found in three of the eight patients who underwent a genetic testing confirming CRMCC syndrome, and were excluded. The remaining five patients had an unremarkable brain MRI and therefore genetic testing was not indicated.

Little is known on initial presentation and outcomes of Coats' disease in females. In a recent study, Daruich and Munier compared the clinical presentation of Coats disease between males and females and found no differences between these two groups in terms of age at diagnosis, presenting signs and symptoms, and severity at diagnosis based on Shields' classification (7).Shields et al. reported a higher likelihood of advanced disease stages in females (5). Several studies found that a younger age at diagnosis is associated with a more advanced stage of the disease and a poorer visual prognosis (4, 10, 19). In our study, females had similar age at diagnosis, presenting symptoms, stage group and VA. However, there was a tendency toward worse visual acuity in female ($p = 0.05$) without reaching statistical significance, which can be due to the limited number of patients.

Furthermore, we found that bilateral involvement was more frequent in females. Eleven patients had bilateral involvement (seven females, 64%) of which 5 had clinically visible anomalies (four females, 80%) while the rest were only diagnosed on FA. All eyes with clinically visible anomalies underwent laser while only one eye with stage 0 was treated for a large peripheral avascular zone. To our knowledge, no other study has investigated this association. In their series of 112 patients, Spitznas et al. (6) did not test the association between bilaterality and gender but found, in the age population of 0–20 years, that 17.6% (three out of 17) of females and 2.4% of males had bilateral involvement, which is similar to our study. It seems that in the first two decades,

TABLE 3 Clinical characteristics of patients with bilateral disease.

Patient N°	Gender	Age at presentation (years)	Presenting sign	Stage		Initial BCVA		Treatment		Final BCVA	
				RE	LE	RE	LE	RE	LE	RE	LE
1	Female	6	Routine examination	2A	0	20/20	20/20	Laser	Observation	20/20	20/20
2	Male	1	Strabismus	2B	3A1	NA	NA	Laser	Laser	NA	NA
3	Female	3	Strabismus	3A1	2A	HM	20/32	Laser	Laser	NA	NA
4	Female	26	Floaters	0	2A	20/20	20/20	Observation	Laser	20/16	20/16
5	Male	4	NA	3A1	0	20/200	20/20	Laser	Observation	CF	20/20
6	Female	9	Strabismus	1	4	20/40	NLP	Laser	Antivegf cyclodiode	20/16	NLP
7	Female	1	Leukocoria	2A	3B	NA	NA	Laser	Vitrectomy	20/20	NLP
8	Male	NA	NA	1	0	NA	NA	Laser	Laser	20/320	20/40
9	Male	8	Routine examination	0	1	NA	NA	Observation	Laser	NA	NA
10	Female	7	Visual impairment	0	2B	20/20	CF	Observation	Laser	20/20	20/250
11	Female	6	Routine examination	2B	1	20/100	20/20	Laser	Laser	20/100	20/20

BCVA, best-corrected visual acuity; LE, left eye; NA, not available; RE, right eye.

TABLE 4 Comparative analysis of outcomes between males and females.

	Females N = 29		Males N = 129		
	n	%	*n*	%	*p*
Final BCVA (*N* = 128)					0.41
≤HM	13	(48.1)	36	(35.6)	
CF	2	(7.4)	15	(14.9)	
20/400–20/100	7	(25.9)	21	(20.8)	
>20/100	5	(18.5)	29	(28.7)	
Anatomical outcome (*N* = 155)					0.82
No retinal detachment	21	(72.4)	98	(77.8)	
Patient requiring vitrectomy	6	(20.7)	21	(16.7)	
phthisis bulbi or total retinectomy or enucleation	2	(6.9)	7	(5.6)	

BCVA, best-corrected visual acuity; CF, counting fingers; CI, confidence interval; HM, hand motion; N, number of patients.

females have more bilateral involvement than males. One hypothesis is the presence since birth of bilateral lesions more frequently in the female population. Another hypothesis is males might develop bilateral involvement later in the course of the disease.

The limitation of the present study is that it is retrospective and that data such as VA was not always available for young children. We believe that the limited number of patients especially in the female group and the lack of VA available at presentation might have limited the statistical power of VA analysis between genders. Furthermore, since our institution is a tertiary referral center, severe and atypical cases maybe overrepresented because of referral bias. Finally, the use of wide-field FA increased the sensitivity of detecting peripheral abnormalities that may have been previously missed in other series.

In conclusion, 18.3% of patients with Coats' disease were females and bilateral involvement (overall 6.9%) was more frequent in females (25.9 vs. 3.4%, $p < 0.001$). Fluorescein angiography can be useful to evaluate contralateral involvement and brain MRI should be performed for all patients with bilateral involvement. Age at presentation, stage groups and VA was similar between genders, with a tendency toward a worse VA at presentation in the female group. It seems that Coats' disease could present or become bilateral more frequently or earlier in female population. Outcomes after treatment

were comparable between genders. Larger studies should be done to better compare VA at presentation between genders and to compare outcomes according to proposed treatments.

Data availability statement

The raw data supporting the conclusions of this article will be made available by the authors, without undue reservation.

Author contributions

GP, TC, and FM contributed to conception and design of the study. GP and TC organized the database. TC performed the statistical analysis. GP wrote the first draft of the manuscript. GP, TC, and YA wrote sections of the manuscript. All authors contributed to manuscript revision, read, and approved the submitted version.

Acknowledgments

Presented at the Congress of the Société Francaise d'Ophtalmologie, Paris, 2020.

Conflict of interest

The authors declare that the research was conducted in the absence of any commercial or financial relationships that could be construed as a potential conflict of interest.

Publisher's note

References

1. COATS G. Forms of retinal diseases with massive exudation. *Roy Lond Ophthalmol Hosp Rep.* (1908) 17:440–525.

2. Morris B, Foot B, Mulvihill A, A. population-based study of Coats disease in the United Kingdom I: epidemiology and clinical features at diagnosis. *Eye.* (2010) 24:1797–801. doi: 10.1038/eye.2010.126

3. Shields JA, Shields CL, Honavar SG, Demirci H, Cater J. Classification and management of Coats disease: the 2000 proctor lecture. *Am J Ophthalmol.* (2001) 131:572–83. doi: 10.1016/S0002-9394(01)00896-0

4. Shields JA, Shields CL, Honavar SG, Demirci H. Clinical variations and complications of coats disease in 150 cases: the 2000 Sanford Gifford memorial lecture. *Am J Ophthalmol.* (2001) 131:561–71. doi: 10.1016/S0002-9394(00)00883-7

5. Shields CL, Udyaver S, Dalvin LA, Lim LA, Atalay HT, Khoo C, et al. Visual acuity outcomes in Coats disease by classification stage in 160 patients. *Br J Ophthalmol.* (2019) 104:422–31. doi: 10.1136/bjophthalmol-2019-314363

6. Spitznas M, Joussen F, Wessing A, Meyer-Schwickerath G. Coat's disease. An epidemiologic and Fluorescein angiographic study. *Albrecht Von Graefes Arch Klin Exp Ophthalmol.* (1975) 195:241–50. doi: 10.1007/bf004 14937

7. Daruich A, Munier FL. Phenotype of coats disease in females. *BMJ Open Ophthalmol.* (2022) 7:e000883. doi: 10.1136/bmjophth-2021-000883

8. Dalvin LA, Udyaver S, Lim LAS, et al. Coats disease: clinical features and outcomes by age category in 351 cases. *J Pediatr Ophthalmol Strabismus.* (2019) 56:288–96. doi: 10.3928/01913913-2019 0716-01

9. Daruich A, Matet A, Tran HV, Gaillard MC, Munier FL. Extramacular fibrosis in coats' disease. *Retina.* (2016) 36:2022–8. doi: 10.1097/IAE.0000000000 001013

10. Daruich AL, Moulin AP, Tran HV, Matet A, Munier FL. Subfoveal nodule in. Coats' disease. *Retina.* (2017) 37:1591–8. doi: 10.1097/IAE.0000000000001399

11. Jeng-Miller KW, Soomro T, Scott NL, et al. Longitudinal examination of fellow-eye vascular anomalies in coats' disease with widefield fluorescein angiography: a multicenter study. *Ophthalmic Surg Lasers Imaging Retina.* (2019) 50:221–7. doi: 10.3928/23258160-20190401-04

12. Jung EH, Kim JH, Kim SJ, Yu YS. Fluorescein angiographic abnormalities in the contralateral eye with normal fundus in children with unilateral Coats' disease. *Korean J Ophthalmol.* (2018) 32:65–9. doi: 10.3341/kjo.2016.0092

13. Rabiolo A, Marchese A, Sacconi R, Cicinelli MV, Grosso A, Querques L, et al. Refining Coats' disease by ultra-widefield imaging and optical coherence tomography angiography. *Graefes Arch Clin Exp Ophthalmol.* (2017) 255:1881–90. doi: 10.1007/s00417-017-3794-7

14. Brockmann C, Löwen J, Schönfeld S, et al. Vascular findings in primarily affected and fellow eyes of middle-aged patients with Coats' disease using multimodal imaging. *Br J Ophthalmol Published online October 31.* (2020). doi: 10.1136/bjophthalmol-2020-317101

15. Wessel MM, Aaker GD, Parlitsis G, Cho M, D'Amico DJ, Kiss S. Ultra–wide-field angiography improves the detection and classification of diabetic retinopathy. *RETINA.* (2012) 32:785–91. doi: 10.1097/IAE.0b013e3182278b64

16. Singer M, Sagong M, van Hemert J, Kuehlewein L, Bell D, Sadda SR. Ultra-widefield imaging of the peripheral retinal vasculature in normal subjects. *Ophthalmology.* (2016) 123:1053–9. doi: 10.1016/j.ophtha.2016.01.022

17. Lu J, Mai G, Luo Y, et al. Appearance of far peripheral retina in normal eyes by ultra-widefield fluorescein angiography. *Am J Ophthalmol.* (2017) 173:84–90. doi: 10.1016/j.ajo.2016.09.024

18. Blair MP, Shapiro MJ, Hartnett ME. Fluorescein angiography to estimate normal peripheral retinal nonperfusion in children. *J AAPOS.* (2012) 16:234–7. doi: 10.1016/j.jaapos.2011.12.157

19. Mrejen S, Metge F, Denion E, Dureau P, Edelson C, Caputo G. Management of retinal detachment in Coats disease. *Study 15 Cases Retina.* (2008) 28:S26–32. doi: 10.1097/IAE.0b013e31816b3158

frontiers | Frontiers in Medicine

TYPE Original Research
PUBLISHED 10 August 2022
DOI 10.3389/fmed.2022.914207

OPEN ACCESS

EDITED BY
Georgios Panos,
Nottingham University Hospitals NHS Trust, United Kingdom

REVIEWED BY
Dhanashree Ratra,
Sankara Nethralaya, India
Murat Gunay,
Karadeniz Technical University, Turkey
Shahid Husain,
Queen Mary University of London, London, United Kingdom
Ugur Acar,
Selcuk University, Turkey

*CORRESPONDENCE
Xiaoyan Ding
dingxiaoyan@gzzoc.com

†These authors have contributed equally to this work and share first authorship

SPECIALTY SECTION
This article was submitted to Ophthalmology, a section of the journal Frontiers in Medicine

RECEIVED 06 April 2022
ACCEPTED 27 June 2022
PUBLISHED 10 August 2022

CITATION
Sun L, Yan W, Huang L, Li S, Liu J, Lu Y, Su M, Li Z and Ding X (2022) ROP-like retinopathy in full/near-term newborns: A etiology, risk factors, clinical and genetic characteristics, prognosis and management. *Front. Med.* 9:914207. doi: 10.3389/fmed.2022.914207

ROP-like retinopathy in full/near-term newborns: A etiology, risk factors, clinical and genetic characteristics, prognosis and management

Limei Sun[1†], Wenjia Yan[1†], Li Huang[1], Songshan Li[1], Jia Liu[2], Yamei Lu[2], Manxiang Su[3], Zhan Li[3] and Xiaoyan Ding[1*]

[1]State Key Laboratory of Ophthalmology, Zhongshan Ophthalmic Center, Sun Yat-sen University, Guangzhou, China, [2]The Sixth Affiliated Hospital of Guangzhou Medical University, Qingyuan, China, [3]Zhuhai Maternity and Child Health Hospital, Zhuhai, China

Purpose: Retinopathy of prematurity (ROP) like retinopathy (ROPLR) could occur in full/near-term newborns. The causes and clinical features are still largely elusive. This study focused on the risk factors, clinical and genetic characteristics, treatment and outcome, and prognosis of ROPLR.

Methods: A total of 47 consecutive full/near-term newborns during 2016–2017 with ROPLR were included. The clinical and genetic characteristics, treatment and outcome, prognosis, and potential underlying etiology of ROPLR were were analyzed.

Results: 91 eyes of 47 infants were found to have ROPLR. The ROPLR regressed completely in 65.9% and partially in 20.9% of eyes without any interventions. Retinal changes of family exudative vitreoretinopathy (FEVR) were allocated in 12 neonates (group A), perinatal hypoxia-ischemia were categorized in 17 neonates (group B), and the other 18 neonates were categorized in group C. Compared to those in group B/C, infants in group A had significantly more severe retinopathy (stage 4/5, $p < 0.001$) and more treatments ($p < 0.00$ risk factor 1).

Conclusions: Perinatal hypoxia-ischemia might be a major risk factor for ROPLR, in which spontaneous regression was common. FEVR, confirmed by positive family findings and genetic testing, might be the second risk factor of ROPLR, in which retinopathy is more severe and treatment is needed.

KEYWORDS

ROP-like retinopathies, full/near-term newborns, risk factor, etiology, family exudative vitreoretinopathy 3/25

Introduction

Retinopathy of prematurity (ROP) is a potentially severe complication of prematurity, characterized by incomplete retinal vascular development of the peripheral retina in premature infants. It is a leading cause of avoidable

childhood blindness worldwide, especially in middle-income countries (1, 2). The leading factors associated with ROP are prematurity, low birth weight, and exposure to high concentrations of O_2 (3). In full term infants, retinopathies can occur with clinical features that can appear similar to ROP (4–6). ROP-like retinopathies (ROPLR) refers to ROP developing in full/near-term neonates at a birth weight heavier than 2400 g (7). Some potential risk factors, such as brain anomalies and defects and poor maternal nutrition, increased oxygen tension in the retina after birth, hypoxic-ischemic encephalopathy (HIE) and family exudative vitreoretinopathy (FEVR) were suspected to be related to the occurrence of ROPLR (8, 9). Additionally, perinatal infection and/or inflammation had been clarified playing important etiologic roles in ROP (10). Based on current knowledge about ROP etiology and pathogenesis, it seems likely that infection and/or inflammation may be a separate insult aside of hypoxia in ROPLR.

Recently, controversy exists regarding whether ROPLR is atypical FEVR or a new clinical entity. FEVR is a congenital retinal vascular development disorder caused by disruption of the Wnt-β signaling pathway (11). The failure of peripheral retinal vascularization results in a similar appearance to the clinical spectrum of ROP. In previous studies, up to 58–76.6% of family members of patients with FEVR had abnormal fundus findings (12). Therefore, careful fundus examination of family members is important to characterize this disease. Nevertheless, to date, there has been no study focusing on fundus findings in family members of term infants with ROPLR. Therefore, the purpose of the present study was to investigate the clinical and genetic characteristics, treatment and outcome, prognosis, and potential underlying etiology of ROPLR.

Methods

Study cohort

This prospective study was conducted in three hospitals (including two community hospitals and a tertiary referral-based pediatric retina clinic). In the two community hospitals, universal newborn eye screening was performed in every neonate. 47 full/near-term neonates diagnosed with ROPLR from 2016–2017 were included. This study was approved by the Institutional Review Board of Zhongshan Ophthalmic Center, Sun Yat-sen University, and accorded with the tenets of the Declaration of Helsinki. Parents of all participants signed informed consent forms. Neonates who were born at 37–41 gestational weeks, with birth weight $>$ 2000 g, were enrolled. Patients with any other congenital ocular disorders, such as persistent fetal vasculature (PFV) or incontinentia pigmenti (IP), were excluded. Handheld slit-lamp and fundus examination (RetCam III, Clarity Medical Systems, Pleasanton, CA, United States) were performed by an ophthalmologist in each neonate within 72 h after birth.

Neonatal factors included gestational age (GA), birth weight (BW), gender, race, post-natal oxygen exposure, cephalhematoma, intracranial hemorrhage, neonatal hyperbilirubinemia, umbilical cord around fetal neck (UCAN), and fetal distress. The antenatal maternal variables such as mode of delivery (vaginal or cesarean), anemia, gestational diabetes mellitus (GDM), hypertensive disorders complicating pregnancy (HDCP), turbidity of amniotic fluid, placenta previa, gestational thyroid disease (hypothyroidism or hyperthyroidism), vaginal wall laceration, perineal laceration, premature rupture of membranes, and placental abruption were recorded and reviewed.

Assessment, treatment, and follow-up

All ophthalmic examinations were performed by qualified ophthalmologists using the 2005 International Classification of Retinopathy of Prematurity (ICROP) (13). The fundus findings of ROPLR were staged according to the international guidelines for ROP (13). The indications for treatment were based on the criteria proposed by the Early Treatment for Retinopathy of Prematurity (ETROP) Study (14). Treatments were carried out by a single surgeon (Ding X). Intravitreal injection of ranibizumab (IVR) in 0.25 mg /0.025 ml or ablative laser photocoagulation (LPC) was performed (15, 16). Surgical management is recommended for stages 4 and 5, as it might halt progression to worse complications (17). Cases with stages 1 or 2 in zone I without plus disease require a follow-up once a week, while stages 1 or 2 in zone II, zone III, or stage 3 in zone II without plus disease should be observed with 2 or 3 weekly follow-up. A repeat IVR, LPC, or surgery was considered if the clinical features were compatible with retinopathies recurrence (16). The follow-up examination was performed weekly for 1 month, biweekly for 2 months, and then less frequently in a gradual pattern, from every 4 weeks to 3 months to 6 months.

Main outcome measures

The main outcome measures were as follows: the percentage of neonates in need of treatment and anatomical outcomes after treatment at the most recent follow-up. The outcomes were defined as the ocular structure status at the final visit according to previous studies (18); Complete regression was defined as an attached macula with full vascularization; Partial regression was defined as an absence of plus disease and neovascularization with the presence of peripheral avascular area; Stable was defined as the retinopathy with neither regression nor progression. Progression was defined as the evolution of the lesion needing treatment or with recurrence.

To investigate the potential underlying etiology and risk factors of ROPLR, a comprehensive ocular examination was performed in all the parents and siblings. All the fundus findings were graded by two experienced pediatric retinal specialists (Sun L and Yan W) to determine the presence and severity of retinopathy.

Genetic analysis

Genomic DNA was extracted from the peripheral blood of each proband and family member using a standardized protocol. All samples underwent whole exon sequencing (WES). The method used for bioinformatics analysis of the pathogenic variants was the same as our previous study (19). Sanger sequencing was conducted to verify the mutation in the probands and family members.

Statistical analysis

Statistical analysis was conducted using SPSS 22.0. Shapiro—Wilk tests were used to analyze the distribution of samples. Continuous variables were compared using the student's test for normally distributed variables and the Wilcoxon rank-sun test for non-normally distributed variables, and $p < 0.05$ was considered statistically 'significant.

Results

Demographic and clinical features of ROPLR

A total of 47 neonates and their biological parents were enrolled in this study. The cohort consisted of 35 boys and 12 girls. The male-to-female ratio was 2.9:1. The average gestational age (GA) was 38.6 ± 1.2 weeks, with a range from 37 to 41 weeks. The average birth weight was 3,087 ± 259g (2,300–3,950g). Retinopathy was found in 91 eyes of 47 infants (3 unilateral, 44 bilateral), including stage 1 lesions in 51 (54.3%) eyes, stage 2 in 20 (21.3%) eyes, stage 3 in 9 (9.5%) eyes, stage 4 in 6 (6.4%) eyes, and stage 5 in 5 (5.3%) eyes. 10 infants (21.3%) presented asymmetry with unilateral ROPLR or a difference of one stage or more between two eyes (Table 1).

Treatment and outcome of ROPLR

Combined with treatment criteria and after careful discussion with parents or guardians, a total of 12 eyes of eight patients received a range of treatments, which were as follows: single IVR in five eyes of five patients, combined IVR with scleral buckling in one eye, combined IVR with LPC in two eyes of two patients, and LPC in four eyes of two patients. The other eyes were left for observation, which included in 6 eyes with stage 3 in zone III without plus disease, 2 eyes with stage 4b presented retinal folds with macula involvement and 5 eyes with stage 5 presented complete retinal detachment. All neonates were followed once a week until the retinal lesion regressed or remained stable after the treatment. The ROPLR completely regressed in 60 eyes (65.9%, 60/91) of 35 infants without any intervention, and partially regressed in 8 eyes of six infants after treatments and in 12 eyes (13.2%, 12/91) of six infants without intervention. None of the neonates presented recurrence that needed retreatment (Table 1). Eleven eyes in 6 patients with stage 4/5 severe retinopathy remained stable, including 4 eyes been treated and 7 eyes under observation. The median follow-up period was 52 months, ranging from 30 to 60 months after the first screening.

There were no statistical differences in age, gender, DM or risk factors ratio between treatment needed eyes and not requiring treatment eyes ($p = 0.952$, 1.000, 0.538, and 1.000). There were significantly larger birth weight and more gene mutations in treatment needed eyes compared to the not requiring treatment eyes ($p = 0.035$, < 0.001) (Table 2).

Fundus findings in the family members in neonates with ROPLR

Typical characteristics of FEVR, including retinal peripheral avascular areas (AVA), increased ramification, and vascular straightening (Supplement Figure), were found in 18 individuals from 12 (25.5%) families. Of the 12 FEVR families, two of them had positive family history because of the affected father, the other 10 declined positive family history until the proband was diagnosed. The diagnosis of FEVR was further confirmed by vascular leakage on FFA (9) and TEMPVIA (18, temporal mid-peripheral vitreoretinal interface abnormality) on SLO. TEMPVIA, described in our prior study (20), is an image biomarker with a high sensitivity and specificity in the quick screening and diagnosis of FEVR. Briefly, it was presented as a grayish-white band located at the temporal retina, while the anterior margin was shown as the boundary of the peripheral vascular and avascular areas.

Genetic findings in neonates with ROPLR and their family members

In total, 35 (35/47, 74.5%) neonates and their family members agreed to receive genetic analysis. Of them, 12 infants all with positive fundus findings in their family members, and the other 23 infants (23/35, 65.7%) with negative family findings.

TABLE 1 Demographic and clinical features, risk factors and treatment of newborns with ROP-like retinopathies.

Case	Gender	BW(g)	GA(w)	DM	Risk factors	IVD(d)	Family history	Eye	Zone	Stage	Treatments	Follow-up(months)	Outcomes	Gene
1	M	2,300	37	VG	None	3	P	OD	III	2	observation	36	PR	FZD4
	M	2,300	37	VG	None	3	P	OS	III	2	observation		PR	
2	M	3,100	38	VG	None	3	P	OD	NA	5	observation	54	stable	NDP
	M	3,100	38	VG	None	3	P	OS	NA	5	observation		stable	
3	M	3,100	39	VG	None	2	P	OD	NA	4b	IV scleral buckling	36	stable	FZD4
	M	3,100	39	VG	None	2	P	OS	NA	4b	IV		stable	
4	M	3,150	38	CS	None	3	P	OD	NA	4b	IV photocoagulation	60	stable	TSPAN12
	M	3,150	38	CS	None	3	P	OS	NA	4b	IV photocoagulation		stable	
5	F	3,600	38	CS	placenta previa	2	P	OD	II	2	photocoagulation	54	PR	TSPAN12
	F	3,600	38	CS	placenta previa	2	P	OS	II	2	photocoagulation		PR	
6	M	2,900	39	VG	None	2	P	OD	NA	4b	observation	50	stable	LRP5
	M	2,900	39	VG	None	2	P	OS	NA	4b	observation		stable	
7	M	3,050	38	CS	None	3	P	OD	NA	5	observation	39	stable	NDP
	M	3,050	38	CS	None	3	P	OS	NA	5	observation		stable	
8	F	3,200	40	VG	None	3	P	OD	NA	5	observation	45	stable	FZD4
	F	3,200	40	VG	None	3	P	OS	II	3	IV		PR	
9	M	2,450	38	CS	None	2	P	OD	II	2	observation	60	PR	N
	M	2,450	38	CS	None	2	P	OS	II	2	observation		PR	
10	M	3,100	40	VG	turbidity of amniotic fluid	2	P	OD	III	2	observation	60	PR	N
	M	3,100	40	VG	umbilical cord around fetal neck			OS	III	2	observation		PR	
11	M	3,300	37	CS	None	3	N	OD	III	2	observation	36	CR	N
	M	3,300	37	CS	None	3	N	OS	III	2	observation		CR	
12	F	2,500	39	VG	None	2	N	OD	III	1	observation	48	CR	N

(Continued)

10.3389/fmed.2022.914207

TABLE 1 Continued

Case	Gender	BW(g)	GA(w)	DM	Risk factors	IVD(d)	Family history	Eye	Zone	Stage	Treatments	Follow-up(months)	Outcomes	Gene
	F	2,500	39	VG	None	2	N	OS	III	1	observation		CR	
13	M	3,000	38	VG	None	3	N	OD	III	1	observation	40	CR	N
	M	3,000	38	VG	None	3	N	OS	III	1	observation		CR	
14	M	3,200	39	VG	None	3	N	OD	III	1	observation	54	CR	N
	M	3,200	39	VG	None	3	N	OS	III	1	observation		CR	
15	F	2,500	40	CS	None	2	N	OD	III	1	observation	60	CR	N
	F	2,500	40	CS	None	2	N	OS	III	1	observation		CR	
16	M	3,300	39	VG	hyperbilirubinemia	2	N	OD	III	1	observation	60	CR	N
	M	3,300	39	VG	hyperbilirubinemia	2	N	OS	III	1	observation		CR	
17	M	3,050	40	VG	None	2	N	OD	III	1	observation	54	CR	N
	M	3,050	40	VG	None	2	N	OS	III	1	observation		CR	
18	M	3,100	39	VG	hyperbilirubinemia	1	N	OD	III	1	observation	45	CR	N
	M	3,100	39	VG	hyperbilirubinemia	1	N	OS	III	1	observation		CR	
19	F	3,350	39	CS	None	2	N	OD	III	1	observation	60	CR	N
	F	3,350	39	CS	None	2	N	OS	III	1	observation		CR	
20	M	3,330	40	VG	maternal anemia	2	N	OD	III	1	observation	60	CR	N
	M	3,330	40	VG	maternal anemia	2	N	OS	III	1	observation		CR	
21	M	2,750	37	VG	fetal distress	2	N	OD	III	1	observation	60	CR	N
	M	2,750	37	VG	fetal distress	2	N	OS	III	1	observation		CR	
22	M	2,750	37	VG	umbilical cord around fetal neck	2	N	OD	III	1	observation	60	CR	N
	M	2,750	37	VG	umbilical cord around fetal neck	2	N	OS	III	1	observation		CR	
23	M	2,950	39	VG	maternal anemia	2	N	OD	III	1	observation	52	CR	N
	M	2,950	39	VG	maternal anemia	2	N	OS	III	1	observation		CR	

(Continued)

10.3389/fmed.2022.914207

TABLE 1 Continued

Case	Gender	BW(g)	GA(w)	DM	Risk factors	IVD(d)	Family history	Eye	Zone	Stage	Treatments	Follow-up(months)	Outcomes	Gene
24	M	3,170	38	CS	umbilical cord around fetal neck	2	N	OD	III	1	observation	60	CR	N
	M	3,170	38	CS	umbilical cord around fetal neck	2	N	OS	III	1	observation		CR	
25	M	2,650	37	CS	umbilical cord around fetal neck	1	N	OD	III	1	observation	60	CR	N
	M	2,650	37	CS	umbilical cord around fetal neck	1	N	OS	-	0	-		-	
26	F	2,750	37	CS	None	2	N	OD	III	1	observation	60	CR	N
	F	2,750	37	CS	None	2	N	OS	III	1	observation		CR	
27	M	3,200	37	CS	None	2	N	OD	III	1	observation	60	CR	N
	M	3,200	37	CS	None	2	N	OS	III	1	observation		CR	
28	M	3,300	39	CS	None	2	N	OD	III	1	observation	60	CR	N
	M	3,300	39	CS	None	2	N	OS	III	1	observation		CR	
29	M	3,300	40	VG	intracerebral hemorrhage	3	N	OD	III	1	observation	45	CR	N
	M	3,300	40	VG	intracerebral hemorrhage	3	N	OS	III	1	observation		CR	
30	M	3,550	40	VG	None	2	N	OD	III	1	observation	54	CR	N
	M	3,550	40	VG	None	2	N	OS	III	1	observation		CR	
31	M	2,700	37	VG	fetal distress	3	N	OD	II	2	IV	60	PR	N
	M	2,700	37	VG	fetal distress	3	N	OS	II	1	observation		CR	
32	M	3,200	40	CS	None	3	N	OD	III	1	observation	54	CR	N
	M	3,200	40	CS	None	3	N	OS	II	3	IV		PR	
33	M	3,500	40	CS	None	3	P	OD	II	2	observation	42	PR	N
	M	3,500	40	CS	None	3	P	OS	II	2	observation		PR	

(Continued)

10.3389/fmed.2022.914207

TABLE 1 Continued

Case	Gender	BW(g)	GA(w)	DM	Risk factors	IVD(d)	Family history	Eye	Zone	Stage	Treatments	Follow-up(months)	Outcomes	Gene
34	F	2,980	40	CS	Intrauterine hypoxia	3	N	OD	III	3	observation	54	PR	N
	F	2,980	40	CS	Intrauterine hypoxia	3	N	OS	III	3	observation		PR	
35	M	3,000	40	VG	None	3	N	OD	III	1	observation	48	CR	N
	M	3,000	40	VG	None	3	N	OS	III	1	observation		CR	
36	M	2,900	37	CS	None	3	N	OD	III	1	observation	54	CR	N
	M	2,900	37	CS	None	3	N	OS	III	2	observation		CR	
37	M	3,500	38	CS	None	3	N	OD	III	1	observation	36	CR	N
	M	3,500	38	CS	None	3	N	OS	II	3	IV		PR	
38	F	2,500	37	CS	None	3	N	OD	III	3	observation	48	CR	N
	F	2,500	37	CS	None	3	N	OS	III	3	observation		CR	
39	F	2,530	37	CS	None	3	N	OD	III	3	observation	48	CR	N
	F	2,530	37	CS	None	3	N	OS	III	3	observation		CR	
40	M	3,700	38	VG	None	3	P	OD	II	1	observation	30	PR	N
	M	3,700	38	VG	None	3	P	OS	II	1	observation		PR	
41	M	3,450	39	VG	None	1	N	OD	II	1	observation	33	CR	N
	M	3,450	39	VG	None	1	N	OS	III	2	observation		CR	
42	F	3,950	37	VG	maternal anemia	2	N	OD	III	1	observation	42	CR	N
	F	3,950	37	VG	maternal anemia	2	N	OS	-	0	-		-	
43	M	3,500	40	VG	turbidity of amniotic fluid	1	N	OD	III	2	observation	36	CR	N
	M	3,500	40	VG	umbilical cord around fetal neck	1	N	OS	III	1	observation		CR	
44	F	2,960	41	VG	maternal anemia	2	N	OD	III	2	observation	42	CR	N

(Continued)

10.3389/fmed.2022.914207

TABLE 1 Continued

Case	Gender	BW(g)	GA(w)	DM	Risk factors	IVD(d)	Family history	Eye	Zone	Stage	Treatments	Follow-up(months)	Outcomes	Gene
	F	2,960	41	VG	maternal anemia	2	N	OS	-	0	-		-	
45	F	3,250	40	VG	turbidity of amniotic fluid	2	N	OD	III	1	observation	33	CR	N
	F	3,250	40	VG	turbidity of amniotic fluid	2	N	OS	III	1	observation		CR	
46	M	3,330	39	VG	premature rupture of membranes	1	N	OD	II	2	photocoagulation	42	PR	
	M	3,330	39	VG	premature rupture of membranes	1	N	OS	II	2	photocoagulation		PR	N
47	M	3,170	37	VG	maternal anemia	2	N	OD	III	2	observation	36	CR	
	M	3,170	37	VG	maternal anemia	2	N	OS	III	1	observation		CR	N

F, female; M, male; BW, birth weight; GA, gestational age; DM, delivery method; VG, vaginal delivery; CS, caesarean section; RF, risk factors; IVD, initial visit date; IV, intravitreal injection; CR, complete regression; PR, partial regression.

10.3389/fmed.2022.914207

TABLE 2 Multivariate analysis between treatment needed eyes and not requiring treatment eyes.

	Treatment needed eyes	Observation eyes	*P* value
Total eyes number	12	79	
Gender			1.000
Male	9 (75.0)	60 (75.9)	
Fmale	3 (25.0)	19 (24.1)	
BW(g)	3,247 ± 250.9	3,058 ± 353.9	0.035
GA(w)	38.58 ± 0.9003	38.58 ± 1.236	0.952
DM			0.538
VG	6 (50.0)	48 (60.8)	
CS	6 (50.0)	31 (39.2)	
Risk factors			1.000
Positive	5 (41.7)	30 (40.0)	
Negative	7 (58.3)	49 (60.0)	
Gene mutations			< 0.001
Positive	7 (58.3)	9 (11.4)	
Negative	5 (41.7)	70 (88.6)	

BW, birth weight; GA, gestational age; DM, delivery method; VG, vaginal delivery; CS, caesarean section.

The results of WES analysis showed that 8 pathogenic mutations in 8 different pedigrees (8/47, 17.0%) were identified (Table 3). All of them were from neonates with positive family findings, revealing a positive rate of 66.7% (8 / 12).

Of these mutations, two different NDP mutations [deletion of exon 2,362 G > A (21)] were identified in two boys presenting as bilateral typical retinal detachment accompanied by a retrolenticular fibrotic mass. The heterozygous LRP5 mutation (2,558 A > G) was found in a two-day-old boy with stage 4 ROPLR in both eyes. The variant was found in his father, who had bilateral stage 1 ROPLR.

There were three variants in FZD4 identified in the cohort, including two missense mutations [757C > T (22), 284A > T] and one frameshift mutation (c49–50insCCCGGGGGCG). The carrier of the variant 757C > T was a three-day-old boy who had bilateral retinal ridge and avascular retinal in the peripheral retina (Figure 1). His father was proband in his family. The variant was inherited from his father, and his sister also harbored the mutation. Although his father and sister had no clinical symptoms, peripheral avascularity of bilateral eyes were observed in FFA (Figures 2, 3). Variant c284A > T was detected in a two-day-old boy with bilateral retinal folds accompanied by vitreous hemorrhage. His father was proband in his family. The mutation was also detected in his father and sister, both of whom had peripheral avascularity and retinal folds. A two-day-old girl with c49–50insCCCGGGGGCG mutation had retinal detachment in the right eye and peripheral neovascularization in the left eye. Her mother, who carried the mutation, had stage 1 ROPLR.

TABLE 3 Variants of mutated genes in newborns with ROP-like retinopathies.

Case	Gene	Genotype	Location	Cdna	Protein	Allele Type	Heredity	Reference	SIFT	Polyphen2	Mutation Assessor	PROVEAN
1	FZD4	heterozygous	exon 2	757 C > T	R253C	Missense	paternal	Zhao et al.[20]	Damaging	Probably damaging	Medium	Damaging
3	FZD4	heterozygous	exon 1	284A>T	Q95L	Missense	paternal	Novel	Damaging	Benign	Neutral	Damaging
6	LRP5	heterozygous	exon12	2558 A >G	Gln853Arg	Missense	paternal	Novel	Damaging	Probably damaging	Medium	Neutral
7	NDP	hemizygous	exon3	362G > A	Arg121Gln	Missense	maternal	Johnson et al.[19]	Damaging	Probably damaging	Low	Damaging
2	NDP	hemizygous	exon 2	CNV		Deletion	maternal	Novel	-	-	-	-
4	TSPAN12	heterozygous	exon 4	285 + 1G > A	IVS4 dsG-A + 1	Splicing	paternal	Novel	-	-	-	-
5	TSPAN12	heterozygous	exon7	518delA	p.E173fs	Frameshift	maternal	Novel	-	-	-	-
8	FZD4	heterozygous	exon 1	c4950insCCCGGGGGCG	p.V17fs	Frameshift	maternal	Novel	-	-	-	-

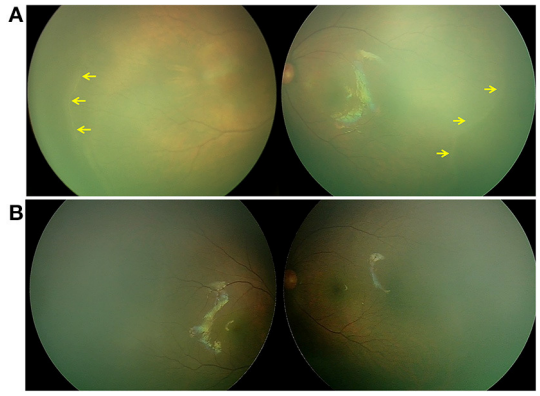

FIGURE 1
Retina imaging of a full-term newborn with FZD4 mutation (case 1, GA 37W, BW 2300g, and IVD 37W^{+3}). **(A)** Fundus picture showing retinal ridges (yellow arrow) in zone II in bilateral eyes and avascular retinal periphery. **(B)** Fundus images of both eyes showing that the ridge resolved spontaneously 26 months after the first visit.

Two different variants in TSPAN12, a splicing mutation (285 + 1G > A) and a frameshift mutation insertion (518delA), were included. Variant 285 + 1G > A was detected in a three-day-old boy with bilateral retinal folds. His father, who carried the same mutation, showed bilateral peripheral avascular areas. A two-day girl with 518delA mutation had bilateral retinal ridge and avascular retinal periphery. Her mother carried the mutation with bilateral peripheral avascularity. We measured no specific associations between phenotype and genotype due to the small size of the cohort.

Perinatal hypoxia-ischemia in neonates with ROPLR

Of the 47 neonates, perinatal risk factors of 9 different variables was found in 19 infants: placenta previa in one infant, turbidity of amniotic fluid in three, umbilical cord around fetal neck in five, hyperbilirubinemia in two, maternal anemia in four, fetal distress in two, intracerebral hemorrhage in one, intrauterine hypoxia in one, and premature rupture of membranes in one. Two neonates had both turbidity of amniotic fluid and umbilical cord around the fetal neck (Table 1).

Sub–grouping of ROPLR neonates and the analysis of the risk factors

In order to clarify the potential etiology and risk factors of ROPLR, all neonates were subdivided into three groups according to the presence of positive findings in family members and perinatal hypoxia-ischemia. Of the 47 neonates with ROPLR, 12 neonates (25.5%) whose family members presented positive fundus findings were allocated to group A, 17 neonates (three unilateral, 14 bilateral, 36.2%) with perinatal hypoxia-ischemia were categorized into group B, and the other 18 neonates (38.3%) were allocated to group C. Two neonates were both with perinatal hypoxia-ischemia, and family members presented positive fundus findings were allocated to group A. The demographic characteristics, clinical features, and treatment outcomes were compared among the groups and listed in Table 4.

Essentially, there were no statistical differences in BW, age, or gender ratio among the three groups ($p = 0.800$, 0.94, and 0.57). There was no significant difference in retinopathy stage between group B and group C ($p = 0.31$). Severe retinopathy (stages 4 and 5) was seen in 45.8% (11/24) eyes in group A; however, none was found in group B and group C. Compared to those in group B and group C, infants in group A had significantly more severe retinopathy ($p < 0.001$). During the follow-up, seven eyes in group A, three eyes in group B, and two eyes in group C (29.2%, 9.7%, and 5.6%) received treatments, respectively. There were significantly more eyes in need of treatment in group A compared to group B and C ($p < 0.001$). Spontaneous complete regression was observed in 26 eyes of 15 neonates (83.9%, 26/31) in group B and in 34 eyes of 18 neonates (94.4%, 34/36) in group C (Figure 4); however, there was no one in group A ($p < 0.001$). For those 12 eyes needing treatment, eight eyes with moderate retinopathy (stage 2/3) resulted in partial regression, while 4 eyes staged 4b stayed stable. The average BCVA (logMAR) at final follow up were 1.53 ± 1.72, 0.217 ± 0.109, 0.167 ± 0.143 in group A, group B, and group C. There was significantly worse vision in group A compared to group B and C ($p < 0.001$). The refractive error at final visit were −2.59 ± 5.47D, 1.28 ± 0.604D, and 1.42 ± 0.674D in group A, group B, and group C. The prevalence of myopia was significantly higher than that in group B and group C ($p < 0.001$).

Discussion

Retinal vascular changes similar to ROP in healthy full/near-term infants with a normal birth weight were sporadically reported in previous studies (5, 7). And among them, most of infants were with supplementary oxygen exposure. The clinical findings were classically described as "ROP-like retinopathy (ROPLR)" with an incidence between 0.42 and 0.9% of healthy babies (4, 23). It has been reported that the pathogenesis of ROPLR is associated with perinatal hypoxia-ischemia (8, 24). A study revealed that meconium-stained amniotic fluid was identified as determinants of birth asphyxia (25). However, there is no consensus regarding the etiology or diagnostic criteria for ROPLR. We herein reported

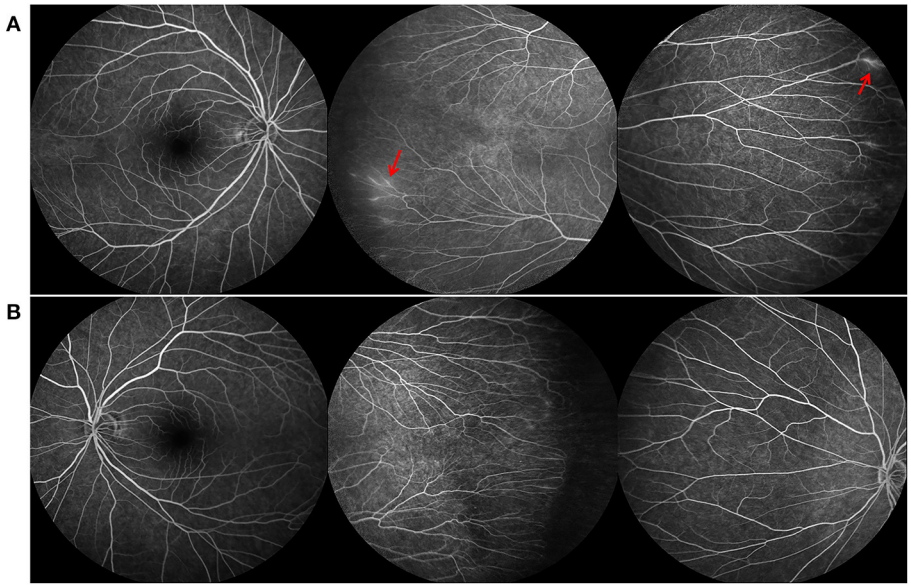

FIGURE 2
Fundus fluorescein angiography (FFA) findings of the father of case 1, who also carried the FZD4 mutation. **(A,B)** are bilateral fundus images, showing temporal avascular area with brush-shaped peripheral retinal vessles and leakage of the dye (red arrow).

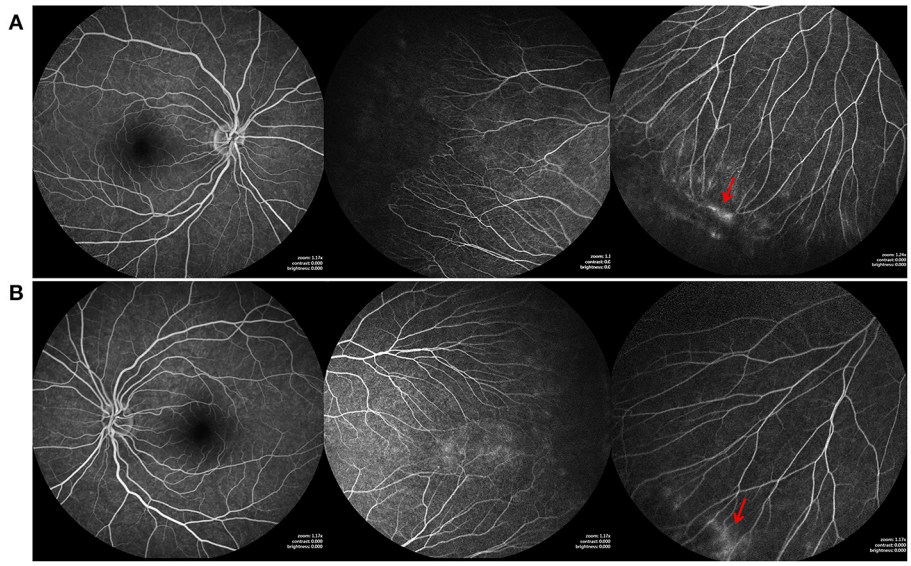

FIGURE 3
Fundus fluorescein angiography (FFA) findings of the elder sister of case1, who also carried the FZD4 mutation. **(A,B)** are bilateral fundus images, showing temporal avascular area with brush-shaped peripheral retinal vessels, avascular retinal periphery and leakage of the dye (red arrow).

47 neonates with ROPLR who were recruited from their birth and followed up for at least 30 months. The clinical features, natural history, treatment and outcome, prognosis, genetic testing, and perinatal hypoxia-ischemia were reviewed and analyzed.

Our study is the first report providing clinical findings, treatment outcomes, and prognosis in neonates with ROPLR. Of the total 47 neonates, the clinical features varied from stage 1 to 5 according to ROP staging criteria. 10 infants presented asymmetry. The ROPLR spontaneously regressed in 79.1% infants without any intervention. According to the ROP criteria, 12 eyes of eight patients received treatments in our study and 8 eyes partially regressed and 4 eyes stable. It was encouraging that the prognosis of ROPLR was favorable after

TABLE 4 Sub-grouping of ROPLR neonates and the analysis of the risk factors and outcomes.

	Group A	Group B	Group C	P values
Total number, *n* (%)	12 (25.5)	17 (36.2)	18 (38.3)	-
Sex, *n* (%)				0.570
Male	10 (83.3)	13 (76.5)	12 (66.7)	
Female	2 (16.7)	4 (23.5)	6 (33.3)	
Birth weight, g	3,096 ± 414	3,126 ± 331	3,043 ± 359	0.800
GA at birth, weeks	38.6 ± 1.0	38.6 ± 1.4	38.5 ± 1.3	0.940
Stage at first visit (eye)	24	34	36	*P* (A-B-C) < 0.001
0	0	3 (8.8)	0	*P* (A-B) < 0.001
1	2 (8.3)	23 (67.6)	26 (72.2)	*P* (A-C < 0.001
2	10 (41.7)	6 (17.6)	4 (11.1)	
3	1 (4.2)	2 (5.9)	6 (16.7)	
4	6 (25)	0	0	
5	5 (20.8)	0	0	
Total eyes	24	31	36	
Observation	17 (70.8)	28 (90.3)	34 (94.4)	P (A-B-C) < 0.001
Treatment needed eyes	7 (29.2)	3 (9.7)	2 (5.6)	P (A-B) < 0.001
LPC	2	2	0	P (A-C) < 0.001
IV	2	1	2	
IV with LPC	2	0	0	
IV with SB	1	0	0	
Outcomes (eyes)	24	31	36	P (A-B-C) < 0.001
CR	0	26 (80.3)	34 (94.4)	P (A-B) < 0.001
PR	13 (54.2)	5 (16.1)	2 (5.6)	P (A-C) < 0.001
Stable	11 (45.8)	0 (0)	0 (0)	
Progression	0(0)	0 (0)	0 (0)	
Gene mutations	8 66.7%)	0 (0)	0 (0)	
BCVA at final visit (logMAR)	1.53 ± 1.72	0.217 ± 0.109	0.167 ± 0.143	P (A-B-C) < 0.001
				P (A-B) < 0.001
				P (A-C) < 0.001
Refractive error at final visit (D)	−2.59 ± 5.47	1.28 ± 0.604	1.42 ± 0.674	P (A-B-C) = 0.003
				P (A-B) < 0.001
				P (A-C) < 0.001

GA, gestational age; ROP, retinopathy of prematurity; IV, Intravitreal injection; LPC, laser photocoagulation; SB, scleral buckling CR, complete regression; PR, partial regression.

prompt treatment. No recurrence or retreatment was presented during a long follow-up period.

According to our previous studies, TEMPVIA revealed by SLO, was found in 88.3% of FEVR patients (20). Our current study has proved further that TEMPVIA, identified in 25.5% of families, could serve as a biomarker. FEVR is a rare disorder of retinal blood vessel development, leading to incomplete vascularization of the peripheral retina and poor vascular differentiation. Most patients have an avascular peripheral retina but expressivity may be asymmetric and is highly variable, ranging from asymptomatic to severe within the same family. Several genes, including FZD4, LPR5, TSPAN12, and NDP, are important components in the Wnt/Norrin signaling pathway that regulates developmental retinal angiogenesis and maintains retinal blood vessel integrity (26–29). Overall, about 44% of FEVR patients could be explained by these four gene mutations. It is noteworthy that 66.7% of these 12 families in our current cohort were confirmed carrying mutated FEVR-related gene mutations, which indicated that at least 17.0% (8/47) neonates with ROPLR actually have FEVR, and this can be confirmed clinically and genetically. Though studies have mentioned that ROP can be developed in near-term infants with normal BW (30) and neonates could behave like FEVR patients but were also with ROP, termed ROPER (ROP vs. FEVR) (31, 32), carefully evaluation of the family members and genetic

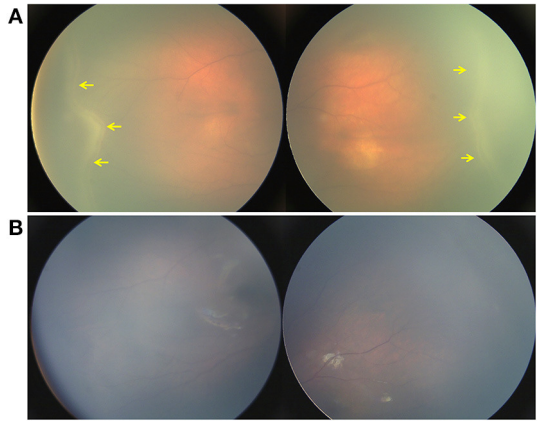

FIGURE 4
Retina imaging showing the disease course of a neonate with ROPLR (GA 37W, BW 2500g, IVD 37W^{+3}). **(A)** Fundus picture showing retinal ridges and peripheral neovascularization (yellow arrow) in zone II in bilateral eyes. **(B)** Fundus images of both eyes showing that the ridges resolved spontaneously 2 months after the first visit. Neither vessel dilation nor tortuosity was found.

analysis are essential for making the final diagnosis. Therefore, we suggest that fundus examination in family members is necessary, sensitive, and helpful for distinguishing FEVR from ROPLR. In general, family history and deliberate fundus examination, not only in babies, but also in their family members, are pivotal for identifying the underlying reasons for ROPLR.

Differential diagnosis of ROPLR is difficult but of great importance. In this study, 12 neonates were diagnosed as FEVR, in which 8 neonates had mutations and 4 neonates had no mutations. Among the 8 neonates with mutations, 6 (75%) had retinal detachment, and 5 had retinal detachment bilaterally. However, the 4 neonates without mutations had stage 1 or 2 FEVR. This result filled in the blanks of the current understanding of FEVR in neonates. However, it is impossible to accurately assess the progression of FEVR to a late stage. Further analysis of novel causative genes may explain the mild clinical findings. Our results showed that retinal folds as well as total retinal detachment could occur for several days after birth (1–3 days). FEVR in young children tends to be very aggressive, usually leading to severe complications (33). No eyes with FEVR could regress without any intervention, while seven eyes progressed to needing treatment in this study. Fortunately, with timely treatments, including IVR, LPC, and scleral buckling, satisfactory outcomes were achieved in most neonates. Severe complications, including total retinal detachment, cataracts, keratopathy, and glaucoma, were not noted in any of the patients receiving timely treatment. However, the development of visual status and refractive error were significantly affected. Therefore, early detection and prompt therapy can restore vision in a timely manner as well as prevent blindness for neonates with FEVR.

The diagnosis of real "ROPLR" can only be made after exclusion of other retinopathies in infants, including PFV, IP, and FEVR. Although the pathogenesis of ROPLR remains elusive, systemic abnormalities such as brain anomalies and defects and poor maternal nutrition, increased oxygen tension and metabolic demands in the retina after birth, and blockage of placental transfer of nutritional factors have been hypothesized as potential reasons for real ROPLR (8, 34, 35). Nineteen neonates (40.4%) with perinatal hypoxia-ischemia were discovered in the study. Twenty-eight of the 31 eyes (90.3%) spontaneously regressed in group B as the neonates grew up and the physiological situation improved. Therefore, we supposed that ROPLR might be associated with perinatal hypoxia-ischemia.

The limitations of our study lie in the limited number of enrolled patients. Moreover, the constitution of FEVR (25.5%) and ROPLR (74.5%) in term neonates might not be representative of the universal population. It should also be noted that perinatal infection/inflammatory and the interactions among risk factors need to be further explored. Therefore, further studies with larger sample sizes are necessary to validate our findings.

In conclusion, we observed 47 neonates with ROPLR. The clinical features mimicking ROP varied widely from stage 1 to stage 5. With timely screening and treatment in these neonates, the prognosis of ROPLR was favorable and encouraging, and childhood blindness might be prevented. Perinatal maternal and/or neonatal hypoxic-ischemia might be the major risk factors of ROPLR, in which the retinopathy spontaneously regressed as the physiological situation improved. FEVR, which is confirmed by positive family findings and genetic testing, might be one of the aetiologic factors of ROPLR. The retinopathy due to FEVR was more severe, and treatment was needed. It is suggested that all neonates should receive universal eye screening within 72 h of birth. Retinal detachment in a newborn suggests another mechanism other than "ROP". Genetic testing and carefully evaluation of the family members should be prompted when a full/near-term newborn presented with retinal fold or retinal detachment. Importantly, with timely recognition and treatment in these neonates, childhood blindness may be prevented. Furthermore, studies with a larger sample size are required to confirm our findings and explore the underlying mechanism of ROPLR.

Data availability statement

The original contributions presented in the study are included in the article/Supplementary material, further inquiries can be directed to the corresponding author.

Ethics statement

The studies involving human participants were reviewed and approved by Institutional Review Board of Zhongshan Ophthalmic Center, Sun Yat-sen University. Written informed consent to participate in this study was provided by the participants' legal guardian/next of kin. Written informed consent was obtained from the individual(s), and minor(s)' legal guardian/next of kin, for the publication of any potentially identifiable images or data included in this article.

Author contributions

LS, WY, and XD conceptualized and designed the study, drafted the initial manuscript, and reviewed and revised the manuscript. LH, SL, MS, JL, YL, and ZL designed the data collection instruments, collected data, carried out the initial analyses, and reviewed and revised the manuscript. All authors contributed to the article and approved the submitted version.

Funding

This study is supported in part by grants from the Fundamental Research Funds of State Key Laboratory of Ophthalmology, Research Funds of Sun Yat-sen University (15ykjxc22d; Guangzhou, Guangdong, China), Science and Technology Program Guangzhou, China (201803010031; Guangzhou, Guangdong, China).

Acknowledgments

We thank the enrolled families for their kind support and cooperation.

Conflict of interest

The authors declare that the research was conducted in the absence of any commercial or financial relationships that could be construed as a potential conflict of interest.

Publisher's note

Supplementary material

The Supplementary Material for this article can be found online at: https://www.frontiersin.org/articles/10.3389/fmed.2022.914207/full#supplementary-material

SUPPLEMENT FIGURE
Representative images of FEVR (case 4, GA 38W, BW 3100g, IVD 38W^{+3}).

References

1. Gilbert C, Fielder A, Gordillo L, Quinn G, Semiglia R, Visintin P, et al. Characteristics of infants with severe retinopathy of prematurity in countries with low, moderate, and high levels of development: implications for screening programs. *Pediatrics.* (2005) 115:e518–25. doi: 10.1542/peds.2004-1180

2. Azad R, Gilbert C, Gangwe AB, Zhao P, Wu WC, Sarbajna P, et al. Retinopathy of prematurity: how to prevent the third epidemics in developing countries. *Asia Pac J Ophthalmol (phila).* (2020) 9:440–8. doi: 10.1097/APO.0000000000000313

3. Askie LM, Darlow BA, Davis PG, Finer N, Stenson B, Vento M, et al. Effects of targeting lower versus higher arterial oxygen saturations on death or disability in preterm infants. *Cochrane Database Syst Rev.* (2017) 4:CD011190. doi: 10.1002/14651858.CD011190.pub2

4. Li LH Li N, Zhao JY, Fei P, Zhang GM, Mao JB, et al. Findings of perinatal ocular examination performed on 3573, healthy full-term newborns. *Br J Ophthalmol.* (2013) 97:588–91. doi: 10.1136/bjophthalmol-2012-302539

5. Ratra D, Akhundova L, Das MK. Retinopathy of prematurity like retinopathy in full-term infants. *Oman J Ophthalmol.* (2017) 10:167–72. doi: 10.4103/ojo.OJO_141_2016

6. Ma Y, Deng G, Ma J, Liu J, Li S, Lu H. Universal ocular screening of 481 infants using wide-field digital imaging system. *BMC Ophthalmol.* (2018) 18:283. doi: 10.1186/s12886-018-0943-7

7. Padhi TR, Rath S, Jalali S, Pradhan L, Kesarwani S, Nayak M, et al. Larger and near-term baby retinopathy: a rare case series. *Eye.* (2015) 29:286–9. doi: 10.1038/eye.2014.253

8. Chen LN HX, Huang LP, A. survey of high risk factors affecting retinopathy in full-term infants in China. *Int J Ophthalmol.* (2012) 5:177–80. doi: 10.3980/j.issn.2222-3959.2012.02.12

9. Savarese M, Spinelli E, Gandolfo F, Lemma V, Di Fruscio G, Padoan R, et al. Familial exudative vitreoretinopathy caused by a homozygous mutation in Tspan12 in a cystic fibrosis infant. *Ophthalmic Genet.* (2014) 35:184–6. doi: 10.3109/13816810.2013.811270

10. Lee J, Dammann O. Perinatal infection, inflammation, and retinopathy of prematurity. *Semin Fetal Neonatal Med.* (2012) 17:26–9. doi: 10.1016/j.siny.2011.08.007

11. Wang Z, Liu CH, Huang S, Chen J. Wnt signaling in vascular eye diseases. *Prog Retin Eye Res.* (2019) 70:110–33. doi: 10.1016/j.preteyeres.2018.11.008

12. Wang Z, Chen C, Sun L, Zhang A, Liu C, Huang L, et al. Symmetry of folds in fevr: a genotype-phenotype correlation study. *Exp Eye Res.* (2019) 186:107720. doi: 10.1016/j.exer.2019.107720

13. International Committee for the Classification of Retinopathy of P. The international classification of retinopathy of prematurity revisited. *Arch Ophthalmol*. (2005) 123:991–9. doi: 10.1001/archopht.123.7.991

14. Early Treatment For Retinopathy Of Prematurity Cooperative G. Revised indications for the treatment of retinopathy of prematurity: results of the early treatment for retinopathy of prematurity randomized trial. *Arch Ophthalmol.* (2003) 121:1684–94. doi: 10.1001/archopht.121.12.1684

15. Emami S, Isaac M, Mireskandari K, Tehrani N. Laser treatment for retinopathy of prematurity: a decade since etrop. *Ophthalmology.* (2019) 126:639–41. doi: 10.1016/j.ophtha.2018.12.012

16. Ling K, Liao P, Wang N, Chao A, Chen K, Chen T, et al. Rates and risk factors for recurrence of retinopathy of prematurity after laser or intravitreal anti-vascular endothelial growth factor monotherapy. *Retina.* (2020) 40:1793–803. doi: 10.1097/IAE.0000000000002663

17. Parag K, Shah VP, Smita S. Karandikar, Ratnesh Ranjan, Venkatapathy Narendran, Narendran Kalpana. Retinopathy of prematurity past, present and future. *World J Clin Pediatr*. (2016) 5:35–46. doi: 10.5409/wjcp.v5.i1.35

18. Titawattanakul Y, Kulvichit K, Varadisai A, Mavichak A. Outcomes of pre-early treatment for retinopathy of prematurity (Pre-Etrop). *Clin Ophthalmol.* (2020) 14:3393–7. doi: 10.2147/OPTH.S268997

19. Chen C, Sun L, Li S, Huang L, Zhang T, Wang Z, et al. The spectrum of genetic mutations in patients with asymptomatic mild familial exudative vitreoretinopathy. *Exp Eye Res.* (2020) 192:107941. doi: 10.1016/j.exer.2020.107941

20. Zhang T, Wang Z, Sun L, Li S, Huang L, Liu C, et al. Ultra-wide-field scanning laser ophthalmoscopy and optical coherence tomography in fevr: findings and its diagnostic ability. *British J Ophthalmol.* (2020) 0:1–7. doi: 10.1136/bjophthalmol-2020-316226

21. Johnson K, Mintz-Hittner H, Conley Y, Ferrell R. X-linked exudative vitreoretinopathy caused by an arginine to leucine substitution (r121l) in the norrie disease protein. *Clin Genet.* (1996) 50:113–5. doi: 10.1111/j.1399-0004.1996.tb02363.x

22. Tian T, Zhang X, Zhang Q, Zhao P. Fzd4variable reduction in norrin signaling activity caused by novel mutations in *FZD4* identified in patients with familial exudative vitreoretinopathy. *Mol Vis.* (2019) 25:60–9.

23. Vinekar A, Govindaraj I, Jayadev C, Kumar AK, Sharma P, Mangalesh S, et al. Universal ocular screening of 1021 term infants using wide-field digital imaging in a single public hospital in India - a pilot study. *Acta Ophthalmol.* (2015) 93:e372–6. doi: 10.1111/aos.12685

24. Huang H, Huang C, Hung P, Chang Y. Hypoxic-ischemic retinal injury in rat pups. *Pediatr Res.* (2012) 72:224–31. doi: 10.1038/pr.2012.74

25. Lemma K, Misker D, Kassa M, Abdulkadir H, Otayto K. Determinants of birth asphyxia among newborn live births in public hospitals of gamo and gofa zones, Southern Ethiopia. *BMC Pediatr.* (2022) 22:280. doi: 10.1186/s12887-022-03342-x

26. Dickinson JL, Sale MM, Passmore A, FitzGerald LM, Wheatley CM, Burdon KP, et al. Mutations in the Ndp gene: contribution to norrie disease, familial exudative vitreoretinopathy and retinopathy of prematurity. *Clin Exp Ophthalmol.* (2006) 34:682–8. doi: 10.1111/j.1442-9071.2006.01314.x

27. Kondo H, Kusaka S, Yoshinaga A, Uchio E, Tawara A, Hayashi K, et al. Mutations in the Tspan12 gene in japanese patients with familial exudative vitreoretinopathy. *Am J Ophthalmol.* (2011) 151:1095–100 e1. doi: 10.1016/j.ajo.2010.11.026

28. Paes K, Wang E, Henze K, Vogel P, Read R, Suwanichkul A, et al. Frizzled 4 Is required for retinal angiogenesis and maintenance of the blood-retina barrier. *Invest Ophthalmol Vis Sci.* (2011) 52:6452–61. doi: 10.1167/iovs.10-7146

29. Lai MB, Zhang C, Shi J, Johnson V, Khandan L, McVey J, et al. Tspan12 is a norrin co-receptor that amplifies frizzled4 ligand selectivity and signaling. *Cell Rep.* (2017) 19:2809–22. doi: 10.1016/j.celrep.2017.06.004

30. Gunay M, Celik G, Tuten A, Karatekin G, Bardak H, Ovali F. Characteristics of severe retinopathy of prematurity in infants with birth weight above 1500 grams at a referral center in Turkey. *PLoS ONE.* (2016) 11:e0161692. doi: 10.1371/journal.pone.0161692

31. John VJ, McClintic JI, Hess DJ, Berrocal AM. Retinopathy of prematurity versus familial exudative vitreoretinopathy: report on clinical and angiographic findings. *Ophthalmic Surg Lasers Imaging Retina.* (2016) 47:14–9. doi: 10.3928/23258160-20151214-02

32. Tanenbaum R, Acon D, El Hamichi S, Negron C, Berrocal AM. Unrecognized roper in a child with a novel pathogenic variant in Znf408 gene. *Ophthalmic Genet*. (2020) 1–4. doi: 10.1080/13816810.2020.1778735

33. Hocaoglu M, Karacorlu M, Sayman Muslubas I, Ersoz M, Arf S. Anatomical and functional outcomes following vitrectomy for advanced familial exudative vitreoretinopathy: a single surgeon's experience. *British J Ophthalmol.* (2017) 101:946–50. doi: 10.1136/bjophthalmol-2016-309526

34. Kim H, Yu Y. Retinopathy of prematurity-mimicking retinopathy in full-term babies. *Korean J Ophthalmol.* (1998) 12:98–102. doi: 10.3341/kjo.1998.12.2.98

35. Smith LE, Hard AL, Hellstrom A. The biology of retinopathy of prematurity: how knowledge of pathogenesis guides treatment. *Clin Perinatol.* (2013) 40:201–14. doi: 10.1016/j.clp.2013.02.002

frontiers | Frontiers in Medicine

TYPE Original Research
PUBLISHED 23 August 2022
DOI 10.3389/fmed.2022.961152

OPEN ACCESS

EDITED BY
Panpan Ye,
Zhejiang University, China

REVIEWED BY
Guoming Zhang,
Shenzhen Eye Hospital, China
Simar Rajan Singh,
Post Graduate Institute of Medical Education and Research (PGIMER), India
Pengyi Zhou,
The First Affiliated Hospital of Zhengzhou University, China

*CORRESPONDENCE
Peiquan Zhao
zhaopeiquan@xinhuamed.com.cn;
zhaopeiquan@126.com
Yu Xu
drxuyu@126.com

†These authors have contributed equally to this work

SPECIALTY SECTION
This article was submitted to Ophthalmology, a section of the journal Frontiers in Medicine

RECEIVED 04 June 2022
ACCEPTED 01 August 2022
PUBLISHED 23 August 2022

CITATION
Peng J, Ren J, Zhang X, Yang Y, Zou Y, Xiao H, Xu Y and Zhao P (2022) Two-step widefield fundus fluorescein angiography-assisted laser photocoagulation in pediatric retinal vasculopathy: A pilot study. *Front. Med.* 9:961152. doi: 10.3389/fmed.2022.961152

Two-step widefield fundus fluorescein angiography-assisted laser photocoagulation in pediatric retinal vasculopathy: A pilot study

Jie Peng†, Jianing Ren†, Xuerui Zhang†, Yuan Yang†, Yihua Zou, Haodong Xiao, Yu Xu* and Peiquan Zhao*

Department of Ophthalmology, Xin Hua Hospital Affiliated to Shanghai Jiao Tong University School of Medicine, Shanghai, China

Purpose: To introduce the procedures of two-step fundus fluorescein angiography (FFA) and evaluate its utility in the management of pediatric retinal vasculopathy.

Materials and methods: In this retrospective study, medical records of 12 patients who received two-step FFA were studied. The two-step FFA consisted of step 1 [low-dose (LD)] FFA at an intravenous dose of 1.5 mg/kg fluorescein, followed by step 2 [reduced dose (RD)] FFA at a dose of 6.2 mg/kg fluorescein. Demographic data, including age, gender, diagnosis, weight, gestational age, birth weight, and weight on the examination day were taken, were collected. The results of two-step FFA and treatment were recorded.

Results: A total of 20 eyes were studied. The top 5 common FFA changes in RD-FFA included peripheral avascular zone (15 eyes), fluorescein leakage (10 eyes), supernumerous vascular branching (10 eyes), neovascularization (NV) (8 eyes), and absence of the foveal avascular zone (6 eyes). LD-FFA was efficient to show all the NV without severe vitreous dye in 8/8 (100.0%) eyes with NV, partial peripheral avascular zone in 11/15 (73.3%) eyes, while RD-FFA always offered more information in all the eyes. Thirteen eyes had laser photocoagulation under the guidance of LD-FFA. In 4 (30.8%) eyes, RD-FFA revealed more lesions and an immediate relaser was performed. Laser photocoagulation was successfully performed in all the 13 eyes in one session without being rearranged. After a median follow-up of 28.1 months, all the eyes were in a stable status.

Conclusion: Step-one LD-FFA acted as a pre-FFA to show the NV, and step-two RD-FFA acted as a double-check. The modified strategy may be a helpful clinical adjuvant in the laser photocoagulation of pediatric retinal disorders, especially for young ophthalmologists.

KEYWORDS

fundus fluorescein angiography (FFA), retinal vasculopathy, neovascularization, laser photocoagulation, fluorescein leakage

Introduction

Widefield fundus fluorescein angiography (WF-FFA) offers more details of microvascular abnormalities, retinal non-perfusion areas, neovascularization, vascular fluorescein leakage (1), and vascular perfusion dynamics than fundoscopy or color image alone, broadening ophthalmologists' understanding of pediatric retinal vascular disorders (2). Fundus fluorescein angiography (FFA) also assisted in the management of pediatric retinal vascular diseases such as retinopathy of prematurity (ROP) (3), Coats disease, familial exudative vitreoretinopathy (FEVR) (4), incontinentia pigmenti (IP) (5), and so on.

Traditional FFA was performed with an intravenous injection of 5% fluorescein dye dosed by weight (7.7 mg/kg) (6, 7). For oral FFA, the applied concentration of fluorescein was 20 mg/kg of body weight as reported (8, 9). Sometimes, the green fluorescein dye extravasated into the vitreous overlying the areas of retinal neovascularization (NV) guiding the ablation of avascular retina (10, 11). Unfortunately, for cases with massive NV, extensive leakage of fluorescein into the vitreous made laser photocoagulation difficult. The treatment should be rescheduled (12), which always needs another general anesthesia for younger children.

Occasionally, we found 1.5 mg/kg fluorescein that could help to show the retinal NV without severe vitreous dye. To avoid secondary interference caused by dye leakage, we came up with this two-step FFA procedure and evaluated its utilization in a real-world setting. The two-step FFA consisted of step 1 [low-dose (LD)] FFA at an intravenous dose of 1.5 mg/kg fluorescein, followed by step 2 (reduced dose of 6.2 mg/kg) FFA to ensure the observation and treatment in pediatric patients. In this pilot study, we postulated that two-step FFA may be increasing as a meaningful clinical adjuvant in the management of pediatric retinal disorders.

Materials and methods

With Institutional Review Board approval by Xinhua Hospital Affiliated to Shanghai Jiao Tong University (XHEC-D-2022-071), a retrospective study was conducted in our department from 6 December 2019 to 15 May 2022. It adhered to the tenets of the Declaration of Helsinki (13). Written informed consent was signed by the guardians for performing FFA and expected interventions, including laser photocoagulation or intravitreal injection of anti-vascular endothelial growth factor (VEGF) agents. Cases were excluded if poor-quality images were acquired due to significant media opacity such as keratopathy, cataract, or vitreous hemorrhage.

Demographic data, including age, gender, diagnosis, weight, gestational age, birth weight, and weight on the examination day were collected. All the FFA and fundus color images were acquired under general anesthesia with RetCam III (Clarity Medical System, Pleasanton, CA, United States). Scleral indentation was performed as needed to show the far periphery of the retina.

After proper general anesthesia and mydriasis, color images were initially taken before step 1 FFA (LD-FFA). Intravenous sodium fluorescein (10%) was injected into the peripheral vein followed by a saline flush. Contact high-resolution WF-FFA images were obtained. To avoid possible neglect of lesions of both eyes, speculums were placed on both eyes simultaneously. FFA images of posterior pole and four quadrants were first taken on the eye with severer abnormalities or possible NV and the camera was shifted to the fellow eye quickly to take the early venous-stage images. After the LD-FFA, we also checked the skin and vital signs for any allergic reactions. Only when no severe allergic reactions occurred, the further procedures performed. LD-FFA-guided laser photocoagulation was carried out wherever required immediately. After laser photocoagulation, step 2 FFA with a dose of 6.2 mg/kg sodium fluorescein FFA [reduced dose FFA (RD-FFA)] was performed to confirm the possible residual lesions and proper laser spots. Relaser treatment can be applied to the skipped areas accordingly. For eyes with massive NV or severe fluorescein leakage, intravitreal injection of ranibizumab could be applied after the laser photocoagulation.

Statistics

Statistical analysis was performed using Statistical Package for the Social Sciences (SPSS) version 26 (IBM Corporation,

Armonk, NY, United States). Data were expressed as the mean ± SD or as median and range.

Results

Twelve patients (6 boys and 6 girls) with a median age of 6.70 (4.63, 47.75) months, and a mean birth weight of 3070.83 ± 751.50 g received two-step FFA were studied. The clinical diagnoses included FEVR (6 cases, 50.0%), IP (3 cases, 25.0%), Coats disease (2 cases, 16.7%), and retinal detachment (RD) with unknown reason (1 case, 8.3%). Eight patients underwent bilateral FFA and four patients underwent unilateral FFA due to simultaneous surgery on the fellow eye. As a result, a total of 20 eyes were studied.

The results are given in Table 1 and shown in Figures 1, 2. Detailed results are shown in Supplementary material. In LD-FFA, due to the low dose, the early stage images are not clear, and it is hard to illustrate accurate arm-retina time (ART) and timing of phases in all the cases. In LD-FFA, the images can be dark sometimes, with built-in software built in Retcam III, the adjusted images can offer more information in all the images (Figures 1C,D, 2D,F, 3B,E,F). The top 5 common FFA changes in RD-FFA included peripheral avascular zone (15 eyes, 75.0%), fluorescein leakage (10 eyes, 50.0%), supernumerous vascular branching (10 eyes, 50.0%), NV (8 eyes, 40.0%), absence of the foveal avascular zone (FAZ) (6 eyes, 30.0%), and vessels tortuosity (5 eyes, 25.0%). The top 5 common FFA changes in LD-FFA included peripheral avascular zone (11 eyes, 55.0%), fluorescein leakage (9 eyes, 45.0%), NV (8 eyes, 40.00%), supernumerous vascular branching (7 eyes, 35.0%), vessels dilatation (4 eyes, 20.0%), and vessels tortuosity (4 eyes, 20.0%). With a higher dose of fluorescein, RD-FFA reveals more lesions than LD-FFA (Table 1). Interestingly, some lesions were only shown in RD-FFA, including microaneurysms, vessels fluorescence staining, absence of the FAZ, bulbous vascular terminals, distinct pruning of vessels, persistent fetal vasculature (PFV), capillary dropout, and peripheral vessels in normal eyes.

Low-dose fundus fluorescein angiography was efficient to show all the NV with fluorescein leakage in 8/8 (100.0%) eyes. In 14 eyes with different kinds of abnormal vessels, LD-FFA always showed less information and neglected some information in 14 (100%) eyes. Among 15 eyes with peripheral avascular zone, LD-FFA showed partial peripheral avascular zone in 11 eyes frontier to abnormal vessels or NV, while LD-FFA was unable to show peripheral avascular zone anterior to normal or fine vessels, and not efficient to show all the peripheral avascular zone in all the 15 eyes as shown in RD-FFA. As a double-edged sword, low-dose (1.5 mg/kg) fluorescein could show NV in LD-FFA without obvious disturbance in the color fundus images in all the 8/8 eyes. With a higher dose, RD-FFA shows more distinct vascular details about peripheral retinal anatomy, vascular network, and non-perfusion areas, and necessary clinical information was obtained in all the cases. As laser spots were performed after the LD-FFA, laser spots were not recorded as an FFA change.

TABLE 1 Results of the two-step FFA.

	Step one, RD-FFA, eye(s)	Step two, LD-FFA, eye(s)	RD-FFA shown more than LD-FFA, eye(s)
Peripheral avascular zone	15	11	4
Fluorescein leakage	10	9	1
Supernumerous vascular branching	10	7	3
Neovascularization	8	8	0
Absence of the FAZ	6	0	6
Vessels tortuosity	5	4	1
Bulbous vascular terminals	5	0	5
Normal	4	0	4
Dragged-disc	4	3	1
Vessels dilatation	4	4	0
Microaneurysms	3	0	3
Messy vessels	3	1	2
Old laser spots	2	2	0
Vessels fluorescence staining	2	0	2
Telangiectasia	3	2	1
Distinct pruning of vessels	2	0	2
Capillary dropout	2	0	2
Fine vessels	1	1	0
Retinal fold	1	1	0
Avascular zone in the posterior pole	1	1	0
Retinal detachment	1	1	0
Venous-venous anastomoses	1	1	0
Persistent fetal vasculature	1	0	1

FAZ, foveal avascular zone; LD-FFA, low dose-fundus fluorescein angiography; RD-FFA, reduced dose-fundus fluorescein angiography.

In total, 13 (65.00%) eyes had laser photocoagulation under the guidance of LD-FFA. In 4 (4/13, 30.77%) eyes of them, RD-FFA revealed more lesions asking for immediate relaser (Figure 3). The reasons for the relaser included more abnormal vessels and non-perfusion areas (2 eyes) and abnormal vessels with local fluorescein leakage (2 eyes). Laser photocoagulation was successfully performed in all the 13 eyes in one session without being rearranged. Four eyes received intravitreal injection of ranibizumab after laser photocoagulation.

All the patients tolerated the procedures without adverse effects during or after the procedures, such as rash, respiratory distress, tachycardia, fever, and local injection site reactions as

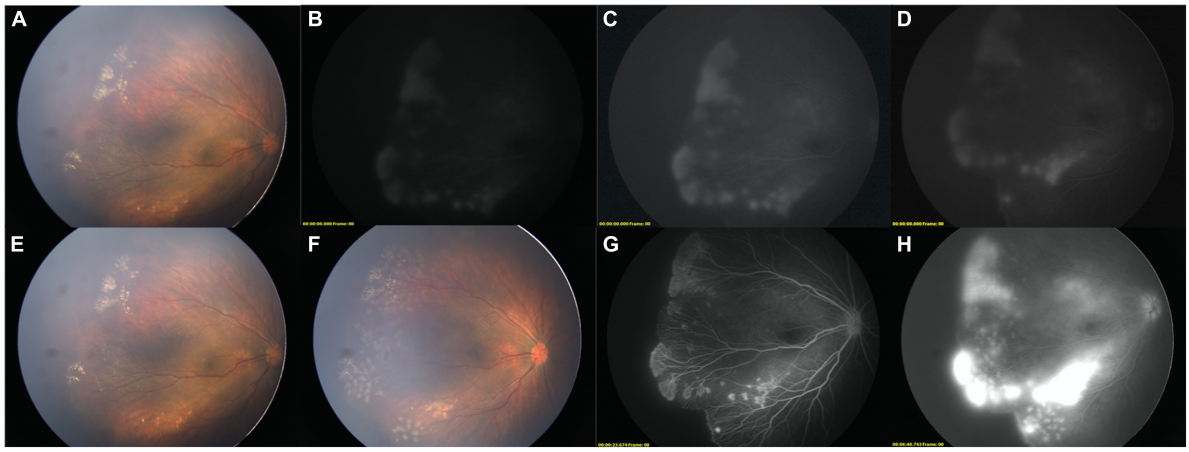

FIGURE 1
Two-step FFA of a FEVR child. **(A)** Color image before FFA (OD). **(B,C)** [adjusted version of **(B)**], LD-FFA image showed supernumerous vascular branching, NV, fluorescein leakage, peripheral avascular zone. **(D)** adjusted version of late phase of LD-FFA, fluorescein leakage remained. **(E)** Color image after LD-FFA. Comparing with **(A)**, no obvious media opacity was noted. **(F)** After laser photocoagulation, the laser spots and retinal vessels are clearly displaced. **(G)** Step-two RD-FFA shown clearly all the detailed retinal vessels and revealed more about the absence of the FAZ, and bulbous vascular terminals. **(H)** Late phase of RD-FFA, severe fluorescein leakage was noted.

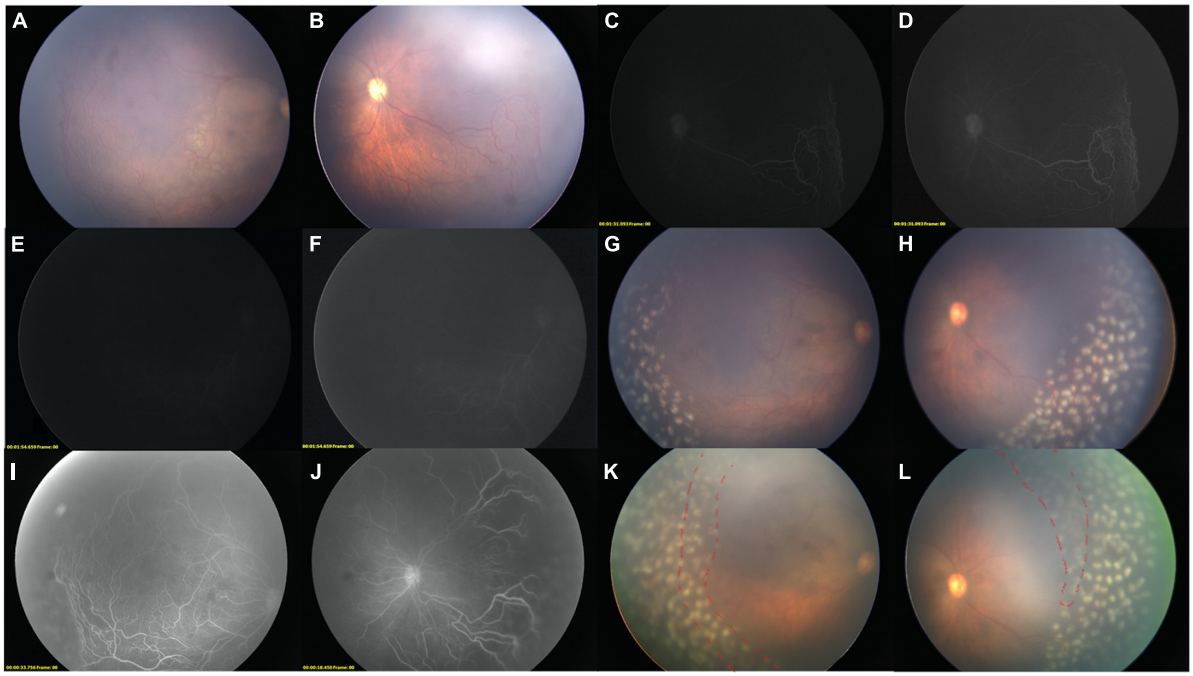

FIGURE 2
Two-step FFA-guided relaser of an IP child. Color images of the right eye before FFA [**(A)** Temporal field; **(B)** Nasal Field]. LD-FFA [**(C)**: 1 m 35 s, **(D)**: Adjusted version of **(C)**; **(E)**: 1 m 54 s, **(F)** adjusted version of **(E)**] showed supernumerous vascular branching, vessels dilatation, vessels tortuosity, and peripheral avascular zone in the nasal field **(D)**, while not so clear in the temporal side **(E,F)**. **(F)** Showed filling of optic disk and sparse posterior retinal vessels. **(G,H)** Color images after laser ablations, the media was clean enough without green stain by the fluorescein. **(I,J)** Step-two RD-FFA reveals all the abnormal vessels, non-perfusion areas, and previous laser spots. **(K,L)** After comparisons, supplementary laser photocoagulation was immediately applied (red dashed line), while the vitreous is greenish due to dye extravasation after RD-FFA.

reported in adults (14). The median follow-up duration was 28.15 (25.78, 28.70) months. On the last visit, all the eyes were in a stable status. No progression of diseases, recurrence of vascular activity, or laser-induced complications, such as rhegmatogenous RD, retinal hole, retinal hemorrhage, exudative RD, or retinal holes, were observed.

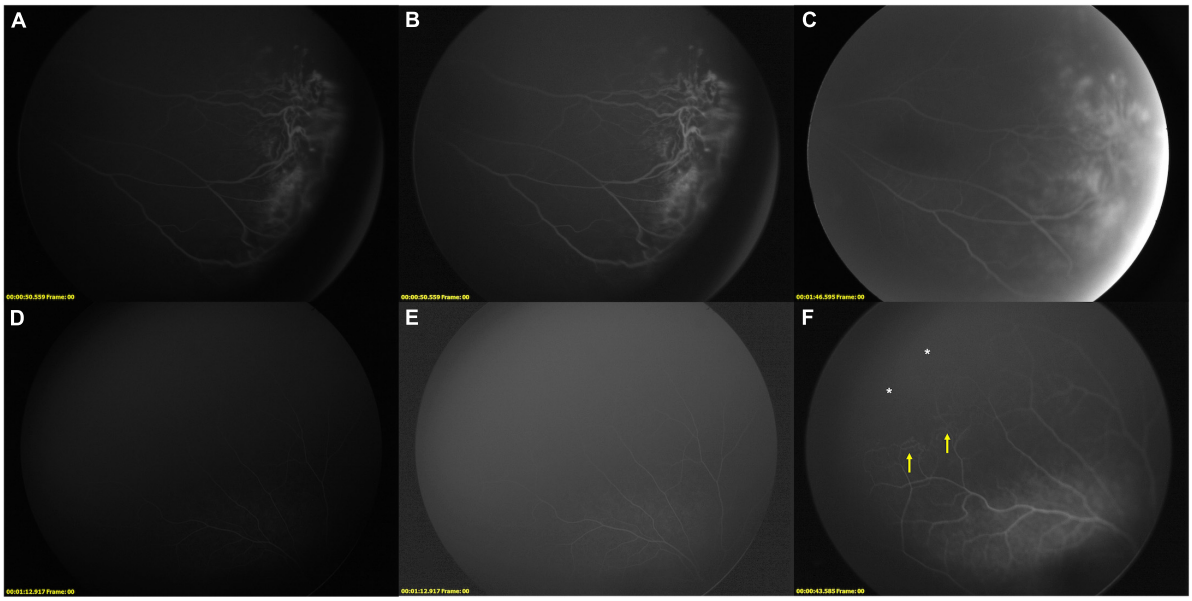

FIGURE 3
Supplementary relaser in the fellow eye after RD-FFA. **(A–F)** FFA images of case 10, a 5-year-old girl with IP. **(A,B)** [**(B)**: adjusted version of **(A)**], LD-FFA (OS): showed dragged-disk, vessels dilatation, vessels tortuosity, messy vessels with fluorescein leakage, and peripheral avascular zone in the temporal field. C, RD-FFA (OS) showed dragged-disk, vessels dilatation, vessels tortuosity, messy vessels, fluorescein leakage, telangiectasis, peripheral avascular zone, and laser spots in the temporal field. **(D,E)** [**(E)**: edited version of **(D)**], LD-FFA (OD) was obscure and showed sparse posterior vessels. **(F)** RD-FFA (OD) showed vessels tortuosity and messy vessels in the periphery (yellow arrow) and peripheral avascular zone (white asterisk) in the superotemporal field.

Discussion

Fundus fluorescein angiography is helpful in clinical situations for a variety of pediatric retinal diseases. In patients with darkly pigmented fundi, such as Asians, the border of the vascularized zone and the demarcation line are barely detectable with an ophthalmoscope. Intraoperative FFA-guided laser photocoagulation in children offered good anatomic outcomes, with preservation of visual acuity in most cases of retinal vascular disease (11, 12, 15). Green fluorescein dye extravasated into the vitreous overlying the areas of retinal neovascularization could guide ablation of the avascular retina (10, 11). However, as time goes by, the dye would diffuse to surrounding areas and stain the area that should not be ablated. Besides, when massive NVs and dye leakage occurred, the dye will be too severe to see the fundus, making simultaneous laser treatment difficult. The treatment should be rescheduled sometimes (12).

Fundus fluorescein angiography was commonly performed with intravenous injection of fluorescein at a dose of 7.7 mg/kg (6, 7) or 3.5 mg/kg (3) and oral intake of fluorescein at a dose of 20 mg/kg (8, 9). The total dose of two-step FFA was also 7.7 mg/kg, same as many other studies (2, 7), which is safely administered intravenously in patients of all the ages, including medically frail, preterm infants (16). The procedures were successfully performed with no fluorescein-related complications in this study. We just made a small modification to divide the common dose into two phases, which are technically safe as traditional ones.

The LD-FFA was able to show all the NV in all the eyes (100.00%), which is helpful in clinical applications. It showed the retinal NVs without strong vitreous staining, making it easy to evaluate the retinal vessels and laser spots under the indirect ophthalmoscope and the camera. A clear view is very important for the doctor to give precise treatment. Inappropriate laser photocoagulation may end up with disease progression, including rhegmatogenous RD, tractional RD, or a combination of both (17). With the guidance of LD-FFA, the NV and abnormal vessels were directed without obvious fluorescein leakage, making precise laser ablations easier to be performed.

For pediatric patients with poor compliance, the FFA and laser photocoagulation are always performed under general anesthesia in the spine position. The laser ablations are conducted with binocular laser indirect ophthalmoscope, which needs a longer learning curve. The procedures are even harder with obscure media. Step-one LD-FFA acted as a pre-FFA to show the NV without obvious vitreous opacity. As a double-edged sword, LD-FFA was surely unable to show all the vascular anomalies, especially for subtle lesions, such as microaneurysms, vessels fluorescence staining, absence of the FAZ, bulbous vascular terminals, distinct pruning of vessels, PFV, and peripheral vessels in normal eyes. Hence, RD-FFA

can serve as a good complement and confirmation on this basis. Step-two RD-FFA reveals more detailed information about retinal vessels and new laser spots, which is the double-check and guides supplementary laser photocoagulation when needed. On the basis of former laser ablation, the residual supplementary laser photocoagulation required less time before excessive fluorescein extravasation blurred the view, which is friendly to surgeons with comfort, especially for young ophthalmologists in their early career.

As a result, in our opinion, we highly recommend this technique to be applied in cases with retinal exudates and suspected NV. An LD-FFA will show whether and where the NV existed without severe media opacity, making the laser treatment easier. With the same pharmacokinetics, the circulation time is the same as traditional ones. So, the NV is always shown within 1 min. If no NVs were noted 1 min after the fluorescein injection, the RD-FFA could be performed immediately to save time. The step-one LD-FFA could be performed as a pretest for NV.

Besides, lesions of the fellow eye could be sometimes neglected since the quality of the angiogram of the fellow eye was suboptimal when performed at a late stage of the angiogram sometimes (12). In case 10 with IP, subtle peripheral messy vessels and avascular zone were noted in RD-FFA and supplementary laser ablation was applied. We believe that an RD-FFA gives us another chance to possibly reveal more signs, which may be neglected in a one-time FFA. After a median follow-up duration of 28.15 months, no laser-induced complications were noted. Besides, all the 13 eyes that received laser photocoagulation were in a stable status without active anomalies. Two-step FFA-guided laser photocoagulation helped to take the active lesions under control.

Furthermore, the LD-FFA could also be considered an allergic test for fluorescein. After the LD-FFA, we also checked the skin and vital signs for any allergic reactions. Only when no severe allergic reactions occurred, the further procedures performed. The LD-FFA instead of a full dose may evoke less severe FFA-associated complications, which could also make the procedure a safer one.

With no doubt, there are drawbacks of this two-step FFA and limitations of the pilot study. First, the modified technique with two steps is more time-consuming than traditional ones, and with more risks for corneal or conjunctival abrasions. Besides, the doses for each step may not be the optimal ones. There was only one dose without a gradient method to test the most suitable dose strategies. The perfect dose should always be one effective enough to show all the abnormal vessels without severe vitreous dye, which is most optimal when personalized. In our opinion, due to disease heterogeneity, the ideal dose should be decided in multiple FFA in the same group of patients in different concentration gradients and choose the best one. However, it is impossible in a clinical set. Furthermore, with LD-FFA, the vessels are commonly obscure; it was harder to fetch good images with the right position and perfect focus, which may rely on an experienced photographer. Other limitations included those biases intrinsic to a retrospective study. The study sample was small, so it was only a pilot study. It was impossible to evaluate all the vascular lesions in this study. At last, ideally, a comparison group with traditional FFA with a regular dose should be arranged to evaluate this two-step FFA's feasibility. However, in this pilot study, we merely want to introduce the concept and first attempts. A further study with a larger scale, gradient doses, and comparison groups is needed.

In summary, we postulated a modified strategy with two-step widefield FFA. The step-one FFA is effective to show retinal NV without severe fluorescein leakage. The step-two FFA could also be a double-check to prevent possible skip areas. The strategy may be a helpful clinical adjuvant in the laser photocoagulation of pediatric retinal disorders, especially for young ophthalmologists early in their careers in laser photocoagulation.

Data availability statement

The original contributions presented in this study are included in the article/**Supplementary material**, further inquiries can be directed to the corresponding authors.

Ethics statement

The studies involving human participants were reviewed and approved by the Institutional Review Board approval by Xinhua Hospital Affiliated to Shanghai Jiao Tong University. Written informed consent to participate in this study was provided by the participants' legal guardian/next of kin.

Author contributions

JP, JR, XZ, YY, YZ, and HX collected, analyzed, and interpreted the data. JP drafted the manuscript. JR, XZ, YY, YZ, and HX carefully revised the manuscript. YX and PZ contributed to the conception of the study. All authors have read and approved the final version of the manuscript.

Funding

This study was partially supported by the Shanghai Sailing Program (No. 20YF1429700), the Shanghai Pujiang Program (No. 18PJ1407500), the Clinical Research Plan of SHDC (No. SHDC2020CR5014-002), and the Hospital Funded Clinical Research Xin Hua Hospital Affiliated to Shanghai Jiao Tong University School of Medicine (No. 21XHDB08).

Conflict of interest

The authors declare that the research was conducted in the absence of any commercial or financial relationships that could be construed as a potential conflict of interest.

Publisher's note

All claims expressed in this article are solely those of the authors and do not necessarily represent those of their affiliated organizations, or those of the publisher, the editors and the reviewers. Any product that may be evaluated in this article, or claim that may be made by its manufacturer, is not guaranteed or endorsed by the publisher.

Supplementary material

The Supplementary Material for this article can be found online at: https://www.frontiersin.org/articles/10.3389/fmed.2022.961152/full#supplementary-material

References

1. Kang KB, Wessel MM, D'Amico DJ, Chan PRV, Tong J. Ultra-widefield imaging for the management of pediatric retinal diseases. *J Pediatr Ophthal Strabismus.* (2013) 50:282–8. doi: 10.3928/01913913-20130528-04

2. Tsui I, Franco-Cardenas V, Hubschman JP, Schwartz SD. Pediatric retinal conditions imaged by ultra wide field fluorescein angiography. *Ophthalmic Surg Lasers Imaging Retina.* (2013) 44:59–67. doi: 10.3928/23258160-20121221-14

3. John VJ, McClintic JI, Hess DJ, Berrocal AM. Retinopathy of prematurity versus familial exudative vitreoretinopathy: report on clinical and angiographic findings. *Ophthalmic Surg Lasers Imaging Retina.* (2016) 47:14–9. doi: 10.3928/23258160-20151214-02

4. Shukla D, Singh J, Sudheer G, Soman M, John R, Ramasamy K, et al. Familial exudative vitreoretinopathy (fevr). *Clin Profile Manage Indian J Ophthalmol.* (2003) 51:323. doi: 10.1016/j.celrep.2013.10.028

5. Peng J, Zhang Q, Long X, Zhang J, Huang Q, Li Y, et al. Incontinentia pigmenti-associated ocular anomalies of paediatric incontinentia pigmenti patients in China. *Acta Ophthalmol (Copenh).* (2019) 97:265–72. doi: 10.1111/aos.13781

6. Kothari N, Pineles S, Sarraf D, Velez F, Heilweil G, Holland G, et al. Clinic-based ultra-wide field retinal imaging in a pediatric population. *Int J Retina Vitr.* (2019) 5:21. doi: 10.1186/s40942-019-0171-1

7. Temkar S, Azad SV, Chawla R, Damodaran S, Garg G, Regani H, et al. Ultra-widefield fundus fluorescein angiography in pediatric retinal vascular diseases. *Indian J Ophthalmol.* (2019) 67:788–94. doi: 10.4103/ijo.IJO_1688_18

8. Sugimoto M, Matsubara H, Miyata R, Matsui Y, Ichio A, Kondo M. Ultra-widefield fluorescein angiography by oral administration of fluorescein. *Acta Ophthalmol (Copenh).* (2014) 92:e417–8. doi: 10.1111/aos.12323

9. Syed M, Ali A, Khan I, Khurram D, Kozak I. Ultra-widefield angiography with oral fluorescein in pediatric patients with retinal disease. *JAMA Ophthalmol.* (2018) 2018:462. doi: 10.1001/jamaophthalmol.2018.0462

10. Trese MT, Kashani AH. Advances in the diagnosis, management and pathophysiology of capillary nonperfusion. *Expert Rev Ophthalmol.* (2014) 7:281–92. doi: 10.1586/eop.12.26

11. Sisk RA. Intravenous sodium fluorescein 10% for laser ablation of subtle retinal neovascularization in FEVR. *J Pediatr Ophthalmol Strabismus.* (2012) 49:126–7. doi: 10.3928/01913913-20111214-01

12. Suzani M, Moore AT. Intraoperative fluorescein angiography-guided treatment in children with early coats' disease. *Ophthalmology.* (2015) 122:1195–202. doi: 10.1016/j.ophtha.2015.02.002

13. World Medical Association. World medical association declaration of Helsinki: ethical principles for medical research involving human subjects. *JAMA.* (2013) 310:2191–4. doi: 10.1001/jama.2013.281053

14. Lapiana FG, Penner R. Anaphylactoid reaction to intravenously administered fluorescein. *Arch Ophthalmol.* (1968) 79:161–2. doi: 10.1001/archopht.1968.03850040163009

15. Cai S, Liu TYA. The role of ultra-widefield fundus imaging and fluorescein angiography in diagnosis and treatment of diabetic retinopathy. *Curr Diab Rep.* (2021) 21:30. doi: 10.1007/s11892-021-01398-0

16. Lepore D, Molle F, Pagliara MM, Baldascino A, Angora C, Sammartino M, et al. Atlas of fluorescein angiographic findings in eyes undergoing laser for retinopathy of prematurity. *Ophthalmology.* (2011) 118:168–75. doi: 10.1016/j.ophtha.2010.04.021

17. Hubbard GB, Li AL. Analysis of predisposing clinical features for worsening traction after treatment of familial exudative vitreoretinopathy in children. *Am J Ophthalmol.* (2021) 223:430–45. doi: 10.1016/j.ajo.2020.07.013

frontiers | Frontiers in Medicine

TYPE Original Research
PUBLISHED 24 October 2022
DOI 10.3389/fmed.2022.976520

OPEN ACCESS

EDITED BY
Xiaoyan Ding,
Sun Yat-sen University, China

REVIEWED BY
Santasree Banerjee,
Beijing Genomics Institute (BGI), China
Zongyi Zhan,
Shenzhen Eye Hospital, China

*CORRESPONDENCE
Ping Fei
feiping@xinhuamed.com.cn
Peiquan Zhao
zhaopeiquan@xinhuamed.com.cn

†These authors have contributed equally to this work and share first authorship

SPECIALTY SECTION
This article was submitted to Ophthalmology, a section of the journal Frontiers in Medicine

RECEIVED 23 June 2022
ACCEPTED 27 September 2022
PUBLISHED 24 October 2022

CITATION
Liu M, Luo J, Feng H, Li J, Zhang X, Zhao P and Fei P (2022) Decrease of *FZD4* exon 1 methylation in probands from *FZD4*-associated FEVR family of phenotypic heterogeneity. *Front. Med.* 9:976520. doi: 10.3389/fmed.2022.976520

Decrease of *FZD4* exon 1 methylation in probands from *FZD4*-associated FEVR family of phenotypic heterogeneity

Miaomiao Liu†, Jia Luo†, Huazhang Feng, Jing Li, Xiang Zhang, Peiquan Zhao* and Ping Fei*

Department of Ophthalmology, Xinhua Hospital Affiliated to Shanghai Jiao Tong University School of Medicine, Shanghai, China

Familial exudative vitreoretinopathy (FEVR) is an important cause of childhood blindness and is clinically characterized by phenotypic heterogeneity. FEVR patients harboring the same genetic mutation vary widely in disease severity. The purpose of this study was to explore non-genetic factors that regulate FEVR phenotypic heterogeneity. We detected methylation levels of 21 CpG sites located at the *FZD4* exon 1 region of 11 probands, 12 asymptomatic/paucisymptomatic carriers and 11 non-carriers from 10 unrelated *FZD4*-associated FEVR families using bisulfite amplicon sequencing (BSAS). Our results showed reduced methylation level of *FZD4* exon 1 in probands, suggesting that *FZD4* exon 1 methylation level may be negatively linked with FEVR disease severity. It provided a new research direction for follow-up research, helping us better understand the complexity of the FEVR-causing mechanism.

KEYWORDS

familial exudative vitreoretinopathy (FEVR), the receptor frizzled-4 (FZD4), phenotypic heterogeneity, DNA methylation, epigenetics

Introduction

Familial exudative vitreoretinopathy (FEVR) is a clinically and genetically heterogeneous ophthalmic disorder characterized by incomplete retinal vascular development. The disease was first described in 1969 by Criswick and Schepens (1), and it is a major cause of vision loss in juveniles. Several sight-threatening complications are considered secondary to retinal avascularity, including retinal neovascularization and exudates, retinal fold and detachments, vitreous hemorrhage, and macular ectopia, ultimately leading to total blindness. The clinical appearance of FEVR varies considerably. The mildly affected patients may have only a small avascular area at the peripheral retina, which is visible only by fundus fluorescein angiography (FFA), while severely affected patients often registered as blind during infancy. With extensive fundus screening, we now realize that the prevalence of FEVR is much higher than we thought before (2). Therefore, it is imperative to study the mechanism underlying FEVR in order to seek for advanced therapy.

In the past decades, research on FEVR has mainly focused on genomics. At least 9 genes have been reported to cause FEVR: norrin cystine knot growth factor *NDP* (*NDP*; MIM: 300658) (3); low-density lipoprotein receptor-related protein 5 (*LRP5*; MIM: 603506) (4), tetraspanin 12 (*TSPAN12*; MIM: 613138) (5), frizzled class receptor 4 (*FZD4*; MIM: 604579) (6, 7), kinesin family member 11 (*KIF11*; MIM:148760) (8, 9), zinc finger protein 408 (*ZNF408*; MIM: 616454) (10), catenin, β-1 (*CTNNB1*; MIM: 116806) (11, 12), jagged 1 (*JAG1*; MIN: 601920) (13), and catenin, α-1 (*CTNNA1*; MIM:116805) (14). These gene mutations explain approximately 50% of FEVR cases. Mutations in six of the nine genes (*FZD4*, *TSPAN12*, *NDP*, *LRP5*, *CTNNB1*, and *CTNNA1*) are related to the Norrin/ Wnt β-catenin signaling pathway, which coordinates retinal development and angiogenesis by regulating cell survival, differentiation, proliferation, and migration (15, 16). The *NDP* gene encodes the extracellular ligand Norrin, which binds specifically to the receptor/coreceptor (*FZD4*, *LRP5* and *TSPAN12*) and forms a ligand-receptor complex. Upon activation of Norrin signaling, β-catenin translocates to the nucleus, binds to *TCF/LEF* (T cell factor/lymphoid-enhancing factor) and subsequently modulates gene expression (17–19). Mutations in *CTNNA1* induce overactivation of Norrin/β-catenin signaling and interrupt cell junctions (20, 21). The inheritance patterns of FEVR include autosomal dominant (AD), autosomal recessive (AR), and X-linked recessive (XL), with AD being the most common mode. Despite clear definition of causative genes, mutations of the same gene often manifest with drastic phenotypic heterogeneity in carriers (2, 22, 23). First-degree relatives of index patients with severe FEVR are often asymptomatic despite carrying the same mutation (24). This suggests that other risk factors beyond genetic mutation may contribute to FEVR pathogenesis.

Gene expression variability is one of the important causes for phenotypic variation. Epigenetic modification affects gene expression. One of the best understood epigenetic modification is DNA methylation. DNA methylation usually occurs in the cytosine guanine (CpG) dinucleotide. It affects gene expression by changing chromatin structure, DNA conformation, DNA stability and protein accessibility to DNA (25, 26). CpG islands are regions in the genome where CpG levels are significantly higher than the average CpG levels of the whole gene. CpG islands usually are found in the promoter or exon 1 region. Although few studies addressed DNA methylation change in FEVR, methylation changes have been demonstrated in other ocular vitreoretinopathy diseases such as age-related macular degeneration (AMD), proliferative vitreoretinopathy (PVR), and diabetic retinopathy (DR) (27–30). Therefore, we hypothesized that DNA methylation changes exist in FEVR causative genes, and such changes could affect gene expression and leading to FEVR phenotypic heterogeneity.

In this study, 10 separate *FZD4*-associated FEVR families were recruited to investigate the *FZD4* methylation status of FEVR probands and their asymptomatic/paucisymptomatic family members carrying the same mutation. Our results showed reduced *FZD4* exon 1 methylation in probands, suggesting that *FZD4* exon 1 methylation level may be negatively linked with FEVR disease severity. To the best of our knowledge, this is the first paper that attempts to investigate the association between DNA methylation and heterogeneous presentation of FEVR.

Methods

Subjects

760 probands were recruited based on a clinical diagnosis of FEVR at the ophthalmology department of Xinhua hospital from May 2010 to August 2019. Next Generation Sequencing (NGS) revealed that 112 probands carried only *FZD4* gene mutations, without other known FEVR-associated gene mutation. We further collected family history information of these 112 *FZD4* Gene mutation probands. Finally, 10 *FZD4*-associated FEVR families met the following inclusion criteria were recruited. each enrolled family contained at least one FEVR proband (Staged 3–5), one asymptomatic/ paucisymptomatic carrier of the mutant allele (clinically healthy or staged 1) and one non-carrier. Stage 2 individuals were excluded to maximize the phenotypic heterogeneity feature in our study design. Clinical staging was based on Trese's 5-stage system (31) and the severity of patients was determined by the highest stage of FEVR in either eye. Subjects with histories of oxygen inhalation and preterm birth were also excluded. all enrolled participants were diagnosed by ophthalmologist with expertise in FEVR Based on clinical manifestations, genotyping, fundus examination and FFA. This study was approved by the Institutional Review Board of Xin Hua Hospital Affiliated to Shanghai Jiao Tong University School of Medicine. All work was performed in accordance with the approved study protocol. written informed content was obtained from all the participants or their parents.

Analysis of *FZD4* Rs10128621 single nucleotide polymorphisms

Cis-regulatory variants might also modify mutation penetrance and contribute to clinical heterogeneity (32). *FZD4* rs10128621 SNP is the only known SNP which could affect FZD4 gene expression (33). We performed Sanger sequencing to analyze *FZD4* rs10128621 SNP in our cohort. The primer sequences were as follows: 5'-ACCTTGGCTTCCTAAAGTGTTG-3' (forward primer) and 5'-CTGCCTGAGAGACAGAGTAAGA-3' (reverse primer). The expected amplicon is 297 bp in length.

Bisulfite amplicon sequencing for methylation analysis

DNA methylation was analyzed by Bisulfite amplicon sequencing (BSAS). About 5 mL of peripheral blood samples were collected from each participant in a standard EDTA tube. Genomic DNA was extracted and purified using QIAamp® DNA Mini kit. One hundred thirty microliter of CT Conversion Reagent was added to 300 ng purified DNA samples as per the manufacturer's instructions. This process converted unmethylated cytosines (C) in CpG sites to uracil (U), whereas methylated C remained C. The primer sequences were as follows: 5′-TTTAGTTTGGGGTTGTTTTTGTAGT-3′ (forward primer) and 5′-CTTTTCCAAAAAAACTATCTCCTTC-3′ (reverse primer). PCR library was constructed using VAHTS Turbo DNA Library Prep Kit for Illumina and sequenced on a Miseq system (Illumina). Quality control was performed using FastQC v 0.11.2. Mapping and calling of the methylation levels were performed using bismark software and methylKit (R package 4.1.0), respectively.

Statistical analysis

Independent Samples *T*-test was used to pairwise compare the methylation differences among probands, carriers and non-carriers. Significant differences were determined as $p < 0.05$. Data analysis was performed using Graphpad 9.0.

Results

Characteristics of subjects

Thirty-four members of 10 *FZD4*-associated FEVR families were recruited in our study, including 11 FEVR probands, 12 asymptomatic/paucisymptomatic carriers of the same mutation, and 11 non-carriers of the mutant alleles. FEVR probands and family members were studied as a whole to best ensure similar genetic and environmental backgrounds. While FEVR probands had the most advanced ocular manifestations early in life, most of the family members carrying the same gene mutation were asymptomatic, only 4 carriers presented with Stage 1 FEVR. The mean age of probands, carriers and non-carriers were 35.1 ± 48.5 months (average ± standard deviation), 32.2 ± 12.2 years and 32.5 ± 14.8 years, respectively. Other than mutations in *FZD4*, no additional known FEVR-associated mutation was found in these subjects. Family No. 2, 5, 8 (chr11-86665923 c.205C>T) and family No. 7, 10 (chr11: 86665894-86665911 c.217_234del) shared the same mutation, respectively. The clinical details and genetic test results were summarized in Table 1. Fundus photographs and FFA of family No. 8 were presented in Figure 1.

Map of CpG island in the *FZD4* exon 1 region

We confirmed the methylation of CpG islands in *FZD4* using a genomic map of *FZD4* (NM_012193.4). *FZD4* is located on the negative strand of chromosome 11. Most of the CpG island (CpG:69) exists in the exon 1 region. Twenty-one CpG sites were identified from a fragment in the exon 1 region at 86,665,722–86,666,073 (Figure 2).

Methylation analysis of 21 CpG sites

Before DNA methylation, we performed Sanger sequencing to analyze *FZD4* rs10128621 SNP in our cohort. Sanger sequencing results showed a complete consistency of G base. Our results did not support the role of *FZD4* rs10128621 SNP in the phenotypic heterogeneity of our FEVR patients. (Supplementary Figure S1)

DNA methylation levels of 21 CpG sites identified above in probands and their family members were presented in Figure 3, except for the non-carrier of family No. 8, whose blood sample was not obtained due to data missing. At almost all tested CpG sites (19 out of 21), FEVR probands held the lowest average methylation level compared to carriers and non-carriers, except for CpG4 and CpG5, where probands had slightly higher methylation levels than carriers. At more than half of the CpG sites (12 out of 21), carriers held lower methylation levels than non-carriers. DNA methylation levels of probands were significantly lower than symptomatic/paucisymptomatic carriers in CpG14 ($p = 0.0009$), CpG15 ($p = 0.0489$) and CpG16 ($p = 0.0320$). DNA methylation levels of probands were significantly lower than non-carriers at CpG1 ($p = 0.0009$), CpG9 ($p = 0.0371$) and CpG13 ($p = 0.0021$). Overall, the results suggested probands had lower DNA methylation compared with carriers and non-carriers in *FZD4* exon 1 region.

The methylation levels of these six significantly different CpG sites in each of the 10 FEVR families were shown in Figure 4. It showed that FEVR probands had lower methylation levels nearly in almost all cases. For example, at CpG14, probands in all 10 families had lower methylation levels. In addition, we noticed a negative correlation at CpG14 between methylation levels and disease severity within three families (No. 2, 5 and 8) that happened to carry the same mutation (chr11-86665923 c.205C>T). Proband from family No. 2 had the most advanced FEVR and the lowest methylation level at CpG14 compared to the rest. Similar negative correlations also existed for CpG15 and CpG16.

TABLE 1 Clinical details and genetic test results of 34 subjects from 10 FEVR families.

Family ID	FEVR probands						Asymptomatic/paucisymptomatic		Non carrier	Genomic coordinate (hg19)	Exon	Nucleotide change	Zygosity
	Gender	Age at diagnose /month	Disease stage (OD/OS)	Retinal folds (OD/OS)	Retinal detachment (OD/OS)	Others	Relation	Disease stage					
1	M	42	5/1	NA/No	NA/No	OD corneal staphyloma	Father	N	Mother	chr11-86662767	Exon2	c.1031dup	het
2	M	12	3b/5a	NA	NA		Mother	N	Father	chr11-86665923	Exon1	c.205C>T	het
3	F	12	1/5	No/No	No/Yes	OS disappearance of anterior chamber	Mother	N	Father brother	chr11-86663328	Exon2	c.470T>C	het
4	M	29	4a/4a	Yes/Yes	Yes/Yes		Mother	N	Father	chr11-86663485	Exon2	c.313A>G	het
5	F	19	5/1	NA	NA		Mother	N	Father	chr11-86665923	Exon1	c.205C>T	het
6	M	6	1/5	No/Yes	No/Yes	OS disappearance of anterior chamber OS vitreous hemorrhage	Father grandfather	1 1	Grandmother	chr11:86662513–86662516	Exon2	c.1282_1285del	het
	F	174	1/5	No/Yes	No/Yes								
7	M	17	5/0	Yes/No	Yes/No		Mother	1	Father	chr11:86665894–86665911	Exon1	c.217_234del	het
8	M	54	4a/0	Yes/No	Yes/No	OD lens opacity	Father	N	Mother	chr11-86665923	Exon1	c.205C>T	het
9	M	5	4a/4a	Yes/Yes	Yes/Yes		Father	1	Mother	chr11-86662817	Exon2	c.981G>A	het
10	M	16	4a/3a	Yes/Yes	Yes/Yes		Father brother	1 N	Mother	chr11:86665894–86665911	Exon1	c.217_234del	het

M, male; F, female; N, normal fundus; het, heterozygous; OD, right eye; OS, left eye; NA, not available.

10.3389/fmed.2022.976520

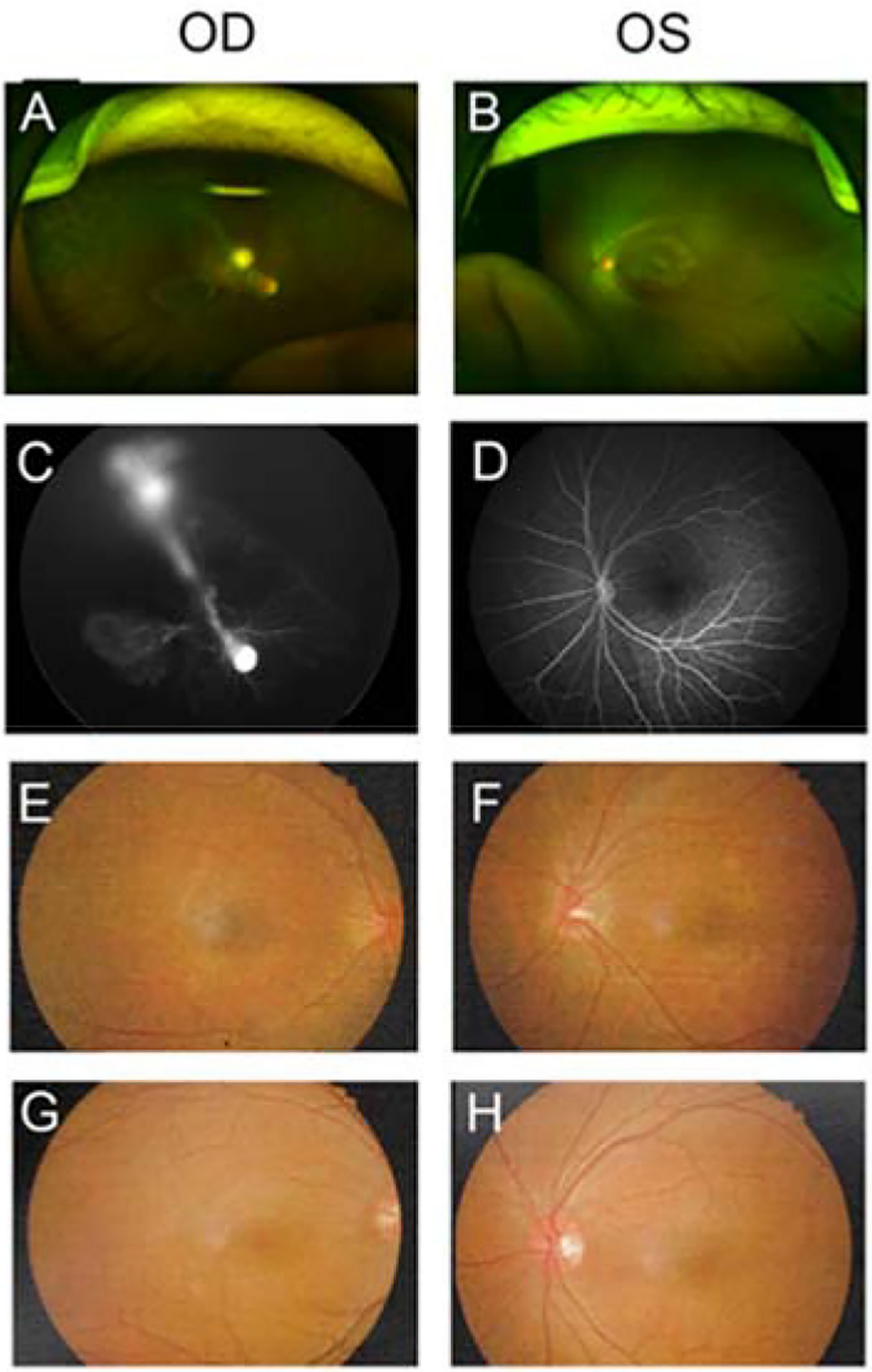

FIGURE 1
Fundus photographs and fundus fluorescein angiography (FFA) of subjects from family No. 8. In this family, the c.205C>T mutation was detected in a 4-year-old proband boy and it was inherited from his father. OD and OS represented right eye and left eye, respectively. **(A–D)** Fundus and FFA photographs of FEVR proband. The proband suffered from monocular FEVR disease in the right eye and was staged 4A. Severe fibrous proliferation membrane connected the optic disc to the lens in the right eye, with subtotal retinal detachment and peripheral avascular zone. The left eye exhibited normal retinal appearance without prolonged filling time or leakage. **(E,F)** Fundus photographs of father. Fundus examination didn't reveal any FEVR presentation although the father carried the c.205C>T mutation. **(G,H)** Fundus photographs of mother. The mother was a non-carrier without any fundus abnormality.

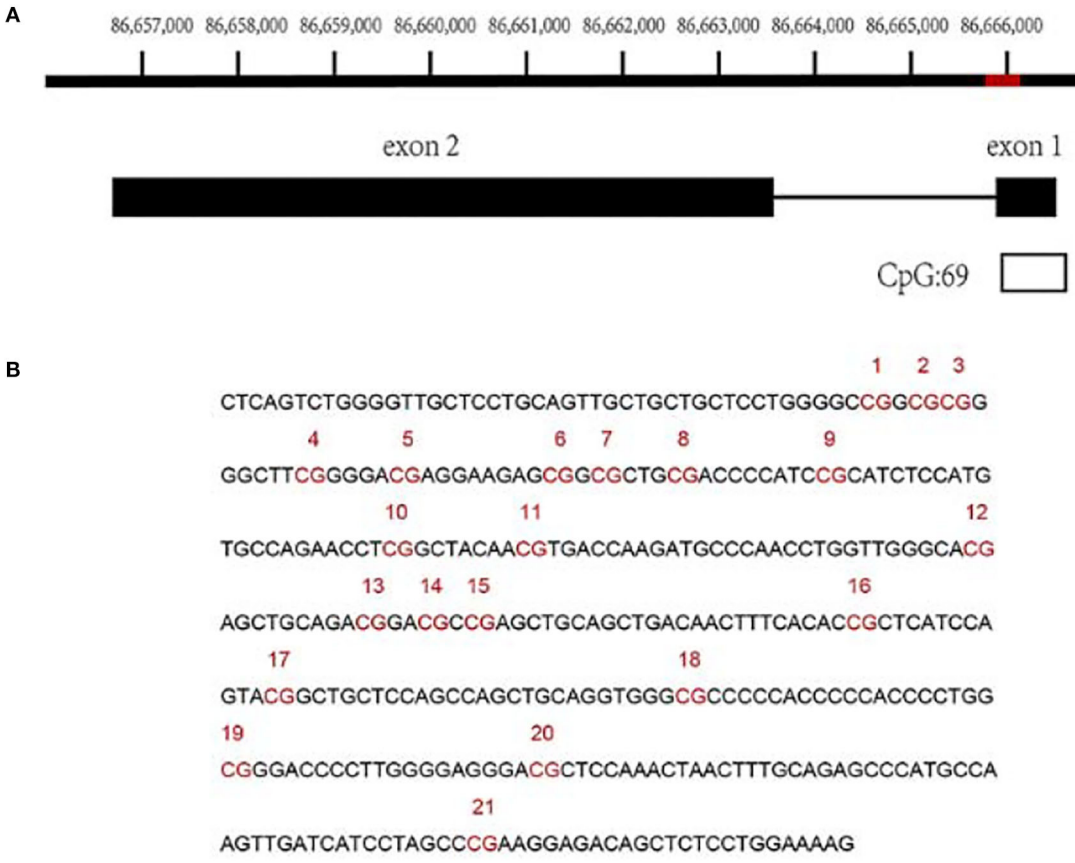

FIGURE 2
Analysis of methylation of CpG sites in the FZD4 exon 1 region. **(A)** The red region showed the location of tested sequence. The black box showed FZD4, black line indicated intergenic region and the white box indicated the CpG island region (CpG: 69) located in the exon 1 region of FZD4. **(B)** The sequence and CpG sites analyzed in this study were presented. The CpG sites were numbered and indicated as red.

Discussion

FEVR is a rare disease featured by peripheral retinal vascular abnormalities (19, 34). It is clinically characterized by phenotypic heterogeneity, suggesting that non-genetic factors are involved in disease etiology (2, 22, 23). Comparing the epigenetic features among FEVR family members with or without mutation would provide important information regarding epigenetic factors which could contribute to phenotypic heterogeneity. DNA methylation is a widely studied epigenetic modification type. Increasing number of evidence supported the role of DNA methylation in modulating the phenotypic expression of diseases (35–37). For example, Coppede et al. found that the increase of global DNA methylation might contribute to disease manifestation in amyotrophic lateral sclerosis (ALS) carriers of not fully penetrant SOD1 mutations (38). DNA methylation at promoter CpG islands (CGI) of Wnt pathway genes showed a significant association with progression-free survival in ovarian tumor patients (39). Although little is known about FEVR disease, altered DNA methylation has been demonstrated in many other vitreoretinopathy diseases such as age-related macular degeneration (AMD), proliferative vitreoretinopathy (PVR), and diabetic retinopathy (DR). Therefore, we hypothesized that DNA methylation changes might play a role in FEVR phenotypic heterogeneity.

Up to date, at least 9 genes have been reported to cause FEVR. In previous studies, we and others showed that with *FZD4* mutations accounting for the greatest proportion of FEVR in Chinese population (23, 40, 41). The *FZD4* gene encodes a 537–amino acid protein, which functions as a receptor of the Wnt signaling pathway (42). According to our previous work, more than half (51.43%) in the *FZD4* group were identified asymmetry, suggesting *FZD4* mutations might initiate the most diverse and asymmetric phenotypes (22). Previous study suggested epigenetic modifications might involve

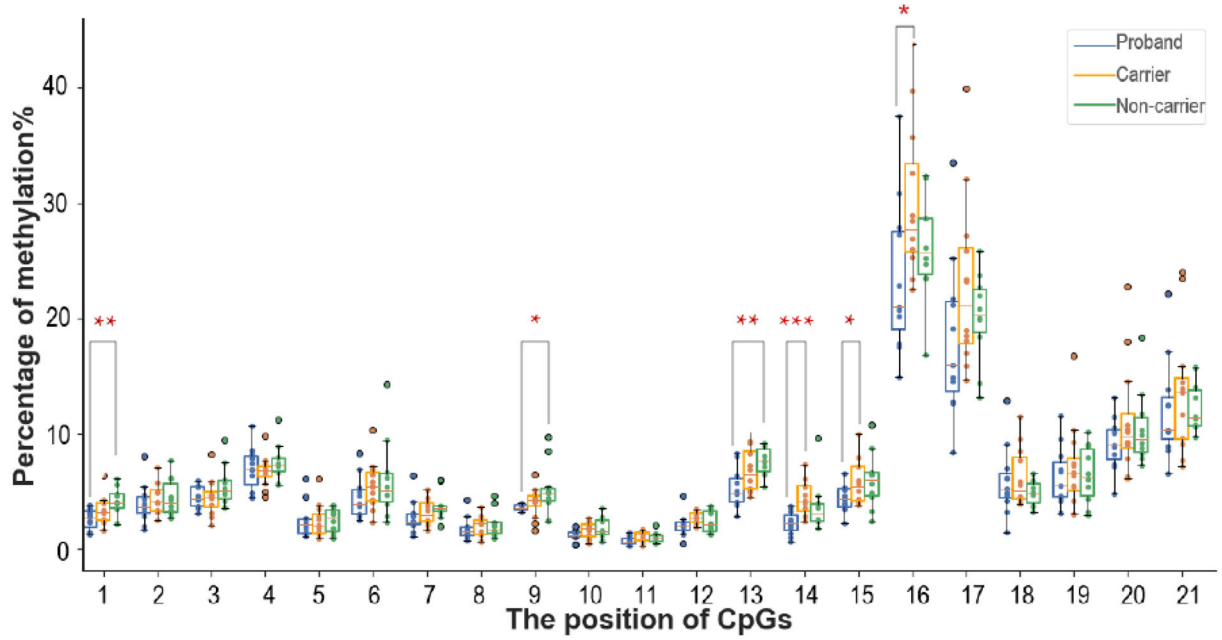

FIGURE 3
The graph showed methylation levels of 21 tested CpG sites. The horizontal axis represented the position of CpG sites and the vertical axis represented percentage of methylation. Blue, orange and green points respectively indicated to 11 FEVR probands, 12 carriers and 11 non-carriers. Box plot data represented range (error bars), median (horizontal line), quartile values (box) and outliers (dots). Median methylation levels of probands, carriers and non-carriers were compared in pair using student's *t*-test. DNA methylation levels of CpG1, CpG9 and CpG13 were significantly different between probands and non-carriers. DNA methylation levels of CpG14, CpG15 and CpG16 were significantly different between probands and carriers. *, $p < 0.05$; **, $p < 0.01$; ***, $p < 0.001$.

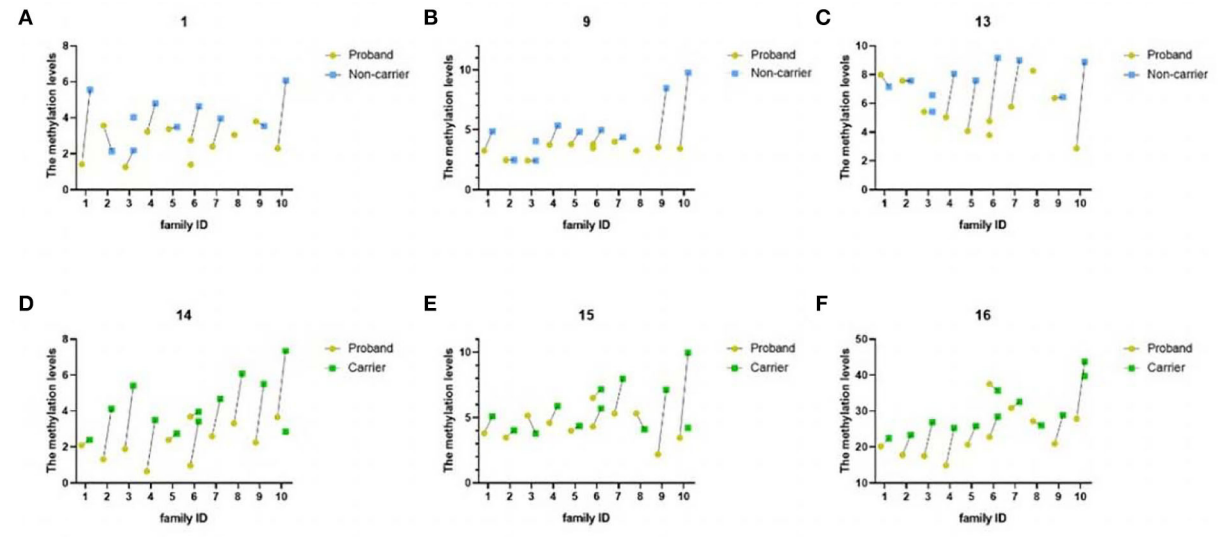

FIGURE 4
The figure above showed methylation levels at six significantly different CpG sites of 10 FEVR families. The horizontal axis represented family ID and the vertical axis represented the methylation level of specific CpG site. **(A–C)** DNA methylation levels of CpG1, CpG9 and CpG13 were significantly different between probands and non-carriers. Yellow and blue points indicated to probands and non-carriers, respectively. **(D–F)** DNA methylation levels of CpG14, CpG15 and CpG16 were significantly different between probands and carriers. Yellow and green points indicated to probands and carriers, respectively.

in the developing fetal retina which caused high asymmetric *FZD4* gene expression (43). Therefore, it is important to study non-genetic factors underlying *FZD4*-associated FEVR phenotypic heterogeneity.

Bisulfite sequencing was first reported by Frommer et al. in (44). The bisulfite treated-DNA is amplified by PCR, and then the cloning and sequencing results of PCR products are used to determine whether the CpG site was methylated. This method has been recognized as one of the most powerful approaches to investigate DNA methylation patterns due to its reliable results, high accuracy and high sensitivity. It allows the determination of methylation at a single-cytosine resolution and has become the "gold standard" for DNA methylation detection (45, 46).

The current study aimed to access evidence of a link between FEVR phenotypic heterogeneity and *FZD4* methylation status. We focused on 10 unrelated clinically heterogeneous FEVR families carrying only *FZD4* gene mutation. In this study, our goal was to investigate whether there was a difference in methylation levels between probands at severe FEVR stage and parents with mild phenotype. Stage 1 FEVR has only peripheral avascular zone seen by fluorescein fundus angiography. Patients with stage 1 FEVR may be stable for decades without any progression. Therefore, we grouped asymptomatic and stage 1 carriers together. Our data indicated a negative correlation between DNA methylation in *FZD4* exon 1 region and FEVR severity, which requires further validation. Among the six significantly different CpG sites, four sites (CpG13, CpG14, CpG15 and CpG16) were adjacent, suggesting that this region might play an important and unique role in the regulation of *FZD4* expression. Although the CpG9 of Family No. 9 and No.10 are obviously different, the probands still had the lowest average methylation level of the three groups and non-carriers had the highest average methylation level when these two families were eliminated. Our study suggests that changes in DNA methylation might contribute to the severity in *FZD4*-associated FEVR patients. The function of intragenic DNA methylation hasn't been well recognized. Brenet et al. found that DNA methylation at the first exon is tightly linked to transcriptional silencing (47), while others believed that the methylation in the body of genes can actually activate gene transcription (48, 49). Although it remains controversial, given that altered methylation of a specific CpG site might be enough to change gene expression [50], FEVR probands with reduced DNA methylation are highly likely to undergo altered gene expression, thus causing different degrees of disease severity.

This study is limited by the number of FEVR families enrolled. For 5 mutations analyzed here, only one family was found for each mutation. Alternatively, we took the approach of comparing the average overall methylation level in probands, carriers and non-carriers, which could have masked the effect of specific mutation on DNA methylation. In addition, age may be an independent factor in the methylation level. However, in this study, after excluding the "grandmother" and "grandfather" subjects in family 6, the probands still had the lowest average methylation level among the three groups, which is in line with our conclusion. What's more, we do not have RNA samples from our patients to validate the expression of *FZD4*. Future study with larger sample size is needed to validate our findings. Nevertheless, our results provided a new mechanism potentially responsible for phenotypic heterogeneity amongst FEVR patients.

Data availability statement

The raw data supporting the conclusions of this article will be made available by the authors, without undue reservation.

Ethics statement

The studies involving human participants were reviewed and approved by the Institutional Review Board of Xin Hua Hospital Affiliated to Shanghai Jiao Tong University School of Medicine. Written informed consent to participate in this study was provided by the participants' legal guardian/next of kin.

Author contributions

ML and JLu are responsible for conceptualization, methodology, software, investigation, and writing original draft. HF is responsible for clinical data collection and writing. JLi and XZ are responsible for software and writing review. PF and PZ are responsible for supervision, writing review and funding acquisition. All authors contributed to the article and approved the submitted version.

Funding

This research was supported by Grant 81770963 from National Natural Science Foundation of China (to FP) and Grant 2018YFA0800801 from National Key Research and Development Program of China (to LJ).

Acknowledgments

The authors thank all the patients and their family members for their participation.

Conflict of interest

The authors declare that the research was conducted in the absence of any commercial or financial relationships that could be construed as a potential conflict of interest.

Publisher's note

All claims expressed in this article are solely those of the authors and do not necessarily represent those of their affiliated organizations, or those of the publisher, the editors and the reviewers. Any product that may be evaluated in this article, or claim that may be made by its manufacturer, is not guaranteed or endorsed by the publisher.

Supplementary material

The Supplementary Material for this article can be found online at: https://www.frontiersin.org/articles/10.3389/fmed.2022.976520/full#supplementary-material

References

1. Criswick VG, Schepens CL. Familial exudative vitreoretinopathy. *Am J Ophthalmol.* (1969) 68:578–94. doi: 10.1016/0002-9394(69)91237-9

2. Kashani AH, Learned D, Nudleman E, Drenser KA, Capone A, Trese MT. High prevalence of peripheral retinal vascular anomalies in family members of patients with familial exudative vitreoretinopathy. *Ophthalmology.* (2014) 121:262–8. doi: 10.1016/j.ophtha.2013.08.010

3. Chen ZY, Battinelli EM, Fielder A, Bundey S, Sims K, Breakefield XO, et al. A mutation in the Norrie disease gene (NDP) associated with X-linked familial exudative vitreoretinopathy. *Nat Genet.* (1993) 5:180–3. doi: 10.1038/ng1093-180

4. Fei P, Zhang Q, Huang L, Xu Y, Zhu X, Tai Z, et al. Identification of two novel LRP5 mutations in families with familial exudative vitreoretinopathy. *Mol Vis.* (2014) 20:395–409.

5. Nikopoulos K, Gilissen C, Hoischen A, van Nouhuys CE, Boonstra FN, Blokland EA, et al. Next-generation sequencing of a 40 Mb linkage interval reveals TSPAN12 mutations in patients with familial exudative vitreoretinopathy. *Am J Hum Genet.* (2010) 86:240–7. doi: 10.1016/j.ajhg.2009.12.016

6. Fei P, Zhu X, Jiang Z, Ma S, Li J, Zhang Q, et al. Identification and functional analysis of novel FZD4 mutations in Han Chinese with familial exudative vitreoretinopathy. *Sci Rep.* (2015) 5:16120. doi: 10.1038/srep16120

7. Robitaille J, MacDonald ML, Kaykas A, Sheldahl LC, Zeisler J, Dube MP, et al. Mutant frizzled-4 disrupts retinal angiogenesis in familial exudative vitreoretinopathy. *Nat Genet.* (2002) 32:326–30. doi: 10.1038/ng957

8. Robitaille JM, Gillett RM, LeBlanc MA, Gaston D, Nightingale M, Mackley MP, et al. Phenotypic overlap between familial exudative vitreoretinopathy and microcephaly, lymphedema, and chorioretinal dysplasia caused by KIF11 mutations. JAMA Ophthalmol. (2014) 132:1393–9. doi: 10.1001/jamaophthalmol.2014.2814

9. Li JK, Fei P, Li Y, Huang QJ, Zhang Q, Zhang X, et al. Identification of novel KIF11 mutations in patients with familial exudative vitreoretinopathy and a phenotypic analysis. *Sci Rep.* (2016) 6:26564. doi: 10.1038/srep26564

10. Collin RW, Nikopoulos K, Dona M, Gilissen C, Hoischen A, Boonstra FN, et al. ZNF408 is mutated in familial exudative vitreoretinopathy and is crucial for the development of zebrafish retinal vasculature. *Proc Natl Acad Sci U S A.* (2013) 110:9856–61. doi: 10.1073/pnas.1220864110

11. Dixon MW, Stem MS, Schuette JL, Keegan CE, Besirli CG. CTNNB1 mutation associated with familial exudative vitreoretinopathy (FEVR) phenotype. *Ophthalmic Genet.* (2016) 37:468–470. doi: 10.3109/13816810.2015.1120318

12. Panagiotou ES, Sanjurjo Soriano C, Poulter JA, Lord EC, Dzulova D, Kondo H, et al. Defects in the cell signaling mediator β-catenin cause the retinal vascular condition FEVR. *Am J Hum Genet.* (2017) 100:960–8. doi: 10.1016/j.ajhg.2017.05.001

13. Zhang L, Zhang X, Xu H, Huang L, Zhang S, Liu W, et al. Exome sequencing revealed Notch ligand JAG1 as a novel candidate gene for familial exudative vitreoretinopathy. *Genet Med.* (2020) 22:77–84. doi: 10.1038/s41436-019-0571-5

14. Zhu X, Yang M, Zhao P, Li S, Zhang L, Huang L, et al. Catenin α 1 mutations cause familial exudative vitreoretinopathy by overactivating Norrin/β-catenin signaling. *J Clin Invest.* (2021) 131:9869. doi: 10.1172/JCI139869

15. Warden SM, Andreoli CM, Mukai S. The Wnt signaling pathway in familial exudative vitreoretinopathy and Norrie disease. *Semin Ophthalmol.* (2007) 22:211–7. doi: 10.1080/08820530701745124

16. Wang Z, Liu CH, Huang S, Chen J. Wnt Signaling in vascular eye diseases. *Prog Retin Eye Res.* (2019) 70:110–33. doi: 10.1016/j.preteyeres.2018.11.008

17. Dan H, Wang D, Huang Z, Shi Q, Zheng M, Xiao Y, et al. Whole exome sequencing revealed 14 variants in NDP, FZD4, LRP5, and TSPAN12 genes for 20 families with familial exudative vitreoretinopathy. *BMC Med Genomics.* (2022) 15:54. doi: 10.1186/s12920-022-01204-0

18. Xiao H, Tong Y, Zhu Y, Peng M. Familial exudative vitreoretinopathy-related disease-causing genes and norrin/β-catenin signal pathway: structure, function, and mutation spectrums. *J Ophthalmol.* (2019) 2019:5782536. doi: 10.1155/2019/5782536

19. Tauqeer Z, Yonekawa Y. Familial exudative vitreoretinopathy: pathophysiology, diagnosis, and management. *Asia Pac J Ophthalmol (Phila).* (2018) 7:176–82. doi: 10.22608/201855

20. He Y, Yang M, Zhao R, Peng L, Dai E, Huang L, et al. Novel truncating variants in CTNNB1 cause familial exudative vitreoretinopathy. *J Med Genet.* (2022). doi: 10.1136/jmedgenet-2021-108259

21. Wang S, Zhang X, Hu Y, Fei P, Xu Y, Peng J, et al. Clinical and genetical features of probands and affected family members with familial exudative vitreoretinopathy in a large Chinese cohort. *Br J Ophthalmol.* (2021) 105:83–6. doi: 10.1136/bjophthalmol-2019-315598

22. Lu J, Huang L, Sun L, Li S, Zhang Z, Jiang Z, et al. FZD4 in a large Chinese population with familial exudative vitreoretinopathy: molecular characteristics and clinical manifestations. *Invest Ophthalmol Vis Sci.* (2022) 63:7. doi: 10.1167/iovs.63.4.7

23. Toomes C, Bottomley HM, Scott S, Mackey DA, Craig JE, Appukuttan B, et al. Spectrum and frequency of FZD4 mutations in familial exudative vitreoretinopathy. *Invest Ophthalmol Vis Sci.* (2004) 45:2083–90. doi: 10.1167/iovs.03-1044

24. Lorincz MC, Dickerson DR, Schmitt M, Groudine M. Intragenic DNA methylation alters chromatin structure and elongation efficiency in mammalian cells. *Nat Struct Mol Biol.* (2004) 11:1068–75. doi: 10.1038/nsmb840

25. Schübeler D, Lorincz MC, Cimbora DM, Telling A, Feng YQ, Bouhassira EE, et al. Genomic targeting of methylated DNA: influence of methylation on transcription, replication, chromatin structure, and histone acetylation. *Mol Cell Biol.* (2000) 20:9103–12. doi: 10.1128/MCB.20.24.9103-9112.2000

26. Hunter A, Spechler PA, Cwanger A, Song Y, Zhang Z, Ying GS, et al. DNA methylation is associated with altered gene expression in AMD. *Invest Ophthalmol Vis Sci.* (2012) 53:2089–105. doi: 10.1167/iovs.11-8449

27. Corso-Díaz X, Jaeger C, Chaitankar V, Swaroop A. Epigenetic control of gene regulation during development and disease: a view from the retina. *Prog Retin Eye Res.* (2018) 65:1–27. doi: 10.1016/j.preteyeres.2018.03.002

28. Shafabakhsh R, Aghadavod E, Ghayour-Mobarhan M, Ferns G, Asemi Z. *Role* of histone modification and DNA methylation in signaling pathways involved in diabetic retinopathy. *J Cell Physiol.* (2019) 234:7839–46. doi: 10.1002/jcp.27844

29. Wei L, Liu B, Tuo J, Shen D, Chen P, Li Z, et al. Hypomethylation of the IL17RC promoter associates with age-related macular degeneration. *Cell Rep.* (2012) 2:1151–8. doi: 10.1016/j.celrep.2012.10.013

30. Pendergast SD, Trese MT. Familial exudative vitreoretinopathy Results of surgical management. *Ophthalmology.* (1998) 105:1015–23. doi: 10.1016/S0161-6420(98)96002-X

31. Wang F, Zhang S, Wen Y, Wei Y, Yan H, Liu H, et al. Revealing the architecture of genetic and epigenetic regulation: a maximum likelihood model. *Brief Bioinform.* (2014) 15:1028–43. doi: 10.1093/bib/bbt076

32. Castel SE, Cervera A, Mohammadi P, Aguet F, Reverter F, Wolman A, et al. Modified penetrance of coding variants by cis-regulatory variation contributes to disease risk. *Nat Genet.* (2018) 50:1327–34. doi: 10.1038/s41588-018-0192-y

33. Gilmour DF. Familial exudative vitreoretinopathy and related retinopathies. *Eye (Lond).* (2015) 29:1–14. doi: 10.1038/eye.2014.70

34. Quiñonez-Silva G, Dávalos-Salas M, Recillas-Targa F, Ostrosky-Wegman P, Aranda DA, Benítez-Bribiesca L. Monoallelic germline methylation and sequence variant in the promoter of the RB1 gene: a possible constitutive epimutation in hereditary retinoblastoma. *Clin Epigenetics.* (2016) 8:1. doi: 10.1186/s13148-015-0167-0

35. Eloy P, Dehainault C, Sefta M, Aerts I, Doz F, Cassoux N, et al. *A parent-of-origin effect impacts the phenotype in low penetrance retinoblastoma families segregating the c.1981C>T/p.Arg661Trp Mutation of RB1. PLoS Genet.* (2016) 12:e1005888. doi: 10.1371/journal.pgen.1005888

36. Pizzolo F, Friso S, Morandini F, Antoniazzi F, Zaltron C, Udali S, et al. Apparent mineralocorticoid excess by a novel mutation and epigenetic modulation by HSD11B2 promoter methylation. *J Clin Endocrinol Metab.* (2015) 100:E1234–41. doi: 10.1210/jc.2015-1760

37. Coppedè F, Stoccoro A, Mosca L, Gallo R, Tarlarini C, Lunetta C, et al. Increase in DNA methylation in patients with amyotrophic lateral sclerosis carriers of not fully penetrant SOD1 mutations. *Amyotroph Lateral Scler Frontotemporal Degener.* (2018) 19:93–101. doi: 10.1080/21678421.2017.1367401

38. Dai W, Teodoridis JM, Zeller C, Graham J, Hersey J, Flanagan JM, et al. Systematic CpG islands methylation profiling of genes in the wnt pathway in epithelial ovarian cancer identifies biomarkers of progression-free survival. *Clin Cancer Res.* (2011) 17:4052–62. doi: 10.1158/1078-0432.CCR-10-3021

39. Li Y, Peng J, Li J, Zhang Q, Li J, Zhang X, et al. The characteristics of digenic familial exudative vitreoretinopathy. *Graefes Arch Clin Exp Ophthalmol.* (2018) 256:2149–56. doi: 10.1007/s00417-018-4076-8

40. Seo SH, Yu YS, Park SW, Kim JH, Kim HK, Cho SI, et al. Molecular Characterization of FZD4, LRP5, and TSPAN12 in Familial Exudative Vitreoretinopathy. *Invest Ophthalmol Vis Sci.* (2015) 56:5143–51. doi: 10.1167/iovs.14-15680

41. Zhang K, Harada Y, Wei X, Shukla D, Rajendran A, Tawansy K, et al. An essential role of the cysteine-rich domain of FZD4 in Norrin/Wnt signaling and familial exudative vitreoretinopathy. *J Biol Chem.* (2011) 286:10210–5. doi: 10.1074/jbc.M110.194399

42. Aldiri I, Xu B, Wang L, Chen X, Hiler D, Griffiths L, et al. *The dynamic epigenetic landscape of the retina during development, reprogramming, and tumorigenesis. Neuron.* (2017) 94:550–68.e10. doi: 10.1016/j.neuron.2017.04.022

43. Frommer M, McDonald LE, Millar DS, Collis CM, Watt F, Grigg GW, et al. A genomic sequencing protocol that yields a positive display of 5-methylcytosine residues in individual DNA strands. *Proc Natl Acad Sci U S A.* (1992) 89:1827–31. doi: 10.1073/pnas.89.5.1827

44. Sibbritt T, Schumann U, Shafik A, Guarnacci M, Clark SJ, Preiss T. Target-specific profiling of RNA m(5)C methylation level using amplicon sequencing methods. *Mol Biol.* (2022) 2404:375–92. doi: 10.1007/978-1-0716-1851-6_21

45. Masser DR, Stanford DR, Freeman WM. Targeted DNA methylation analysis by next-generation sequencing. *J Vis Exp.* (2015) 96:52488. doi: 10.3791/52488

46. Brenet F, Moh M, Funk P, Feierstein E, Viale AJ, Socci ND, et al. DNA methylation of the first exon is tightly linked to transcriptional silencing. *PLoS ONE.* (2011) 6:e14524. doi: 10.1371/journal.pone.0014524

47. Baylin SB, Jones PA. A decade of exploring the cancer epigenome - biological and translational implications. *Nat Rev Cancer.* (2011) 11:726–34. doi: 10.1038/nrc3130

48. Rivera RM, Bennett LB. Epigenetics in humans: an overview. *Curr Opin Endocrinol Diabetes Obes.* (2010) 17:493–9. doi: 10.1097/MED.0b013e3283404f4b

49. Ferreira HJ, Heyn H, Moutinho C, Esteller M. CpG island hypermethylation-associated silencing of small nucleolar RNAs in human cancer. *RNA Biol.* (2012) 9:881–90. doi: 10.4161/rna.19353

frontiers | Frontiers in Medicine

TYPE Case Report
PUBLISHED 17 April 2023
DOI 10.3389/fmed.2023.1119623

OPEN ACCESS

EDITED BY
Peiquan Zhao,
Shanghai Jiao Tong University, China

REVIEWED BY
Zongyi Zhan,
Shenzhen Eye Hospital, China
Gabriela Corina Zaharie,
Iuliu Haţieganu University of Medicine and Pharmacy, Romania
Wei-Chi Wu,
Linkou Chang Gung Memorial Hospital, Taiwan

*CORRESPONDENCE
Hou-Tai Chang
houtai38@gmail.com

†These authors have contributed equally to this work and share first authorship

SPECIALTY SECTION
This article was submitted to Ophthalmology, a section of the journal Frontiers in Medicine

RECEIVED 09 December 2022
ACCEPTED 29 March 2023
PUBLISHED 17 April 2023

CITATION
Lee C-T, Hsieh T-H, Chu C-C, Hsu Y-R, Wang J-H, Wang J-K, Zhao Z and Chang H-T (2023) Hyperbaric oxygen therapy as rescue therapy for pediatric frosted branch angiitis with Purtscher-like retinopathy: a case report. *Front. Med.* 10:1119623. doi: 10.3389/fmed.2023.1119623

Hyperbaric oxygen therapy as rescue therapy for pediatric frosted branch angiitis with Purtscher-like retinopathy: a case report

Chi-Tai Lee[1,2†], Tzu-Han Hsieh[3†], Chan-Ching Chu[1,2], Yung-Ray Hsu[3,4], Jia-Horng Wang[5], Jia-Kang Wang[3,4], Zhanqi Zhao[6,7] and Hou-Tai Chang[1,5,8*]

[1]Center of Hyperbaric Oxygen, Far Eastern Memorial Hospital, New Taipei City, Taiwan, [2]Department of Chest Medicine, Far Eastern Memorial Hospital, New Taipei City, Taiwan, [3]Department of Ophthalmology, Far Eastern Memorial Hospital, New Taipei City, Taiwan, [4]Department of Electrical Engineering, Yuan Ze University, Taoyuan, Taiwan, [5]Department of Critical Care Medicine, Far Eastern Memorial Hospital, New Taipei City, Taiwan, [6]Department of Biomedical Engineering, Fourth Military Medical University, Xi'an, China, [7]Institute of Technical Medicine, Furtwangen University, Villingen-Schwenningen, Germany, [8]Department of Industrial Engineering and Management, Yuan Ze University, Taoyuan, Taiwan

Introduction: Frosted branch angiitis (FBA) is an uncommon uveitis characterized by fulminant retinal vasculitis. Purtscher-like retinopathy (PuR) is a rare retinal angiopathy associated with a non-traumatic etiology. Both FBA and PuR can cause profound visual impairments.

Case report: We describe the case of a 10-year-old male who presented with sudden bilateral painless visual loss due to FBA with concurrent PuR, with notable viral prodrome 1 month prior to presentation. Systemic investigations revealed a recent herpes simplex virus 2 infection with a high titer of IgM, positive antinuclear antibody (ANA) (1:640), and abnormal liver function tests. After administration of systemic corticosteroids, anti-viral agents, and subsequent immunosuppressive medications, the FBA was gradually alleviated. However, fundoscopy and optical coherence tomography (OCT) revealed persistent PuR and macular ischemia. Hence, hyperbaric oxygen therapy was administered as a rescue strategy, which resulted in gradual bilateral visual acuity improvement.

Conclusion: Hyperbaric oxygen therapy may be a beneficial rescue treatment for retinal ischemia secondary to FBA with PuR.

KEYWORDS

frosted branch angiitis, Purtscher-like retinopathy, hyperbaric oxygen therapy, positive antinuclear antibody, atmosphere absolute, best-corrected visual acuity, optical coherence tomography

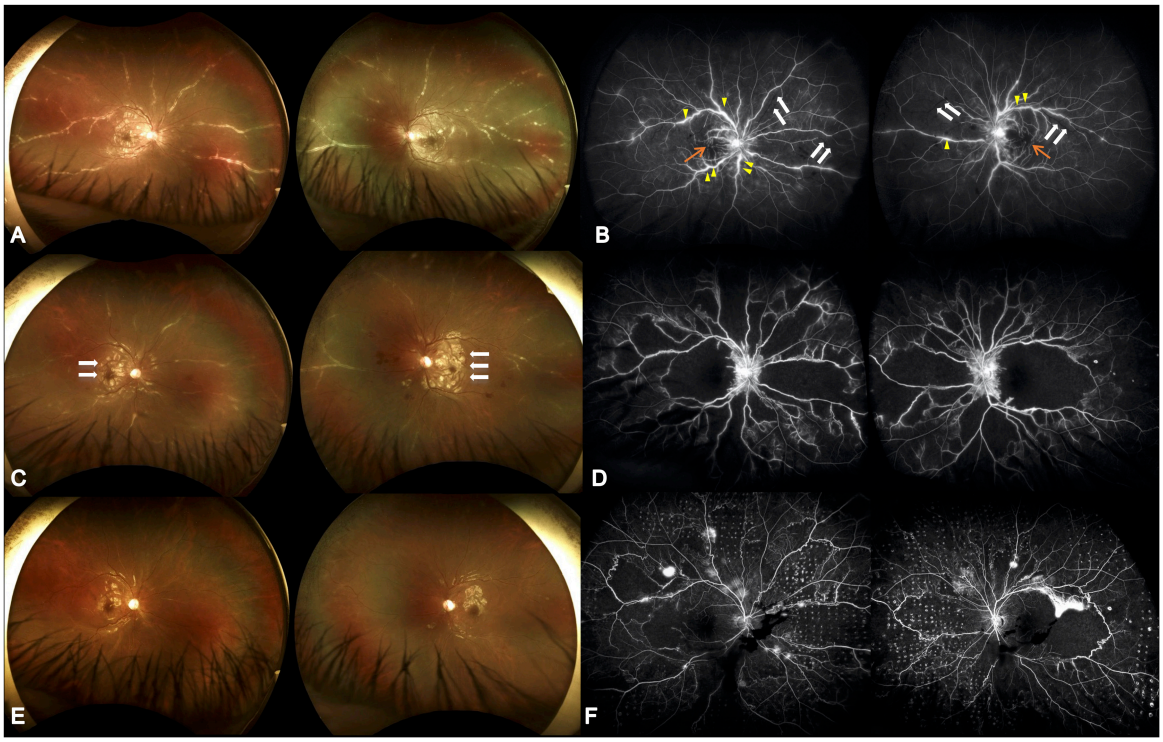

FIGURE 1
Serial ultrawide-field fundus photographs. **(A)** Initial presentation showed diffuse perivascular sheathing with frosted branch angiitis appearance. **(B)** Initial fluorescein angiography revealed multiple segmental phlebitis (yellow arrow) with occlusive arteritis (white arrow) and retinal non-perfusion (orange arrow). The visual acuity was 0.025 (both eyes). **(C)** Four weeks later, partial resolution of the perivasculitis following systemic corticosteroid and antiviral treatment was seen; however, aggravated Purtscher-like retinopathy was demonstrated (white arrow). **(D)** Twenty-one weeks after initial visit and 8 weeks following HBOT, alleviated vascular leakage, however, with extensive macular and midperipheral retinal non-perfusion was shown. The visual acuity was 0.16 (both eyes). **(E)** Nineteen weeks after initial visit, reduced Purtscher fleckens was note. Frosted branch angiitis almost completely resolved following combined corticosteroid, antiviral agent, and immunosuppressive medications. **(F)** Thirty-nine weeks after initial visit and 26 weeks following HBOT as well as 15 weeks after retinal photocoagulation, there were vascular leakage with few vitreous hemorrhage. The visual acuity was 0.1 (right) and 0.16 (left).

Introduction

Uveitis is a group of ocular inflammatory diseases encompassing non-infectious and infectious causes. Frosted branch angiitis (FBA) is an uncommon retinal vasculitis characterized by widespread perivascular sheathing that simulates frost on a tree branch. Apart from lymphoma or leukemic cell infiltration, or definite infectious diseases such as cytomegalovirus retinitis, most reported cases of FBA are idiopathic, with presumed viral prodromes before the ocular manifestations (1).

Purtscher-like retinopathy (PuR) is a clinical phenomenon characterized by diffuse white plaques, namely Purtscher fleckens confined within the macular area, with precapillary arteriole occlusion. Optical coherence tomography (OCT) often reveals the pattern of paracentral acute middle maculopathy (2). PuR results from various non-traumatic etiologies (3), and among which, viral infections are extremely rare.

Hyperbaric oxygen therapy (HBOT) has been used to treat blindness, including central retinal artery occlusion, macular edema due to diabetes, and specific optic neuropathy (4–6). We report a case utilizing HBOT as a rescue treatment for macular ischemia in post-viral infection-induced FBA and PuR.

Abbreviations: ATA, atmosphere absolute; BCVA, best-corrected visual acuity; FBA, frosted branch angiitis; HBOT, hyperbaric oxygen therapy; OCT, optical coherence tomography; PuR, Purtscher-like retinopathy; ANA, antinuclear antibody.

Case report

A 10-year-old male consulted our ophthalmology department due to bilateral blurred vision for one week. He had experienced a 1-week episode of flu-like symptoms, including fever and general malaise, 1 month before the ocular presentation. The best-corrected visual acuity (BCVA) was 0.025 (both eyes, BE). The intraocular pressure was within the normal range. Slit lamp examinations revealed 0.5+ anterior chamber cells (BE) with otherwise normal anterior segment structures. Indirect ophthalmoscopy revealed bilateral diffuse perivascular sheathing of the arteries and veins, Purtscher fleckens, and mild optic papillitis. Necrotizing retinitis was not observed (**Figures 1A, B**). OCT revealed profound macular edema with intraretinal fluid, subretinal fluid, and inner to middle retinal layer hyperreflectiveness (**Figure 2A**). Ultrawide-field fluorescein angiography revealed bilateral segmental phlebitis, occlusive arteritis, and retinal non-perfusion with macular ischemia. Due to previous systemic

prodromes, a pediatrician was consulted for multidisciplinary care.

Physical examination results aside from the ocular findings were unremarkable. Abdominal ultrasonography revealed mild hepatomegaly. Initial hematology and serology investigations revealed an elevated erythrocyte sedimentation rate at 58 mm/h, alanine aminotransferase at 160 U/L, and positive antinuclear antibody (1:640). A systemic infection survey targeting retinal vasculitis and hepatitis revealed negative results for HSV-1, CMV, VZV, EBV, HTLV, HBV, HCV, Quantiferon-TB Gold, syphilis, and toxoplasma serology. However, a highly positive titer of HSV 2 IgM (5.10) was noted. An aqueous tap was not performed because of its invasiveness considering the age of the patient. In addition, the associated autoimmune profiles were positive for anti-smooth muscle antibody (Ab), but negative for anti-dsDNA, anti-mitochondria Ab, or anti-liver kidney microsome Ab (anti-LKM Ab). Therefore, this patient was diagnosed with post-HSV-2 infection-related FBA, PuR, and concurrent autoimmune hepatitis. The patient was initially prescribed prednisolone (40 mg/day), valaciclovir (500 mg every 12 h), and acetylsalicylic acid (100 mg every other day) (Figure 3).

Although the bilateral FBA and macular edema gradually alleviated (Figures 1C, 2B) after several weeks of medical treatment, the BCVA improvement was minimal (0.05, right eye; counting finger, left eye) (Table 1). Persistent macular ischemia, with clinical presentations of profound PuR and compatible ischemic hyperreflective changes on OCT (Figures 1C, 2C), was identified to be the main cause of poor vision. Therefore, HBOT was initiated with 2.0 atmosphere absolute (ATA) for 75 min per session, 1 session per day, 5 days per week. After a total of 39 sessions of HBOT, the visual acuity steadily improved to 0.16 (RE) and 0.2 (LE), with gradual resolution of Purtscher flecken (Table 1). Subsequent immunosuppressive medications, including methotrexate (10 mg/week) and cyclosporine (50 mg/day), were also initiated for FBA treatment and corticosteroid tapering (Figure 3). Follow-up fundus photograph and fluorescein angiography performed 21 weeks after the initial visit and 8 weeks following HBOT revealed almost completely resolution of FBA and decrease in size of PuR, but extensive macular and mid-peripheral retinal ischemia (Figures 1D, E). Therefore, retinal photocoagulation on the non-perfusion area was performed 13 weeks after the initiation of HBOT to prevent further neovascular complications, such as vitreous hemorrhage, tractional retinal detachment, and neovascular glaucoma (Figure 1F).

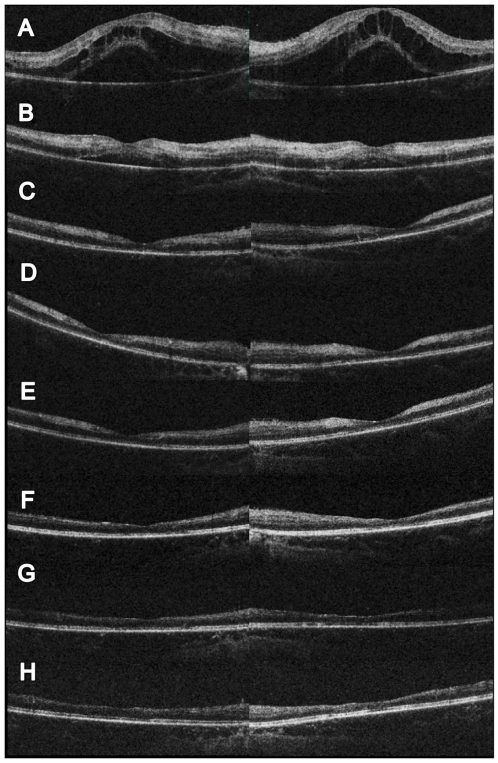

FIGURE 2
Serial changes in OCT. **(A)** Initial OCT showed profound macular edema with combine intraretinal and subretinal fluid. **(B)** Two weeks after initial visit, partial resolution of the macular edema; however, hyperreflective change could be noted at the inner and middle retinal layers. The visual acuity was 0.1 (right) and 0.05 (left). **(C)** Eleven weeks after initial visit, complete resolution of the macular edema. CFT 156 μm (right) and 147 μm (left). The visual acuity was 0.05 (right) and counting finger 30 cm (left). **(D)** Seventeen weeks after initial visit and 4 weeks following HBOT. Slightly reduce hyperreflectivity at the left eye could be noted. The visual acuity was 0.1 (both). **(E)** Twenty-one weeks after initial visit and 8 weeks following HBOT. Extensive retinal thinning with ellipsoid zone loss was noted. The visual acuity was 0.16 (both). **(F)** Twenty-eight weeks after initial visit and 15 weeks following HBOT. Reduced inner retinal thinning was noted. The visual acuity was 0.16 (right) and 0.2 (left). **(G)** Forty-three weeks after initial visit and 30 weeks following HBOT. Reduced inner retinal thinning was noted. The visual acuity was 0.05 (right) and 0.16 (left). **(H)** Sixty weeks after initial visit and 47 weeks following HBOT. Reduced inner retinal thinning was noted. The visual acuity was 0.1 (right) and 0.16 (left).

Discussion

This case raises three important issues for clinicians. First, the clinical appearance of the fundus showed typical FBA; however, the clinical course was prolonged compared to typical FBA cases. Second, with bilateral retinal vasculitis and high titer of HSV-2 IgM in the serology survey, non-necrotizing herpetic retinopathy, which is the immunopathological reaction to the herpes virus, is the most likely pathophysiology. Combined immunosuppressive therapy was effective. Third, extensive arterial occlusions and PuR with macular ischemia made the visual prognosis limited. All three possibilities are relatively rare, with limited information in the extant literature.

The most relevant literature includes limited case reports and case series. Lee et al. (7) conducted 4 case series and an extensive literature review of 236 cases in which 105 cases (43.8%) were classified as idiopathic etiology. More bilateral manifestations were associated with younger age (<10 years) and better visual prognosis (7). A review by Walker et al. (1) of 57 case reports within 27 years (1976–2003) worldwide reported similar results in that nearly half of the cases were from the pediatric-age group. Most patients were characterized by Asian ethnicity and idiopathic etiology (1), including our case. The clinical presentation in the current case also coincides with another uncommon factor, non-necrotizing herpetic retinopathy, as reported by Bodaghi et al. (8) and Wensing et al.

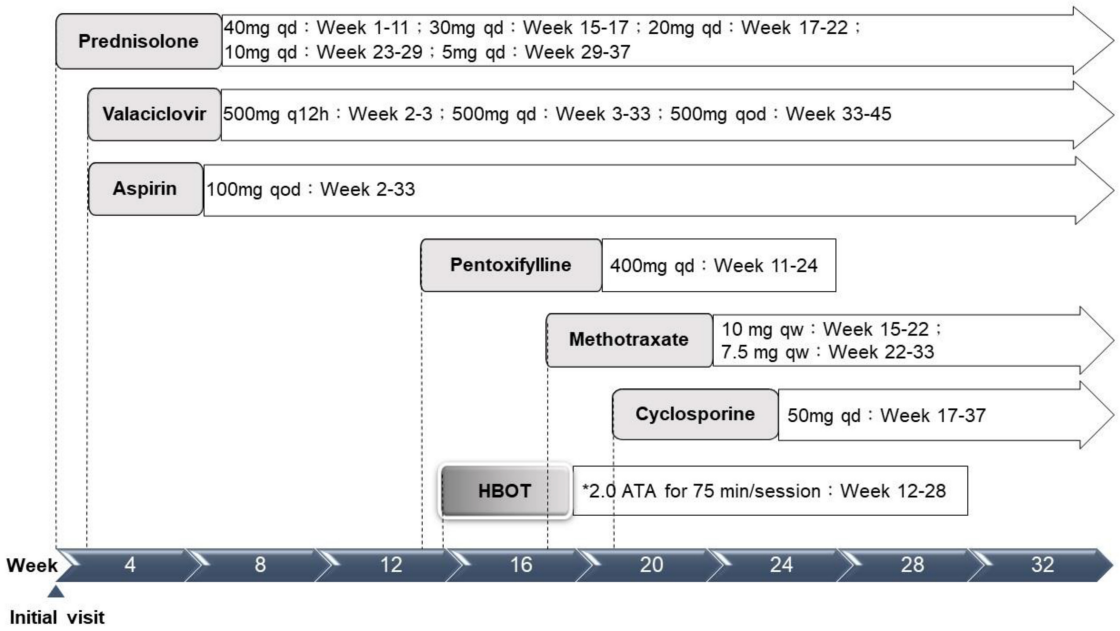

FIGURE 3
Treatment timeline. ATA, atmosphere absolute; HBOT, hyperbaric oxygen therapy; qd, every day; q12h, every 12 hours; qod, every other day; qw, every week. *Treatment protocol: 2.0 ATA for 75 min per session, 1 session per day, 5 days per week.

(9). The hallmark of the final diagnosis of the case was the absence of typical rapidly progressive necrotizing retinitis seen in acute retinal necrosis. As Bodaghi et al. (8) proposed, the constellation of papillitis and retinal vasculitis is an immunopathological phenomenon rather than a direct viral cytopathic effect. Therefore, systemic corticosteroids and immunosuppressive therapies were the mainstay of treatment with adjunctive low-dose prophylactic anti-viral agents in the current case.

The visual prognosis of FBA is excellent. However, similar to our case, a minority (10%) may present with poor final visual acuity (<0.1) due to structural complications such as macular pathologies, optic atrophy, and retinal vascular occlusions (1). Kwon et al. (10) reported a 39-year-old male with an unusual case of unilateral FBA associated with Behçet's disease. Neovascularization of the disc was found, despite panretinal photocoagulation for non-perfusion areas. Foveal atrophy and disruption of the photoreceptor layer in the macular area developed with final vision limited to hand movement, 8 months later (10). In our patient, although initial macular edema responded favorably to treatment, macular ischemia with PuR was refractory to combined anti-inflammatory and antiplatelet therapy. Follow-up fluorescein angiography revealed extensive arterial and capillary dropout, and further neovascular complications, such as vitreous hemorrhage, retinal vascular occlusion, iris rubeosis, and neovascular glaucoma require close monitoring (7). As most ophthalmological treatment modalities, such as intravitreal anti-VEGF injections and panretinal photocoagulation, are only capable of suppressing VEGF release and avoiding further neovascular complications, few options are available to rescue retinal perfusion in such challenging scenarios. Therefore, HBOT is a viable option for physicians. As the patient had received numerous medications, it was not possible to evaluate the sole effect of HBOT. However, considering the significant structural changes in macular ischemia and foveal thinning on follow-up images (**Figures 1C–F**, **2D–H**), the salvage effect of HBOT may have played a role in the visual recovery process.

Hyperbaric oxygen therapy is a treatment option for hypoxic tissue that increases tissue oxygen tension. It improves the oxygen supply because dissolved oxygen can diffuse into hypoxic tissue via tissue fluid, even if tissue vascularity is devastated. Most importantly, according to Henry's law, the amount of dissolved oxygen increases in proportion to the increased

TABLE 1 Hyperbaric oxygen therapy sessions and visual acuity and ocular findings monitoring.

Week	HBOT (cumulative sessions)*	BCVA		CFT (μm)	
		OD	OS	OD	OS
Initial	0	0.025	0.025	394	396
2nd week	0	0.1	0.05	320	210
5th week	0	0.1	0.16	204	196
11th week	0	0.05	CF 30 cm	156	147
15th week	12	0.1	CF 20 cm	153	137
17th week	22	0.1	0.1	152	142
19th week	30	0.1	0.1	155	140
21st week	30	0.16	0.16		
28th week	39	0.16	0.2	158	143

HBOT, hyperbaric oxygen therapy; BCVA, best-corrected visual acuity; CFT, central foveal thickness on optical coherence tomography; OD, right eye; OS, left eye.
*Treatment protocol: 2.0 atmosphere absolute (ATA) for 75 min per session.

partial pressure of oxygen. For instance, if 100% oxygen is breathed at 3 ATA (≈ 2,280 mmHg), dissolved oxygen rises from 0.31 to 6.02 vol%, which theoretically provides sufficient oxygen to maintain the basic metabolism of the human body without oxygen from hemoglobin (6). In an earlier animal study by Landers, the visual evoked response (VER) was restored to normal despite retinal artery occlusion while 1 ATA oxygen was administered. Normal VER indicated that the inner retinal layers were adequately oxygenated in this model (6, 11).

The human retina has a dual blood supply system (12). The retinal circulation supplies the inner layers of the retina (ganglion, bipolar, and Muller glial cells) and the choroidal circulation supplies the outer layers (photoreceptors and retinal pigment epithelium) (12). Therefore, in the model of central retinal artery occlusion, it is postulated that higher partial pressure of oxygen could diffuse farther from the choroidal circulation or other patent retinal vessels to reach the ischemic retina using HBOT (13). HBOT should be able to lessen the degree of ischemia neuronal injury and restart cellular metabolism. The circumstance of ischemic neuronal damage within the retina begins with a hypoxia event, just as it takes place in the ischemic stroke within central nervous system (14). According to Kim et al., patients with central retinal artery occlusion (CRAO) benefit from HBOT, with greater visual improvement (5). HBOT is not only supposed to improve visual acuity via increased oxygen concentration to ischemic retinas, it also reduces retinal apoptosis according to animal models (4, 15). Recently, another case demonstrated visual acuity improvement for mumps-associated FBA after sessions of HBOT (16).

The pathophysiology of PuR remains uncertain, but the most widely accepted theory is an embolic phenomenon, resulting in occlusion of the precapillary arterioles and subsequently ischemia (3). We believed that HBOT could also improve tissue oxygenation to the macular ischemia. Lin et al. reported HBOT improved visual function and retinal appearance in a case with Purtscher's retinopathy secondary to chest injury (17). In addition, Haji and Frenkel also reported a case of radiation-induced macular ischemia, who benefited from HBOT with macular perfusion improvement (18). In the present case, signs of avascular area and vasculitis appeared at the first visit. Although HBOT was not initiated immediately after diagnosis, visual acuity steadily improved under sessions of HBOT with successful corticosteroid tapering.

The novel information provided by this case is that the prognosis of FBA is not always favorable. With concurrent structural complications, such as macular pathologies, optic atrophy, and retinal vascular occlusions, aggressive corticosteroid with combined immunomodulatory therapy is necessary. We recommend early intervention with HBOT to salvage severe macular ischemia. Long-term management should monitor for and attempt to prevent neovascular complications.

Conclusion

Hyperbaric oxygen therapy may be a beneficial rescue treatment for retinal ischemia secondary to FBA with PuR. Further clinical and basic research is needed to evaluate the effectiveness of HBOT for uveitis with occlusive retinal vasculitis.

Ethics statement

The study was approved by the FEMH Ethics Committee in Taiwan (FEMH-111106-C). Written informed consent for publication was obtained from the involved patient and his parents. Written informed consent to participate in this study was provided by the participants' legal guardian/next of kin.

Author contributions

C-TL and H-TC: conceptualization. T-HH: data curation. H-TC: funding acquisition and supervision. T-HH and ZZ: investigation. Y-RH: methodology and resources. C-CC and J-HW: project administration. C-TL, T-HH, and ZZ: writing—original draft. Y-RH, H-TC, and J-KW: writing—review and editing. All authors contributed to the article and approved the submitted version.

Funding

This study was financially supported by the project Far Eastern Memorial Hospital (FEMH-2020-C-008).

Acknowledgments

We thank Mei-Yun Chang (Center of Hyperbaric Oxygen, Far Eastern Memorial Hospital).

Patient consent

The patient provided written informed consent for inclusion of his clinical and imaging details in the manuscript for the purpose of publication.

Conflict of interest

The authors declare that the research was conducted in the absence of any commercial or financial relationships that could be construed as a potential conflict of interest.

Publisher's note

References

1. Walker S, Iguchi A, Jones N. Frosted branch angiitis: a review. *Eye.* (2004) 18:527–33. doi: 10.1038/sj.eye.6700712

2. Miguel A, Henriques F, Azevedo L, Loureiro A, Maberley D. Systematic review of Purtscher's and Purtscher-like retinopathies. *Eye.* (2013) 27:1–13. doi: 10.1038/eye.2012.222

3. Ang L, Chang B. Purtscher-like retinopathy - A rare complication of acute myocardial infarction and a review of the literature. *Saudi J Ophthalmol.* (2017) 31:250–6. doi: 10.1016/j.sjopt.2017.05.009

4. Murphy-Lavoie H, Butler F, Hagan C. Central retinal artery occlusion treated with oxygen: a literature review and treatment algorithm. *Undersea Hyperb Med.* (2012) 39:943–53.

5. Kim Y, Nam M, Park E, Lee Y, Kim H, Kim S, et al. The effect of adjunctive hyperbaric oxygen therapy in patients with central retinal artery occlusion. *Undersea Hyperb Med.* (2020) 47:57–64.

6. Butler F, Hagan C, Murphy-Lavoie H. Hyperbaric oxygen therapy and the eye. *Undersea Hyperb Med.* (2008) 35:333–87.

7. Lee, K, Jung S, Chin H. Frosted branch angiitis; Case series and literature review. *Ocul Immunol Inflamm.* (2022). doi: 10.1080/09273948.2022.2148112 [Epub ahead of print].

8. Bodaghi B, Rozenberg F, Cassoux N, Fardeau C, LeHoang P. Nonnecrotizing herpetic retinopathies masquerading as severe posterior uveitis. *Ophthalmology.* (2003) 110:1737–43. doi: 10.1016/S0161-6420(03)00580-3

9. Wensing B, de Groot-Mijnes J, Rothova A. Necrotizing and nonnecrotizing variants of herpetic uveitis with posterior segment involvement. *Arch Ophthalmol.* (1960) 2011:403–8. doi: 10.1001/archophthalmol.2010.313

10. Kwon S, Park D, Shin J. Frosted branch angiitis as ocular manifestation of Behçet's disease: unusual case report and literature review. *Korean J Ophthalmol.* (2013) 27:466–9.

11. Landers M III. Retinal oxygenation via the choroidal circulation. *Trans Am Ophthalmol Soc.* (1978) 76:528–56.

12. Hadanny A, Maliar A, Fishlev G, Bechor Y, Bergan J, Friedman M, et al. Reversibility of retinal ischemia due to central retinal artery occlusion by hyperbaric oxygen. *Clin Ophthalmol.* (2017) 11:115–25.

13. Elder M, Rawstron J, Davis M. Hyperbaric oxygen in the treatment of acute retinal artery occlusion. *Diving Hyperb Med.* (2017) 47:233–8.

14. Celebi A. Hyperbaric oxygen therapy for central retinal artery occlusion: patient selection and perspectives. *Clin Ophthalmol.* (2021) 15:3443–57. doi: 10.2147/OPTH.S224192

15. Gaydar V, Ezrachi D, Dratviman-Storobinsky O, Hofstetter S, Avraham-Lubin B, Goldenberg-Cohen N. Reduction of apoptosis in ischemic retinas of two mouse models using hyperbaric oxygen treatment. *Invest Ophthalmol Vis Sci.* (2011) 52:7514–22. doi: 10.1167/iovs.11-7574

16. Sayadi J, Ksiaa I, Malek I, Ben Sassi R, Essaddam L, Khairallah M, et al. Hyperbaric oxygen therapy for mumps-associated outer retinitis with frosted branch angiitis. *Ocul Immunol Inflamm.* (2021) 30:1001–4. doi: 10.1080/09273948.2020.1841243

17. Lin Y-C, Yang C-M, Lin C-L. Hyperbaric oxygen treatment in purtscher's retinopathy induced by chest injury. *J Chin Med Assoc.* (2006) 69:444–8.

18. Haji S, Frenkel R. Hyperbaric oxygen therapy for the treatment of radiation-induced macular ischemia. *Clin Ophthalmol.* (2010) 4:433–6. doi: 10.2147/opth.s9803

Frontiers in Medicine

Translating medical research and innovation into improved patient care

A multidisciplinary journal which advances our medical knowledge. It supports the translation of scientific advances into new therapies and diagnostic tools that will improve patient care.

Discover the latest Research Topics

See more →

Frontiers

Avenue du Tribunal-Fédéral 34
1005 Lausanne, Switzerland
frontiersin.org

Contact us

+41 (0)21 510 17 00
frontiersin.org/about/contact